QUANTIZED MASSIVE SPIN ½ FIELDS ON STATIC SPHERICALLY SYMMETRIC WORMHOLE SPACETIMES

A Thesis Presented to the Faculty of the Graduate School

At the University of Missouri

In Partial Fulfillment of the Requirement for the Degree

Doctor of Philosophy

By

ZHIYONG SHEN

Dr. Aigen Li, Thesis Supervisor

Dr. David Retzloff, Thesis Co-Supervisor

July 2012

The undersigned, appointed by the Dean of the Graduate School, have examined the dissertation entitled:

QUANTIZED MASSIVE SPIN ½ FIELDS ON STATIC SPHERICALLY SYMMETRIC WORMHOLE SPACETIMES

presented by Zhiyong Shen,

a candidate for the degree of Doctor of Philosophy and hereby certify that, in their opinion, it is worthy of acceptance.

_____

Dr. Aigen Li

_____

Dr. Sergei Kopeikin

_____

Dr. Adam Helfer

_____

Dr. David Retzloff

_____

Dr. Carsten Ullrich

ACKNOWLEDGMENTS

I would like to thank my advisor Dr. Aigen Li and co-advisor Dr. David Retzloff. Their support and help made it possible for me to complete this thesis. I would also like to thank Dr. Adam Helfer who gave me valuable advice on improving this thesis. At last but not least, I acknowledge the Department of Physics and Astronomy for support and hospitality during the period of my studying and working at the University of Missouri.

TABLE OF CONTENTS

LIST OF TABLES

LIST OF FIGURES

Figure Page

ABSTRACT

Traversable wormholes have become a subject of intensive studies since 1988 when Morris and Thorne published their paper which put forward the energy conditions for traversable wormholes. A number of researchers have calculated the stress-energy tensors of different fields but failed to find one that meets the requirement of the wormhole geometry. Some others find different schemes to sustain traversable wormholes but either on the Planck scale or hypothetically on a macroscopic scale.

Groves has developed a method to compute the renormalized stress-energy tensor for a quantized massive spin ½ field in a general static spherically symmetric spacetime. Using this method, I have computed the renormalized stress-energy tensors of two quantized massive spin ½ fields in four static spherically symmetric wormhole spacetimes. The results of my calculation suggest that these two fields can be considered exotic. However, due to the technical difficulties in implementing this method, a series of approximations are used in the computation in order to make the problem mathematically tractable; but it is not clear under what physical circumstances these approximations could hold. Besides, the cases that I investigated turned out to involve unphysically large energy densities. Because of these reasons, no firm physical conclusions can be drawn.

Chapter 1. Introduction

The name wormhole was coined by John A. Wheeler in 1957. It refers to a hypothetical topological feature of spacetime that would be a "shortcut" through spacetime. It is like a tunnel with two ends each in separate points in spacetime. A wormhole has the property of traversing a very large distance in an otherwise impossibly small amount of local time as measured by the traveler.

There is no observational evidence of wormhole. It is a theoretical solution to Einstein's field equations. Although it is speculative, a large number of serious research has been done on this subject. This started with Einstein and Rosen's paper in 1935 on the Einstein-Rosen bridge [1] that consists of a Schwarzschild black hole connected to a white hole. The hypothesis was that one-way travel could occur into the black hole and then out of the white hole. However, Wheeler and Fuller [2] showed later that this configuration was unstable, with the bridge connecting the two spacetimes collapsing before any signal could pass through.

In the 1950s Wheeler utilized a wormhole as the framework for a new

elementary entity called a geon that was a bundle of electromagnetic waves held together by gravity [3]. He considered wormholes as objects of the quantum foam connecting different regions of spacetime and operating on the Planck scale. However, these wormholes were not traversable, and furthermore would develop some type of singularity [4].

After the work of Wheeler, the field of wormhole lay dormant until 1988 when Morris and Thorne published a paper [5] that reinvigorated the study on this subject. They explored what kind of energy and matter would be required to hold open a wormhole metric satisfying Einstein's field equations and if such a wormhole could be made safely traversable by people in a finite amount of time.

The metric of a general spherically symmetric spacetime can be written as

$$ds^2 = -f(r)dt^2 + h(r)dr^2 + r^2(d\theta^2 + sin^2\theta d\phi^2). \tag{1.1}$$

In their paper [5], Morris and Thorne parameterized the metric for a static spherically symmetric wormhole spacetime in the form

$$ds^2 = -e^{2\Phi(r)}dt^2 + \frac{dr^2}{1 - b(r)/r} + r^2(d\theta^2 + sin^2\theta d\phi^2). \tag{1.2}$$

These two metric equations are connected by

$$f(r) = e^{2\Phi(r)}, \tag{1.3}$$

$$h(r) = [1 - \frac{b(r)}{r}]^{-1}. \tag{1.4}$$

In Eq. (1.2), $\Phi(r)$ is called the redshift function because it determines the gravitational redshift of an observer traveling through the wormhole; and $b(r)$ is called the shape function, since it is related to the spatial shape of the wormhole. The coordinate r lies in the range $r_0 \leq r < \infty$, with $2\pi r_0$ being the circumference of a circle centered on the wormhole's throat at $r = r_0$.

However, Eq. (1.2) does not represent the metric of a wormhole spacetime unless we put some restrictions on the functions $\Phi(r)$ and $b(r)$. One restriction is that the spatial geometry must become flat as r approaches infinity. Therefore, the following limits must hold [9]:

$$\lim_{r\to\infty} \Phi(r) = 0, \tag{1.5}$$

$$\lim_{r\to\infty} \frac{b(r)}{r} = 0. \tag{1.6}$$

Besides, a wormhole does not have an event horizon or a singularity. To ensure there is no event horizon at $r = r_0$, we must demand that

$$\lim_{r\to r_0} \Phi(r) > -\infty. \tag{1.7}$$

The function $b(r)$ must be chosen so that

$$\lim_{r\to r_0} h(r) = \infty. \tag{1.8}$$

Eq. (1.8) implies that

$$b(r_0) = r_0. \tag{1.9}$$

Moreover, we want $h(r)$ to be positive and finite as r increases above r_0. This requires

$$\frac{d}{dr}[\frac{1}{h(r)}]|_{r=r_0} > 0. \tag{1.10}$$

Substituting the metric function for $h(r)$ from Eq. (1.4) into Eq. (1.10) and making use of Eq. (1.9), we have the inequality

$$\frac{1}{r_0^2} - \frac{b'(r_0)}{r_0^2} > 0, \tag{1.11}$$

where a prime denotes a derivative with respect to r. Utilizing the Einstein field equations, the energy density at the wormhole's throat is expressed as

$$\rho_0 = -\frac{G_t^t}{8\pi} = -T_t^t = \frac{b'(r_0)}{8\pi r_0^2}; \tag{1.12}$$

and the radial tension at the throat is written as

$$\tau_0 = -\frac{G_r^r}{8\pi} = -T_r^r = \frac{1}{8\pi r_0^2}. \tag{1.13}$$

Substituting these results into Eq. (1.11) yields the inequality for the energy condition of a traversable wormhole derived by Morris and Thorne [5]:

$$\tau_0 - \rho_0 > 0. \tag{1.14}$$

Besides, Eq. (1.13) requires

$$\tau_0 > 0. \tag{1.15}$$

Normally, a matter satisfies Eq. (1.15) but does not satisfy Eq. (1.14). A matter that satisfies Eq. (1.14) would violate the weak energy condition, which states that the local energy density as viewed by any observer is non-negative so that [6]

$$T_{\mu\nu}U^\mu U^\nu \geq 0 \tag{1.16}$$

for all time-like vector U^μ. However, Eq. (1.14) implies that an observer traveling through the wormhole's throat with a radial velocity close to the speed of light ($\gamma \gg 1$) will observe negative energy density. In this observer's reference frame, the energy density is [5, 9]:

$$\rho' = \gamma^2(\rho_0 - \tau_0) + \tau_0. \tag{1.17}$$

As γ increases, the first term on the right-hand side, which is negative, takes over the second term on the right-hand side, which is positive. So ρ' becomes negative. Such a stress-energy tensor required by a wormhole violates the weak energy condition. Therefore, a matter with such a stress-energy tensor is called "exotic matter".

In nature, a matter usually satisfies the weak energy condition. The closest known candidate of exotic matter is the negative pressure density

reflected by a small attractive force between two close parallel metalic plates. This phenomenon was predicted by the Dutch physicist Hendrick Casimir in 1948 and is called Casimir effect. The origin of the Casimir effect is attributed to quantum fluctuations. Due to the quantum fluctuation, the mean value of the square of the dipole moment is not equal to zero. This leads to what is referred to as dispersion forces. For atomic separations of the orders of angstrom and nanometer, which are much less than the characteristic absorption wavelength of the virtual photon emitted by the atom, the dispersion force is usually called the Van der Waals force. At relatively large atomic separations, of order or larger than the characteristic absorption wavelength of the virtual photon, the dispersion force is usually called Casimir force for interaction between two macroscopic bodies [7].

Casimir developed a theoretical approach to the atom-wall interaction. The finite energy and pressure per unit area between two infinitely large parallel ideal metal walls separated by a distance a were found as the difference between the energies and pressures of zero-point (vacuum) oscillations of the electromagnetic field in the presence and in the absence of walls as [7]

$$E = -\frac{\pi^2 \hbar c}{720 a^3}, \qquad P = -\frac{\pi^2 \hbar c}{240 a^4} \tag{1.18}$$

A more general theory about the Casimir effect was developed by Lifshitz, who unified the Van der Waals force and the Casimir force as two limiting cases of the single dispersion force. Lifshitz's theory describes dispersion

forces as a physical phenomenon caused by the fluctuating electromagnetic field. Using the fluctuation-dissipation theorem, Lifshitz derived the general formulas for the free energy and force of the dispersion interaction.

A lot of experiments on the Casimir effect have been carried out. Before 1990 many experiments were done to demonstrate the existence of the Casimir force. However, the experiment by van Blockland and Overbeek in 1978 with metallic surfaces was considered as the only unambiguous demonstration. In more recent experiments, more precise laboratory techniques were used to measure small forces and short distances. The first of these experiments was done in 1997 by Lamoreaux who used a torsion balance to measure the Casimir force between a gold coated spherical lens and a plate. The most precise measurements of the Casimir force between metallic surfaces were performed in a series of experiments by Decca et al. between 2003 and 2007. Using the new technique of a micromechanical torsional oscillator, they could determine the Casimir pressure between two parallel plates. In the last of this series of experiments, they reported a 0.2 % total experimental error at a separation of $160nm$ [7].

In spite of these fruitful experiments, a problem lies in the disparity between the experimental results and the theory, and this disparity is caused by the difficulty in modeling real materials. Both Casimir's and Lifshiftz's theories consider dispersion forces between two parallel plates. However, real bodies may have different geometric configurations, and a distinctive feature of the Casimir force is its geometry dependence. For example, the Casimir

force can be repulsive for an ideal spherical shell. Another example is that, in ideal metal rectangular boxes, the Casimir force may either be repulsive or attractive depending on the ratio of the size of the sides [7].

Another feature of real material bodies differentiating them from ideal metal plates are connected with the realistic material properties and thermal effects. In the Lifshitz theory of dispersion forces, the free energy and other thermodynamic quantities are expressed as functionals of the frequency-dependent dielectric permittivity, and the calculational results depend strongly on the model of dielectric permittivity used to describe real material. However, different physical processes contribute to the value of the dielectric permittivity, which are not distinguished in the Lifshitz theory [7].

Due to these difficulties in modeling real materials, it is still not known how to properly compare the experimental results on the Casimir effect with theories. In addition, it should be noted that all the above-mentioned experiments are to test the Casimir force, while the Casimir energy density has not been measured.

Apart from the Casimir effect, there seems no sign of evidence of exotic matter in nature. However, a number of people have made efforts to theoretically explore the existence of the exotic matter that could support wormhole spacetimes. Using the DeWitt-Schwinger approximation, Taylor, Hiscock, and Anderson [8] analytically computed the stress-energy of a quantized massive scalar field in five static spherically symmetric Lorentzian wormhole spacetimes. They found that in all five cases, for both minimally and con-

formally coupled scalar fields, the stress-energy does not even qualitatively have the properties needed to support the wormhole geometry.

W. H. Hirsch [9] numerically computed the fully renormalized stress-energy tensor for a massless spin 1/2 field on and outside the throat of three static spherically symmetric Lorentzian wormhole spactimes. The full stress-energy tensors are analyzed in terms of an arbitrary renormalization parameter μ to see if the exotic energy condition needed to keep such an object from collapsing is met. The results show that no wormhole geometry studied is found to be a self-consistent solution when quantum fluctuations of the spin 1/2 field are considered.

On the other hand, some other researchers claimed that certain materials can sustain wormhole geometries. Barcelo and Visser [10] reported that the energy-momentum tensor of a massless scalar field conformally coupled to gravity can violate the weak energy condition (i.e., has negative energy density) and thus can support wormhole geometries, even at the classical level and even in flat Minkowski spacetime. They found a three-parameter class of exact solutions to the Einstein equation for such a field. These exact solutions include the Schwarzschild geometry, assorted naked singularities, and a large class of traversable wormholes. However, their results have a drawback that the effective Newtonian constant has opposite signs in the two asymptotic regions connected by the wormhole.

Hochberg, Popov and Sushkov [11] reported that quantum effects of a scalar field can maintain a wormhole. They presented the results of a self-

consistent solution of the semi-classical Einstein field equations corresponding to a Lorentzian wormhole coupled to a quantum scalar field. The solution represents a wormhole connecting two asymptotically spatially flat regions. However, the throat of the wormhole turned out to be on the order of the Planck scale, i.e., nontraversable.

Garattini [12] considered the graviton quantum fluctuations around a traversable wormhole background. The fluctuations, contained in the perturbed Einstein tensor, play the role of the exotic matter. He computed the graviton one-loop contribution to the classical energy in the background. Such a contribution is evaluated by means of a variational approach with Gaussian trial wavefunctionals. A zeta function regularization is involved to handle divergences. The results suggest that the finite one-loop energy can sustain a wormhole smaller than a Planck length.

It is worth mentioning that Ford, Roman and Pfenning studied the constraints on negative energy fluxes and introduced Quantum Inequality (QI) applied to energy densities [13, 14]. The QI was proven directly from quantum field theory in four-dimensional Minkowski spacetime. The inequality limits the magnitude of the negative energy violations and the time for which they are allowed to exist. When QI is applied to wormhole geometries, a small spacetime volume around the throat of the wormhole is considered so that all the dimensions of this volume are much smaller than the minimum proper radius of curvature in the region. Thus the spacetime can be considered approximately flat in this region. The result of the analysis is that the

wormhole possesses a throat size only slightly larger than the Planck length. Ford and Roman concluded that the existence of macroscopic traversable wormholes is very improbable [15].

Krasnikov [16, 17] circumvented the "exotic matter" and constructed a class of static traversable Lorentzian wormholes by using a two-component matter field, one of which satisfies the weak energy condition (having positive energy density), while the other is produced by vacuum fluctuations of the neutrino, electromagnetic or massless scalar (conformally coupled) fields that constitute the source of the weak energy condition violation. He claimed that static macroscopic wormholes are possible as long as Ω and K, two smooth positive even functions in the metric equation, behave properly as the radial distance $\xi \to \infty$. However, Krasnikov did not find out a physical substance that could enable Ω and K to behave properly.

Some authors propose that the phantom energy, a kind of dark energy with the property $\omega(r) = p(r)/\rho(r) < -1$ [where $p(r)$ is the pressure and $\rho(r)$ is the density of the dark energy], may be the source of supporting traversable wormholes. Zaslavskii [18] finds a simple exact solution of spherically symmetric Einstein equations describing a wormhole for an inhomogeneous distribution of the phantom energy. The equation of state is linear but highly anisotropic: while the radial pressure is negative, the transversal one is positive.

Sushkov [19] also finds an exact solution describing a static spherically symmetric wormhole with phantom energy and shows that a spatial distri-

bution of the phantom energy is mainly restricted by the vicinity of the wormhole's throat. The maximum size of the spherical region, surrounding the throat and containing most of the phantom energy, depends on the equation-of-state parameter $\omega(r)$ and cannot exceed some upper limit.

Some researchers, while confirming phantom energy to be the source of traversable wormholes, expect that the expansion of the universe will increase the size of the wormhole. Lobo [20] investigates the physical properties of traversable wormholes using the equation of state $p(r) = \omega(r)\rho(r)$, with $\omega(r) < -1$, and verifies that it is theoretically possible to construct wormhole geometries with vanishing amounts of averaged weak energy condition violating phantom energy. He argues that, because of the accelerating expansion of the universe, macroscopic wormholes could naturally grow from the submicroscopic constructions that originally pervaded the quantum foam. Gonzalez-Diaz [21] reports that, relative to the initial embedding-space coordinate system, whereas the shape of the wormholes is always preserved with time, their size is driven by the expansion of the universe to increase by a factor proportional to the scale factor of the universe.

In this thesis, I calculate the stress-energy tensors of two quantized massive spin 1/2 fields to investigate whether they satisfy Eqs. (1.14) and (1.15) so that they can be considered exotic matter. A further aim is to explore whether the stress-energy tensors of these fields satisfy the semiclassical Einstein equation

$$G_{\mu\nu} = 8\pi < T_{\mu\nu} > \tag{1.19}$$

whose solution is a wormhole spacetime, so that these fields could be semi-classically support the wormhole geometry.

Due to technical difficulties in calculation, some approximations are used. In the range of these approximations, the results of my calculation show that these two fields satisfy Eqs. (1.14) and (1.15) but do not satisfy Eq. (1.19). Thus, these two fields can be qualitatively considered to be exotic matter, but are not enough to produce wormholes by themselves. However, it is not clear under what physical circumstances these approximations could hold. Moreover, for the parameter values used in my calculation, some resulting energy densities are unphysically high. Because of these reasons, no firm physical conclusions can be drawn.

Chapter 2 introduces the method to compute the renormalized stress-energy tensor of a quantized massive spin 1/2 field in a general static spherically symmetric spacetime developed by P. Groves. Chapter 3 introduces the calculation of the stress-energy tensor of quantized massive spin 1/2 fields in a static spherically symmetric spacetime carried out in this thesis. Chapter 4 presents the results of the calculation in a zero-temperature vacuum state. Chapter 5 presents the results of the calculation in thermal states. Chapter 6 summarizes the findings in the previous chapters.

Chapter 2. Method to Compute the Stress-Energy Tensor of A Quantized Massive Spin 1/2 Field in A Static Spherically Symmetric Spacetime

2.1 Quantum field theory in curved spacetime

A key idea of general relativity is that matter influences the spacetime curvature, which is expressed by Einstein's field equation:

$$G_{\mu\nu} = 8\pi T_{\mu\nu}, \tag{2.1}$$

where the left-hand side is the Einstein tensor that describes the geometry of the spacetime, and the right-hand side is the stress-energy tensor for any matter present in the spacetime. An exact treatment of this equation requires that the gravitational field be quantized, i.e., a theory of quantum gravity is needed. However, a major difficulty in developing quantum gravity is

that, higher order terms in the expansion of the gravitational action produce graviton Feynman diagrams with multiple loops, and with increasing number of loops one encounters more and more virulent divergences. This fact renders quantum gravity unrenormalizable – with each new order more new physical quantities are needed to absorb the infinities. It is for this reason that a satisfactory theory of quantum gravity has not been developed.

An alternative approach is to assume the quantum nature of gravity does not play a crucial role, so that gravitation can be described by a classical curved spacetime as in the framework of general relativity, while other fields are treated as quantum fields propagating in the classical curved background of spacetime. Such an approach is called quantum field theory in curved spacetime (QFTCS).

In quantum field theory in flat spacetime, the Poincare group plays a key role in picking out a preferred vacuum state and defining the notion of particle. However, in a general curved spacetime, there does not appear to be any preferred notion of particles [22]. For a noncompact space, in cases where natural notions of particles are available in both the asymptotic past and future, the representations of the canonical commutation relations corresponding to these two notions are in general unitarily inequivalent. This difficulty in formulating QFTCS is cured by an algebraic approach, which allows one to consider all states arising in all the different (i.e. unitarily inequivalent) Hilbert space constructions of the theory on an equal footing. The mathematical formulation of QFTCS is based mainly on such an alge-

braic approach to field theory initiated by Haag and Kastler, as well as on the work of Segal and others on the general theory of linear dynamical system. The theory thereby obtained directly describes the expectation values of all observables.

Due to the weakness of gravity, as Birrell and Davies point out [23], any possibility of direct observational verification of quantum effects of gravity is precluded. Therefore, QFTCS must rely entirely on theoretical consideration. This is the case at least for the time being and foreseeable future.

One expects that QFTCS should have limited range of validity. In particular, it should certainly break down and be replaced by a quantum theory of gravity coupled to matter when the spacetime curvature approaches Planck scales. However, as Wald notes, the precise criteria for the validity of QFTCS will be known only when the ultimate theory of quantum gravity is available [22]. On the other hand, QFTCS is considered valid for describing elementary particles and gravitation at energies below the Planck scales [24]. Birrell and Davies argues that, in the early days of quantum theory, many calculations were undertaken in which the electromagnetic field was considered as a classical background field interacting with quantized matter. Such a semiclassical approximation readily yields some results that are in complete accordance with the full theory of quantum electrodynamics. One may therefore hope that a similar regime exists for quantum aspects of gravity, which validates QFTCS [23].

Many studies in QFTCS have produced fruitful results. It has been shown

how gravitation and quantum field theory are intimately connected to give a consistent description of black holes having entropy and satisfying the second law of thermodynamics; and it has been explained how the inhomogeneities and anisotropies observed today in the cosmic microwave background and in the large-scale structure of the universe were created in a brief stage of inflation [24]. Specifically, an important result is Hawking's study of quantum black holes and the discovery of their thermal emission. This is important in that it establishes a strong connection between black holes and thermodynamics that was thought to be purely formal before the application of quantum theory to black holes. However, both Hawking's prediction of the blackhole's thermal radiation and the application of QFTCS to inflation are afflicted with the trans-Planckian problem, and thus are questionable for their validity.

As mentioned above, all observables are described by their expectation values in QFTCS. By taking the expection value of the stress-energy tensor and treating the Einstein tensor as a c-number, Eq. (2.1) takes the form

$$G_{\mu\nu} = 8\pi < T_{\mu\nu} >, \tag{2.2}$$

where both sides are c-numbers instead of operators as in the context of quantum field theory.

This thesis is concerned with whether two quantized massive spin 1/2 fields can be considered exotic matter, and whether they can semiclassically

support wormhole geometry. Passing from QFTCS to semiclassical approximation amounts to imposing the constraint of Eq. (2.2). Finding whether a quantum field can semiclassically support a wormhole means finding a solution to Eq. (2.2) that represents a wormhole gemoetry.

2.2 Method to compute the stress-energy tensor of a quantized massive spin $1/2$ field in a curved spacetime

Because of the difficulty in solving quantum field equations in curved spacetime and summing over the modes for quantized fields, the expectation value of the stress-energy tensor in four dimensions is a quantity that has been historically and continues to be very difficult to calculate. As a result, most calculations are approximations, with rare exact calculations.

There are four approaches to calculating the stress-energy tensor of a quantized field in a static spherically symmetric spacetime [25]. One is to constrain the form of the stress-energy tensor by integrating the conservation equation and using the symmetry properties of the state that the field is in. This approach has been used in Schwarzschild spacetime for fields that are static and spherically symmetric [26, 27].

A second approach is to derive an analytic approximation for the stress-energy tensor. This approach has been used for conformally invariant fields of spin 0, 1/2, and 1 in Schwarzschild spacetime [28, 29]. For massive fields

the DeWitt-Schwinger expansion [30] can often be used to obtain a good approximation for the stress-energy tensor. This approximation has been derived for massive scalar fields in Schwarzschild spacetime [31] and in a general static spherically symmetric spacetime [32]. It has also been derived for massive spin 1/2 and spin 1 fields in Reissner-Nordstrom spacetimes [33].

A third approach is to numerically compute the stress-energy tensor. This has been done for conformally invariant spin 0 and spin 1 fields in Schwarzschild spacetime [34, 35]. Numerical calculations of the stress-energy tensor for both massive and massless scalar fields with arbitrary curvature couplings in Schwarzschild and Reissner-Nordstrom spacetimes have also been done [32].

The fourth approach is the most accurate and the most difficult. It is to analytically compute the full renormalized stress-energy tensor. This has been done for scalar fields with arbitrary mass and curvature coupling in de Sitter space [36, 37]. The stress-energy tensor for the massless spin 1 field has also been computed analytically on the event herizon of a Schwarzschild black hole. Finally a computation of the stress-energy tensor for the massless spin 1/2 field has been done in a global monopole spacetime [38].

Adopting QFTCS, Groves, Anderson, and Carlson [25] have developed a method that can be used to analytically (and partially numerically) compute the expectation value of full renormalized stress-energy tensor for the massless spin 1/2 field in a general static spherically symmetric spacetime. They proceed from the Dirac equation for massless spin 1/2 field, writing it

in terms of the Euclidean Green's function. Then they derived an expression of the unrenormalized stress-energy tensor in terms of the Euclidean Green's function for the field. They use the method of point splitting to renormalize the stress-energy tensor, with the point-splitting counter-terms for the spin 1/2 field computed by Christensen [39]. In the process of renormalization, the WKB approximation is used to isolate the divergences. Their result is an expression for the renormalized stress-energy tensor of a massless spin 1/2 field in a general static spherically symmetric spacetime. The field can either be in a vacuum state or in a thermal state at an arbitrary temperature. In the derivation the stress-energy tensor is divided into two parts. One part depends on sums and integrals over radial mode functions. This part usually needs to be computed numerically. The other part consists of an analytic tensor with a trace equal to the trace anomaly for the spin 1/2 field.

Groves, leading author of [25], has generalized this method into one that includes both the massive case and massless case in his Ph.D. dissertation [40], namely, a general method to compute the renormalized stress-energy tensors of both massive and massless spin 1/2 fields in a static spherically symmetric spacetime. The derivation of this general method is similar to that in [25], except that he uses the Dirac equation for massive spin 1/2 field instead of the Dirac equation for massless spin 1/2 field. The resulting expressions for the renormalized stress-energy tensor components include mass terms as well as massless terms. If one sets the mass terms to zero, the expressions for the renormalized stress-energy tensor components reduce to

those for massless case.

The following sections are a brief review of the derivation of the renormalized stress-energy tensor for a quantized massive spin 1/2 field in a curved spacetime in [40].

2.2.1 The Dirac equation in Minkowski space

The action for a massive spin 1/2 field in Minkowski space is [41]

$$S = \int d^4x \frac{i}{2}[\overline{\Psi}(x)\gamma^a(\partial_a\Psi(x)) - (\partial_a\overline{\Psi}(x))\gamma^a\Psi(x)] - m\overline{\Psi}(x)\Psi(x) \tag{2.3}$$

with

$$\overline{\Psi} \equiv \Psi^\dagger\gamma^0 \tag{2.4}$$

The variation of Eq. (2.3) with respect to $\overline{\Psi}$ yields the Dirac equation in Minkowski space [42, 43]

$$(i\gamma^a\partial_a - m)\Psi(x) = 0, \tag{2.5}$$

where γ^a are the Dirac matrices. Upon second quantization, the Dirac equation becomes an equation for a spin 1/2 field rather than a single particle [41, 44], and the parameter m is interpreted as the mass of the field quantum.

Similarly, the variation of Eq. (2.3) with respect to Ψ gives

$$\overline{\Psi}(i\gamma^a\overleftarrow{\partial_a} + m) = 0 \tag{2.6}$$

2.2.2 The vierbein formalism

Spinors in curved space may be dealt with through the use of the vierbein or tetrad formalism. In general relativity, it is always possible to find coordinates ξ^a_X such that the curved space metric at the point X is equal to the flat space metric η_{ab}. The coordinates ξ^a_X are called locally inertial coordinates. The vierbein or tetrad function is defined as

$$e^a_\mu(X) \equiv \frac{\partial \xi^a_X}{\partial x^\mu}|_{x=X} \tag{2.7}$$

It plays the role to connect the contravariant components of a vector V^μ in the general coordinate system at point X and its contravariant components V^a in the locally inertial coordinate system ξ^a_X:

$$V^a = e^a_\mu(X) V^\mu. \tag{2.8}$$

The components of a tensor $S^{\alpha\beta\gamma\cdots}_{\delta\sigma\rho\cdots}$ with respect to the locally inertial coordinate system at the point X are

$$S^{abc\cdots}_{def\cdots} = (e^a_\alpha e^b_\beta e^c_\gamma \cdots)(e^\delta_d e^\sigma_e e^\rho_f \cdots) S^{\alpha\beta\gamma\cdots}_{\delta\sigma\rho\cdots}. \tag{2.9}$$

When defining the covariant derivative of a spinor in curved space, it is desirable to retain the Lorentz transformation property of the partial derivative of a spinor in flat space. In flat space, the partial derivative of a spinor

$\psi(x)$ transforms under Lorentz transformation as

$$\partial_a \psi(x) \to \partial_a \psi'(x) = \Lambda_a^b R_{1/2}(\Lambda) \partial_b \psi(x). \tag{2.10}$$

We may define a spinor covariant ∇_a such that under Lorentz transformation transforms as

$$\nabla_a \psi(x) \to \nabla_a \psi'(x) = \Lambda_a^b R_{1/2}(\Lambda(x)) \nabla_b \psi(x). \tag{2.11}$$

Comparing Eqs. (2.10) and (2.11) and using the vierbein formalism, we obtain the full covariant derivative of a spin 1/2 field in curved space:

$$\nabla_a \psi = e_a^\mu (\partial_\mu + \Gamma_\mu) \psi, \tag{2.12}$$

where

$$\Gamma_\mu = \frac{1}{2} \sigma^{ab} e_a^\nu e_{b\nu;\mu}, \tag{2.13}$$

$$\sigma^{ab} = -\frac{1}{4} [\gamma^a, \gamma^b]. \tag{2.14}$$

2.2.3 The Dirac equation in a static spherically symmetric spacetime

By replacing the partial derivative in Eq. (2.5) with the covariant derivative of Eq. (2.12), one may write the Dirac equation for a spin 1/2 field in

an arbitrarily curved spacetime as

$$(i\gamma^a\nabla_a - m)\psi(x) = 0. \tag{2.15}$$

The line element for a general static spherically symmetric spacetime is written in Eq. (1.1). Using Eq. (1.1) and Eq. (2.12), the Dirac equation Eq. (2.15) is written more explicitly as

$$(i[e_a^t\gamma^a(\partial_t + \Gamma_t) + e_a^r\gamma^a(\partial_r + \Gamma_r) + e_a^\theta\gamma^a(\partial_\theta + \Gamma_\theta) + e_a^\phi\gamma^a(\partial_\phi + \Gamma_\phi)] - m)\psi = 0, \tag{2.16}$$

where Γ_μ are defined by Eq. (2.13). Employing Eq. (2.14) and the relation

$$\overrightarrow{\sum} = \begin{pmatrix} \overrightarrow{\sigma} & 0 \\ 0 & \overrightarrow{\sigma} \end{pmatrix} \tag{2.17}$$

the Dirac equation Eq. (2.16) can be written in the form

$$i\frac{\gamma^0\partial_t\psi}{f^{1/2}} + i\frac{\tilde{\gamma}}{rf^{1/4}h^{1/2}}\partial_r(rf^{1/4}\psi) - i\frac{\tilde{\gamma}(\overrightarrow{\sum}\bullet\overrightarrow{L} + 1)}{r}\psi - m\psi = 0, \tag{2.18}$$

where $\overrightarrow{L}$ is the angular momentum vector; f and h are functions of r in Eq. (1.1); and $\tilde{\gamma}$ is defined as

$$\tilde{\gamma} \equiv sin\theta cos\phi\gamma^1 + sin\theta sin\phi\gamma^2 + cos\theta\gamma^3. \tag{2.19}$$

Eq. (2.18) can be solved by separation of variables. The solutions are:

$$\psi_1(x) = \frac{e^{i\omega\tau}}{rf^{1/4}} \begin{pmatrix} F^1_{\omega,j}(r)\Psi^{m_j}_{j,+}(\theta,\phi) \\ G^1_{\omega,j}(r)\Psi^{m_j}_{j,-}(\theta,\phi) \end{pmatrix}, \tag{2.20}$$

$$\psi_2(x) = \frac{e^{i\omega\tau}}{rf^{1/4}} \begin{pmatrix} G^2_{\omega,j}(r)\Psi^{m_j}_{j,-}(\theta,\phi) \\ F^2_{\omega,j}(r)\Psi^{m_j}_{j,+}(\theta,\phi) \end{pmatrix}, \tag{2.21}$$

with

$$\Psi^m_{j,+} = \begin{pmatrix} \sqrt{\frac{j+m}{2j}}Y^{m-1/2}_{j-1/2} \\ \sqrt{\frac{j-m}{2j}}Y^{m+1/2}_{j-1/2} \end{pmatrix} \text{ and } \Psi^m_{j,-} = \begin{pmatrix} \sqrt{\frac{j+1-m}{2j+2}}Y^{m-1/2}_{j+1/2} \\ -\sqrt{\frac{j+1+m}{2j+2}}Y^{m+1/2}_{j+1/2} \end{pmatrix}, \tag{2.22}$$

$$(\frac{\omega}{f^{1/2}} - im)F^1_{\omega,j} = (\frac{1}{h^{1/2}}\partial_r + \frac{j+1/2}{r})G^1_{\omega,j}, \tag{2.23}$$

$$(\frac{\omega}{f^{1/2}} + im)G^1_{\omega,j} = (\frac{1}{h^{1/2}}\partial_r - \frac{j+1/2}{r})F^1_{\omega,j}, \tag{2.24}$$

,

$$(\frac{\omega}{f^{1/2}} + im)F^2_{\omega,j} = (\frac{1}{h^{1/2}}\partial_r + \frac{j+1/2}{r})G^2_{\omega,j}, \tag{2.25}$$

$$(\frac{\omega}{f^{1/2}} - im)G^2_{\omega,j} = (\frac{1}{h^{1/2}}\partial_r - \frac{j+1/2}{r})F^2_{\omega,j}, \tag{2.26}$$

.

2.2.4 Stress-energy tensor

A. Derivation of unrenormalized stress-energy tensor

The action for a massive spin 1/2 field in an arbitrary spacetime is

$$S = \int d^4x\sqrt{-g}\frac{i}{2}[\overline{\psi}(x)\gamma^a\nabla_a\psi(x) - (\nabla_a\overline{\psi}(x))\gamma^a\psi(x)] - m\overline{\psi}(x)\psi(x) \quad (2.27)$$

The stress-energy tensor can be derived by making variation of the action with respect to the metric $g_{\mu\nu}$ [45]:

$$T^{\mu\nu}(x) = \frac{2}{\sqrt{-g(x)}}\frac{\delta S}{\delta g_{\mu\nu}(x)}. \quad (2.28)$$

The result is:

$$T_{\mu\nu}(x) = -\frac{i}{2}[\overline{\psi}(x)\gamma_{(\mu}\nabla_{\nu)}\psi(x) - \nabla_{(\mu}\overline{\psi}(x)\gamma_{\nu)}\psi(x)]. \quad (2.29)$$

Using the relations

$$\overline{\psi}\psi = Tr(\overline{\psi}\psi), \quad (2.30)$$

$$S^{(1)}(x,x') =< [\psi(x), \overline{\psi}(x')] >, \quad (2.31)$$

$$S^{(1)}(x,x') = iS_F(x,x') - iS_F^c(x,x'), \quad (2.32)$$

$$S_E(it, \overrightarrow{x}; it', \overrightarrow{x'}) = iS_F(t, \overrightarrow{x}; t', \overrightarrow{x'}), \quad (2.33)$$

where $S^{(1)}$, S_F, and S_E are the Hadamard Green's function, Feynman Green's function, and Euclidean Green's function respectively, Eq. (2.29) can be written in terms of the Euclidean Green's function and its charge conjugate:

$$< T_{\mu\nu} >_{unren} = -\frac{1}{4} \lim_{x' \to x} ImTr[\gamma_{(\mu}(\nabla_{\nu}[S_E + S_E^c] - g_{\nu)}^{\lambda'} \nabla_{\lambda'}[S_E + S_E^c]) I(x', x)], \tag{2.34}$$

where $g_{\nu'}^{\mu}$ is bi-vector of parallel transport that transforms a vector at x' to a vector at x; $I(x', x)$ is bi-spinor of parallel transport that transforms a spinor at x' to a spinor at x:

$$V_{\parallel}^{\mu} = g_{\nu'}^{\mu} V^{\nu'}, \tag{2.35}$$

$$\psi(x)_{\parallel} = I(x', x)\psi(x'). \tag{2.36}$$

B. Renormalization of the stress-energy tensor

In a general spacetime, the expectation value of a quantized stress-energy tensor is divergent. A renormalization scheme is point splitting, which works for any spacetime. To use this scheme, the stress-energy tensor is written in terms of the Green's function, which is a function of two points in spacetime. Although the stress-energy tensor is divergent when the points come together, it is finite with the points split. Point-splitting renormalization is achieved by subtracting off the renormalization counter-terms from the unrenormalized stress-energy tensor and taking the limit $x' \to x$. In this way one forms the renormalized stress-energy tensor

$$< T_{\mu\nu} >_{ren} = \lim_{x' \to x} (< T_{\mu\nu} >_{unren} - < T_{\mu\nu} >_{DS}), \tag{2.37}$$

where DS denotes the counter-terms obtained by the use of the DeWitt-Schwinger expansion [46, 47].

(a) *Point splitting.* In [40], the points are chosen to be split in the time direction so that

$$\varepsilon \equiv t - t', r = r', \theta = \theta', \phi = \phi'. \tag{2.38}$$

With this point-splitting, $S_E(t, x; t', x), g^{\mu}_{\nu'}$, and $I(x', x)$ can be expanded in powers of ε; and so $< T_{\mu\nu} >_{unren}$ [Eq. (2.34)] can be calculated in powers of ε. The results are:

$$\begin{aligned}
< T^t_t >_{unren} &= 2Re \int \frac{d\omega}{4\pi r^2}[-\omega^2 cos[\omega(\tau - \tau')] I_1 (g^{tt} + g^{tt'}) A_1 \\
&\quad -i\omega sin[\omega(\tau - \tau')] I_1 g^{tr'} \frac{h^{1/2}}{r} A_3 - \omega^2 cos[\omega(\tau - \tau')] I_2 g^{tr'} \frac{h^{1/2}}{f^{1/2}} A_1 \\
&\quad -i\omega sin[\omega(\tau - \tau')] I_2 (g^{tt} - g^{tt'}) \frac{f'}{4 f^{1/2} h^{1/2}} A_1 \\
&\quad +\omega cos[\omega(\tau - \tau')] I_2 g^{tr'} \frac{h^{1/2}}{r} A_2 \\
&\quad +i\omega sin[\omega(\tau - \tau')] I_1 g^{tr'} (\frac{1}{r} - \frac{h^{1/2}}{r} + \frac{f'}{4f}) A_1 \\
&\quad +i\omega sin[\omega(\tau - \tau')] I_1 g^{tr'} h^{1/2} m A_4 \\
&\quad -\omega cos[\omega(\tau - \tau')] I_2 g^{tr'} h^{1/2} m A_5],
\end{aligned} \tag{2.39}$$

$$\begin{aligned}
< T^r_r >_{unren} &= 2Re \int \frac{d\omega h^{1/2}}{4\pi r^2 f^{1/2}}[-i\omega sin[\omega(\tau - \tau')] I_2 (g^{rr} - g^{rr'}) \\
&\quad \times (\frac{1}{r} - \frac{h^{1/2}}{r} + \frac{f'}{4f}) A_1 + i\omega sin[\omega(\tau - \tau')] I_2 (g^{rr} - g^{rr'}) \frac{h^{1/2}}{r} A_3 \\
&\quad -\omega^2 cos[\omega(\tau - \tau')] I_2 g^{rt'} A_1
\end{aligned}$$

$$
\begin{aligned}
&-\omega^2 cos[\omega(\tau-\tau')]I_1(g^{rr}+g^{rr'})\frac{h^{1/2}}{f^{1/2}}A_1 \\
&+\omega cos[\omega(\tau-\tau')]I_1(g^{rr}+g^{rr'})\frac{h^{1/2}}{r}A_2 \\
&+i\omega sin[\omega(\tau-\tau')]I_1 g^{rt'}\frac{f'}{4f^{1/2}h^{1/2}}A_1 \\
&-\omega cos[\omega(\tau-\tau')]I_1(g^{rr}+g^{rr'})h^{1/2}mA_5 \\
&-i\omega sin[\omega(\tau-\tau')]I_2(g^{rr}-g^{rr'})h^{1/2}mA_4], \qquad (2.40)
\end{aligned}
$$

$$
\begin{aligned}
< T^{\theta}_{\theta} >_{unren} \;=\; & 2Re\int\frac{d\omega}{4\pi r^3 f^{1/2}}[-\omega cos[\omega(\tau-\tau')]I_1A_2 \\
& -i\omega sin[\omega(\tau-\tau')]I_2A_3 \\
& +i\omega sin[\omega(\tau-\tau')]I_2(\frac{1}{h^{1/2}}-1)A_1], \qquad (2.41)
\end{aligned}
$$

where I_1, I_2 are bi-spinors expressed in terms of f, h and ε; A_1 through A_5 [whose expressions are given by Eqs. (A11) through (A15) in Appendix A] are functionals of $F_{\omega,l}(r)$ and $G_{\omega,l}(r)$; and

$$
\tau-\tau' = i(t-t')+i\epsilon. \qquad (2.42)
$$

(b) *Derivation of the counter-term* $< T_{\mu\nu} >_{DS}$. The Hadamard function $G^{(1)}(x,x')$ is defined as

$$
S^{(1)}(x,x') = (i\gamma^{\mu}\nabla_{\mu}+m)G^{(1)}(x,x'). \qquad (2.43)
$$

Using relations between $S^{(1)}, S_F, S_E$ [Eqs. (2.31), (2.32) and (2.33)], Eq.

(2.34) can be written in terms of $G^{(1)}(x,x')$ as

$$< T_{\mu\nu} >= \frac{1}{2} \lim_{x' \to x} Tr[\gamma_{(\mu}\gamma^{\rho}(G^{(1)}_{;\rho\nu)} - G^{(1)}_{;\rho\nu')})]. \tag{2.44}$$

Christensen [39] finds the DeWitt-Schwinger expansion for $G^{(1)}(x,x')$:

$$\begin{aligned} G^{(1)}(x,x') &= \frac{\Delta^{1/2}}{4\pi^2}(a_0[\frac{1}{\sigma} + m^2 L(1 + \frac{1}{4}m^2\sigma + ...) - \frac{1}{2}m^2 - \frac{5}{16}m^4\sigma + ...] \\ &\quad -a_1[L(1 + \frac{1}{2}m^2\sigma + ...) - \frac{1}{2}m^2\sigma - ...] \\ &\quad +a_2\sigma[L(\frac{1}{2} + \frac{1}{8}m^2\sigma + ...) - \frac{1}{4} - ...] + \frac{1}{2m^2}[a_2 + ...] \\ &\quad +...), \end{aligned} \tag{2.45}$$

where $\Delta(x,x') \equiv g^{-1/2}(x) det(\sigma_{;\mu\nu}) g^{-1/2}(x'), L \equiv C + \frac{1}{2}\ln(\frac{1}{2}m^2\sigma)$; C being the Euler's constant; a_0, a_1, a_2 being functions of $I(x,x'), \varepsilon$, and $R_{\alpha\beta\gamma\delta}$; and $\sigma(x,x')$ being the geodesic interval, which is half of the square of the proper distance along a geodesic that connects x' and x:

$$\sigma(x,x') = \frac{1}{2}(\sigma_\mu \sigma^\mu) \tag{2.46}$$

where $\sigma^\mu \equiv \sigma^{;\mu}$ is the tangent vector to $\sigma(x,x')$ at the point x [40]. Substituting Eq. (2.45) into Eq. (2.44) and calculating derivatives, we get $< T_{\mu\nu} >_{DS}$.

(c) *Renormalized stress-energy tensor.* Substituting $< T_{\mu\nu} >_{DS}$ into Eq. (2.37), we get renormalized stress-energy tensor. However, a direct numerical computation of Eq. (2.37) is difficult. An alternative is to isolate the

divergent structure of $< T_{\mu\nu} >_{unren}$ by using the WKB approximation for the radial modes $F_{\omega,j}$ and $G_{\omega,j}$. The divergent part of this expression is labeled $< T_{\mu\nu} >_{WKBdiv}$. It can be added and subtracted on the right-hand side of Eq. (2.37):

$$\begin{aligned} < T_{\mu\nu} >_{ren} &= \lim_{x' \to x} (< T_{\mu\nu} >_{unren} - < T_{\mu\nu} >_{WKBdiv} \\ &\quad + < T_{\mu\nu} >_{WKBdiv} - < T_{\mu\nu} >_{DS}) \\ &= < T_{\mu\nu} >_{numeric} + < T_{\mu\nu} >_{analytic} \end{aligned} \tag{2.47}$$

where

$$< T_{\mu\nu} >_{numeric} \equiv \lim_{x' \to x} (< T_{\mu\nu} >_{unren} - < T_{\mu\nu} >_{WKBdiv}) \tag{2.48}$$

$$< T_{\mu\nu} >_{analytic} \equiv \lim_{x' \to x} (< T_{\mu\nu} >_{WKBdiv} - < T_{\mu\nu} >_{DS}) \tag{2.49}$$

Since $< T_{\mu\nu} >_{WKBdiv}$ contains all the divergences in $< T_{\mu\nu} >_{unren}$, both $< T_{\mu\nu} >_{numeric}$ and $< T_{\mu\nu} >_{analytic}$ are finite. They are so named because $< T_{\mu\nu} >_{numeric}$ must usually be computed numerically, while $< T_{\mu\nu} >_{analytic}$ may be computed analytically. The resulting expressions of $< T_{\mu\nu} >_{numeric}$ and $< T_{\mu\nu} >_{analytic}$ include equations for four components of the stress-energy tensor. The expressions of the components of $< T_{\mu\nu} >_{analytic}$ involve the variables $f(r), h(r)$ [metric functions in Eq. (1.1)] and their derivatives, as well as m, mass of the field quantum, and κ, a parameter that includes the temperature T. The zero-temperature case is obtained by setting $\kappa = 0$ in

these equations. The expressions of the components of $< T_{\mu\nu} >_{numeric}$ also involve $f(r), h(r)$ and their derivatives, the field quantum m, as well as $A_1(r)$ through $A_5(r)$ which are functionals of the radial modes $F_{\omega,l}(r)$ and $G_{\omega,l}(r)$. These expressions are listed in Appendix A.

Chapter 3. Calculation of Stress-Energy Tensor of A Quantized Massive Spin 1/2 Field in A Static Spherically Symmetric Spacetime

As introduced in Chapter 2, Groves [40] has developed a method to compute the stress-energy tensor of a quantized massive spin 1/2 field in a static spherically symmetric spacetime. The general formulae of the renormalized stress-energy tensor components, which are derived by Groves in [40], are listed in Appendix A. To compute $< T_{\mu\nu} >_{analytic}$ [Eq. (A1)], add up Eqs. (A2) through (A6) for different components, using Eq. (A5) for the zero-temperature state and Eq. (A6) for thermal states.

To compute $< T_{\mu\nu} >_{numeric}$, the radial mode equations Eqs. (2.23) – (2.26) need to be solved so as to get an expression for the radial functions A_1 through A_5 [Eqs. (A11) – (A15)]. However, Eqs. (2.23) – (2.26) cannot be solved exactly and difficult to solve numerically. But they can be solved by WKB approximation.

3.1 WKB approximation to solve radial mode equations

To solve the radial mode equations (2.23) – (2.26), using the ansatz

$$G^q_{\omega,j}(r) = \frac{1}{\sqrt{2W}} \exp[-\int W(r)(\frac{h}{f})^{1/2}(1 - \frac{imf^{1/2}}{\omega})dr] \tag{3.1}$$

$$G^p_{\omega,j}(r) = \frac{1}{\sqrt{2W}} \exp[\int W(r)(\frac{h}{f})^{1/2}(1 - \frac{imf^{1/2}}{\omega})dr] \tag{3.2}$$

and substituting into Eqs. (2.23) and (2.25) gives

$$F^q_{\omega,j} = \frac{G^q_{\omega,j}}{\omega - imf^{1/2}}[-W + \frac{imf^{1/2}W}{\omega} - \frac{f^{1/2}W'}{2h^{1/2}W} + (j + \frac{1}{2})\frac{f^{1/2}}{r}] \tag{3.3}$$

$$F^p_{\omega,j} = \frac{G^p_{\omega,j}}{\omega - imf^{1/2}}[W - \frac{imf^{1/2}W}{\omega} - \frac{f^{1/2}W'}{2h^{1/2}W} + (j + \frac{1}{2})\frac{f^{1/2}}{r}] \tag{3.4}$$

Eqs. (2.23) – (2.26) may be combined to form the uncoupled second-order equations

$$\begin{aligned} 0 \;=\; & \frac{f^{1/2}}{h^{1/2}}\partial_r(\frac{f^{1/2}}{h^{1/2}}\partial_r F_{\omega,j}) - \frac{f}{h^{1/2}}F_{\omega,j}\partial_r(\frac{j+1/2}{r}) - f(\frac{j+1/2}{r})^2 F_{\omega,j} \\ & -(\omega^2 + m^2 f)F_{\omega,j} - \frac{f'}{2h^{1/2}}(\frac{j+1/2}{r})F_{\omega,j} \\ & -\frac{imf'}{2h^{1/2}}\frac{(\omega f^{1/2} - imf)}{\omega^2 + m^2 f}(\frac{1}{h^{1/2}}\partial_r - \frac{j+1/2}{r})F_{\omega,j} \end{aligned} \tag{3.5}$$

$$0 \;=\; \frac{f^{1/2}}{h^{1/2}}\partial_r(\frac{f^{1/2}}{h^{1/2}}\partial_r G_{\omega,j}) + \frac{f}{h^{1/2}}G_{\omega,j}\partial_r(\frac{j+1/2}{r}) - f(\frac{j+1/2}{r})^2 G_{\omega,j}$$

$$-(\omega^2+m^2f)G_{\omega,j}+\frac{f'}{2h^{1/2}}(\frac{j+1/2}{r})G_{\omega,j}$$
$$+\frac{imf'}{2h^{1/2}}\frac{(\omega f^{1/2}+imf)}{\omega^2+m^2f}(\frac{1}{h^{1/2}}\partial_r+\frac{j+1/2}{r})G_{\omega,j} \tag{3.6}$$

Substituting Eqs. (3.1) and (3.3) into Eq. (3.5) gives

$$\begin{aligned} W^2 &= \frac{\omega^2}{(\omega-imf^{1/2})^2}[\Omega^2+\Gamma[W] \\ &\quad -\frac{1}{\omega-imf^{1/2}}(-\frac{imf'W'f^{1/2}}{4hW}+\frac{imf'(j+1/2)}{2h^{1/2}r})] \end{aligned} \tag{3.7}$$

with

$$\Omega^2\equiv\omega^2+m^2f-\frac{(j+1/2)f'}{2h^{1/2}r}+\frac{(j+1/2)f}{h^{1/2}r}+\frac{(j+1/2)^{1/2}f}{r^2} \tag{3.8}$$

and

$$\Gamma[W]\equiv\frac{fW''}{2hW}-\frac{3fW'^2}{4hW^2}-\frac{fh'W'}{4h^2W}+\frac{f'W'}{4hW} \tag{3.9}$$

Eq. (3.7) may be solved iteratively. To zeroth order,

$$W=\frac{\omega\Omega}{\omega-imf^{1/2}} \tag{3.10}$$

Each iteration yields terms containing two more derivatives than the previous iteration. Therefore the first iteration of Eq. (3.7) yields the second-order W:

$$W = \frac{\omega\Omega}{\omega-imf^{1/2}}+\frac{\omega}{2(\omega-imf^{1/2})\Omega}[\Gamma[W]$$

$$-\frac{1}{\omega - imf^{1/2}}(-\frac{imf'\Omega' f^{1/2}}{4h\Omega} + \frac{imf'(j+1/2)f^{1/2}}{2h^{1/2}r})] \quad (3.11)$$

Substituting Eq. (3.11) into Eq. (3.7), we get the fourth-order W. Then, substituting the fourth-order W into Eqs. (3.1) – (3.4), we get the fourth-order WKB approximation of the mode functions $F_{\omega,j}(r)$ and $G_{\omega,j}(r)$.

In general, Eqs. (3.5) and (3.6) have two sets of linearly independent solutions. One set, labeled $(F^q_{\omega,j}, G^q_{\omega,j})$, is finite at large r but diverges at $r = 0$ or the throat of the wormhole. The other set, labeld $(F^p_{\omega,j}, G^p_{\omega,j})$, is finite at $r = 0$ or the throat of the wormhole but diverges at large r [40]. In solving these equations by the WKB approximation method, no boundary conditions are imposed.

The WKB approximation is a good approximation if the successive derivatives of the metric functions $f(r)$ and $h(r)$ become smaller. The approximation is also good for ω and j large enough [40]. However, the uncertainties caused by the WKB approximation are unassessed; and to what extent it is justifiable to use the WKB approximation for finding the stress-energy remains an open question.

3.2 WKB approximation of radial functions

The expressions of the radial functions $A_1(r)$ through $A_5(r)$ are given by Eqs. (A11) – (A15) in Appendix A. Since they contain the radial modes $F_{\omega,j}(r)$ and $G_{\omega,j}(r)$, they also cannot be computed exactly, but can be computed by WKB approximation.

From Eqs. (3.1) – (3.4) we can get

$$G^q_{\omega,l-\frac{1}{2}}(r)G^p_{\omega,l-\frac{1}{2}}(r) = \frac{1}{2W} \tag{3.12}$$

$$\begin{aligned} F^q_{\omega,l+\frac{1}{2}}(r)F^p_{\omega,l+\frac{1}{2}}(r) &= \frac{1}{2W(\omega - imf^{1/2})^2}[\frac{fW'^2}{4hW^2} - \frac{(l+1)fW'}{h^{1/2}rW} - W^2 \\ &\quad \frac{(l+1)^2 f}{r^2} + \frac{2imf^{1/2}W^2}{\omega} + \frac{m^2 fW^2}{\omega^2}] \end{aligned} \tag{3.13}$$

Substituting Eqs. (3.12) and (3.13) into Eq. (A11), we get

$$\begin{aligned} A_1 &= Re\sum_{l=0}^{\infty}(\frac{l+1}{2(\omega - imf^{1/2})^2}[\frac{fW'^2}{4hW^3} - \frac{(l+1)fW'}{h^{1/2}rW^2} + \frac{(l+1)^2 f}{r^2 W} \\ &\quad +(\frac{2imf^{1/2}}{\omega} + \frac{m^2 f}{\omega^2} - 1)W] - \frac{l}{2W} + \frac{r}{f^{1/2}}) \end{aligned} \tag{3.14}$$

The fourth-order WKB approximation of A_1 is obtained by first substituting the fourth-order W into Eq. (3.14); then expanding in inverse powers of ω and keeping only terms of order ω^{-1} or higher, because terms of order ω^{-3} and lower do not contribute to the divergence; finally, summing over l by using the Plana sum formula, which says that for a function $g(k)$

$$\begin{aligned} \sum_{j=k}^{\infty} g(j) &= \frac{1}{2}g(k) + \int_k^{\infty} g\tau d\tau \\ &\quad +i\int_0^{\infty} \frac{dt}{e^{2\pi t} - 1}[g(k+it) - g(k-it)] \end{aligned} \tag{3.15}$$

The resulting expression of the fourth-order WKB approximation of A_1

is a function of ω as well as $f(r), h(r)$ and their derivatives. The fourth-order WKB approximations of A_2 through A_5 are also obtained in a similar fashion.

3.3 Calculation of $< T_{\mu\nu} >_{numeric}$

The expressions of the components of $< T_{\mu\nu} >_{numeric}$ are given by Eqs. (A8) – (A10) in Appendix A. To compute these components, it requires numerical solutions of the mode equations [Eqs. (2.23) – (2.26)] for a very large number of modes, which is an arduous task.

An approximation method to compute $< T_{\mu\nu} >_{numeric}$ is introduced in [48]. In this method, $< T_{\mu\nu} >_{unren}$ is approximated by the sixth-order WKB approximation. Therefore, Eq. (2.48) becomes

$$< T_{\mu\nu} >_{numeric} = \lim_{x' \to x} (< T_{\mu\nu} >_{6th-orderWKB} - < T_{\mu\nu} >_{WKBdiv}) \qquad (3.16)$$

where $< T_{\mu\nu} >_{WKBdiv}$ is the fourth-order WKB approximation mentioned in Chapter 2. Both $< T_{\mu\nu} >_{WKBdiv}$ and $< T_{\mu\nu} >_{6th-orderWKB}$ contain the divergent part of $< T_{\mu\nu} >_{unren}$, so their difference is finite.

$< T_{\mu\nu} >_{WKBdiv}$ is obtained by substituting the fourth-order WKB approximations of A_1 through A_5, which are introduced above, into Eqs. (2.39) – (2.41) and integrating over ω. Likewise, $< T_{\mu\nu} >_{6th-orderWKB}$ is obtained by first solving Eq. (3.7) iteratively to the sixth order; the solution, the sixth-order W, is substituted into Eq. (3.14) and the like to get the sixth-order WKB approximations of A_1 through A_5. Then these A_1 through A_5

are expanded in inverse powers of ω to the ω^{-5} order. Next, the Plana sum formula [Eq. (3.15)] is used to sum over l. The resulting expressions of A_1 through A_5 are substituted into the expressions of $< T_{\mu\nu} >_{unren}$ [Eqs. (2.39) – (2.41)]. After integration over ω, we get $< T_{\mu\nu} >_{6th-orderWKB}$. Substituting $< T_{\mu\nu} >_{6th-orderWKB}$ and $< T_{\mu\nu} >_{WKBdiv}$ into Eq. (3.16), we obtain $< T_{\mu\nu} >_{numeric}$.

In my calculation, however, I compute the difference of $< T_{\mu\nu} >_{6th-orderWKB}$ and $< T_{\mu\nu} >_{WKBdiv}$ directly rather than first compute these two quantities separatly and then take their difference. This is achieved by first taking the differences of the sixth-order WKB approximations of A_1 through A_5 and the fourth-order WKB approximations of A_1 through A_5, then substituting these differences into Eqs. (2.39) – (2.41), and finally integrating over ω. The results are the components of $< T_{\mu\nu} >_{numeric}$. This way of calculation avoids much repetitive work in computing $< T_{\mu\nu} >_{6th-orderWKB}$ and $< T_{\mu\nu} >_{WKBdiv}$ separately.

3.4 Renormalized stress-energy tensor

After $< T_{\mu\nu} >_{analytic}$ and $< T_{\mu\nu} >_{numeric}$ are computed, one gets $< T_{\mu\nu} >_{ren}$ simply by adding them up [Eq. (2.37)]. The resulting expressions of the renormalized stress-energy tensor components of a quantized massive spin 1/2 field in a static spherically symmetric spacetime are listed in Appendix B.

3.5 Approximations used in computation

The fourth-order W is a basic element contained in many quantities including the radial modes $F_{\omega,j}(r)$ and $G_{\omega,j}(r)$, and the radial functions $A_1(r)$ through $A_5(r)$, which are in turn contained in the expressions of $< T_{\mu\nu} >_{unren}, < T_{\mu\nu} >_{WKBdiv}$ and $< T_{\mu\nu} >_{numeric}$. However, the expression of the fourth-order W is so complicated that it is intractable manually. Other quantities that contain the fourth-order W are even more intractable. All these quantities are calculated by using the computer program Mathematica with approximations. To manipulate these quantities, Taylor expansion is widely used and only significant parts are kept.

3.5.1 Approximation in computing the fourth-order W

To compute the fourth-order W, various terms in Eq. (3.11) are multiplied by a dimensionless parameter e to different powers so as to track the order of the WKB expansion. The zeroth-order $\Gamma[W]$ [Eq. (3.9)], which contains zeroth-order W and its derivatives, is multiplied by e^2. The first derivative of the zeroth-order $\Gamma[W]$, which is $\Gamma_0[W]'$, is multiplied by another e; and the second derivative of the zeroth-order $\Gamma[W]$, which is $\Gamma_0[W]''$, is multiplied by an additional e to the derivative of $\Gamma[W]'$. The second-order $\Gamma[W]$, which is $\Gamma_2[W]$, is multiplied by e^2. Besides, the first derivative of $f(r)$ and $h(r)$, which are $f'(r)$ and $h'(r)$ respectively, are each multiplied by an e. The second derivative of $f(r)$ and $h(r)$, which are $f''(r)$ and $h''(r)$ respectively, are each multiplied by an additional e to the derivative of $f'(r)$ and $h'(r)$.

With various terms multiplied by different powers of e, the right-hand side of Eq. (3.11) is expanded to the fourth-power e, and terms with higher powers of e are truncated. By setting $e = 1$ in the remaining expression, the fourth-order W is obtained.

3.5.2 Approximation in computing the radial functions

As introduced in section 3.2, the radial functions $A_1(r)$ through $A_5(r)$ [Eqs. (A11) – (A15)] are also computed by WKB approximation. For example, $A_1(r)$ is calculated by substituting the fourth-order W into Eq. (3.14). The expression is expanded in inverse power of ω to the ω^{-1} order; terms with order ω^{-3} or lower are truncated. This expansion is valid because we are only looking for the divergent part of $< T_{\mu\nu} >_{unren}$, and those truncated terms do not contribute to divergence.

3.5.3 Approximation in computing $< T_{\mu\nu} >_{numeric}$

$< T_{\mu\nu} >_{numeric}$ is computed by approximating $< T_{\mu\nu} >_{unren}$ by the sixth-order WKB approximation. This is explained in section 3.3.

3.5.4 Approximation in numerical results

Given the uncertainties in the approximations used in the computation and the poorly known value of the neutrino mass, one significant figure is used in numerical results of the stress-energy tensor components. However, while discussing numerical results in graphs, two significant figures are used

in order to tell possible difference between different graphs.

3.6 Verification of previous work

The calculation in this thesis is based on the method developed by P. Groves [40], who used the renormalization counter-terms calculated by Christensen [45]. I have checked and verified most equations in [40]. A few equations are not checked due to technical difficulties. As for the renormalization counter-terms in [45], I have checked and verified only one term, which is the simplest one. The rest terms are too complicated to compute due to the complicated form of tensor indices. These tensor indices are so complicated that current computer programs, including Mathematica and Maple, are helpelessly to manipulate. To carry on the calculation of the renormalization counter-terms, Christensen particularly developed the computer software MathTensor to manipulate the tensor indices. This software is commercially available at present.

Chapter 4. Stress-Energy Tensor of Two Quantized Massive Spin 1/2 Fields in Four Static Spherically Symmetric Wormhole Spacetimes at Zero Temperature

4.1 Conditions of calculating stress-energy tensor for two fields in four wormhole spacetimes

In this thesis, the method in [40] is applied to computing the renormalized stress-energy tensor of two quantized massive spin 1/2 fields in four static spherically symmetric wormhole spacetimes. One field is the quantized neutrino field, and the other is the quantized proton field. Although it is not very clear whether the neutrino is a Dirac particle, I model it so in this thesis. The neutrino mass is not very well known. However, a set of experiments [49, 50] have pinned down the mass of the neutrino in the range of $0.05eV/c^2 < m_\nu < 0.28eV/c^2$. Within this range, a good estimation of the

mass of the electronic neutrino is $m_\nu = 0.24eV/c^2$ [51]. I take this value for the neutrino mass. As for the proton field, the mass of the field quantum is $m_p = 938MeV/c^2$.

In my calculation, I use the sign conventions of Misner, Thorne and Wheeler [52], and adopt Planck units. In this unit system, the mass of the neutrino and the mass of proton are:

$$m_\nu = 1.96 \times 10^{-29} m_{Planck}, \tag{4.1}$$

$$m_p = 7.67 \times 10^{-20} m_{Planck}, \tag{4.2}$$

where $m_{Planck} = 2.17651 \times 10^{-8} kg$. A unit length is the Planck length, $l_p = 1.616199 \times 10^{-35} m$. c (the speed of light), G (the Newtonian gravitational constant) and $\hbar$ (the reduced Planck constant) are set to be 1.

To be exotic matter, the stress-energy of the field must violate the weak energy condition. To examine this, I plot τ_0 and $\zeta_0 = (\tau_0 - \rho_0)$ as functions of r_0 (the radius of the wormhole's throat) to see for what values of r_0 that Eqs. (1.14) and (1.15) are satisfied.

Moreover, I examine violation of the weak energy condition outside of the wormhole's throat. This requires the following two equations

$$\tau = - < T^r_r > = \frac{b/r - 2(r-b)\Phi'}{8\pi r^2} > 0, \tag{4.3}$$

$$\tau - \rho = < T^t_t > - < T^r_r > = \frac{b/r - 2(r-b)\Phi' - b'}{8\pi r^2} > 0, \tag{4.4}$$

be satisfied for $r > r_0$ to some extent. I plot τ and $\zeta = (\tau - \rho)$ as functions of r to see the values of r for which Eqs. (4.3) and (4.4) are satisfied.

. The renormalized stress-energy tensor components of a quantized massive spin 1/2 field in a general static spherically symmetric spacetime are computed and the resulting expressions are listed in Appendix B. For a specific wormhole spacetime, I substitute $f(r)$ and $h(r)$ in these equations [(B1), (B2) and (B3)] by their specific functions in the metric equation for this wormhole spacetime, and m by the neutrino mass [Eq. (4.1)] or proton mass [Eq. (4.2)]. I set $\kappa = 0$ for the zero-temperature case. Finally, I expand these components of $< T^{\nu}_{\mu} >_{ren}$ in powers of r_0 (for values at the throat of the wormhole) or in powers of r (for values beyond the throat of the wormhole). These stress-energy components are expressed in the units of F_p/l_p^2, where $F_p = 1.21027 \times 10^{44} N$ is the Planck force; $l_p^2 = 2.61223 \times 10^{-70} m^2$ is the Planck area.

In the following section, I will present and discuss the results of my calculation. It should be noted that, as a result of using the parameter values explained above, the stress-energy tensor components of these two fields turn out to have unphysically large values in many cases. These large values make the physical model not credible. However, in the interest of exploring the mathematical structure of the physical model, I will check when the energy conditions hold. Besides, some assertions are made for $r < r_0$. They are based on the formulae derived for $r > r_0$ that may not be valid for $r < r_0$.

4.2 Stress-energy tensor of two quantized massive spin 1/2 fields in four wormhole spacetimes

4.2.1 Zero-tidal-force wormhole

The first class of wormhole examined is a particularly simple set of wormholes whose metric functions satisfy:

$$\phi(r) = 0, \tag{4.5}$$

$$b(r) = r_0 = constant. \tag{4.6}$$

Accordingly,

$$f(r) = 1, \tag{4.7}$$

$$h(r) = (1 - \frac{r_0}{r})^{-1}. \tag{4.8}$$

This type of wormhole is called a "zero-tidal-force wormhole" because an observer at the throat of the wormhole experiences zero tidal force.

A. The neutrino field

The stress-energy tensor components of a quantized neutrino field at the throat of this type of wormhole are computed to be:

$$< T_t^t >_0 \quad = \quad \frac{1.6 \times 10^{54}}{r_0^8} - \frac{5.9 \times 10^{54}}{r_0^6} - \frac{0.01}{r_0^4} - \frac{2.0 \times 10^{-60}}{r_0^2}, \tag{4.9}$$

$$< T_r^r >_0 = -\frac{1.6 \times 10^{54}}{r_0^8} - \frac{4.0 \times 10^{54}}{r_0^6} - \frac{0.01}{r_0^4} + \frac{0.0008}{r_0^3} - \frac{0.00003}{r_0^2} - \frac{3.2 \times 0^{-7}}{r_0}, \quad (4.10)$$

$$< T_\theta^\theta >_0 = 1.6 \times 10^{-117} + \frac{5.0 \times 10^{54}}{r_0^6} - \frac{0.007}{r_0^4} - \frac{2.1 \times 10^{-60}}{r_0^2}. \quad (4.11)$$

In these expressions, higher inverse orders of r_0 have much bigger coefficients than those of lower inverse orders of r_0. For example, in Eq. (4.9), the $1/r_0^8$ term has a coefficient to the order of 10^{54}, while the coefficient of the $1/r_0^2$ term is to the order of 10^{-60}. This implies that large values of r_0 are suppressed, while small values of r_0 are preferred. In other words, small values of r_0 contribute more to the stress-energy tensor.

Figure 4.1 is plotted for ζ_0 and τ_0 as functions of r_0. From this figure we see that $\zeta_0 > 0$ for $r_0 < 1.26 l_p$, while $\tau_0 > 0$ for all values of r_0 in the plotted range. So, both ζ_0 and τ_0 are positive for $r_0 < 1.26 l_p$. This means that the neutrino field is exotic for this type of wormhole up to the throat radius $r_0 < 1.26 l_p$.

I have solved the equation $\zeta_0 = 0$ to get its roots. I find that $r_0 = 1.26 l_p$ is the only root in the range of $r_0 > 0$. Other roots are either negative or imaginary. This means that in Figure 4.1, as r_0 increases beyond $1.26 l_p, \zeta_0$ will never become positive, thus assuring that the neutrino field is not exotic for wormholes with larger values of r_0.

The stress-energy tensor components of the quantized neutrino field in

the entire spacetime for this type of wormhole geometry are too complicated to list here. I list them in Appendix C. However, I plot the radial tension τ and $\zeta = (\tau - \rho)$ as functions of r in Figure 4.2 and Figure 4.3. Figure 4.2 is plotted for a zero-tidal-force wormhole with maximum possible throat radius, $r_0 = 1.26 l_p$, for which the quantized neutrino field is exotic. From this figure we see that $\zeta > 0$ for r up to $r_0 = 1.26 l_p$ and $\tau > 0$ for $r < 1.29 l_p$. This means that the weak energy condition is violated up to the boundary of the wormhole's throat for which the neutrino field is exotic.

Figure 4.3 is plotted for a zero-tidal-force wormhole with a smaller throat radius, $r_0 = 0.50 l_p$, for which the quantized neutrino field is exotic. In this figure we see that $\zeta > 0$ for $r < 0.521 l_p$, while $\tau > 0$ for $r < 0.524 l_p$. This indicates that the weak energy condition violation extends a little beyond the throat of the wormhole. However, for this type of wormhole, the maximum radial distance to which the weak energy condition is violated occurs with a wormhole that has the maximum throat radius for which the quantized neutrino field is exotic.

B. The proton field

The stress-energy tensor components of a quantized proton field at the throat of the wormhole are computed to be:

$$< T_t^t >_0 \;\; = \;\; \frac{1.0 \times 10^{35}}{r_0^8} - \frac{3.9 \times 10^{35}}{r_0^6} - \frac{0.01}{r_0^4} - \frac{3.0 \times 10^{-41}}{r_0^2}, \quad (4.12)$$

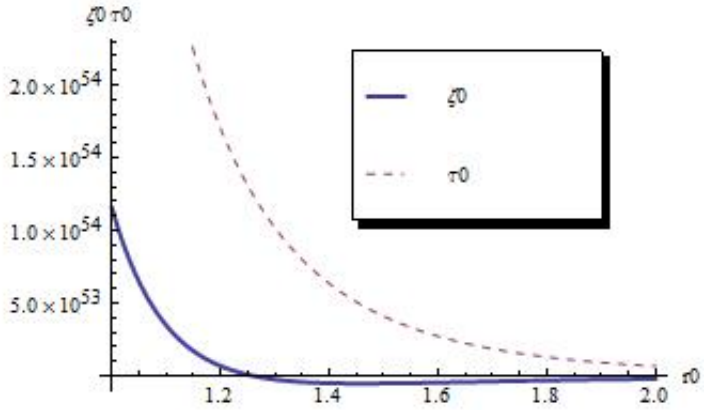

Figure 4. 1: ζ_0 and τ_0 of a quantized neutrino field as functions of r_0 for zero-tidal-force wormholes. $\zeta_0 > 0$ for $r_0 < 1.26 l_p$; and $\tau_0 > 0$ for all values of r_0.

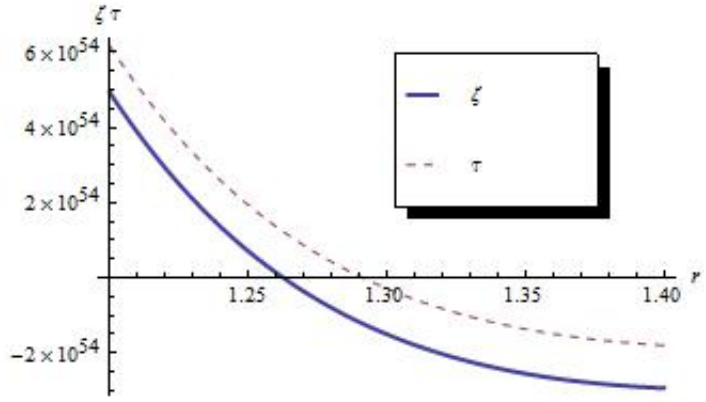

Figure 4. 2: ζ and τ of a quantized neutrino field as functions of r for a zero-tidal-force wormhole with throat radius $r_0 = 1.26 l_p$. $\zeta > 0$ for $r < 1.26 l_p$, while $\tau > 0$ for $r < 1.29 l_p$.

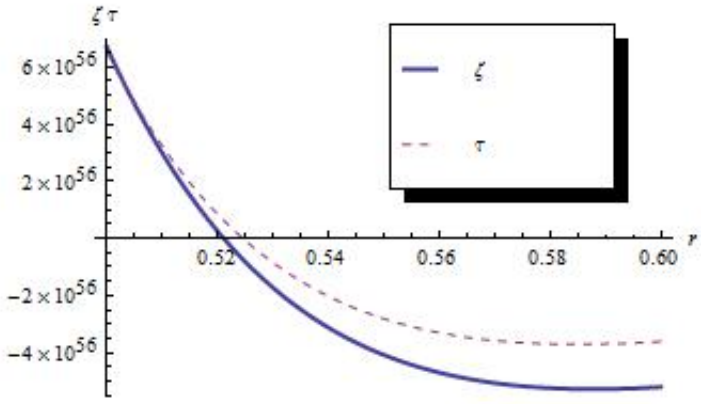

Figure 4. 3: ζ and τ of a quantized neutrino field as functions of r for a zero-tidal-force wormhole with throat radius $r_0 = 0.50l_p$. $\zeta > 0$ for $r < 0.521l_p$, while $\tau > 0$ for $r < 0.524l_p$.

$$< T_r^r >_0 = -\frac{1.0 \times 10^{35}}{r_0^8} - \frac{2.6 \times 10^{35}}{r_0^6} - \frac{0.01}{r_0^4} + \frac{0.0008}{r_0^3} + \frac{2.8 \times 10^{-17}}{r_0^2} + \frac{8.7 \times 10^{-19}}{r_0}, \tag{4.13}$$

$$< T_\theta^\theta >_0 = 3.7 \times 10^{-79} + \frac{3.3 \times 10^{35}}{r_0^6} - \frac{0.007}{r_0^4} - \frac{3.3 \times 10^{-41}}{r_0^2}. \tag{4.14}$$

Similar to the case of the neutrino field, these expressions exhibit a hierarchy of coefficients such that the higher inverse orders of r_0 have much bigger coefficients than those of lower orders of r_0. This also implies that smaller values of r_0 contribute more than larger values of r_0 to the stress-energy tensor.

Figure 4.4 is plotted for ζ_0 and τ_0 as functions of r_0 for zero-tidal-force wormholes. $\zeta_0 > 0$ for $r_0 < 1.26l_p$; and $\tau_0 > 0$ for all values of r_0. So, both ζ_0 and τ_0 are positive for $r_0 < 1.26l_p$. This implies that the quantized proton field is also exotic for this type of wormhole up to the throat radius $r_0 < 1.26l_p$. As in the case of the neutrino field, I solve the equation $\zeta_0 = 0$ and find $r_0 = 1.26l_p$ is the only root for $r_0 > 0$. So, ζ_0 will never become positive as r_0 increases beyond this value. This result is the same as in the case of the neutrino field.

The stress-energy tensor components of the quantized proton field in the entire spacetime for this type of wormhole geometry are also listed in Appendix C. However, I plot τ and ζ as functions of r in Figure 4.5 and Figure 4.6. Figure 4.5 is plotted for a wormhole with the maximum possible throat radius, $r_0 = 1.26l_p$, for which the quantized proton field is exotic. In the graph, we see that $\zeta > 0$ for $r < 1.26l_p$, while $\tau > 0$ for $r < 1.29l_p$. This suggests that the weak energy condition violation is limited to the boundary of the wormhole's throat.

Figure 4.6 is plotted for a wormhole with a smaller throat radius, $r_0 = 0.50l_p$, for which the proton field is exotic. $\zeta > 0$ for $r < 0.521l_p$; while $\tau > 0$ for $r < 0.524l_p$. This indicates that the weak energy condition violation extends a little beyond the throat of the wormhole. As in the case of the neutrino field, the maximum radial distance to which the weak energy condition is violated occurs with a wormhole that has the maximum throat radius for which the proton field is exotic, with the same numerical value.

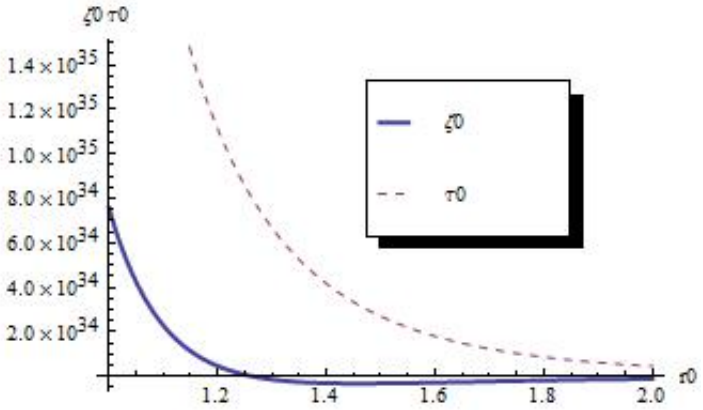

Figure 4. 4: ζ_0 and τ_0 of a quantized proton field as functions of r_0 for zero-tidal-force wormholes. $\zeta_0 > 0$ for $r_0 < 1.26 l_p$; and $\tau_0 > 0$ for all values of r_0.

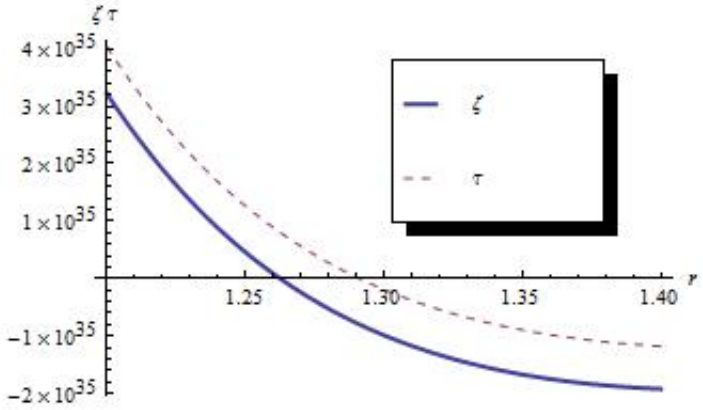

Figure 4. 5: ζ and τ of a quantized proton field as functions of r for a zero-tidal-force wormhole with a throat radius $r_0 = 1.26 l_p$. $\zeta > 0$ for $r < 1.26 l_p$; $\tau > 0$ for $r < 1.29 l_p$.

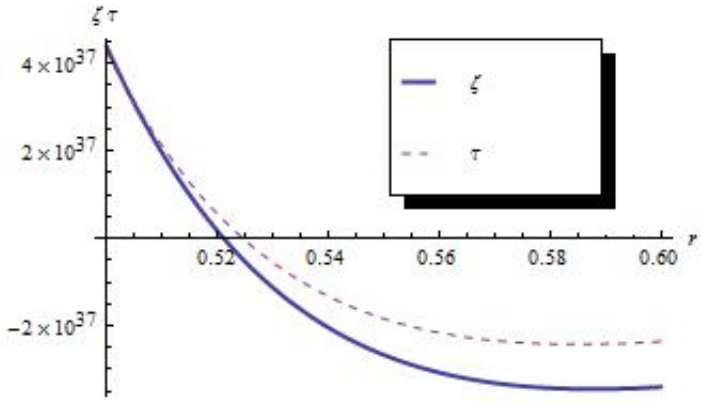

Figure 4. 6: ζ and τ of a quantized proton field as functions of r for a zero-tidal-force wormhole with a throat radius $r_0 = 0.50 l_p$. $\zeta > 0$ for $r < 0.521 l_p$; $\tau > 0$ for $r < 0.524 l_p$.

4.2.2 The simple wormhole

This type of wormhole has the metric functions:

$$\Phi(r) = 0, \tag{4.15}$$

$$b(r) = \frac{r_0^2}{r}. \tag{4.16}$$

Accordingly,

$$f(r) = 1, \tag{4.17}$$

$$h(r) = (1 - \frac{r_0^2}{r^2})^{-1}. \tag{4.18}$$

This wormhole is discussed by Morris and Thorne [5] as an example of traversable wormhole.

A. The neutrino field

I find the stress-energy tensor components of a quantized neutrino field at the throat of this type of wormhole are:

$$< T_t^t >_0 \;=\; \frac{1.6\times 10^{54}}{r_0^8} - \frac{6.1\times 10^{54}}{r_0^6} - \frac{0.02}{r_0^4} - \frac{1.8\times 10^{-60}}{r_0^2}, \quad (4.19)$$

$$< T_r^r >_0 \;=\; -\frac{1.6\times 10^{54}}{r_0^8} - \frac{6.4\times 10^{55}}{r_0^6} - \frac{0.05}{r_0^4} + \frac{0.002}{r_0^3} - \frac{2.1\times 10^{-17}}{r_0^2} + \frac{2.6\times 10^{-18}}{r_0}, \quad (4.20)$$

$$< T_\theta^\theta >_0 \;=\; 1.6\times 10^{-117} + \frac{3.5\times 10^{55}}{r_0^6} - \frac{0.02}{r_0^4} - \frac{3.1\times 10^{-60}}{r_0^2}. \quad (4.21)$$

These expressions exhibit a similar hierarchy of coefficients as those of the zero-tidal-force wormholes. The explanation is similar: smaller values of r_0 contribute more to the stress-energy tensor than larger values of r_0. In other words, the stress-energy tensor is stronger for smaller values of r_0.

Figure 4.7 is plotted for ζ_0 and τ_0 as functions of r_0. From this figure we see that $\zeta_0 > 0$ for $r_0 < 3.32\times 10^{19} l_p$, and $\tau > 0$ for $r_0 < 3.42\times 10^{19} l_p$. So, both ζ_0 and τ_0 are positive in the range $r_0 < 3.32\times 10^{19} l_p$. This implies that a quantized neutrino field is exotic for simple wormholes with a throat radius

$r_0 < 3.32 \times 10^{19} l_p$.

The stress-energy tensor components of the quantized neutrino field for the simple wormhole in the entire spacetime are listed in Appendix C. Figure 4.8 through Figure 4.10 are plotted for ζ and τ as functions of r for a simple wormhole with maximum possible throat radius, $r_0 = 3.32 \times 10^{19} l_p$, for which the quantized neutrino field is exotic. I solve $\zeta = 0$ and get only one positive root, $r = r_0 = 3.32 \times 10^{19} l_p$; for $r > r_0$, there is no root. Solving $\tau = 0$, I get two positive roots: $r = 3.32 \times 10^{19} l_p$ and $r = 3.29 \times 10^{34} l_p$. Figure 4.8 shows that both ζ and τ are positive beyond the wormhole's throat, i.e., for $r > r_0 = 3.32 \times 10^{19} l_p$. However, Figure 4.9 and Figure 4.10 show that τ becomes negative for $r > 3.29 \times 10^{34} l_p$. Since there is no other root of r beyond this value, we know that τ will never become positive for larger values of r. Therefore, the weak energy condition violation extends to the radial distance $r = 3.29 \times 10^{34} l_p$.

Figure 4.11 and Figure 4.12 are plotted for ζ and τ as functions of r for a simple wormhole with a smaller throat radius $r_0 = 10^{10} l_p$ for which the quantized neutrino field is exotic. I solve $\zeta = 0$ and get four positive roots: $r = 1.02 \times 10^{10} l_p, 1.49 \times 10^{10} l_p, 3.86 \times 10^{12} l_p$, and $6.84 \times 10^{30} l_p$; I solve $\tau = 0$ and get three positive roots: $r = 1.03 \times 10^{10} l_p, 1.42 \times 10^{10} l_p$, and $2.07 \times 10^{30} l_p$. These roots tell us that ζ and τ are positive in the two regions: $10^{10} l_p < r < 1.02 \times 10^{10} l_p$ and $1.49 \times 10^{10} l_p < r < 3.86 \times 10^{12} l_p$, as shown in Figures 4.11 and 4.12. Therefore, the weak energy condition is violated in these regions.

The above two cases tell us that, for simple wormholes of different size, the weak energy condition is violated in different regions of the entire spacetime. However, the violation extends to the maximum radial distance, $r = 3.29 \times 10^{34} l_p$, for a simple wormhole that has the maximum throat radius $r_0 = 3.32 \times 10^{19} l_p$ for which the quantized neutrino field is exotic.

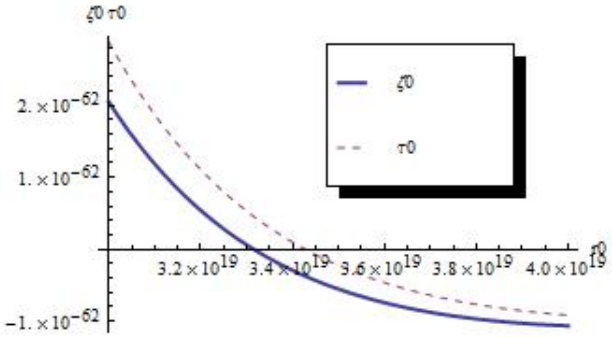

Figure 4. 7: ζ_0 and τ_0 of a quantized neutrino field as functions of r_0 for simple wormholes. $\zeta_0 > 0$ for $r_0 < 3.32 \times 10^{19} l_p$; and $\tau_0 > 0$ for $r_0 < 3.43 \times 10^{19} l_p$.

B. The proton field

The stress-energy tensor components of a quantized proton field at the throat of the simple wormhole are:

$$< T_t^t >_0 \;=\; \frac{1.0 \times 10^{35}}{r_0^8} - \frac{4.0 \times 10^{35}}{r_0^6} - \frac{0.02}{r_0^4} - \frac{2.7 \times 10^{-41}}{r_0^2}, \quad (4.22)$$

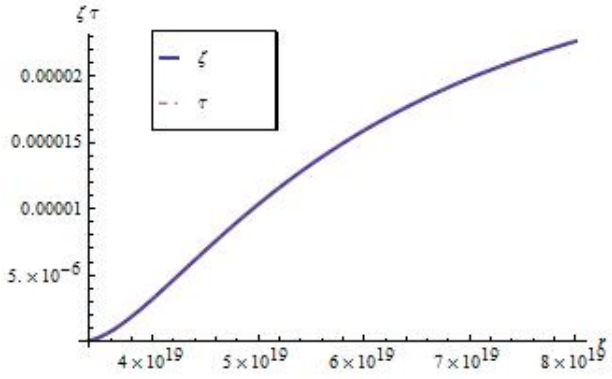

Figure 4. 8: ζ and τ of a quantized neutrino field as functions of r for a simple wormhole whose throat radius is $r_0 = 3.32 \times 10^{19} l_p$. Both ζ and τ are positive for r beyond the throat: $r > r_0 = 3.32 \times 10^{19} l_p$.

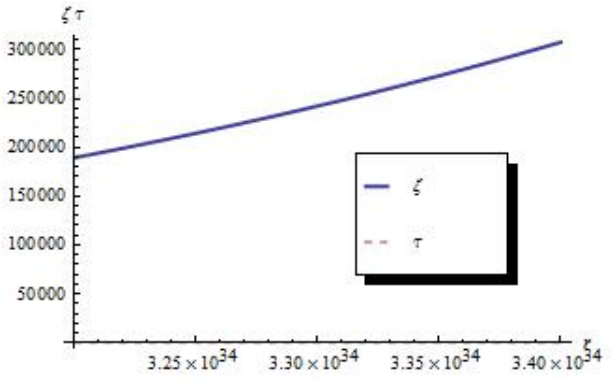

Figure 4. 9: ζ and τ of a quantized neutrino field as functions of r for a simple wormhole whose throat radius is $r_0 = 3.32 \times 10^{19} l_p$. Both ζ and τ are positive for $r < 3.29 \times 10^{34} l_p$. However, τ becomes negative for $r > 3.29 \times 10^{34} l_p$. Note that the graph of τ is indistinguishable from the r_0 axis.

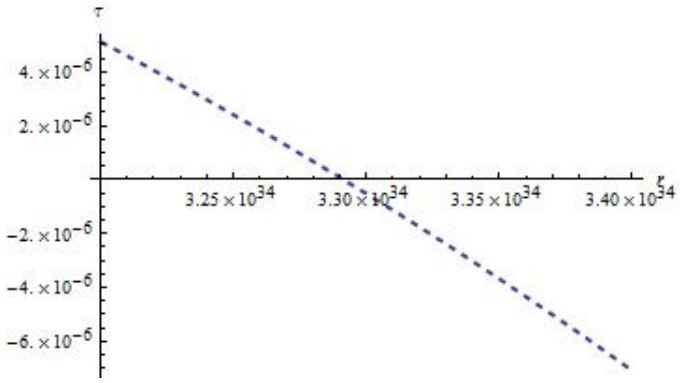

Figure 4. 10: Detail of Figure 4.9. τ becomes negative for $r > 3.29 \times 10^{34} l_p$.

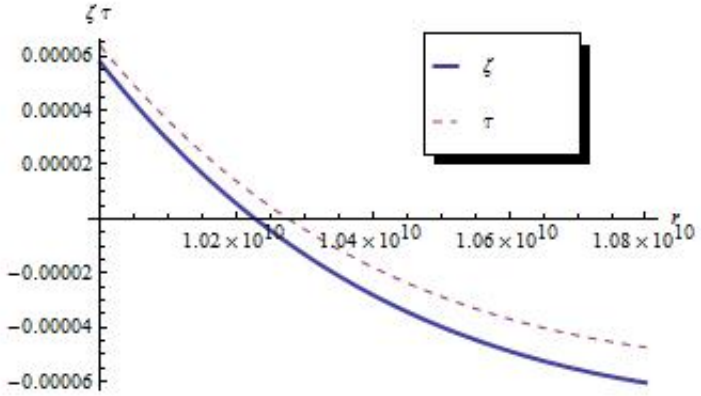

Figure 4. 11: ζ and τ of a quantized neutrino field as functions of r for a simple wormhole whose throat radius is $r_0 = 10^{10} l_p$. $\zeta > 0$ for $10^{10} l_p < r < 1.02 \times 10^{10} l_p$; $\tau > 0$ for $10^{10} l_p < r < 1.03 \times 10^{10} l_p$. Both ζ and τ are positive in the range $10^{10} l_p < r < 1.02 \times 10^{10} l_p$.

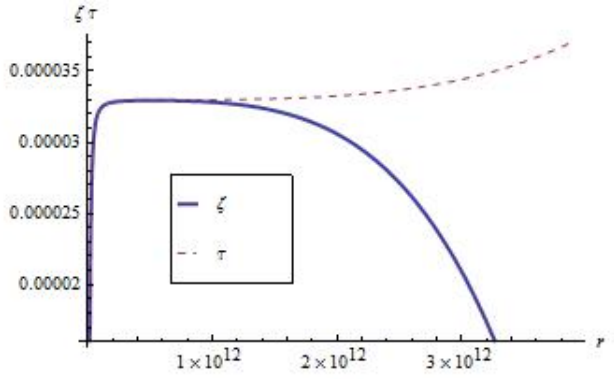

Figure 4. 12: ζ and τ of a quantized neutrino field as functions of r for a simple wormhole whose throat radius is $r_0 = 10^{10} l_p$. Both ζ and τ are positive in the range $1.49 \times 10^{10} l_p < r < 3.86 \times 10^{12} l_p$.

$$< T_r^r >_0 \;=\; -\frac{1.0 \times 10^{35}}{r_0^8} - \frac{4.2 \times 10^{36}}{r_0^6} - \frac{0.05}{r_0^4} + \frac{0.002}{r_0^3} - \frac{2.1 \times 10^{-17}}{r_0^2} + \frac{2.6 \times 10^{-18}}{r_0}, \tag{4.23}$$

$$< T_\theta^\theta >_0 \;=\; 3.7 \times 10^{-79} + \frac{2.3 \times 10^{36}}{r_0^6} - \frac{0.02}{r_0^4} - \frac{4.7 \times 10^{-41}}{r_0^2}. \tag{4.24}$$

The coefficients of these expressions have a similar hierarchy as those in the previous cases. Its implication is the same: the stress-energy tensor is stronger for smaller values of r_0.

Figure 4.13 is plotted for ζ_0 and τ_0 as functions of r_0. $\zeta_0 > 0$ for $r_0 < 1.34 \times 10^{13} l_p$; and $\tau_0 > 0$ for $r_0 < 1.38 \times 10^{13} l_p$. So, both ζ_0 and τ_0 are positive for $r_0 < 1.34 \times 10^{13} l_p$. This means that a quantized proton field is

exotic for this type of wormhole with a throat radius $r_0 < 1.34 \times 10^{13} l_p$. I solve the equation $\zeta_0 = 0$ and find that $r_0 = 1.34 \times 10^{13} l_p$ is the only real root. Similarly, solving $\tau_0 = 0$ I find $r_0 = 1.38 \times 10^{13} l_p$ is the only real root. So we are convinced that both ζ_0 and τ_0 will not become positive as r_0 increases beyond these values, assuring the quantized proton field is not exotic for wormholes with larger values of r_0.

The stress-energy tensor components of the quantized proton field in the entire spacetime for this type of wormhole geometry are listed in Appendix D. However, I plot τ and ζ as functions of r for two simple wormholes of different size. Figure 4.14 through Figure 4.16 are plotted for a simple wormhole with the maximum possible throat radius, $r_0 = 1.34 \times 10^{13} l_p$, for which the quantized proton field is exotic. I solve the equation $\zeta = 0$ and find two positive roots: $r = 1.34 \times 10^{13} l_p$ and $r = 7.65 \times 10^{22} l_p$. Similarly, solving $\tau = 0$ I also find two positive roots: $r = 1.34 \times 10^{13} l_p$ and $r = 7.23 \times 10^{23} l_p$. These roots tell us that both ζ and τ are positive in the range $1.34 \times 10^{13} l_p < r < 7.65 \times 10^{22} l_p$. This means that the weak energy condition is violated up to the radial distance $r = 7.65 \times 10^{22} l_p$.

I further plot τ and ζ as functions of r for a simple wormhole whose throat radius is $r_0 = 10^8 l_p$. I solve $\zeta = 0$ and find the only positive root is $r = 3.20 \times 10^{20} l_p$; solving $\tau = 0$ I find the only positive root is $r = 5.76 \times 10^{21} l_p$. From these roots we know that both ζ and τ are positive for $r < 3.20 \times 10^{20} l_p$, as shown in Figure 4.17 through Figure 4.19. This means that the weak energy condition is violated up to the radial distance $r = 3.20 \times 10^{20} l_p$ for

this wormhole geometry.

Comparing the above two wormholes, we see that the weak energy condition is violated to the maximum radial distance $r = 7.65 \times 10^{22} l_p$ for a wormhole that has the maximum throat radius $r_0 = 1.34 \times 10^{13} l_p$ for which the quantized proton field is exotic.

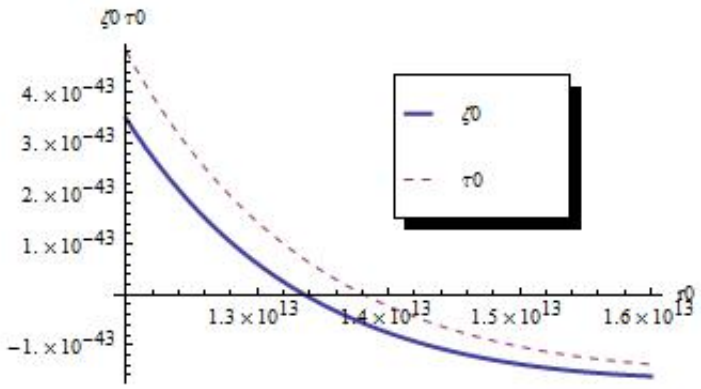

Figure 4. 13: ζ_0 and τ_0 of a quantized proton field as functions of r_0 for simple wormholes. $\zeta_0 > 0$ for $r_0 < 1.34 \times 10^{13} l_p$; $\tau_0 > 0$ for $r_0 < 1.38 \times 10^{13} l_p$.

4.2.3 Proximal Schwarzschild wormhole

The metric of this type of wormhole is similar to the Schwarzschild metric except for an additional term in g_{tt}:

$$-g_{tt} = 1 - \frac{r_0}{r} + \frac{\epsilon}{r^2}. \tag{4.25}$$

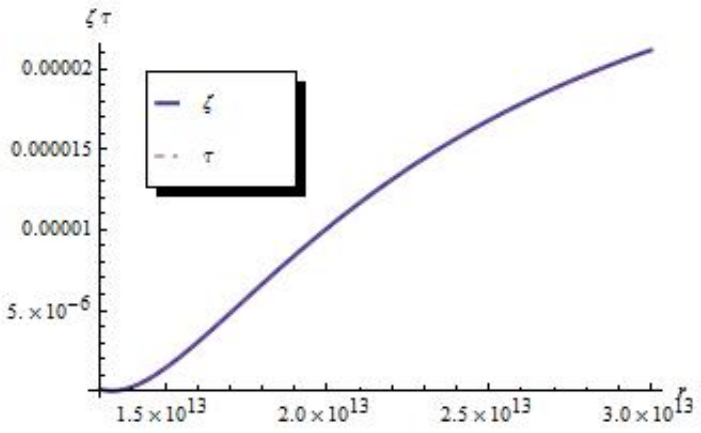

Figure 4. 14: ζ and τ of a quantized proton field as functions of r for a simple wormhole whose throat radius is $r_0 = 1.34 \times 10^{13} l_p$. Both $\zeta > 0$ and $\tau > 0$ for r beyond the throat radius: $r > r_0 = 1.34 \times 10^{13} l_p$.

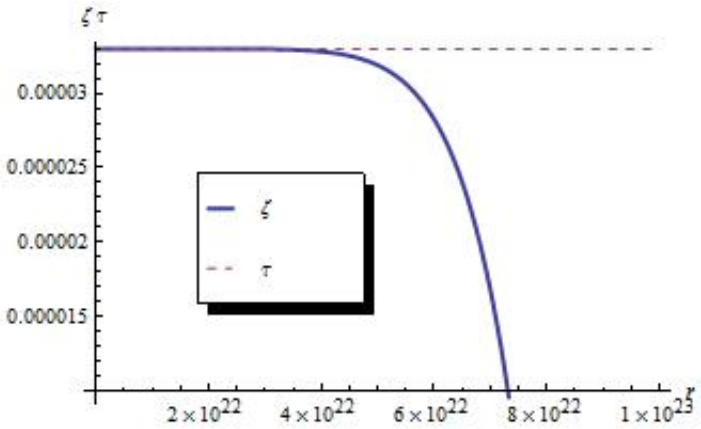

Figure 4. 15: ζ and τ of a quantized proton field as functions of r for a simple wormhole whose throat radius is $r_0 = 1.34 \times 10^{13} l_p$. Both ζ and τ are positive up to $r = 7.65 \times 10^{22} l_p$.

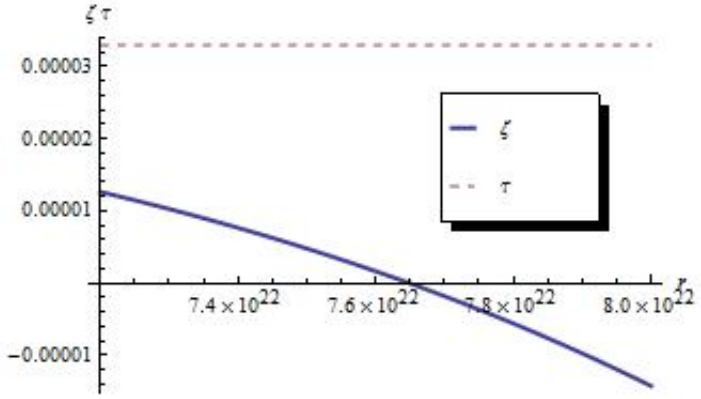

Figure 4. 16: Detail of Figure. 4.15. ζ becomes negative for $r > 7.65 \times 10^{22} l_p$.

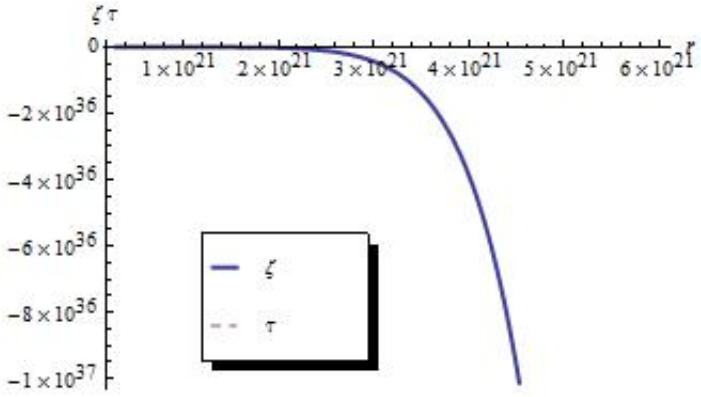

Figure 4. 17: ζ and τ of a quantized proton field as functions of r for a simple wormhole whose throat radius is $r_0 = 10^8 l_p$. Both ζ and τ are positive for $r = 3.20 \times 10^{20} l_p$. The graph τ is indistinguishable from the r_0 axis.

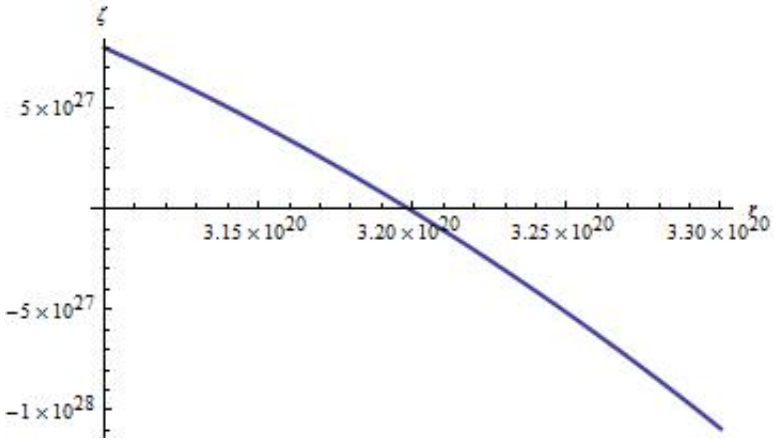

Figure 4. 18: Detail of Figure 3.17. ζ becomes negative for $r > 3.20 \times 10^{20} l_p$.

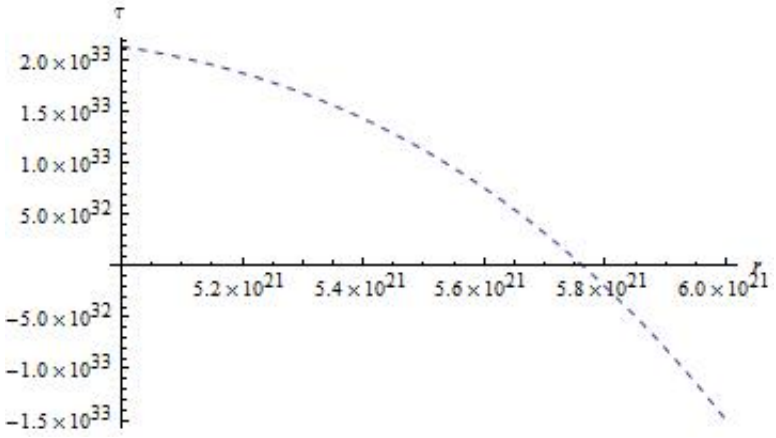

Figure 4. 19: Detail of Figure 4.17. τ becomes negative for $r > 5.76 \times 10^{21} l_p$.

The parameter ϵ is a small positive constant which satisfies $\epsilon \ll r_0^2$ [53]. This parameter prevents the appearance of an event horizon in this wormhole spacetime and keeps the wormhole traversable. Due to its similarity to the Schwarzschild spacetime, this type of wormhole is called proximal Schwarzschild wormhole. For this type of wormhole,

$$\Phi(r) = \frac{1}{2}\ln(1 - \frac{r_0}{r} + \frac{\epsilon}{r^2}), \tag{4.26}$$

$$b(r) = r_0. \tag{4.27}$$

Accordingly,

$$f(r) = 1 - \frac{r_0}{r} + \frac{\epsilon}{r^2}, \tag{4.28}$$

$$h(r) = (1 - \frac{r_0}{r})^{-1}. \tag{4.29}$$

A. The neutrino field

For the proximal Schwarzschild wormhole, I calculate the stress-energy tensor components of a quantized neutrino field for the entire spacetime by using the equations in Appendix A. The results are listed in Appendix E. By setting $r = r_0$ in Eqs. (E1) and (E2), we get Eqs. (E3) and (E4), expressions of the stress-energy components at the throat of the wormhole.

I plot ζ_0 and τ_0 as functions of r_0 and ϵ in Figures 4.20 and 4.21. Figure 4.20 is plotted for ϵ up to 10^8, and Figure 4.21 is plotted for ϵ up to 10^{18}. In both cases, the weak energy condition is violated for wormholes with throat radius r_0 up to $3.57 \times 10^{19} l_p$. So I conclude that a quantized neutrino field

is exotic for proximal Schwarzschild wormholes with a throat radius r_0 up to $3.57 \times 10^{19} l_p$.

In Figure 4.22 and Figure 4.23, I plot ζ and τ as functions of r and ϵ to see the weak energy condition is violated to what extent in the entire spacetime of this wormhole geometry for which the quantized neutrino field is exotic. To better illustrate these figures, I define r_c to be the critical value of r below which the weak energy condition is violated, and ϵ_c to be the critical value of ϵ above which the weak energy condition is violated. Figure 4.22 is plotted for a proximal Schwarzschild wormhole with a throat radius $r_0 = 3.57 \times 10^{19} l_p$. ϵ starts from 1 (since it is a positive constant), and r starts from $r_0 = 3.57 \times 10^{19} l_p$. Since ϵ must satisfies $\epsilon \ll r_0^2$, I plot ϵ up to 10^{36} to ensure that ϵ is less than 1% of r_0^2. In the shaded area, both ζ and τ are positive, which means that the weak energy condition is violated. Figure 4.22 shows that, within the range of plot, the value of r_c is in linear proportion to the value of ϵ_c. As ϵ_c reaches its maximum value of $10^{36}, r_c$ reaches its maximum value of $1.3 \times 10^{102} l_p$.

Figure 4.23 is plotted for a proximal Schwarzschild wormhole with a smaller throat radius $r_0 = 10^{10} l_p$, and ϵ is plotted to 10^{18} to ensure that ϵ is less than 1% of r_0^2. In the shaded area both ζ and τ are positive, which means that the weak energy condition is violated. This figure also shows that within the range of plot, the value of r_c is in linear proportion to the value of ϵ_c. As ϵ_c reaches its maximum value of $10^{18}, r_c$ reaches its maximum value of $1.04 \times 10^{65} l_p$.

Comparing Figure 4.22 and Figure 4.23, we see that the extent to which the weak energy condition is violated depends on the size of the wormhole (the throat radius r_0) as well as on the value of ϵ. The violation extends to the maximum radial value of $r_c = 1.3 \times 10^{102} l_p$ for a wormhole that has the maximum possible throat radius $r_0 = 3.57 \times 10^{19} l_p$ for which the quantized neutrino field is exotic.

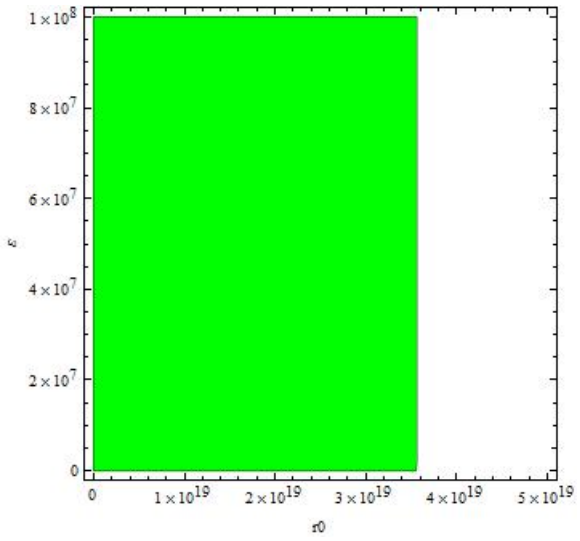

Figure 4. 20: ζ_0 and τ_0 of a quantized neutrino field as functions of r_0 and ϵ for proximal Schwarzschild wormholes. In the shaded area ($10^5 l_p < r_0 < 3.57 \times 10^{19} l_p$), both ζ_0 and τ_0 are positive.

B. The proton field

The stress-energy tensor components of a quantized proton field for the entire spacetime of the proximal Schwarzschild wormhole geometry are listed in Eqs. (E5) and (E6) in Appendix E. By setting $r = r_0$ in these two equations, we get Eqs. (E7) and (E8), expressions of the stress-energy com-

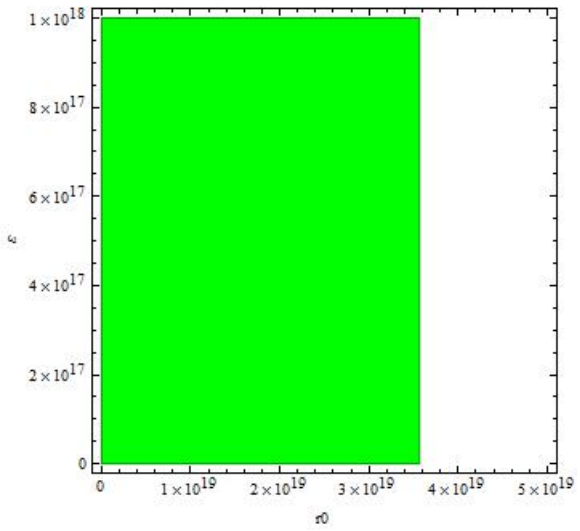

Figure 4. 21: ζ_0 and τ_0 of a quantized neutrino field as functions of r_0 and ϵ for proximal Schwarzschild wormholes. In the shaded area ($10^5 l_p < r_0 < 3.57 \times 10^{19} l_p$), both ζ_0 and τ_0 are positive.

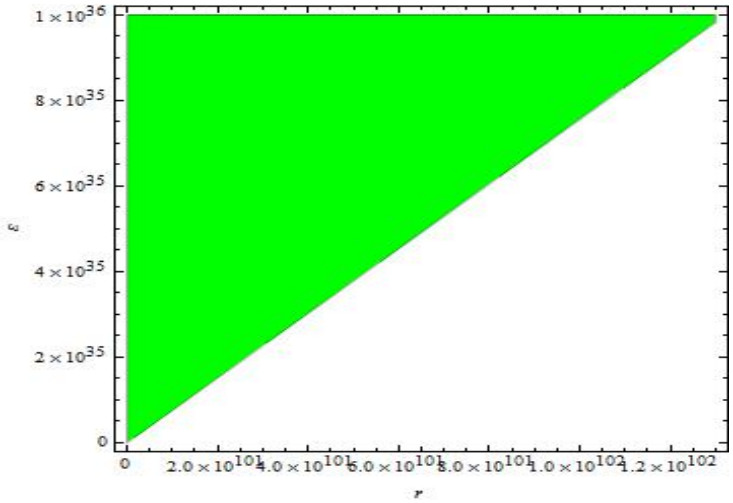

Figure 4. 22: ζ and τ of a quantized neutrino field as functions of r and ϵ for a proximal Schwarzschild wormhole with a throat radius $r_0 = 3.57 \times 10^{19} l_p$. In the shaded area, both ζ and τ are positive, i.e., weak energy condition is violated.

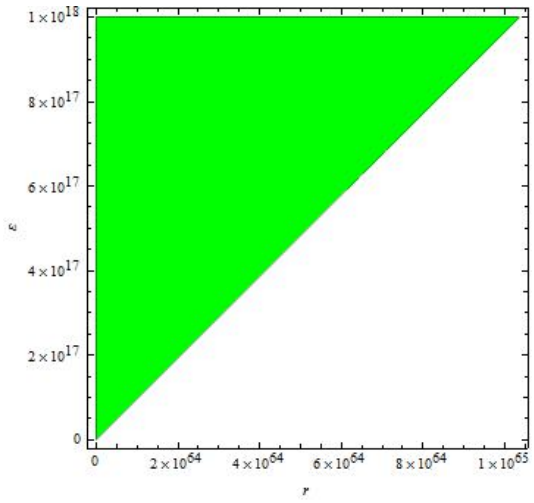

Figure 4. 23: ζ and τ of a quantized neutrino field as functions of r and ϵ for a proximal Schwarzschild wormhole with a throat radius $r_0 = 10^{10} l_p$. In the shaded area, both ζ and τ are positive, i.e., weak energy condition is violated.

ponents at the throat of the wormhole. I plot ζ_0 and τ_0 as functions of r_0 and ϵ in Figure 4.24 and Figure 4.25. In the shaded area, both ζ_0 and τ_0 are positive. Figure 4.24 shows that, for ϵ up to 10^8, the quantized proton field is exotic for wormholes with $r_0 < 1.41 \times 10^{13} l_p$. Figure 4.25 shows that, for ϵ up to 10^{18}, the quantized proton field is exotic for wormholes also with $r_0 < 1.41 \times 10^{13} l_p$. So I conclude that a quantized proton field is exotic for proximal Schwarzschild wormholes with $r_0 < 1.41 \times 10^{13} l_p$.

I also plot ζ and τ as functions of r and ϵ to see weak energy condition is violated to what extent in the entire spacetime for this wormhole geometry. Figure 4.26 through Figure 4.29 are plotted for a proximal Schwarzschild wormhole with the biggest possible throat radius $r_0 = 1.41 \times 10^{13} l_p$ for

which the quantized proton field is exotic. In these figures, r starts from the minimum value $r_0 = 1.41 \times 10^{13} l_p$, and ϵ starts from 1. From Figure 4.26 we see that, for ϵ_c up to $10^8, r_c$ is linearly proportional to ϵ_c. For $\epsilon_c = 10^8, r_c = 3.76 \times 10^{51} l_p$.

Figure 4.27 shows that, as ϵ is greater than about 10^8, the value of r_c increases not in linear proportion to the value of ϵ_c, but follows a curved relationship. Figure 4.28 and Figure 4.29 show that, as ϵ reaches the value of about $10^{11}, r_c$ reaches its maximum value of $1.02 \times 10^{52} l_p$; as ϵ further increases, this value of r_c does not change.

In Figure 4.30 through Figure 4.33, I plot ζ and τ as functions of r and ϵ for a proximal Schwarzschild wormhole with a smaller throat radius, $r_0 = 10^8 l_p$, for which the quantized proton field is exotic. Figure 4.30 shows that, for ϵ up to $10^8, r_c$ is in linear proportion to ϵ_c. For $\epsilon_c = 10^8, r_c = 1.90 \times 10^{41} l_p$.

Figure 4.31 shows that, as ϵ is greater than about 10^8, the value of r_c is not in linear proportion to the value of ϵ_c, but follows a curved relationship. Figure 4.32 and Figure 4.33 show that, as ϵ reaches the value of about $10^{10}, r_c$ reaches its maximum value of $5.0 \times 10^{41} l_p$; as ϵ further increases, this value of r_c does not change.

Figure 4.26 through Figure 4.33 show that r_c depends on both the size of the wormhole (the value of the throat radius r_0) and the value of ϵ. The maximum value of $r_c (1.02 \times 10^{52} l_p)$ occurs with a wormhole that has the maximum throat radius $r_0 = 1.41 \times 10^{13} l_p$ for which the quantized proton field is exotic.

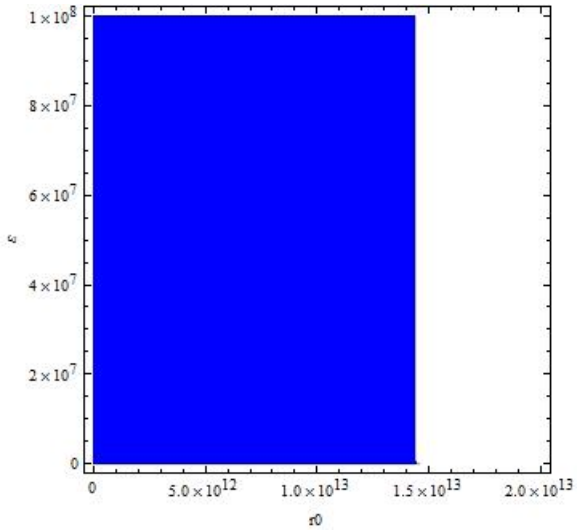

Figure 4. 24: ζ_0 and τ_0 of a quantized proton field as functions of r_0 and ϵ for proximal Schwarzschild wormholes. In the shaded area ($r_0 < 1.41 \times 10^{13} l_p$), both ζ_0 and τ_0 are positive.

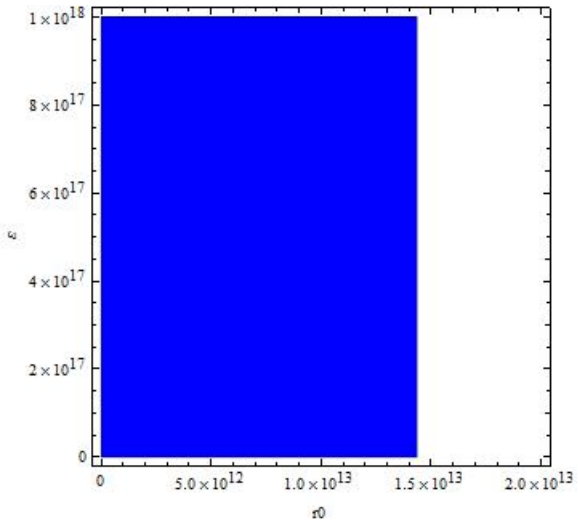

Figure 4. 25: ζ_0 and τ_0 of a quantized proton field as functions of r_0 and ϵ for proximal Schwarzschild wormholes. In the shaded area ($r_0 < 1.41 \times 10^{13} l_p$), both ζ_0 and τ_0 are positive.

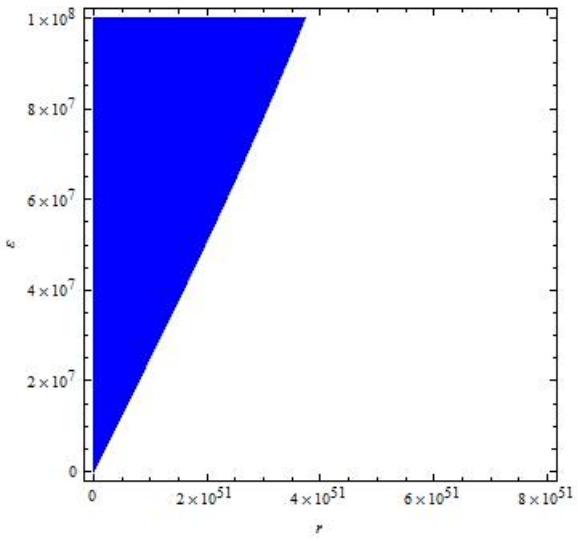

Figure 4. 26: ζ and τ of a quantized proton field as functions of r and ϵ for a proximal Schwarzschild wormhole with throat radius $r_0 = 1.41 \times 10^{13} l_p$. In the shaded area, both ζ and τ are positive. r_c is in linear proportion to ϵ_c.

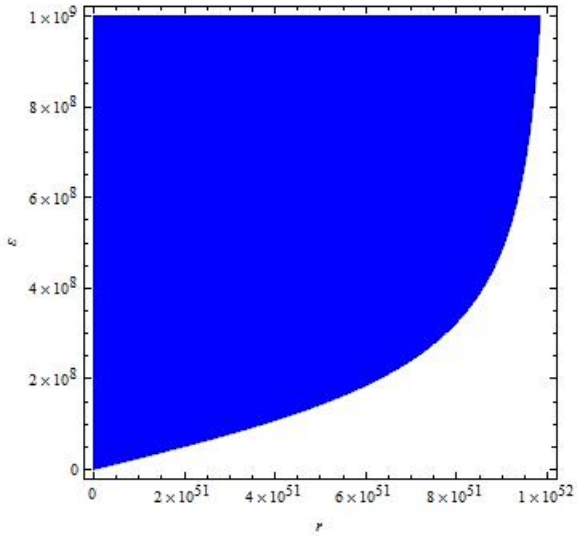

Figure 4. 27: ζ and τ of a quantized proton field as functions of r and ϵ for a proximal Schwarzschild wormhole with throat radius $r_0 = 1.41 \times 10^{13} l_p$. In the shaded area, both ζ and τ are positive.

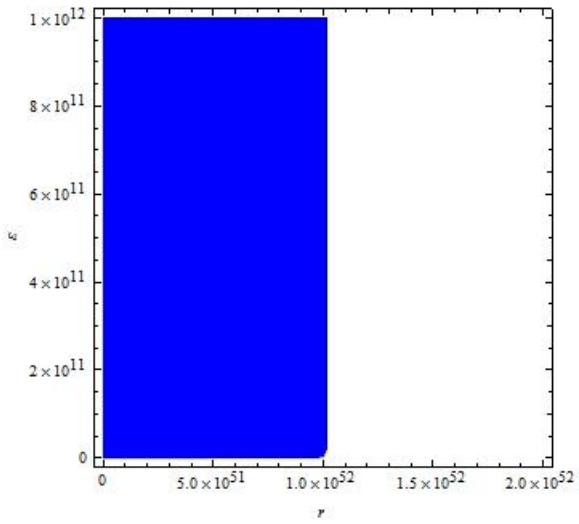

Figure 4. 28: ζ and τ of a quantized proton field as functions of r and ϵ for a proximal Schwarzschild wormhole with throat radius $r_0 = 1.41 \times 10^{13} l_p$. In the shaded area ($r < 1.02 \times 10^{52} l_p$), both ζ and τ are positive.

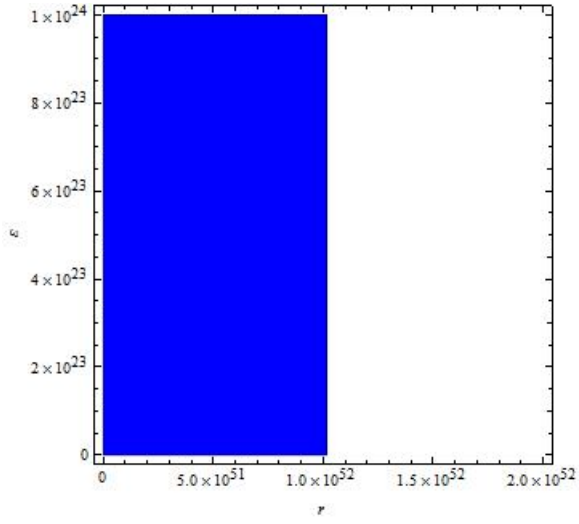

Figure 4. 29: ζ and τ of a quantized proton field as functions of r and ϵ for a proximal Schwarzschild wormhole with throat radius $r_0 = 1.41 \times 10^{13} l_p$. In the shaded area ($r < 1.02 \times 10^{52} l_p$), both ζ and τ are positive.

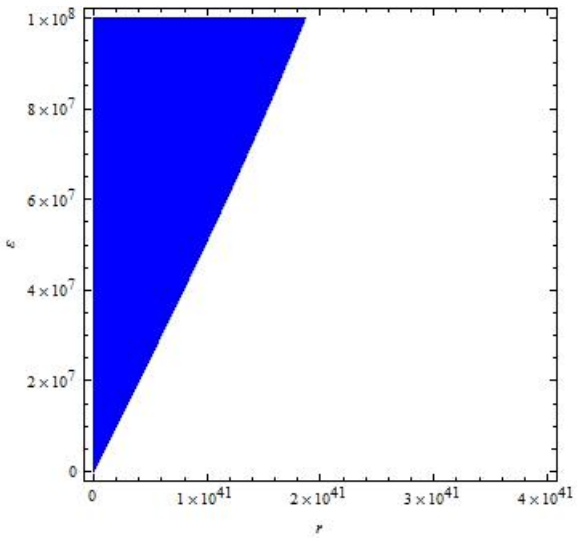

Figure 4. 30: ζ and τ of a quantized proton field as functions of r and ϵ for a proximal Schwarzschild wormhole with throat radius $r_0 = 10^8 l_p$. In the shaded area, both ζ and τ are positive. r_c is in linear proportion to ϵ_c.

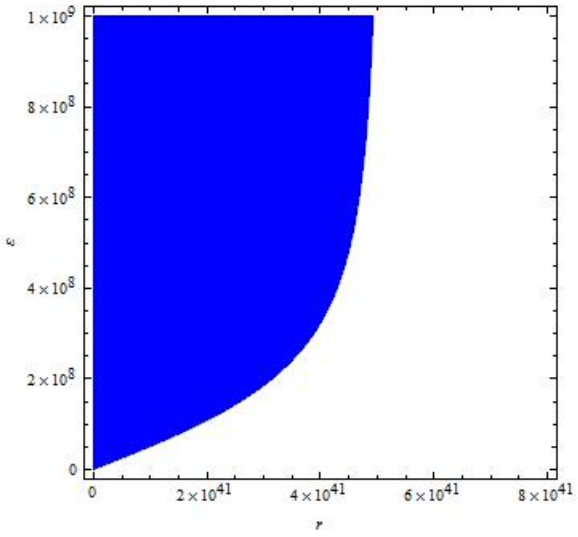

Figure 4. 31: ζ and τ of a quantized proton field as functions of r and ϵ for a proximal Schwarzschild wormhole with throat radius $r_0 = 10^8 l_p$. In the shaded area, both ζ and τ are positive.

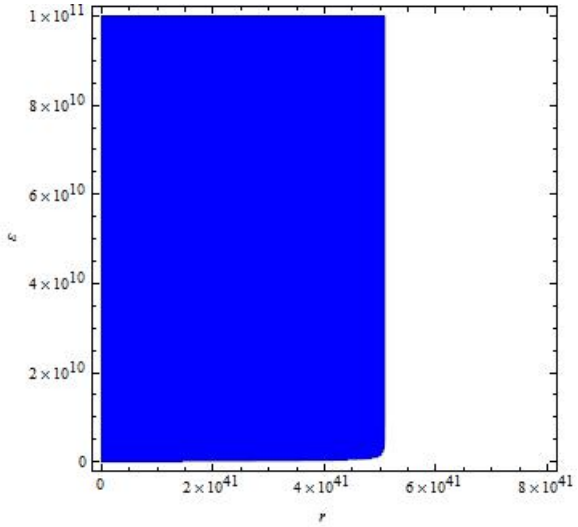

Figure 4. 32: ζ and τ of a quantized proton field as functions of r and ϵ for a proximal Schwarzschild wormhole with throat radius $r_0 = 10^8 l_p$. In the shaded area ($r < 5.10 \times 10^{41} l_p$), both ζ and τ are positive.

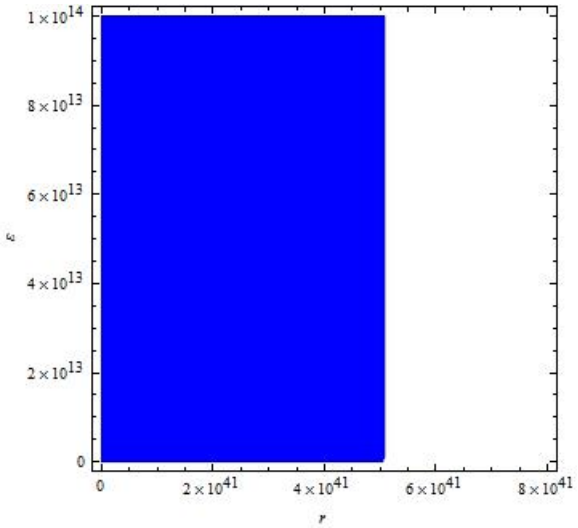

Figure 4. 33: ζ and τ of a quantized proton field as functions of r and ϵ for a proximal Schwarzschild wormhole with throat radius $r_0 = 10^8 l_p$. In the shaded area ($r < 5.10 \times 10^{41} l_p$), both ζ and τ are positive.

4.2.4 Wormhole with finite radial cutoff of stress-energy

The last type of wormhole that I examine is the wormhole with finite radial cutoff of the stress-energy tensor. The metric for this type of wormhole is:

$$\Phi(r) = 0, \tag{4.30}$$

$$b(r) = r_0(\frac{r}{r_0})^{1-\eta}. \tag{4.31}$$

where η is a constant bounded by $0 < \eta < 1$. Accordingly,

$$f(r) = 1, \tag{4.32}$$

$$h(r) = [1 - (\frac{r_0}{r})^{\eta}]^{-1}. \tag{4.33}$$

A. The neutrino field

The stress-energy tensor components of a quantized neutrino field for this type of wormhole in the entire spacetime are also too complicated to list here. So I put them in Eqs. (F1) and (F2) in Appendix F. By setting $r = r_0$ in these two equations, we get Eqs. (F3) and (F4), the stress-energy tensor components of a quantized neutrino field at the throat of this type of wormhole.

Figure 4.34 is plotted for ζ_0 and τ_0 as functions of r_0 and η. In this figure we see that both ζ_0 and τ_0 are positive for r_0 up to around $0.6l_p$. This means that a quantized neutrino field is exotic for this type of wormhole with a throat radius r_0 up to around $0.6l_p$. However, the maximum value of the

throat radius r_0 varies slightly as η varies. For $\eta = 0$, the maximum value of r_0 is $r_0 = 0.59l_p$; for $\eta = 1$, the maximum value of r_0 is $r_0 = 0.62l_p$.

I further plot ζ and τ as functions of r and η in the neighborhood of the wormhole to see the quantity of the weak energy condition violation in the entire spacetime. Figure 4.35 is plotted for a wormhole whose throat radius is $r_0 = 0.59l_p$ for which the quantized neutrino field is exotic. From the figure we see that the value of r_c increases as η increases, ranging from $0.59l_p$ (for $\eta = 0$) to $0.62l_p$ (for $\eta = 1$). Figure 4.36 is plotted for a wormhole whose throat radius is $0.40l_p$ for which the quantized neutrino field is exotic. The value of r_c also increases as η increases, ranging from $0.59l_p$ (for $\eta = 0$) to $0.62l_p$ (for $\eta = 1$), exactly as in the case of $r_0 = 0.59l_p$. However, Figure 4.36 looks different from Figure 4.35 because it is plotted for different range of r. If we magnify part of Figure 4.36 into Figure 4.37, for the same range of r as in Figure 4.35, we see that Figure 4.37 looks exactly the same as Figure 4.35. This tells us that the extent to which the weak energy condition is violated in a quantized neutrino field for this type of wormhole is independent of the throat radius of the wormhole for which the quantized neutrino field is exotic. For a wormhole that has the maximum throat radius (r_0 ranges between $0.59l_p$ and $0.62l_p$ depending on the value of η), the weak energy condition violation is limited to the boundary of the wormhole's throat ($r_c = r_0$) for all values of η; while for a wormhole that has a smaller throat radius ($r_0 < 0.59l_p$), the weak energy condition violation extends beyond the boundary of the wormhole's throat.

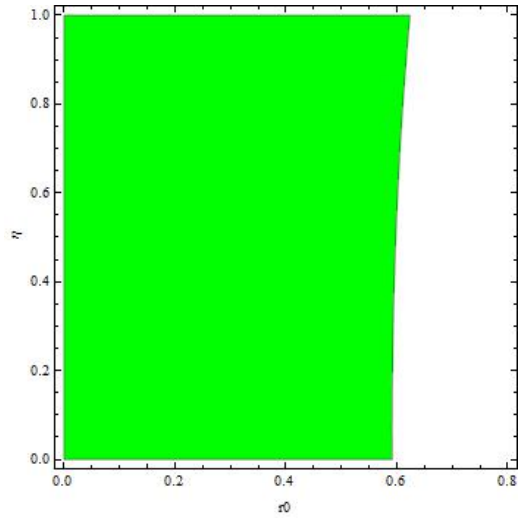

Figure 4. 34: ζ_0 and τ_0 of a quantized neutrino field as functions of r_0 and η for wormholes with finite radial cutoff of stress-energy tensor. In the shaded area, both ζ_0 and τ_0 are positive.

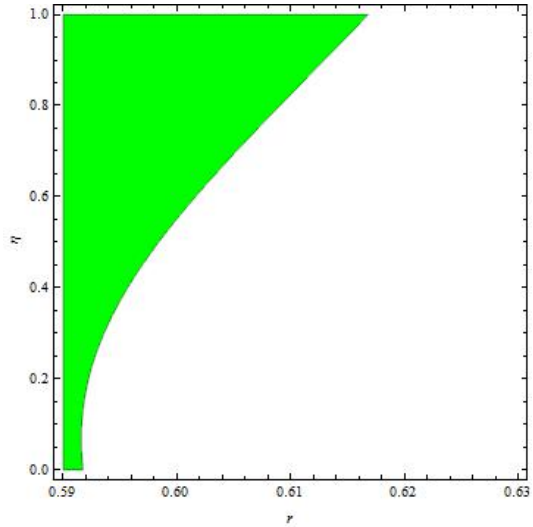

Figure 4. 35: ζ and τ of a quantized neutrino field as functions of r and η for a wormhole with finite radial cutoff of stress-energy tensor whose throat radius is $r_0 = 0.59 l_p$. In the shaded area, both ζ and τ are positive.

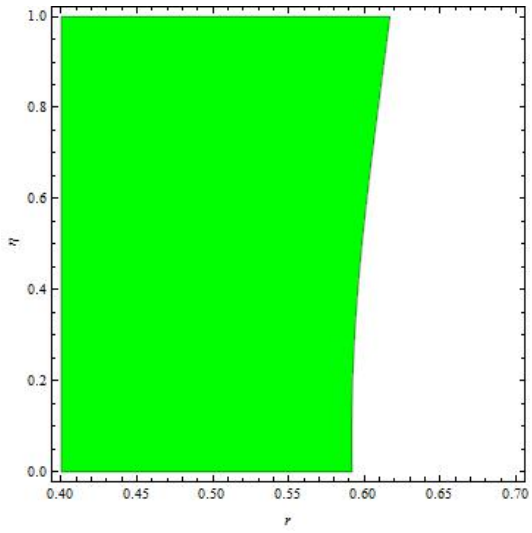

Figure 4. 36: ζ and τ of a quantized neutrino field as functions of r and η for a wormhole with finite radial cutoff of stress-energy tensor whose throat radius is $r_0 = 0.40 l_p$. In the shaded area, both ζ and τ are positive.

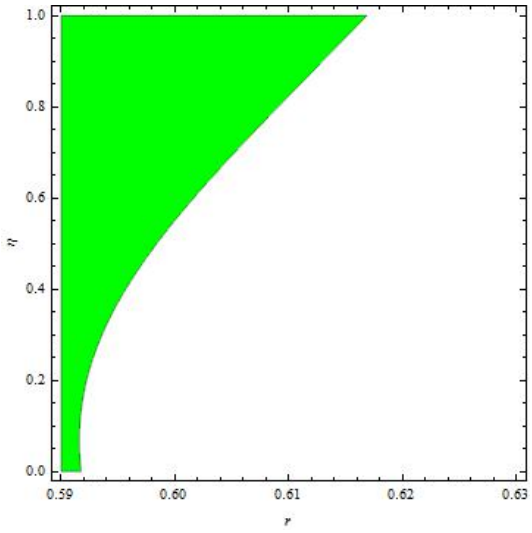

Figure 4. 37: Detail of Figure 4.36. For $\eta = 0, r_c = 0.59 l_p$; for $\eta = 1, r_c = 0.62 l_p$.

B. The proton field

The stress-energy tensor components of a quantized proton field for this type of wormhole in the entire spacetime are listed in Eqs. (F5) and (F6) in Appendix F. By setting $r = r_0$ in these two equations, we get the expressions for the stress-energy tensor components at the throat of the wormhole.

I plot ζ_0 and τ_0 as functions of r_0 and η in Figure 4.38. This figure shows that ζ_0 and τ_0 are positive for r_0 up to around $0.6l_p$. This means that a quantized proton field is exotic for this type of wormhole with a throat radius up to around $0.6l_p$. However, the maximum radius of the throat r_0 varies slightly as η varies, ranging from $0.59l_p$ (for $\eta = 0$) to $0.62l_p$ (for $\eta = 1$). This is the same as in the case of the quantized neutrino field.

I further plot ζ and τ as functions of r and η in the neighborhood of the wormhole to see the quantity of the weak energy condition violation in the entire spacetime. Figure 4.39 is plotted for a wormhole whose throat radius is $r_0 = 0.59l_p$. From the graph we see that the value of r_c increases as η increases, ranging from $0.59l_p$ (for $\eta = 0$) to $0.62l_p$ (for $\eta = 1$). Figure 4.40 is plotted for a wormhole whose throat radius is $r_0 = 0.40l_p$. The value of r_c also increases as η increases, ranging from $0.59l_p$ (for $\eta = 0$) to $0.66l_p$ (for $\eta = 1$), almost the same as in the case of $r_0 = 0.59l_p$. This tells us that the extent to which the weak energy condition is violated in a quantized proton field for this type of wormhole is almost independent of the throat radius of the wormhole, the same as in the case of the quantized neutrino field. For a wormhole that has the maximum throat radius (r_0 ranges between $0.59l_p$ and

$0.62l_p$ depending on the value of η), the weak energy condition violation is limited to the boundary of the wormhole's throat ($r_c = r_0$) for all values of η; while for a wormhole that has a smaller throat radius ($r_0 < 0.59l_p$), the weak energy condition violation extends beyond the boundary of the wormhole's throat.

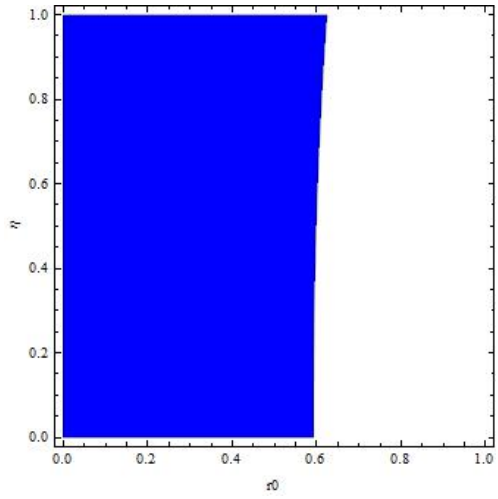

Figure 4. 38: ζ_0 and τ_0 of a quantized proton field as functions of r_0 and η for wormholes with finite radial cutoff of stress-energy tensor. In the shaded area, both ζ_0 and τ_0 are positive.

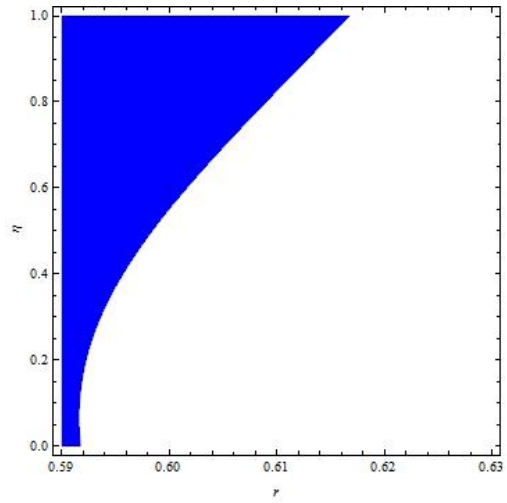

Figure 4. 39: ζ and τ of a quantized proton field as functions of r and η for a wormhole with finite radial cutoff of stress-energy tensor whose throat radius is $r_0 = 0.59 l_p$. In the shaded area, both ζ and τ are positive.

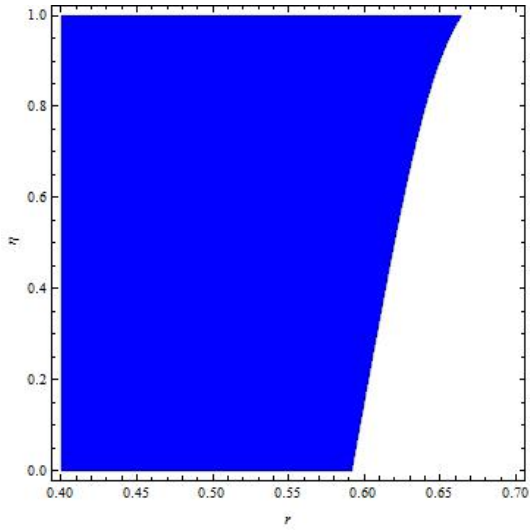

Figure 4. 40: ζ and τ of a quantized proton field as functions of r and η for a wormhole with finite radial cutoff of stress-energy tensor whose throat radius is $r_0 = 0.40 l_p$. In the shaded area, both ζ and τ are positive.

Chapter 5. Stress-Energy Tensor of Two Quantized Massive Spin 1/2 Fields in Four Static Spherically Symmetric Wormhole Spacetimes in Thermal States

5.1 Introduction

As introduced in Chapter 2, we take expectation value of the stress-energy tensor in Eq. (2.2). In thermal states, the expectation value of an observable is defined to be its thermal average, which is based on the equipartition theorem. In classical statistical mechanics, the equipartition theorem is a general formula that relates the temperature of a system with its average energies. The original idea of equipartition theorem was that, in thermal equilibrium, energy is shared equally among all of its various forms. For example, the average kinetic energy per degree of freedom in the translational motion of a molecule should equal that of its rotational motions.

The equipartition theorem makes quantitative predictions. Like the virial theorem, it gives the total average of kinetic and potential energies for a system at a given temperature, from which the system's heat capacity can be calculated. It also gives the average values of individual components of the energy, such as the kinetic energy of a particle. For example, it predicts that every molecule in a monoatomic ideal gas has an average kinetic energy of $\frac{3}{2}k_BT$ in thermal equilibrium, where k_B is the Boltzmann constant and T is the temperature.

However, the equipartition law becomes inaccurate when quantum effects are significant, and it breaks down when the thermal energy k_BT is significantly smaller than the spacing between energy levels. This happens, for instance, at a very low temperature. Equipartition no longer holds because it is a poor approximation to assume that the energy levels form a smooth continuum, which is required in the derivation of the equipartition theorem. In such circumstances, the mechanism of thermal equilibrium is unclear. My calculation of the stress-energy tensor of quantized massive spin 1/2 fields in thermal states is thus a somewhat formal and natural work not yet supported by a detailed picture of the physical mechanisms involved.

5.2 Stress-energy tensor of two quantized massive spin 1/2 fields in four wormhole spacetimes

The stress-energy tensor components of a quantized massive spin 1/2 field in a general static spherically symmetric spacetime in thermal states are calculated and their resulting expressions are listed in Appendix B. In this chapter, I use the equations in Appendix B to calculate the stress-energy tensor of the quantized neutrino field and quantized proton field for four wormhole spacetimes in thermal states. For each wormhole spacetime, I substitute $f(r)$ and $h(r)$ by their specific functions in the line element for this wormhole spacetime, and m by the neutrino mass [Eq. (3.1)] or proton mass [Eq. (3.2)]. Finally, I expand the expressions of $< T^{\nu}_{\mu} >_{ren}$ in powers of r_0 (for values at the throat of the wormhole) or in powers of r (for values beyond the throat of the wormhole).

In Planck units, a unit temperature is $T_p = 1.416833 \times 10^{32} K$. It should be noted that neutrinos and antineutrinos were decoupled from other particles at a temperature $T \approx 1.3 \times 10^{11} K (\approx 10^{-21} T_p)$ [54]. At a temperature $T \approx 10^{12} K (\approx 10^{-20} T_p)$, neutrons and protons appeared to be a very small contamination among other particles [54]. So, in my calculation, I consider temperature up to $10^{-21} T_p$ for the neutrino field and up to $10^{-20} T_p$ for the proton field.

In the following subsections, I will present and discuss the results of my calculation. It should be noted that, as a result of using the parameter values

that I have chosen, the stress-energy tensor components of these two fields turn out to have unphysically large values in many cases. These large values make the physical model not credible. However, in the interest of exploring the mathematical structure of the physical model, I will check when the energy conditions hold. Besides, some assertions are made for $r < r_0$. They are based on the formulae derived for $r > r_0$ that may not be valid for $r < r_0$.

5.2.1 Zero-tidal-force wormhole

The first class of wormhole examined is a particularly simple set of wormholes whose metric functions satisfy:

$$\Phi(r) = 0, \tag{5.1}$$

$$b(r) = r_0 = constant. \tag{5.2}$$

Accordingly,

$$f(r) = 1, \tag{5.3}$$

$$h(r) = (1 - \frac{r_0}{r})^{-1}. \tag{5.4}$$

This type of wormhole is called a zero-tidal-force wormhole because an observer at the throat of the wormhole experiences zero tidal force.

A. The neutrino field

The stress-energy tensor components of a quantized neutrino field at the throat of this type of wormhole in thermal states are computed to be (in

units of F_p/l_p^2):

$$< T_t^t >_0 = \frac{1.6\times 10^{54}}{r_0^8} - \frac{5.9\times 10^{54}}{r_0^6} - \frac{0.08}{r_0^4} - \frac{2.0\times 10^{-60}}{r_0^2} + 3.2\times 10^{-59}T^2 + \frac{2.2\times 10^{-16}T^2}{r_0^2} - 1.2T^4 - \frac{0.0009(\ln T)}{r_0^4}, \quad (5.5)$$

$$< T_r^r >_0 = -\frac{1.6\times 10^{54}}{r_0^8} - \frac{4.0\times 10^{54}}{r_0^6} - \frac{0.1}{r_0^4} + \frac{0.0008}{r_0^3} + \frac{2.8\times 10^{-17}}{r_0^2} + \frac{8.7\times 10^{-19}}{r_0} - 3.2\times 10^{-59}T^2 - \frac{0.01T^2}{r_0^2} + 0.4T^4 - \frac{0.002(\ln T)}{r_0^4}, \quad (5.6)$$

$$< T_\theta^\theta >_0 = 1.6\times 10^{-117} + \frac{5.0\times 10^{54}}{r_0^6} - \frac{0.2}{r_0^4} - \frac{2.1\times 10^{-60}}{r_0^2} - 3.2\times 10^{-59}T^2 + \frac{0.007T^2}{r_0^2} + 0.4T^4 - \frac{0.003(\ln T)}{r_0^4}. \quad (5.7)$$

In these expressions, the terms with higher inverse orders of r_0 have a much bigger coefficient than those terms with lower inverse orders of r_0. This implies that smaller values of r_0 contribute more to the stress-energy tensor. In other words, the magnitude of the stress-energy tensor is larger for smaller values of r_0. Meanwhile, those terms involving temperature have relatively small coefficients. This implies that temperature plays a small and even negligible part in the stress-energy tensor. This is all the more true considering that the temperatures considered are less than $10^{-21}T_p$.

Figure 5.1 is plotted for ζ_0 and τ_0 as functions of T and r_0. In the shaded area, which is to the left of the line $r_0 = 1.26l_p$, both $\zeta_0 > 0$ and $\tau_0 > 0$. This means that a quantized neutrino field is exotic for this type of wormhole with throat radius $r_0 < 1.26l_p$. This numerical result is the same as that in the zero-temperature case. Figure 5.1 shows that temperature has no effect on the result.

I have also computed the stress-energy tensor components in the entire spacetime of the zero-tidal-force wormhole geometry for which the quantized neutrino field is exotic. They are too complicated to list here. So I list them in Appendix C. However, I plot ζ and τ as functions of T and r to see the domain of the weak energy condition violation in the neighborhood of the wormhole. Figure 5.2 is plotted for a zero-tidal-force wormhole that has the maximum possible throat radius, $r_0 = 1.26l_p$, for which the quantized neutrino field is exotic. This figure shows that both ζ and τ are positive for $r < 1.26l_p$, independent of the temperature. So, the weak energy condition violation for this wormhole is limited to the boundary of its throat.

Figure 5.3 is plotted for a zero-tidal-force wormhole whose throat radius is $r_0 = 0.50l_p$ for which the quantized neutrino field is exotic. The figure shows that both ζ and τ are positive for $r < 0.52l_p$, also independent of the temperature. This means that the weak energy condition violation for this wormhole extends a little beyond its throat.

B. The proton field

Similarly, the stress-energy tensor components of a quantized proton field

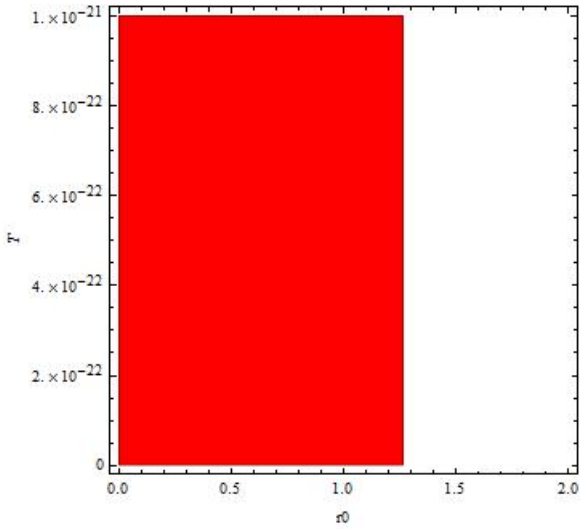

Figure 5. 1: ζ_0 and τ_0 of a quantized neutrino field as functions of T and r_0 for zero-tidal-force wormholes. Both $\zeta_0 > 0$ and $\tau_0 > 0$ for $r_0 < 1.26 l_p$.

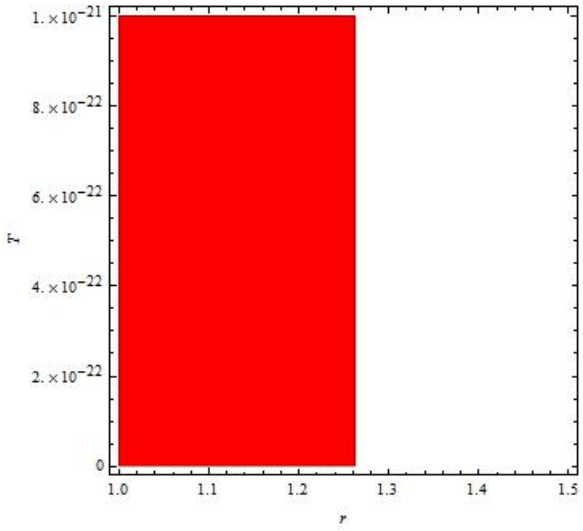

Figure 5. 2: ζ and τ of a quantized neutrino field as functions of T and r for a zero-tidal-force wormhole whose throat radius is $r_0 = 1.26 l_p$. Both $\zeta > 0$ and $\tau > 0$ for $r < 1.26 l_p$.

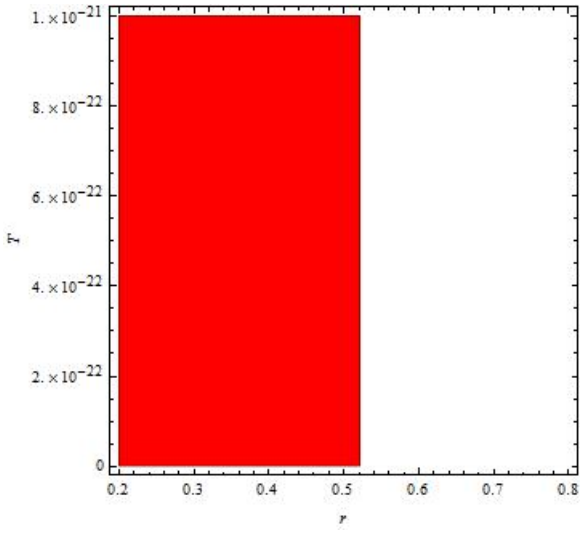

Figure 5. 3: ζ and τ of a quantized neutrino field as functions of T and r for a zero-tidal-force wormhole whose throat radius is $r_0 = 0.50 l_p$. Both $\zeta > 0$ and $\tau > 0$ for $r < 0.52 l_p$.

at the throat of the zero-tidal-force wormhole in thermal states are computed to be (in units of F_p/l_p^2):

$$< T_t^t >_0 = \frac{1.0 \times 10^{35}}{r_0^8} - \frac{3.9 \times 10^{35}}{r_0^6} - \frac{0.05}{r_0^4} - \frac{3.0 \times 10^{-41}}{r_0^2} + 4.9 \times 10^{-40} T^2 + \frac{2.2 \times 10^{-16} T^2}{r_0^2} - 1.2 T^4 - \frac{0.0009 (\ln T)}{r_0^4}, \quad (5.8)$$

$$< T_r^r >_0 = -\frac{1.0 \times 10^{35}}{r_0^8} - \frac{2.6 \times 10^{35}}{r_0^6} - \frac{0.09}{r_0^4} + \frac{0.0008}{r_0^3} + \frac{2.8 \times 10^{-17}}{r_0^2} + \frac{8.7 \times 10^{-19}}{r_0} - 4.9 \times 10^{-40} T^2 - \frac{0.01 T^2}{r_0^2} + 0.4 T^4 - \frac{0.002 (\ln T)}{r_0^4}, \quad (5.9)$$

$$< T^{\theta}_{\theta} >_0 = 3.7 \times 10^{-79} + \frac{3.3 \times 10^{35}}{r_0^6} - \frac{0.1}{r_0^4} - \frac{3.3 \times 10^{-41}}{r_0^2} - 4.9 \times 10^{-40} T^2 + \frac{0.007 T^2}{r_0^2} + 0.4 T^4 - \frac{0.003(\ln T)}{r_0^4}. \quad (5.10)$$

These expressions exhibit a similar hierarchy of coefficients as in the case of the neutrino field. The terms with higher inverse orders of r_0 have a much bigger coefficient than those terms with lower inverse orders of r_0. The implication is similar: smaller values of r_0 contribute more to the stress-energy tensor; or in other words, the magnitude of the stress-energy tensor is larger for smaller values of r_0. As in the case of the neutrino field, those terms involving temperature have relatively small coefficients. This implies that temperature plays a small and even negligible part in the stress-energy tensor. This is all the more true considering that temperature has a maximum value of only $10^{-20} T_p$.

ζ_0 and τ_0 are plotted in Figure 5.4 as functions of T and r_0. Both $\zeta_0 > 0$ and $\tau_0 > 0$ for $r_0 < 1.26 l_p$. This implies that the quantized proton field is also exotic for this type of wormhole with the radius $r_0 < 1.26 l_p$. Figure 5.4 shows that temperature has no effect on this result.

I have computed the stress-energy components of the quantized proton field in the entire spacetime for the zero-tidal-force wormhole geometry in thermal states, and list them in Appendix C. Here I present figures of ζ and τ as functions of T and r for two zero-tidal-force wormholes of different size for which the quantized proton field is exotic. Figure 5.5 is plotted for a

wormhole with the maximum possible throat radius, $r_0 = 1.26l_p$, for which the quantized proton field is exotic. The figure shows that both ζ and τ are positive for $r < 1.26l_p$, independent of the temperature. This implies that the weak energy condition violation is limited to the boundary of the wormhole's throat. This is the same as in the zero-temperature case.

Figure 5.6 is plotted for a zero-tidal-force wormhole whose throat radius is $r_0 = 0.50l_p$. This figure shows that both ζ and τ are positive for $r < 0.52l_p$, independent of the temperature. This implies that the weak energy condition violation extends a little beyond the wormhole's throat. This result is the same as in the case of zero temperature.

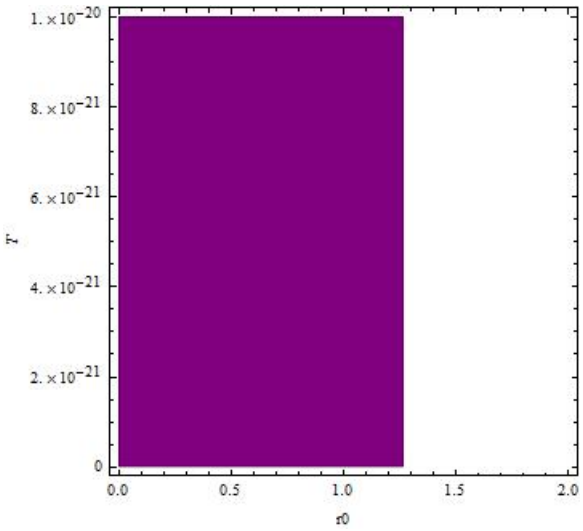

Figure 5. 4: ζ_0 and τ_0 of a quantized proton field as functions of T and r_0 for zero-tidal-force wormholes. Both $\zeta_0 > 0$ and $\tau_0 > 0$ for $r_0 < 1.26l_p$.

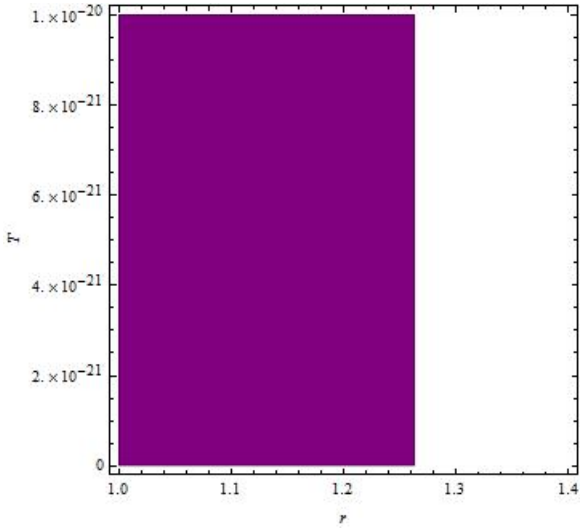

Figure 5. 5: ζ and τ of a quantized proton field as functions of T and r for a zero-tidal-force wormhole whose throat radius is $r_0 = 1.26l_p$. Both $\zeta > 0$ and $\tau > 0$ for $r < 1.26l_p$.

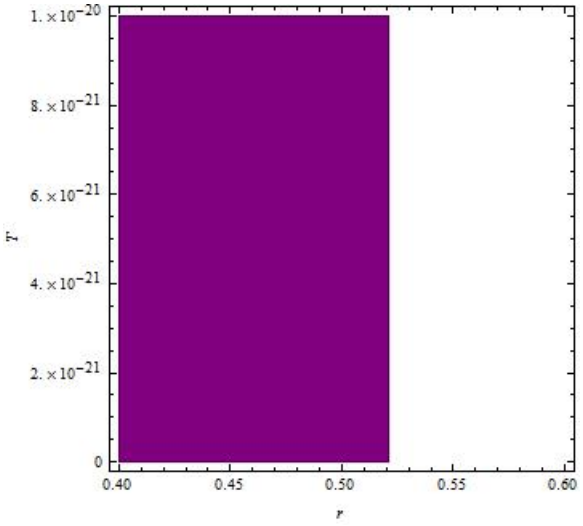

Figure 5. 6: ζ and τ of a quantized proton field as functions of T and r for a zero-tidal-force wormhole whose throat radius is $r_0 = 0.50l_p$. Both $\zeta > 0$ and $\tau > 0$ for $r < 0.52l_p$.

5.2.2 The simple wormhole

This type of wormhole has the metric functions:

$$\Phi(r) = 0, \tag{5.11}$$

$$b(r) = \frac{r_0^2}{r}. \tag{5.12}$$

Accordingly,

$$f(r) = 1, \tag{5.13}$$

$$h(r) = (1 - \frac{r_0^2}{r^2})^{-1}. \tag{5.14}$$

This wormhole is discussed by Morris and Thorne [5] as an example of traversable wormhole.

A. The neutrino field

I find the stress-energy tensor components of a quantized neutrino field at the throat of the simple wormhole to be (in units of F_p/l_p^2):

$$\begin{aligned} < T_t^t >_0 &= \frac{1.6 \times 10^{54}}{r_0^8} - \frac{6.1 \times 10^{54}}{r_0^6} - \frac{0.02}{r_0^4} - \frac{1.8 \times 10^{-60}}{r_0^2} + 3.2 \times 10^{-59} T^2 \\ &\quad - \frac{0.01 T^2}{r_0^2} - 1.2 T^4 - \frac{1.6 \times 10^{-11} (\ln T)}{r_0^4}, \end{aligned} \tag{5.15}$$

$$\begin{aligned} < T_r^r >_0 &= -\frac{1.6 \times 10^{54}}{r_0^8} - \frac{6.4 \times 10^{55}}{r_0^6} - \frac{1.0}{r_0^4} + \frac{0.002}{r_0^3} - \frac{2.1 \times 10^{-17}}{r_0^2} \\ &\quad + \frac{2.6 \times 10^{-18}}{r_0} - 3.2 \times 10^{-59} T_2 - \frac{0.01 T^2}{r_0^2} + 0.4 T^4 \end{aligned}$$

$$-\frac{0.01(\ln T)}{r_0^4}, \tag{5.16}$$

$$\begin{aligned} < T_\theta^\theta >_0 &= 1.6 \times 10^{-117} + \frac{3.5 \times 10^{55}}{r_0^6} - \frac{0.4}{r_0^4} - \frac{3.1 \times 10^{-60}}{r_0^2} - 3.2 \times 10^{-59} T^2 \\ &+ \frac{0.01 T^2}{r_0^2} + 0.4 T^4 - \frac{0.005(\ln T)}{r_0^4}. \end{aligned} \tag{5.17}$$

The coefficients of these expressions have the same hierarchy as in the previous cases. Its implication is the same: smaller values of r_0 contribute more to the stress-energy tensor. Besides, terms involving temperature have relatively small coefficients. This implies that temperature plays a negligible part in the stress-energy tensor.

Figure 5.7 is plotted for ζ_0 and τ_0 as functions of T and r_0. Both $\zeta_0 > 0$ and $\tau_0 > 0$ for $r_0 < 3.32 \times 10^{19} l_p$. This implies that a quantized neutrino fieldis exotic for simple wormholes with a throat radius $r_0 < 3.32 \times 10^{19} l_p$. Figure 5.7 also shows that temperature exerts no influence on ththis result. It is the same as in the zero-temperature case.

I also have computed the stress-energy tensor components in the entire spacetime for the simple wormhole geometry for which the quantized neutrino field is exotic in thermal states. I list them in Appendix D. Here I present Figure 5.8 through Figure 5.10 that show ζ and τ as functions of T and r for two simple wormholes of different size. Figure 5.8 is plotted for a simple wormhole with the maximum possible throat radius, $r_0 = 3.32 \times 10^{19} l_p$, for which the quantized neutrino field is exotic. This figure shows that both

$\zeta > 0$ and $\tau > 0$ for $r < 3.29 \times 10^{34} l_p$. This suggests that the weak energy condition violation for this wormhole extends well beyond the wormhole's throat.

Figure 5.9 and Figure 5.10 are plotted for a simple wormhole whose throat radius is $r_0 = 10^{10} l_p$. Figure 5.9 shows that both $\zeta > 0$ and $\tau > 0$ for $10^{10} l_p < r < 1.02 \times 10^{10} l_p$, while Figure 5.10 shows that both $\zeta > 0$ and $\tau > 0$ for $1.49 \times 10^{10} l_p < r < 3.86 \times 10^{12} l_p$. Therefore, the weak energy violation condition is violated in two regions beyond the throat of this wormhole. This result is also the same as that of the zero-temperature case.

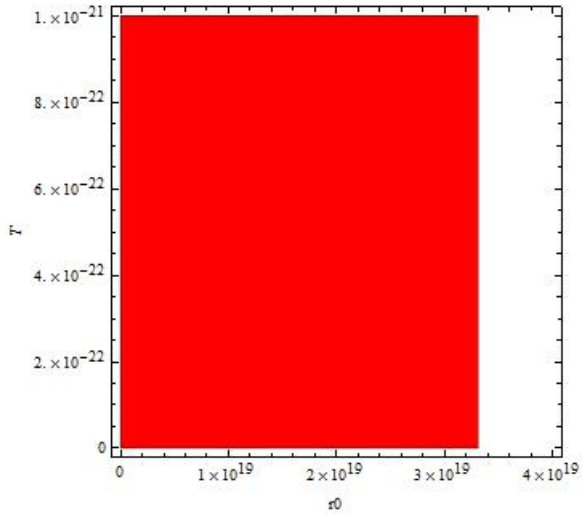

Figure 5. 7: ζ_0 and τ_0 of a quantized neutrino field as functions of T and r_0 for simple wormholes. Both $\zeta_0 > 0$ and $\tau_0 > 0$ for $r_0 < 3.32 \times 10^{19} l_p$.

B. The proton field

The stress-energy tensor components of a quantized proton field at the

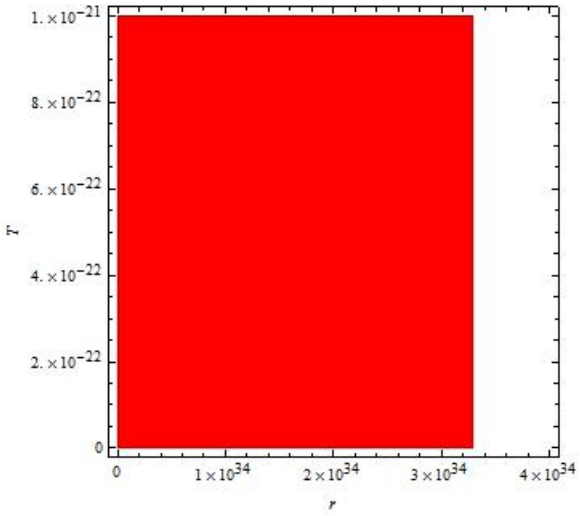

Figure 5. 8: ζ and τ of a quantized neutrino field as functions of T and r for a simple wormhole whose throat radius is $r_0 = 3.32 \times 10^{19} l_p$. Both $\zeta > 0$ and $\tau > 0$ for $r < 3.29 \times 10^{34} l_p$.

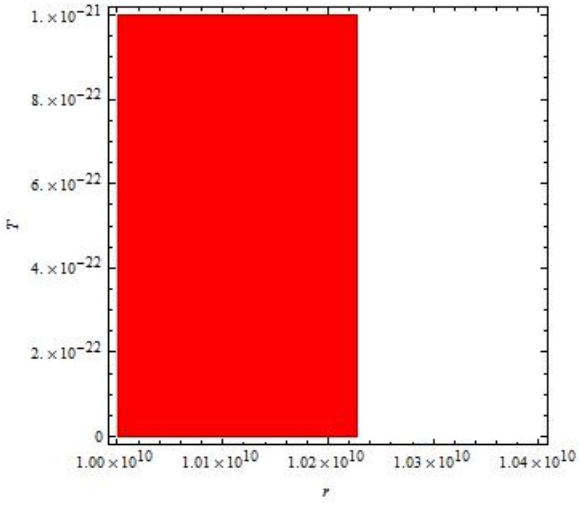

Figure 5. 9: ζ and τ of a quantized neutrino field as functions of T and r for a simple wormhole whose throat radius is $r_0 = 10^{10} l_p$. Both $\zeta > 0$ and $\tau > 0$ for $10^{10} l_p < r < 1.02 \times 10^{10} l_p$.

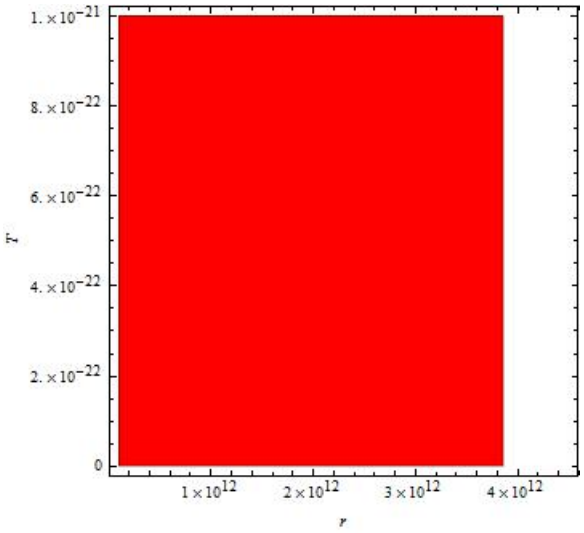

Figure 5. 10: ζ and τ of a quantized neutrino field as functions of T and r for a simple wormhole whose throat radius is $r_0 = 10^{10} l_p$. Both $\zeta > 0$ and $\tau > 0$ for $1.49 \times 10^{10} l_p < r < 3.86 \times 10^{12} l_p$.

throat of the simple wormhole are found to be (in units of F_p/l_p^2):

$$< T_t^t >_0 = \frac{1.0 \times 10^{35}}{r_0^8} - \frac{4.0 \times 10^{35}}{r_0^6} - \frac{0.02}{r_0^4} - \frac{2.7 \times 10^{-41}}{r_0^2} + 4.9 \times 10^{-40} T^2 - \frac{0.01 T^2}{r_0^2} - 1.2 T^4 - \frac{1.6 \times 10^{-11} (\ln T)}{r_0^4}, \tag{5.18}$$

$$< T_r^r >_0 = -\frac{1.0 \times 10^{35}}{r_0^8} - \frac{4.2 \times 10^{36}}{r_0^6} - \frac{0.5}{r_0^4} + \frac{0.002}{r_0^3} - \frac{2.1 \times 10^{-17}}{r_0^2} + \frac{2.6 \times 10^{-18}}{r_0} - 4.9 \times 10^{-40} T^2 - \frac{0.01 T^2}{r_0^2} + 0.4 T^4 - \frac{0.01 (\ln T)}{r_0^4}, \tag{5.19}$$

$$< T^{\theta}_{\theta} >_0 = 3.7 \times 10^{-79} + \frac{2.3 \times 10^{36}}{r_0^6} - \frac{0.2}{r_0^4} - \frac{4.7 \times 10^{-41}}{r_0^2} - 4.9 \times 10^{-40} T^2 + \frac{0.01 T^2}{r_0^2} + 0.4 T^4 - \frac{0.005 (\ln T)}{r_0^4}. \quad (5.20)$$

These expressions exhibit the same hierarchy of coefficients as in the previous cases. The implication is the same: smaller values of r_0 contribute more to the stress-energy tensor, and temperature plays a negligible part.

Figure 5.11 is plotted for ζ_0 and τ_0 as functions of T and r_0 for simple wormholes in thermal states. Both $\zeta_0 > 0$ and $\tau_0 > 0$ for $r_0 < 1.34 \times 10^{13} l_p$. This means that a quantized proton field is exotic for simple wormholes with a throat radius $r_0 < 1.34 \times 10^{13} l_p$ in thermal states. It is the same as in the zero-temperature case.

I also have computed the stress-energy tensor components in the entire spacetime for simple wormhole geometry in thermal states. I list them in Appendix D. Here I present Figure 5.12 and Figure 5.13 to show ζ and τ as functions of T and r for two simple wormholes of different size for which the quantized proton field is exotic. Figure 5.12 is plotted for a simple wormhole with the maximum possible throat radius, $r_0 = 1.34 \times 10^{13} l_p$. The figure shows that both $\zeta > 0$ and $\tau > 0$ for $1.34 \times 10^{13} l_p < r < 7.65 \times 10^{22} l_p$. This suggests that the weak energy condition violation extends well beyond the throat of the wormhole, and is independent of temperature.

Figure 5.13 is plotted for a simple wormhole whose throat radius is $r_0 = 10^8 l_p$. The figure shows that both $\zeta > 0$ and $\tau > 0$ for $10^8 l_p < r < 5.76 \times$

$10^{21} l_p$. This implies that the weak energy condition is violated in this region, independent of temperature.

It should be noted that for both wormholes, the magnitudes of the weak energy condition violation in the entire spacetime of the wormhole geometry for which the field is exotic are the same as in the zero-temperature case.

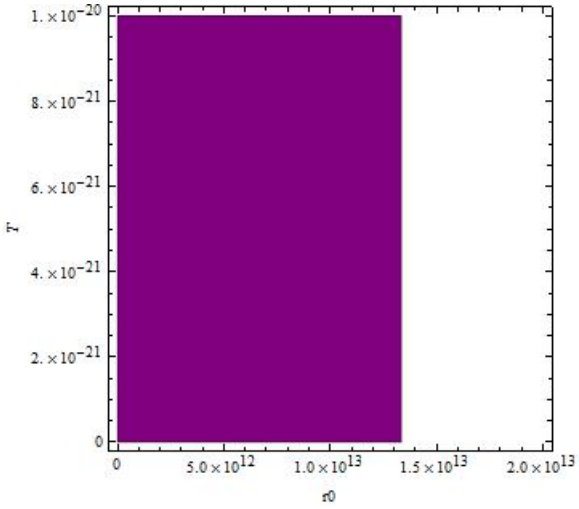

Figure 5. 11: ζ_0 and τ_0 of a quantized proton field as functions of T and r_0 for simple wormholes. Both $\zeta_0 > 0$ and $\tau_0 > 0$ for $r_0 < 1.34 \times 10^{13} l_p$.

5.2.3 Proximal Schwarzschild wormhole

The metric of this type of wormhole is similar to the Schwarzschild metric except for an additional term in g_{tt}:

$$-\mathrm{g_{tt}} = 1 - \frac{\mathrm{r_0}}{\mathrm{r}} + \frac{\epsilon}{\mathrm{r^2}}. \tag{5.21}$$

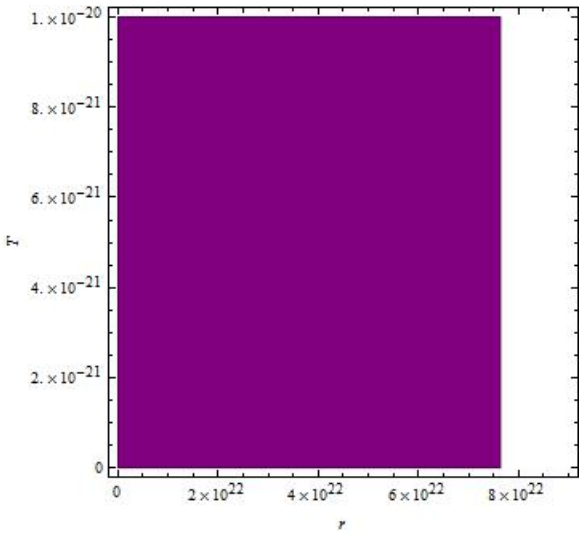

Figure 5. 12: ζ and τ of a quantized proton field as functions of T and r for a simple wormhole whose throat radius is $r_0 = 1.34 \times 10^{13} l_p$. Both $\zeta > 0$ and $\tau > 0$ for $1.34 \times 10^{13} l_p < r < 7.65 \times 10^{22} l_p$.

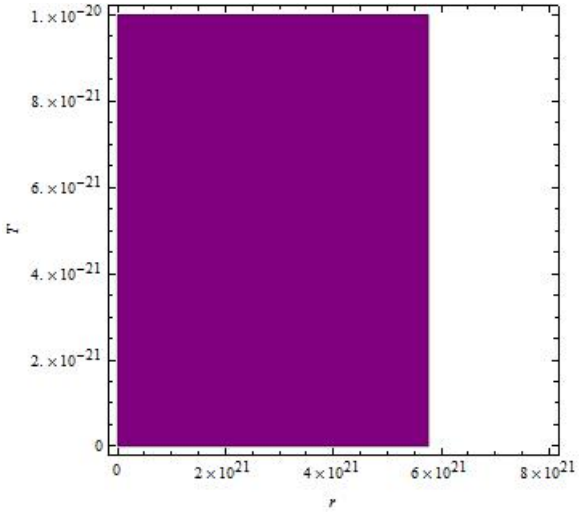

Figure 5. 13: ζ and τ of a quantized proton field as functions of T and r for a simple wormhole whose throat radius is $r_0 = 10^8 l_p$. Both $\zeta > 0$ and $\tau > 0$ for $10^8 l_p < r < 5.76 \times 10^{21} l_p$.

The parameter ϵ is a small positive constant which satisfies $\epsilon \ll r_0^2$ [39]. This parameter prevents the appearance of an event horizon in this wormhole spacetime and keeps the wormhole traversable. Due to its similarity to the Schwarzschild spacetime, this type of wormhole is called proximal Schwarzschild wormhole. For this type of wormhole,

$$\Phi(r) = \frac{1}{2}\ln(1 - \frac{r_0}{r} + \frac{\epsilon}{r^2}), \tag{5.22}$$

$$b(r) = r_0. \tag{5.23}$$

Accordingly,

$$f(r) = 1 - \frac{r_0}{r} + \frac{\epsilon}{r^2}, \tag{5.24}$$

$$h(r) = (1 - \frac{r_0}{r})^{-1}. \tag{5.25}$$

A. The neutrino field

For the proximal Schwarzschild wormhole, the stress-energy tensor components of a quantized neutrino field are too complicated to list here. So I list them in Appendix E. However, I plot the graphs of ζ and τ as functions of r, ϵ and T at the wormhole's throat as well as in the entire spacetime.

Figure 5.14 is plotted for ζ_0 and τ_0 as functions of r_0, ϵ and T. The figure shows that both ζ_0 and τ_0 are positive for $r_0 < 3.57 \times 10^{19} l_p$, independent of temperature. This means that a quantized neutrino field is exotic for this type of wormhole with a throat radius $r_0 < 3.57 \times 10^{19} l_p$. It is the same as that of the zero-temperature case.

Figure 5.15 and Figure 5.16 are plotted for ζ and τ as functions of r, ϵ and T in the entire spacetime of this wormhole geometry for which the quantized neutrino field is exotic. To illustrate the figures more conveniently, I define r_c to be the critical value of r below which the weak energy condition is violated, and ϵ_c the critical value of ϵ above which the weak energy condition is violated. Figure 5.15 is plotted for a proximal Schwarzschild wormhole that has the maximum possible throat radius, $r_0 = 3.57 \times 10^{19} l_p$ for which the quantized neutrino field is exotic. I plot ϵ up to 10^{36} to ensure that $\epsilon < 1\%$ of r_0^2. This figure shows that r_c increases as ϵ_c increases. For $\epsilon_c = 10^{36}, r_c \approx 2.9 \times 10^{34} l_p$. This maximum coordinate distance is smaller than that of the zero-temperature case, which is $1.3 \times 10^{102} l_p$.

Figure 5.16 is plotted for a proximal Schwarzschild wormhole with a smaller throat radius, $r_0 = 10^{10} l_p$. I plot ϵ up to 10^{18} to ensure that $\epsilon < 1\%$ of r_0^2. This figure shows a similar pattern as that of Figure 5.10: r_c increases as ϵ_c increases; as ϵ_c reaches its maximum value of $10^{18}, r_c \approx 8 \times 10^{15} l_p$. Comparing this with the results shown in Figure 5.15, we see that the weak energy condition violation extends to the maximum coordinate distance of $r_c \approx 2.9 \times 10^{34} l_p$ for this type of wormhole. It occurs with a wormhole that has the maximum throat radius for which the quantized neutrino field is exotic.

B. The proton field

I have computed the stress-energy tensor components of a quantized proton field in the entire spacetime of the proximal Schwarzschild wormhole

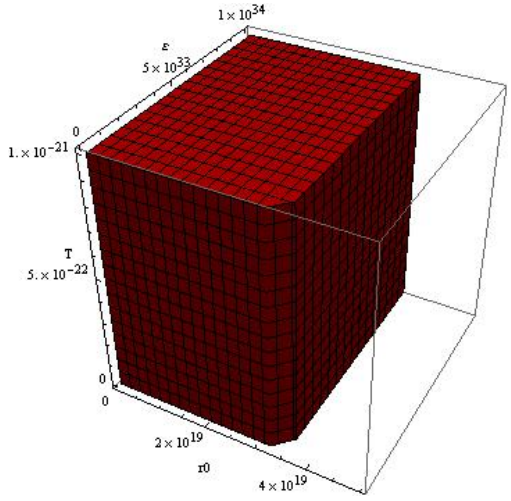

Figure 5. 14: ζ_0 and τ_0 of a quantized neutrino field as functions of r_0, ϵ, and T for proximal Schwarzschild wormholes. Both $\zeta_0 > 0$ and $\tau_0 > 0$ in the solid region.

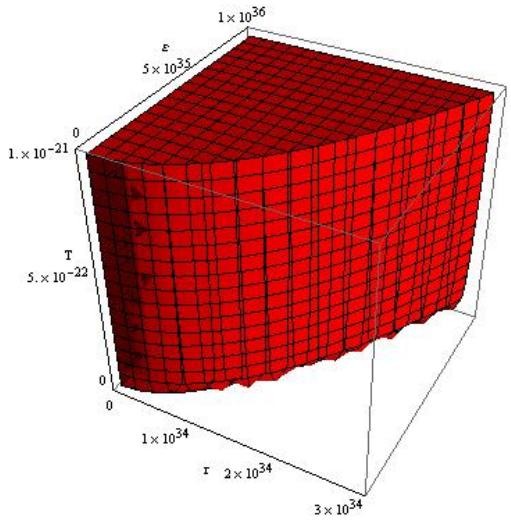

Figure 5. 15: ζ and τ of a quantized neutrino field as functions of T, r, and ϵ for a proximal Schwarzschild wormhole whose throat radius is $r_0 = 3.57 \times 10^{19} l_p$. Both $\zeta_0 > 0$ and $\tau_0 > 0$ in the solid region.

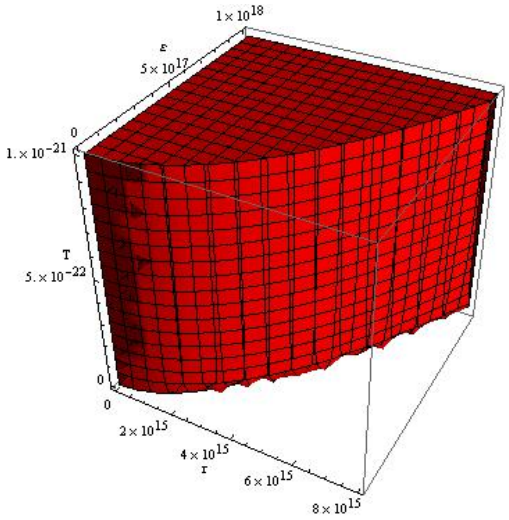

Figure 5. 16: ζ and τ of a quantized neutrino field as functions of T, r, and ϵ for a proximal Schwarzschild wormhole whose throat radius is $r_0 = 10^{10} l_p$. Both $\zeta_0 > 0$ and $\tau_0 > 0$ in the solid region.

geometry as well as at the wormhole's throat. They are too complicated to list here. So I put them in Appendix E.

Figure 5.17 is a plot of ζ_0 and τ_0 as functions of r_0, ϵ, and T for proximal Schwarzschild wormholes. I plot ϵ up to 10^{21} to ensure that the condition $\epsilon \ll r_0^2$ be met. This figure shows that both ζ_0 and τ_0 are positive for $r_0 < 1.41 \times 10^{13} l_p$, independent of the values of ϵ and T. So a quantized proton field is exotic for proximal Schwarzschild wormholes with $r_0 < 1.41 \times 10^{13} l_p$. This is the same as in the case of zero temperature.

Figure 5.18 is plotted for ζ and τ as functions of r, ϵ, and T for a proximal Schwarzschild wormhole that has the maximum possible throat radius, $r_0 = 1.41 \times 10^{13} l_p$, for which the quantized proton field is exotic. I plot ϵ up to 10^{24}

to ensure $\epsilon < 1\%$ of r_0^2. This figure shows that r_c increases as ϵ_c increases. As $\epsilon_c = 10^{24}, r_c \approx 8 \times 10^{21} l_p$. So, the weak energy condition is violated up to the coordinate distance $r \approx 8 \times 10^{21} l_p$ for this wormhole.

Figure 5.19 is plotted for ζ and τ as functions of r, ϵ, and T for a proximal Schwarzschild wormhole that has a smaller throat radius, $r_0 = 10^8 l_p$. I plot ϵ up to 10^{14} to ensure $\epsilon < 1\%$ of r_0^2. This figure also shows that r_c increases as ϵ_c increases. As $\epsilon_c = 10^{14}, r_c \approx 8 \times 10^{11} l_p$. So, the weak energy condition is violated up to the coordinate distance $r \approx 8 \times 10^{11} l_p$ for this wormhole.

Comparing Figure 5.18 and Figure 5.19, we see that the weak energy condition violation extends further in the spacetime for a bigger wormhole. The maximum violation in the spacetime, $r \approx 8 \times 10^{21} l_p$, occurs with a wormhole that has the maximum throat radius for which the quantized proton field is exotic. However, this value is smaller than that of the zero-temperature case, which is $1.0 \times 10^{52} l_p$.

5.2.4 Wormhole with finite radial cutoff of stress-energy

The last type of wormhole that I examine is the wormhole with finite radial cutoff of the stress-energy. The metric of this type of wormhole is:

$$\Phi(r) = 0, \tag{5.26}$$

$$b(r) = r_0 (\frac{r}{r_0})^{1-\eta}. \tag{5.27}$$

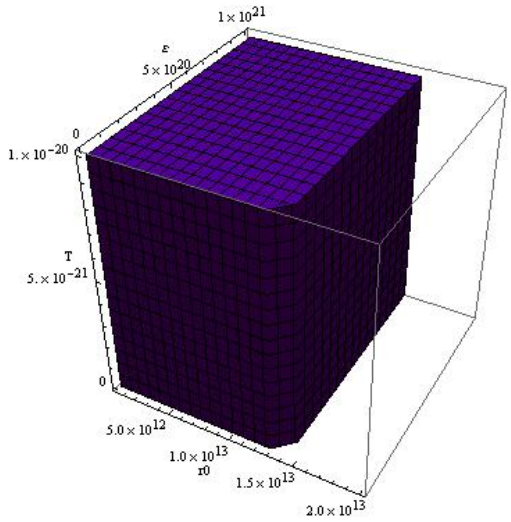

Figure 5. 17: ζ_0 and τ_0 of a quantized proton field as functions of T, r_0, and ϵ for proximal Schwarzschild wormholes. Both $\zeta_0 > 0$ and $\tau_0 > 0$ in the solid region ($r_0 < 1.41 \times 10^{13} l_p$).

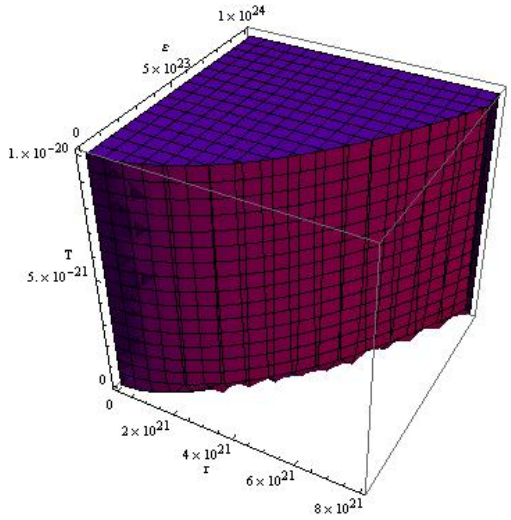

Figure 5. 18: ζ and τ of a quantized proton field as functions of T, r, and ϵ for a proximal Schwarzschild wormhole whose throat radius is $r_0 = 1.41 \times 10^{13} l_p$. Both $\zeta > 0$ and $\tau > 0$ in the solid region.

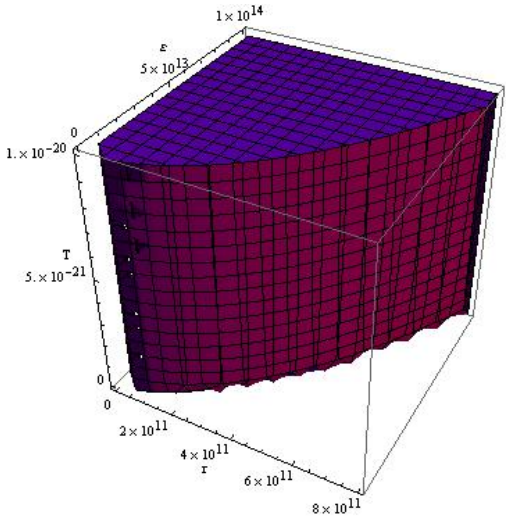

Figure 5. 19: ζ and τ of a quantized proton field as functions of T, r, and ϵ for a proximal Schwarzschild wormhole whose throat radius is $r_0 = 10^8 l_p$. Both $\zeta > 0$ and $\tau > 0$ in the solid region.

where η is a constant bounded by $0 < \eta < 1$. Accordingly,

$$f(r) = 1, \tag{5.28}$$

$$h(r) = [1 - (\frac{r_0}{r})^{\eta}]^{-1}. \tag{5.29}$$

I have computed the stress-energy tensor components in the entire spacetime for this type of wormhole as well as those at the wormhole's throat. They are also too complicated to list here. So I put them in Appendix F.

A. The neutrino field

Figure 5.20 is plotted for ζ_0 and τ_0 as functions of r_0 and η. This figure shows that both ζ_0 and τ_0 are positive for r_0 up to around $0.6 l_p$, independent

of temperature. So a quantized neutrino field is exotic for this type of wormhole with a throat radius r_0 up to around $0.6l_p$. This is the same as that in the zero-temperature case.

Figure 5.21 and Figure 5.22 are plotted to examine the weak energy condition violation in the entire spacetime for two wormholes of different size for which the quantized neutrino field is exotic. Figure 5.21 is plotted for a wormhole whose throat radius is $r_0 = 0.59l_p$. This figure shows that r_c increases slightly as η increases. For $\eta = 0, r_c = 0.592l_p$. For $\eta = 1, r_c = 0.617l_p$. Figure 5.22 is plotted for a wormhole whose throat radius is $r_0 = 0.4l_p$. This figure shows the same pattern as in Figure 5.21. r_c increases slightly as η increases. For $\eta = 0, r_c = 0.59l_p$. For $\eta = 1, r_c = 0.62l_p$. From these two figures we see that the region of the weak energy condition violation in the entire spacetime for this type of wormhole is independent of the wormhole's size, and also independent of temperature. It varies slightly as η varies, however. The maximum violation extends to the coordinate distance $r_c = 0.62l_p$, which occurs for $\eta = 1$. This result is the same as that of the zero-temperature case.

B. The proton field

Figure 5.23 is plotted for ζ_0 and τ_0 as functions of r_0, η, and T for wormholes with finite radial cutoff of stress-energy. This figure shows that both ζ_0 and τ_0 are positive for r_0 up to around $0.6l_p$, independent of temperature. This means that a quantized proton field is exotic for this type of wormhole with a throat radius around $0.6l_p$. It is the same as in the case of the

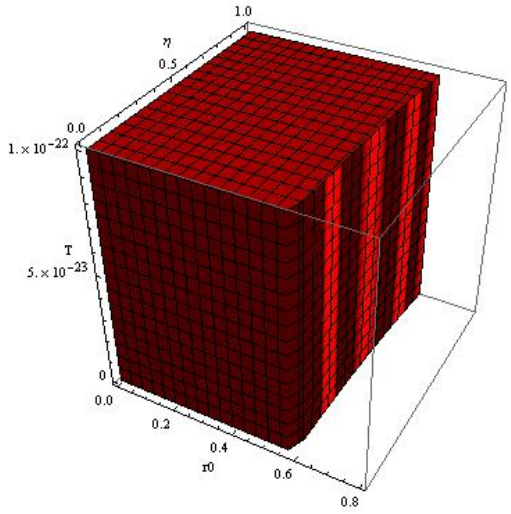

Figure 5. 20: ζ_0 and τ_0 of a quantized neutrino field as functions of T, r_0, and η for wormholes with finite radial cutoff of stress-energy. Both $\zeta_0 > 0$ and $\tau_0 > 0$ in the solid region.

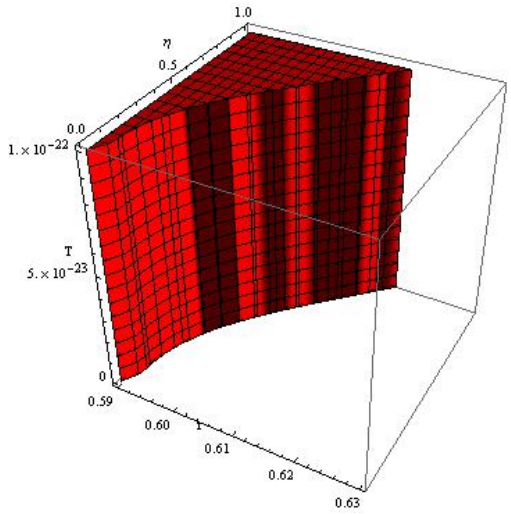

Figure 5. 21: ζ and τ of a quantized neutrino field as functions of T, r, and η for a wormhole with finite radial cutoff of stress-energy, whose throat radius is $r_0 = 0.59 l_p$. Both $\zeta_0 > 0$ and $\tau_0 > 0$ in the solid region.

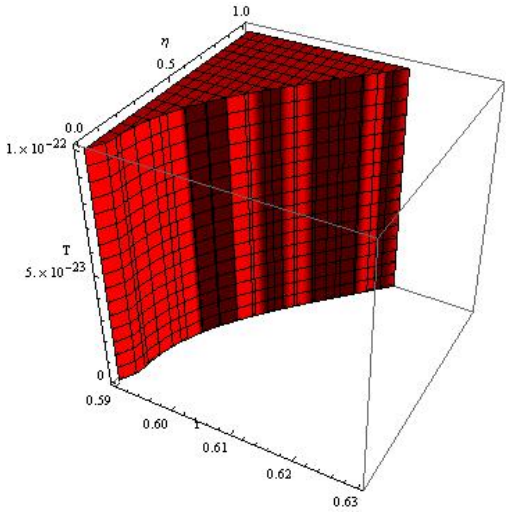

Figure 5. 22: ζ and τ of a quantized neutrino field as functions of T, r, and η for a wormhole with finite radial cutoff of stress-energy, whose throat radius is $r_0 = 0.40l_p$. Both $\zeta_0 > 0$ and $\tau_0 > 0$ in the solid region.

quantized neutrino field.

In Figure 5.24 and Figure 5.25 I plot ζ and τ as functions of r, η, and T beyond the wormhole's throat to examine the weak energy condition violation in the entire spacetime. Figure 5.24 is plotted for a wormhole whose throat radius is $r_0 = 0.59l_p$. The figure shows that r_c increases slightly as η increases. For $\eta = 0, r_c = 0.59l_p$. For $\eta = 1, r_c = 0.62l_p$. Figure 5.25 is plotted for a wormhole with a smaller throat radius, $r_0 = 0.40l_p$. However, this figure shows the same pattern as Figure 5.24. r_c increases slightly as η increases. For $\eta = 0, r_c = 0.59l_p$. For $\eta = 1, r_c = 0.62l_p$.

These two figures show that the weak energy condition violation is independent of the wormhole's size, and also independent of temperature. How-

ever, it varies slightly for different values of η. The maximum violation extends to the radial distance $r_c = 0.62 l_p$, which occurs for $\eta = 1$. This result is the same as that of the neutrino field, and also the same as that of the zero-temperature case.

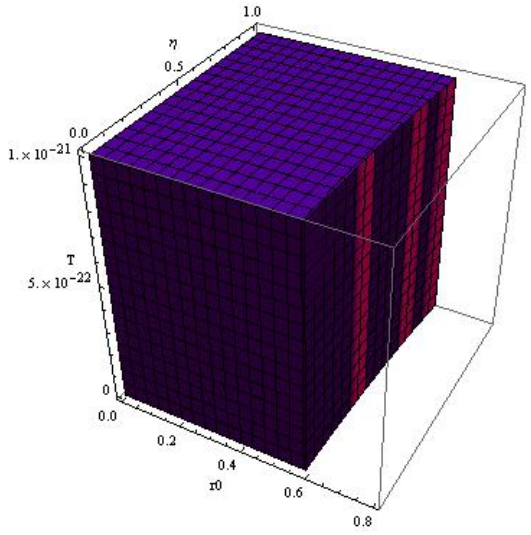

Figure 5. 23: ζ_0 and τ_0 of a quantized proton field as functions of T, r_0, and η for wormholes with finite radial cutoff of stress-energy. Both $\zeta_0 > 0$ and $\tau_0 > 0$ in the solid region.

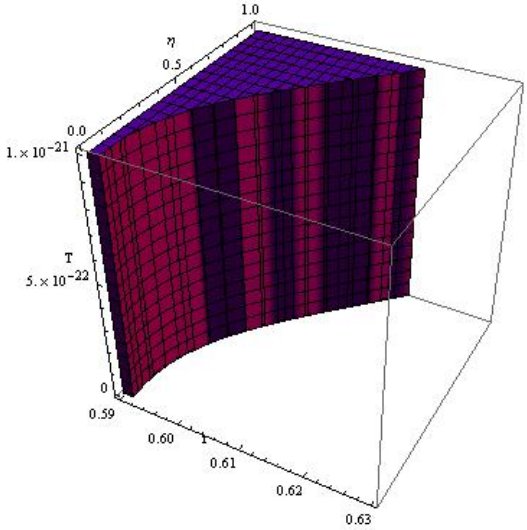

Figure 5. 24: ζ and τ of a quantized proton field as functions of T, r, and η for a wormhole with finite radial cutoff of stress-energy, whose throat radius is $r_0 = 0.59 l_p$. Both $\zeta > 0$ and $\tau > 0$ in the solid region.

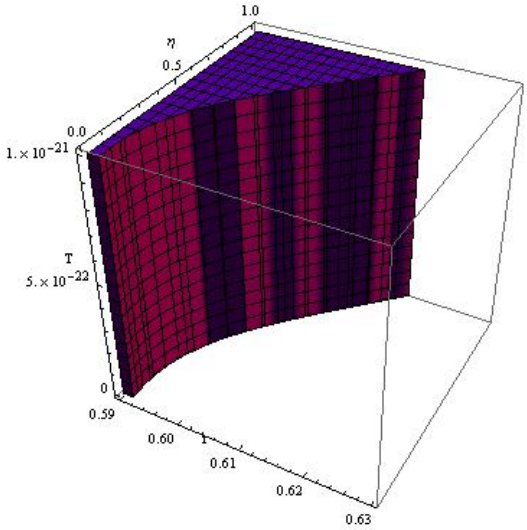

Figure 5. 25: ζ and τ of a quantized proton field as functions of T, r, and η for a wormhole with finite radial cutoff of stress-energy, whose throat radius is $r_0 = 0.40 l_p$. Both $\zeta > 0$ and $\tau > 0$ in the solid region.

Chapter 6. Summary and Concluding Remarks

I have calculated the stress-energy tensor of a quantized Dirac neutrino field and a quantized proton field for four types of wormhole spacetime in a zero-temperature vacuum state as well as in thermal states. I have also examined the weak energy condition violation at the throat of these wormholes as well as in the entire spacetime of these wormhole geometries. I find that, both in the zero-temperature vacuum state and in thermal states, the weak energy condition is violated at the throats of all the four types of wormhole to different size, and the violation extends more or less beyond the wormholes' throats. These findings suggest that the two fields are exotic for the four wormhole geometries up to different radial distances, and temperature does not exert influence on the results.

However, the results of computation show that some components of the stress-energy tensor have values well beyond the Planckian scale. For example, in Figure 4.1 and Figure 4.2, ζ_0 and τ_0 are on the scale of 10^{54} Planckian energy density units; in Figure 4.3, ζ_0 and τ_0 are on the scale of 10^{56} Planck-

ian energy density units. At such high energy levels, quantum field theory in curved spacetime is not credible. In addition, some approximations are used in the computation, for which the uncertainties are difficult to assess. Due to these reasons, no firm physical conclusions can be drawn.

In the following sections, I will summarize the mathematical structure that I have found.

6.1 Zero-temperature vacuum state

6.1.1 At the throat of the wormhole

First, for the zero-tidal-force wormhole, both a quantized neutrino field and a quantized proton field are exotic for wormholes with throat radius $r_0 < 1.26 l_p$. Second, for the simple wormhole, a quantized neutrino field is exotic for wormholes with $r_0 < 3.32 \times 10^{19} l_p$, while a quantized proton field is exotic for wormholes with $r_0 < 1.33 \times 10^{13} l_p$. Third, for the proximal Schwarzschild wormhole, a quantized neutrino field is exotic for wormholes with $r_0 < 3.57 \times 10^{19} l_p$, while a quantized proton field is exotic for wormholes with $r_0 < 1.41 \times 10^{13} l_p$. Fourth, for the wormhole with finite radial cutoff in background stress-energy tensor, both quantized neutrino field and quantized proton field are exotic for wormholes with a throat radius r_0 up to around $0.6 l_p$.

Of the four types of wormhole spacetime, the two fields under investigation are exotic around a Planck length for two types of wormhole spacetime

(the zero-tidal-force wormhole and the wormhole with finite radial cutoff of the stress-energy tensor); for the other two types of wormhole spacetime (the simple wormhole and the proximal Schwarzschild wormhole), these two fields are exotic up to a throat radius much bigger than the Planck length, but the throat is still too small for human beings to traverse. Of all the wormholes for which these two fields are exotic, the biggest is the proximal Schwarzschild wormhole for which the quantized neutrino field is exotic, with a throat radius up to $3.57 \times 10^{19} l_p$. This is the scale of a proton.

6.1.2 In the vicinity of the wormhole's throat

My calculations show that the weak energy condition is violated more or less in the vicinity of the four types of wormholes at zero temperature. For two types of wormhole (the zero-tidal-force wormhole and the wormhole with radial cutoff of energy), the violation of the weak energy condition is limited to the boundary of the maximum radius of the throat for which these two fields are exotic; for the other two types of wormholes (the simple wormhole and the proximal Schwarzschild wormhole), the violation extends beyond the wormholes' throat for which these two fields are exotic. The maximum extension of the weak energy condition violation, which is $1.3 \times 10^{102} l_p$, occurs with the proximal Schwarzschild wormhole for which the quantized neutrino field is exotic.

6.2 Thermal states

6.2.1 At the throat of the wormhole

In thermal states, both quantized neutrino field and quantized proton field are exotic for all the four types of wormholes under investigation. The sizes of these wormholes for which these two fields are exotic are identical to those in the zero-temperature case. This shows that temperature exerts no influence on the exotic nature of these two fields in the four wormhole geometries.

6.2.2 In the vicinity of the wormhole's throat

In thermal states, the violation of the weak energy condition also extends to some degree beyond the wormholes' throat. However, for the proximal Schwarzschild wormhole, the weak energy condition violation is limited in a smaller region in the thermal states than that of the zero-temperature state. For the other three types of wormhole, the weak energy condition violation extends to the same extent as those of the zero-temperature case.

6.3 Semiclassical Einstein equation

Although the quantized neutrino field and the quantized proton field violate the weak energy condition and can be considered exotic matter, their stress-energy components do not satisfy Eq. (2.2) whose solution is a wormhole spacetime. First, the underlying assumption of the quantum field theory

in curved spacetime is that the energy and spacetime curvature are well below the Planckian scale, so the left-hand side of Eq. (2.2), which is the curvature of the wormhole spacetime, must be non-Planckian scale; but the right-hand side of Eq. (2.2), which are components of the two fields under investigation, are sometime on Planckian scale. Second, the renormalized stress-energy tensor components of a quantized massive spin 1/2 field are given by Eqs. (B1) through (B3). For a given wormhole spacetime at a given temperature, the parameters f, h, r_0 and κ are fixed and the spacetime curvature $G_{\mu\nu}$, the left-hand side of Eq. (2.2), is fixed; however, for different fields, the field quanta m are different, thus the stress-energy tensor components, the right-hand side of Eq. (2.2), have different values and cannot be equal to the left-hand side of this equation. Due to these reasons, these two fields cannot be the source of matter of wormhole spacetimes.

6.4 Summary of findings

I summarize my findings in the following three tables.

Category	Quantized neutrino field	Quantized proton field
Zero-tidal-force wormhole	$1.26 l_p$	$1.26 l_p$
Simple wormhole	$3.32 \times 10^{19} l_p$	$1.33 \times 10^{13} l_p$
Proximal Schwarzschild wormhole	$3.57 \times 10^{19} l_p$	$1.41 \times 10^{13} l_p$
Wormhole with radial energy cutoff	around $0.6 l_p$	around $0.6 l_p$

Table 1: Maximum value of r_0 for which the quantized massive spin 1/2 fields are exotic, both at zero temperature and in thermal states.

Category	Quantized neutrino field	Quantized proton field
Zero-tidal-force wormhole	$1.26 l_p$	$1.26 l_p$
Simple wormhole	$3.29 \times 10^{34} l_p$	$7.65 \times 10^{22} l_p$
Proximal Schwarzschild wormhole	$1.3 \times 10^{102} l_p$	$1.0 \times 10^{52} l_p$
Wormhole with radial energy cutoff	around $0.6 l_p$	around $0.6 l_p$

Table 2: Maximum radial extension of the weak energy condition violation beyond the wormhole's throat at zero temperature.

Category	Quantized neutrino field	Quantized proton field
Zero-tidal-force wormhole	$1.26 l_p$	$1.26 l_p$
Simple wormhole	$3.29 \times 10^{34} l_p$	$7.65 \times 10^{22} l_p$
Proximal Schwarzschild wormhole	$2.9 \times 10^{34} l_p$	$8 \times 10^{21} l_p$
Wormhole with radial energy cutoff	$0.62 l_p$	$0.62 l_p$

Table 3: Maximum radial extension of the weak energy condition violation beyond the wormhole's throat in thermal states.

6.5 Topics for future study

My research and some previous research [11, 12] have confirmed that exotic matter exists for microscopic wormholes. However, for human beings to make use of wormholes, exotic matter must be found for macroscopic wormholes. Such wormholes are proposed in [12, 13, 16, 17], yet they are speculative and lack evidence of existence. Topics for future study include exploration on the possibility of macroscopic wormholes. Specifically, one topic is to find what substance can make Ω and K, two functions in [13, 14], behave properly so that a macroscopic wormhole can be sustained. Another topic is to verify the existence of the phantom energy proposed in [16, 17], and the wormholes supported by the phantom energy. A third topic is to verify that macroscopic wormholes can truly grow out of microscopic ones

due to the accelerating expansion of the universe, as proposed in [16, 17].

Appendix A: Stress-Energy Tensor of A Quantized Massive Spin 1/2 Field in A Static Spherically Symmetric Spacetime

As introduced in Chapter 2, P. Groves [40] derived an expression for the renormalized stress-energy tensor of a quantized massive spin 1/2 field in a static spherically symmetric spacetime, which is given by Eq. (2.47). In this equation, $< T_{\mu\nu} >_{analytic}$ also includes two parts:

$$< T_{\mu\nu} >_{analytic} = (T_{\mu\nu})_0 + (T_{\mu\nu})_{log} \tag{A1}$$

with [40]

$$\begin{aligned}(T_t^t)_0 \;=\; & \frac{1}{240\pi^2}[-\frac{15m^4}{2}+\frac{1}{r^4}-\frac{5m^2}{r^2}-\frac{7\kappa^4}{4f(r)^2}+\frac{5\kappa^2m^2}{f(r)}+\frac{5\kappa^2}{6r^2f(r)} \\ & -\frac{1}{r^4h(r)^2}+\frac{5m^2}{r^2h(r)}-\frac{5\kappa^2}{6r^2f(r)h(r)}+\frac{5\kappa^2f'(r)}{3rf(r)^2h(r)}+\frac{10m^2f'(r)}{rf(r)h(r)} \\ & +\frac{43f'(r)^2}{24r^2f(r)^2h(r)^2}-\frac{25\kappa^2f'(r)^2}{24f(r)^3h(r)}-\frac{5m^2f'(r)^2}{4f(r)^2h(r)}-\frac{5f'(r)^2}{8r^2f(r)^2h(r)}\end{aligned}$$

$$
\begin{aligned}
&-\frac{9f'(r)^3}{2rf(r)^3h(r)^2}+\frac{77f'(r)^4}{192f(r)^4h(r)^2}-\frac{2h'(r)}{r^3h(r)^3}-\frac{5m^2h'(r)}{rh(r)^2}\\
&+\frac{5\kappa^2h'(r)}{6rf(r)h(r)^2}+\frac{15f'(r)h'(r)}{4r^2f(r)h(r)^3}-\frac{5\kappa^2f'(r)h'(r)}{12f(r)^2h(r)^2}-\frac{5m^2f'(r)h'(r)}{2f(r)h(r)^2}\\
&-\frac{5f'(r)h'(r)}{12r^2f(r)h(r)^2}-\frac{15f'(r)^2h'(r)}{8rf(r)^2h(r)^3}+\frac{f'(r)^3h'(r)}{24f(r)^3h(r)^3}-\frac{7h'(r)^2}{4r^2h(r)^4}\\
&-\frac{3f'(r)h'(r)^2}{2rf(r)h(r)^4}-\frac{19f'(r)^2h'(r)^2}{32f(r)^2h(r)^4}+\frac{7h'(r)^3}{rh(r)^5}-\frac{7f'(r)h'(r)^3}{4f(r)h(r)^5}\\
&-\frac{5f''(r)}{6r^2f(r)h(r)^2}+\frac{5\kappa^2f''(r)}{6f(r)^2h(r)}+\frac{5m^2f''(r)}{f(r)h(r)}+\frac{5f''(r)}{6r^2f(r)h(r)}\\
&+\frac{5f'(r)f''(r)}{6rf(r)^2h(r)^2}-\frac{f'(r)^2f''(r)}{12f(r)^3h(r)^2}-\frac{2h'(r)f''(r)}{rf(r)h(r)^3}\\
&+\frac{9f'(r)h'(r)f''(r)}{8f(r)^2h(r)^3}+\frac{19h'(r)^2f''(r)}{8f(r)h(r)^4}-\frac{3f''(r)^2}{8f(r)^2h(r)^2}+\frac{h''(r)}{r^2h(r)^3}\\
&+\frac{f'(r)h''(r)}{2rf(r)h(r)^3}+\frac{f'(r)^2h''(r)}{4f(r)^2h(r)^3}-\frac{13h'(r)h''(r)}{2rh(r)^4}+\frac{13f'(r)h'(r)h''(r)}{8f(r)h(r)^4}\\
&-\frac{f''(r)h''(r)}{f(r)h(r)^3}+\frac{2f^{(3)}(r)}{rf(r)h(r)^2}-\frac{f'(r)f^{(3)}(r)}{2f(r)^2h(r)^2}-\frac{3h'(r)f^{(3)}(r)}{2f(r)h(r)^3}\\
&+\frac{h^{(3)}}{rh(r)^3}-\frac{f'(r)h^{(3)}(r)}{4f(r)h(r)^3}+\frac{f^{(4)}(r)}{2f(r)h(r)^2}],
\end{aligned}
\tag{A2}
$$

$$
\begin{aligned}
(T_r^r)_0 \;=\;& \frac{1}{240\pi^2}[\frac{45m^4}{2}+\frac{5m^2}{r^2}+\frac{7\kappa^4}{12f(r)^2}-\frac{5\kappa^2m^2}{f(r)}-\frac{5\kappa^2}{6r^2f(r)}-\frac{5m^2}{r^2h(r)}\\
&+\frac{5\kappa^2}{6r^2f(r)h(r)}+\frac{2f'(r)}{r^3f(r)h(r)^2}-\frac{5\kappa^2f'(r)}{6rf(r)^2h(r)}+\frac{5m^2f'(r)}{rf(r)h(r)}\\
&-\frac{5f'(r)^2}{8r^2f(r)^2h(r)^2}+\frac{5\kappa^2f'(r)^2}{24f(r)^3h(r)}+\frac{5m^2f'(r)^2}{4f(r)^2h(r)}\\
&+\frac{5f'(r)^2}{24r^2f(r)^2h(r)^3}-\frac{7f'(r)^3}{24rf(r)^3h(r)^2}+\frac{f'(r)^4}{192f(r)^4h(r)^2}\\
&+\frac{f'(r)h'(r)}{2r^2f(r)h(r)^3}-\frac{f'(r)^2h'(r)}{4rf(r)^2h(r)^3}+\frac{f'(r)^3h'(r)}{16f(r)^3h(r)^3}-\frac{7f'(r)h'(r)^2}{4rf(r)h(r)^4}
\end{aligned}
$$

$$+\frac{7f'(r)^2h'(r)^2}{32rf(r)^2h(r)^4}-\frac{2f''(r)}{r^2f(r)h(r)^2}+\frac{2f'(r)f''(r)}{rf(r)^2h(r)^2}-\frac{f'(r)^2f''(r)}{8f(r)^3h(r)^2}$$
$$+\frac{h'(r)f''(r)}{rf(r)h(r)^3}-\frac{f'(r)h'(r)f''(r)}{4f(r)^2h(r)^3}-\frac{f''(r)^2}{8f(r)^2h(r)^2}+\frac{f'(r)h''(r)}{rf(r)h(r)^3}$$
$$-\frac{f'(r)^2h''(r)}{8f(r)^2h(r)^3}-\frac{f^{(3)}(r)}{rf(r)h(r)^2}+\frac{f'(r)f^{(3)}(r)}{4f(r)^2h(r)^2}] \qquad \text{(A3)}$$

$$(T^{\theta}_{\theta})_0 = (T^{\phi}_{\phi})_0=\frac{1}{240\pi^2}[\frac{45m^4}{2}+\frac{7\kappa^4}{12f(r)^2}-\frac{5\kappa^2m^2}{f(r)}-\frac{f'(r)}{r^3f(r)h(r)^2}$$
$$+\frac{5m^2h'(r)}{2rh(r)^2}+\frac{5m^2f'(r)}{2rf(r)h(r)}+\frac{5\kappa^2f'(r)^2}{12f(r)^3h(r)}-\frac{3f'(r)^3}{16rf(r)^3h(r)^2}$$
$$+\frac{29f'(r)^4}{64f(r)^4h(r)^2}-\frac{5\kappa^2f'(r)}{12rf(r)^2h(r)}-\frac{5\kappa^2h'(r)}{12rf(r)h(r)^2}-\frac{3f'(r)h'(r)}{2r^2f(r)h(r)^3}$$
$$+\frac{5\kappa^2f'(r)h'(r)}{24f(r)^2h(r)^2}-\frac{5m^2f'(r)h'(r)}{4f(r)h(r)^2}-\frac{7f'(r)^2h'(r)}{16rf(r)^2h(r)^3}+\frac{73f'(r)^3h'(r)}{96f(r)^3h(r)^3}$$
$$-\frac{3f'(r)h'(r)^2}{4rf(r)h(r)^4}+\frac{31f'(r)^2h'(r)^2}{32f(r)^2h(r)^4}+\frac{7f'(r)h'(r)^3}{4f(r)h(r)^5}+\frac{f''(r)}{r^2f(r)h(r)^2}$$
$$-\frac{5\kappa^2f''(r)}{12f(r)^2h(r)}+\frac{5m^2f''(r)}{2f(r)h(r)}+\frac{7f'(r)f''(r)}{12rf(r)^2h(r)^2}-\frac{73f'(r)^2f''(r)}{48f(r)^3h(r)^2}$$
$$+\frac{11h'(r)f''(r)}{4rf(r)h(r)^3}-\frac{2f'(r)h'(r)f''(r)}{f(r)^2h(r)^3}-\frac{19h'(r)^2f''(r)}{8f(r)h(r)^4}+\frac{7f''(r)^2}{8f(r)^2h(r)^2}$$
$$+\frac{f'(r)h''(r)}{4rf(r)h(r)^3}-\frac{3f'(r)^2h''(r)}{8f(r)^2h(r)^3}-\frac{13f'(r)h'(r)h''(r)}{8f(r)h(r)^4}+\frac{f''(r)h''(r)}{f(r)h(r)^3}$$
$$-\frac{3f^{(3)}(r)}{2rf(r)h(r)^2}+\frac{3f'(r)f^{(3)}(r)}{4f(r)^2h(r)^2}+\frac{3h'(r)f^{(3)}(r)}{2f(r)h(r)^3}+\frac{f'(r)h^{(3)}(r)}{4f(r)h(r)^3}$$
$$-\frac{f^{(4)}(r)}{2f(r)h(r)^2}] \qquad \text{(A4)}$$

$$(T^{\nu}_{\mu})_{log}=-\frac{1}{4\pi^2}U^{\nu}_{\mu}\ln(\frac{\mu f^{1/2}}{2\lambda}) \qquad if T=0 \qquad \text{(A5)}$$

$$(T^{\nu}_{\mu})_{log}=-\frac{1}{4\pi^2}U^{\nu}_{\mu}[\ln(\frac{2\mu f^{1/2}}{\kappa})+C] \qquad if T\neq 0 \qquad \text{(A6)}$$

In Eqs. (A5) and (A6), for the massive case, μ is the mass of the field quantum, while for the massless case, it is an arbitrary renormalization parameter with dimensions of mass. In Eq. (A5), λ is an infrared cutoff, which is necessary only in the zero-temperature case, and C is the Euler's constant. Besides, U_μ^ν is given by [40]

$$\begin{aligned} U_\mu^\nu &= \frac{1}{10}(R^\nu_{\rho\mu\tau}R^{\rho\tau} - \frac{1}{4}R^{\rho\tau}R_{\rho\tau}g^\nu_\mu) - \frac{1}{30}R(R^\nu_\mu - \frac{1}{4}Rg^\nu_\mu) + \frac{1}{20}(R^\nu_\mu)_{;\rho}{}^{\rho} \\ &\quad -\frac{1}{60}R_{;\mu}{}^{\nu} - \frac{1}{120}R_{;\rho}{}^{\rho}g^\nu_\mu \end{aligned} \tag{A7}$$

The quantity $< T_{\mu\nu} >_{numeric}$ is finite in the limit that the points come together. As a result, one can simply set $\tau' = \tau$ in the expression of $< T_{\mu\nu} >_{unren}$ [Eqs. (2.39) through (2.41)] to get the components of $< T_{\mu\nu} >_{numeric}$ [40]:

$$\begin{aligned} < T_t^t >_{num} &= 4\int \frac{d\mu}{r^2 f}[\omega^2 A_1 - \frac{r^2\omega^3}{f} - \omega(\frac{1}{12} - \frac{1}{12h} + \frac{rf'}{6fh} - \frac{5r^2f'^2}{48f^2h} \\ &\quad + \frac{rh'}{12h^2} - \frac{r^2f'h'}{24fh^2} + \frac{r^2f''}{12fh} + \frac{m^2r^2}{2})] + \int \frac{d\mu}{\omega}U_t^t \end{aligned} \tag{A8}$$

$$\begin{aligned} < T_r^r >_{num} &= 4\int \frac{d\mu}{r^2 f}[\frac{\omega A_2 f^{1/2}}{r} - \omega^2 A_1 - f^{1/2}\omega m A_5 + \frac{r^2\omega^3}{3f} + \omega(\frac{1}{12} \\ &\quad -\frac{1}{12h} + \frac{rf'}{12fh} - \frac{r^2f'^2}{48f^2h} + \frac{m^2r^2}{2})] + \int \frac{d\mu}{\omega}U_r^r \end{aligned} \tag{A9}$$

$$< T_\theta^\theta >_{num} = < T_\phi^\phi >_{num} = 2\int \frac{d\mu}{r^2 f}[-\frac{\omega A_2 f^{1/2}}{r} + \frac{2r^2\omega^3}{3f} + \omega(\frac{rf'}{12fh}$$

$$-\frac{r^2 f'^2}{12 f^2 h} + \frac{r h'}{12 h^2} - \frac{r^2 f' h'}{24 f h^2} + \frac{r^2 f''}{12 f h} + m^2 r^2)]$$
$$+ \int \frac{d\mu}{\omega} U^{\theta}_{\theta} \tag{A10}$$

where A_1 through A_5 are functionals of the radial modes $F_{\omega,l}(r)$ and $G_{\omega,l}(r)$, given by:

$$A_1 = Re \sum_{l=0}^{\infty} [(l+1) F^q_{\omega,l+\frac{1}{2}}(r) F^p_{\omega,l+\frac{1}{2}}(r) - l G^q_{\omega,l-\frac{1}{2}}(r) G^p_{\omega,l-\frac{1}{2}}(r) + \frac{r}{f^{1/2}}] \tag{A11}$$

$$\begin{aligned} A_2 &= Re \sum_{l=0}^{\infty} [l(l+1)(G^q_{\omega,l+\frac{1}{2}}(r) F^p_{\omega,l+\frac{1}{2}}(r) + F^q_{\omega,l-\frac{1}{2}}(r) G^p_{\omega,l-\frac{1}{2}}(r)) \\ &\quad - \frac{l(l+1)}{\omega} + \frac{r^2 \omega}{2f}] \end{aligned} \tag{A12}$$

$$\begin{aligned} A_3 &= Re \sum_{l=0}^{\infty} [l(l+1)(F^q_{\omega,l+\frac{1}{2}}(r) F^p_{\omega,l+\frac{1}{2}}(r) + G^q_{\omega,l-\frac{1}{2}}(r) G^p_{\omega,l-\frac{1}{2}}(r)) - \frac{r}{2 f^{1/2}} \\ &\quad + \frac{r}{2 f^{1/2} h^{1/2}} - \frac{r^2 f'}{4 f^{3/2} h^{1/2}} + \frac{m^2 r^2}{2\omega}] \end{aligned} \tag{A13}$$

$$A_4 = Im \sum_{l=0}^{\infty} [(l+1) F^q_{\omega,l+\frac{1}{2}}(r) G^p_{\omega,l+\frac{1}{2}}(r) + l G^q_{\omega,l-\frac{1}{2}}(r) F^p_{\omega,l-\frac{1}{2}}(r)] \tag{A14}$$

$$A_5 = Im \sum_{l=0}^{\infty} [(l+1) G^q_{\omega,l+\frac{1}{2}}(r) G^p_{\omega,l+\frac{1}{2}}(r) + l F^q_{\omega,l-\frac{1}{2}}(r) F^p_{\omega,l-\frac{1}{2}}(r) + \frac{mr}{\omega}] \tag{A15}$$

Appendix B: Resulting Expression of Stress-Energy Tensor of A Quantized Massive Spin 1/2 Field in A Static Spherically Symmetric Spacetime

Using Eqs. (A1) through A(15), the renormalized stress-energy tensor components of a quantized massive spin 1/2 field in a static spherically symmetric spacetime are calculated to be:

$$
\begin{aligned}
< T_t^t >_{ren} \;=\; & -\frac{7\kappa^4}{960f^2\pi^2} + \frac{\kappa^2 m^2}{48f\pi^2} - \frac{m^4}{32\pi^2} + \frac{fm^4}{32\pi^2} + \frac{423f^2}{71680m^2\pi^2r^8} \\
& + \frac{7f^2}{15360h^{3/2}m^2\pi^2r^8} + \frac{991f^2}{161280hm^2\pi^2r^8} + \frac{125f^2}{10752m^2\pi^2r^8} \\
& + \frac{1747f^2}{53760\pi^2r^6} + \frac{9f^2}{5120h\pi^2r^6} + \frac{79f^2}{2560\pi^2r^6} - \frac{1781f}{80640m^2\pi^2r^6} \\
& + \frac{f}{64h^3m^2\pi^2r^6} - \frac{f}{640h^{5/2}m^2\pi^2r^6} + \frac{f}{64h^{3/2}m^2\pi^2r^6} \\
& - \frac{f}{512hm^2\pi^2r^6} - \frac{29f}{1280m^2\pi^2r^6} + \frac{1}{240\pi^2r^4} - \frac{71f}{1280\pi^2r^4} \\
& - \frac{1}{240h^2\pi^2r^4} + \frac{117f}{64h^2\pi^2r^4} + \frac{f}{64h^{3/2}\pi^2r^4} - \frac{3f}{128\pi^2r^4}
\end{aligned}
$$

$$-\frac{49f^2m^2}{5120\pi^2r^4}+\frac{f^2m^2}{512\pi^2r^4}+\frac{\kappa^2}{288f\pi^2r^2}-\frac{\kappa^2}{288fh\pi^2r^2}-\frac{m^2}{48\pi^2r^2}$$
$$-\frac{9fm^2}{256\pi^2r^2}+\frac{m^2}{48h\pi^2r^2}+\frac{13fm^2}{64h\pi^2r^2}-\frac{3fm^2}{64\pi^2r^2}+\frac{f^2m^4}{1536\pi^2r^2}$$
$$+\frac{\ln[\frac{\sqrt{f}}{8\pi^2}]}{240\pi^2r^4}+\frac{\ln[\frac{\sqrt{f}}{8\pi^2}]}{80h^2\pi^2r^4}-\frac{\ln[\frac{\sqrt{f}}{8\pi^2}]}{60h\pi^2r^4}-\frac{7ff'}{10240h^{3/2}m^2\pi^2r^7}$$
$$-\frac{991ff'}{161280hm^2\pi^2r^7}-\frac{125ff'}{21504m^2\pi^2r^7}-\frac{143ff'}{15360h\pi^2r^5}-\frac{127ff'}{5120\pi^2r^5}$$
$$+\frac{43f'}{192h^3m^2\pi^2r^5}+\frac{19f'}{768h^{5/2}m^2\pi^2r^5}-\frac{f'}{64h^{3/2}m^2\pi^2r^5}$$
$$+\frac{19f'}{7680hm^2\pi^2r^5}+\frac{29f'}{2560m^2\pi^2r^5}-\frac{187f'}{64h^2\pi^2r^3}+\frac{f'}{128h^{3/2}\pi^2r^3}$$
$$+\frac{17f'}{768\pi^2r^3}+\frac{15fm^2f'}{1024\pi^2r^3}+\frac{\kappa^2f'}{144f^2h\pi^2r}-\frac{11m^2f'}{32h\pi^2r}+\frac{m^2f'}{24fh\pi^2r}$$
$$+\frac{3m^2f'}{128\pi^2r}+\frac{\ln[\frac{\sqrt{f}}{8\pi^2}]f'}{40fh^2\pi^2r^3}-\frac{\ln[\frac{\sqrt{f}}{8\pi^2}]f'}{40fh\pi^2r^3}-\frac{5\kappa^2f'^2}{1152f^3h\pi^2}-\frac{m^2f'^2}{64f^2h\pi^2}$$
$$+\frac{83m^2f'^2}{768fh\pi^2}+\frac{7f'^2}{20480h^{3/2}m^2\pi^2r^6}+\frac{991f'^2}{645120hm^2\pi^2r^6}$$
$$-\frac{f'^2}{3072h^{3/2}\pi^2r^4}+\frac{23f'^2}{6144h\pi^2r^4}-\frac{797f'^2}{1536fh^3m^2\pi^2r^4}$$
$$-\frac{5f'^2}{1536fh^{5/2}m^2\pi^2r^4}+\frac{f'^2}{512fh^{3/2}m^2\pi^2r^4}-\frac{31f'^2}{30720fhm^2\pi^2r^4}$$
$$+\frac{43f'^2}{5760f^2h^2\pi^2r^2}+\frac{2315f'^2}{1536fh^2\pi^2r^2}-\frac{11f'^2}{768fh^{3/2}\pi^2r^2}$$
$$-\frac{f'^2}{384f^2h\pi^2r^2}-\frac{7f'^2}{3072fh\pi^2r^2}+\frac{11m^2f'^2}{6144h\pi^2r^2}+\frac{29\ln[\frac{\sqrt{f}}{8\pi^2}]f'^2}{960f^2h^2\pi^2r^2}$$
$$-\frac{7f'^3}{122880fh^{3/2}m^2\pi^2r^5}+\frac{f'^3}{6144fh^{3/2}\pi^2r^3}+\frac{613f'^3}{1536f^2h^3m^2\pi^2r^3}$$
$$-\frac{f'^3}{128f^2h^{5/2}m^2\pi^2r^3}-\frac{19f'^3}{2880f^3h^2\pi^2r}-\frac{547f'^3}{1536f^2h^2\pi^2r}$$
$$-\frac{f'^3}{384f^2h^{3/2}\pi^2r}-\frac{5\ln[\frac{\sqrt{f}}{8\pi^2}]f'^3}{192f^3h^2\pi^2r}+\frac{77f'^4}{46080f^4h^2\pi^2}+\frac{61f'^4}{1536f^3h^2\pi^2}$$

$$-\frac{31f'^4}{256f^3h^3m^2\pi^2r^2}+\frac{5f'^4}{1536f^3h^{5/2}m^2\pi^2r^2}+\frac{59\ln[\frac{\sqrt{f}}{8\pi^2}]f'^4}{3840f^4h^2\pi^2}$$
$$+\frac{11f'^5}{1024f^4h^3m^2\pi^2r}-\frac{17f'^5}{61440f^4h^{5/2}m^2\pi^2r}+\frac{11f'^6}{24576f^5h^3m^2\pi^2}$$
$$+\frac{95fh'}{384h^4m^2\pi^2r^5}-\frac{7fh'}{384h^{7/2}m^2\pi^2r^5}+\frac{fh'}{128h^{5/2}m^2\pi^2r^5}$$
$$+\frac{fh'}{1920h^2m^2\pi^2r^5}-\frac{h'}{120h^3\pi^2r^3}+\frac{27fh'}{64h^3\pi^2r^3}+\frac{fh'}{32h^{5/2}\pi^2r^3}$$
$$+\frac{\kappa^2h'}{288fh^2\pi^2r}-\frac{m^2h'}{48h^2\pi^2r}+\frac{fm^2h'}{64h^2\pi^2r}+\frac{\ln[\frac{\sqrt{f}}{8\pi^2}]h'}{60h^3\pi^2r^3}-\frac{\ln[\frac{\sqrt{f}}{8\pi^2}]h'}{120h^2\pi^2r^3}$$
$$-\frac{\kappa^2f'h'}{576f^2h^2\pi^2}+\frac{m^2f'h'}{128h^2\pi^2}-\frac{m^2f'h'}{96fh^2\pi^2}+\frac{ff'h'}{768h^{5/2}\pi^2r^4}$$
$$+\frac{29ff'h'}{15360h^2\pi^2r^4}-\frac{77f'h'}{192h^4m^2\pi^2r^4}+\frac{25f'h'}{768h^{7/2}m^2\pi^2r^4}$$
$$-\frac{5f'h'}{768h^{5/2}m^2\pi^2r^4}-\frac{f'h'}{3840h^2m^2\pi^2r^4}-\frac{113f'h'}{768h^3\pi^2r^2}+\frac{f'h'}{64fh^3\pi^2r^2}$$
$$-\frac{f'h'}{32h^{5/2}\pi^2r^2}-\frac{5f'h'}{768h^2\pi^2r^2}-\frac{f'h'}{576fh^2\pi^2r^2}-\frac{fm^2f'h'}{512h^2\pi^2r^2}$$
$$-\frac{11\ln[\frac{\sqrt{f}}{8\pi^2}]f'h'}{480fh^3\pi^2r^2}-\frac{f'^2h'}{1536h^{5/2}\pi^2r^3}+\frac{217f'^2h'}{1536fh^4m^2\pi^2r^3}$$
$$-\frac{19f'^2h'}{1024fh^{7/2}m^2\pi^2r^3}+\frac{f'^2h'}{3072fh^{5/2}m^2\pi^2r^3}-\frac{f'^2h'}{128f^2h^3\pi^2r}$$
$$-\frac{85f'^2h'}{384fh^3\pi^2r}+\frac{f'^2h'}{512fh^{5/2}\pi^2r}-\frac{\ln[\frac{\sqrt{f}}{8\pi^2}]f'^2h'}{48f^2h^3\pi^2r}+\frac{f'^3h'}{5760f^3h^3\pi^2}$$
$$+\frac{229f'^3h'}{3072f^2h^3\pi^2}+\frac{f'^3h'}{24f^2h^4m^2\pi^2r^2}+\frac{5f'^3h'}{1536f^2h^{7/2}m^2\pi^2r^2}$$
$$+\frac{13\ln[\frac{\sqrt{f}}{8\pi^2}]f'^3h'}{640f^3h^3\pi^2}+\frac{f'^4h'}{2048f^3h^{7/2}m\pi^2}-\frac{55f'^4h'}{2048f^3h^4m^2\pi^2r}$$
$$+\frac{f'^4h'}{12288f^3h^{7/2}m^2\pi^2r}+\frac{11f'^5h'}{4096f^4h^4m^2\pi^2}+\frac{fh'^2}{192h^5m^2\pi^2r^4}$$
$$+\frac{fh'^2}{384h^{7/2}m^2\pi^2r^4}-\frac{7h'^2}{960h^4\pi^2r^2}-\frac{29fh'^2}{512h^4\pi^2r^2}+\frac{fh'^2}{64h^{7/2}\pi^2r^2}$$

$$+\frac{3\ln[\frac{\sqrt{f}}{8\pi^2}]h'^2}{320h^4\pi^2r^2}-\frac{311f'h'^2}{768h^5m^2\pi^2r^3}+\frac{3f'h'^2}{256h^{9/2}m^2\pi^2r^3}$$
$$-\frac{f'h'^2}{768h^{7/2}m^2\pi^2r^3}+\frac{143f'h'^2}{512h^4\pi^2r}-\frac{f'h'^2}{160fh^4\pi^2r}-\frac{f'h'^2}{128h^{7/2}\pi^2r}$$
$$-\frac{7\ln[\frac{\sqrt{f}}{8\pi^2}]f'h'^2}{960fh^4\pi^2r}-\frac{19f'^2h'^2}{7680f^2h^4\pi^2}-\frac{593f'^2h'^2}{6144fh^4\pi^2}+\frac{1313f'^2h'^2}{6144fh^5m^2\pi^2r^2}$$
$$-\frac{3f'^2h'^2}{512fh^{9/2}m^2\pi^2r^2}+\frac{67\ln[\frac{\sqrt{f}}{8\pi^2}]f'^2h'^2}{3840f^2h^4\pi^2}-\frac{35f'^3h'^2}{1024f^2h^5m^2\pi^2r}$$
$$+\frac{f'^3h'^2}{1024f^2h^{9/2}m^2\pi^2r}-\frac{f'^4h'^2}{3072f^3h^5m^2\pi^2}+\frac{13fh'^3}{96h^6m^2\pi^2r^3}$$
$$+\frac{7h'^3}{240h^5\pi^2r}-\frac{7fh'^3}{128h^5\pi^2r}-\frac{7\ln[\frac{\sqrt{f}}{8\pi^2}]h'^3}{240h^5\pi^2r}+\frac{7f'h'^3}{384h^5\pi^2}-\frac{7f'h'^3}{960fh^5\pi^2}$$
$$-\frac{157f'h'^3}{768h^6m^2\pi^2r^2}+\frac{7\ln[\frac{\sqrt{f}}{8\pi^2}]f'h'^3}{480fh^5\pi^2}+\frac{271f'^2h'^3}{3072fh^6m^2\pi^2r}$$
$$-\frac{61f'^3h'^3}{6144f^2h^6m^2\pi^2}+\frac{35fh'^4}{768h^7m^2\pi^2r^2}-\frac{35f'h'^4}{768h7m^2\pi^2r}$$
$$+\frac{35f'^2h'^4}{3072fh^7m^2\pi^2}+\frac{\kappa^2f''}{288f^2h\pi^2}-\frac{m^2f''}{64h\pi^2}+\frac{m^2f''}{48fh\pi^2}$$
$$-\frac{ff''}{384h^{3/2}\pi^2r^4}-\frac{29ff''}{7680h\pi^2r^4}+\frac{31f''}{384h^3m^2\pi^2r^4}-\frac{f''}{96h^{5/2}m^2\pi^2r^4}$$
$$+\frac{f''}{192h^{3/2}m^2\pi^2r^4}+\frac{f''}{1920hm^2\pi^2r^4}+\frac{5f''}{96h^2\pi^2r^2}-\frac{f''}{288fh^2\pi^2r^2}$$
$$+\frac{f''}{32h^{3/2}\pi^2r^2}+\frac{5f''}{384h\pi^2r^2}+\frac{f''}{288fh\pi^2r^2}+\frac{fm^2f''}{256h\pi^2r^2}$$
$$+\frac{f'f''}{768h^{3/2}\pi^2r^3}-\frac{11f'f''}{768fh^3m^2\pi^2r^3}+\frac{5f'f''}{512fh^{5/2}m^2\pi^2r^3}$$
$$-\frac{f'f''}{1536fh^{3/2}m^2\pi^2r^3}+\frac{f'f''}{288f^2h^2\pi^2r}+\frac{37f'f''}{96fh^2\pi^2r}-\frac{f'f''}{256fh^{3/2}\pi^2r}$$
$$+\frac{9\ln[\frac{\sqrt{f}}{8\pi^2}]f'f''}{160f^2h^2\pi^2r}-\frac{f'^2f''}{2880f^3h^2\pi^2}-\frac{229f'^2f''}{1536f^2h^2\pi^2}-\frac{223f'^2f''}{3072f^2h^3m^2\pi^2r^2}$$
$$-\frac{f'^2f''}{512f^2h^{5/2}m^2\pi^2r^2}-\frac{13\ln[\frac{\sqrt{f}}{8\pi^2}]f'^2f''}{320f^3h^2\pi^2}+\frac{83f'^3f''}{2048f^3h^3m^2\pi^2r}$$

$$-\frac{f'^3 f''}{6144 f^3 h^{5/2} m^2 \pi^2 r} - \frac{11 f'^4 f''}{2048 f^4 h^3 m^2 \pi^2} + \frac{113 h' f''}{768 h^4 m^2 \pi^2 r^3}$$
$$-\frac{3 h' f''}{512 h^{7/2} m^2 \pi^2 r^3} + \frac{h' f''}{512 h^{5/2} m^2 \pi^2 r^3} - \frac{61 h' f''}{192 h^3 \pi^2 r} - \frac{h' f''}{120 f h^3 \pi^2 r}$$
$$+\frac{3 h' f''}{256 h^{5/2} \pi^2 r} + \frac{7 \ln[\frac{\sqrt{f}}{8\pi^2}] h' f''}{480 f h^3 \pi^2 r} + \frac{3 f' h' f''}{640 f^2 h^3 \pi^2} + \frac{91 f' h' f''}{512 f h^3 \pi^2}$$
$$-\frac{109 f' h' f''}{768 f h^4 m^2 \pi^2 r^2} + \frac{3 f' h' f''}{512 f h^{7/2} m^2 \pi^2 r^2} - \frac{37 \ln[\frac{\sqrt{f}}{8\pi^2}] f' h' f''}{960 f^2 h^3 \pi^2}$$
$$+\frac{209 f'^2 h' f''}{6144 f^2 h^4 m^2 \pi^2 r} - \frac{3 f'^2 h' f''}{2048 f^2 h^{7/2} m^2 \pi^2 r} + \frac{f'^3 h' f''}{12288 f^3 h^4 m^2 \pi^2}$$
$$-\frac{19 h'^2 f''}{768 h^4 \pi^2} + \frac{19 h'^2 f''}{1920 f h^4 \pi^2} + \frac{277 h'^2 f''}{3072 h^5 m^2 \pi^2 r^2} - \frac{19 \ln[\frac{\sqrt{f}}{8\pi^2}] h'^2 f''}{960 f h^4 \pi^2}$$
$$-\frac{29 f' h'^2 f''}{384 f h^5 m^2 \pi^2 r} + \frac{187 f'^2 h'^2 f''}{12288 f^2 h^5 m^2 \pi^2} + \frac{15 h'^3 f''}{512 h 6 m^2 \pi^2 r}$$
$$-\frac{15 f' h'^3 f''}{1024 f h 6 m^2 \pi^2} - \frac{f''^2}{640 f^2 h^2 \pi^2} - \frac{27 f''^2}{512 f h^2 \pi^2} + \frac{19 f''^2}{1536 f h^3 m^2 \pi^2 r^2}$$
$$+\frac{19 \ln[\frac{\sqrt{f}}{8\pi^2}] f''^2}{960 f^2 h^2 \pi^2} - \frac{23 f' f''^2}{3072 f^2 h^3 m^2 \pi^2 r} + \frac{f'^2 f''^2}{1536 f^3 h^3 m^2 \pi^2}$$
$$+\frac{5 h' f''^2}{1024 f h^4 m^2 \pi^2 r} - \frac{5 f' h' f''^2}{2048 f^2 h^4 m^2 \pi^2} - \frac{f h''}{12 h^4 m^2 \pi^2 r^4}$$
$$+\frac{f h''}{256 h^{7/2} m^2 \pi^2 r^4} - \frac{f h''}{768 h^{5/2} m^2 \pi^2 r^4} + \frac{h''}{240 h^3 \pi^2 r^2} + \frac{f h''}{64 h^3 \pi^2 r^2}$$
$$-\frac{f h''}{128 h^{5/2} \pi^2 r^2} - \frac{\ln[\frac{\sqrt{f}}{8\pi^2}] h''}{240 h^3 \pi^2 r^2} + \frac{7 f' h''}{48 h^4 m^2 \pi^2 r^3} - \frac{3 f' h''}{512 h^{7/2} m^2 \pi^2 r^3}$$
$$+\frac{f' h''}{1536 h^{5/2} m^2 \pi^2 r^3} - \frac{89 f' h''}{768 h^3 \pi^2 r} + \frac{f' h''}{480 f h^3 \pi^2 r} + \frac{f' h''}{256 h^{5/2} \pi^2 r}$$
$$+\frac{\ln[\frac{\sqrt{f}}{8\pi^2}] f' h''}{160 f h^3 \pi^2 r} + \frac{f'^2 h''}{960 f^2 h^3 \pi^2} + \frac{f'^2 h''}{24 f h^3 \pi^2} - \frac{119 f'^2 h''}{1536 f h^4 m^2 \pi^2 r^2}$$
$$+\frac{3 f'^2 h''}{1024 f h^{7/2} m^2 \pi^2 r^2} - \frac{\ln[\frac{\sqrt{f}}{8\pi^2}] f'^2 h''}{160 f^2 h^3 \pi^2} + \frac{25 f'^3 h''}{2048 f^2 h^4 m^2 \pi^2 r}$$
$$-\frac{f'^3 h''}{2048 f^2 h^{7/2} m^2 \pi^2 r} + \frac{f'^4 h''}{4096 f^3 h^4 m^2 \pi^2} - \frac{11 f h' h''}{96 h^5 m^2 \pi^2 r^3}$$

$$-\frac{13h'h''}{480h^4\pi^2r}+\frac{13fh'h''}{256h^4\pi^2r}+\frac{13\ln[\frac{\sqrt{f}}{8\pi^2}]h'h''}{480h^4\pi^2r}-\frac{13f'h'h''}{768h^4\pi^2}$$
$$+\frac{13f'h'h''}{1920fh^4\pi^2}+\frac{67f'h'h''}{384h^5m^2\pi^2r^2}-\frac{13\ln[\frac{\sqrt{f}}{8\pi^2}]f'h'h''}{960fh^4\pi^2}$$
$$-\frac{469f'^2h'h''}{6144fh^5m^2\pi^2r}+\frac{109f'^3h'h''}{12288f^2h^5m^2\pi^2}-\frac{47fh'^2h''}{768h^6m^2\pi^2r^2}$$
$$+\frac{47f'h'^2h''}{768h^6m^2\pi^2r}-\frac{47f'^2h'^2h''}{3072fh^6m^2\pi^2}+\frac{f''h''}{96h^3\pi^2}-\frac{f''h''}{240fh^3\pi^2}$$
$$-\frac{13f''h''}{384h^4m^2\pi^2r^2}+\frac{\ln[\frac{\sqrt{f}}{8\pi^2}]f''h''}{120fh^3\pi^2}+\frac{89f'f''h''}{3072fh^4m^2\pi^2r}$$
$$-\frac{37f'^2f''h''}{6144f^2h^4m^2\pi^2}-\frac{25h'f''h''}{1024h^5m^2\pi^2r}+\frac{25f'h'f''h''}{2048fh^5m^2\pi^2}$$
$$+\frac{13fh''^2}{1536h^5m^2\pi^2r^2}-\frac{13f'h''^2}{1536h^5m^2\pi^2r}+\frac{13f'^2h''^2}{6144fh^5m^2\pi^2}$$
$$-\frac{7f^3}{192h^3m^2\pi^2r^3}+\frac{f^3}{256h^{5/2}m^2\pi^2r^3}-\frac{f^3}{768h^{3/2}m^2\pi^2r^3}$$
$$+\frac{19f^3}{128h^2\pi^2r}+\frac{f^3}{120fh^2\pi^2r}-\frac{f^3}{128h^{3/2}\pi^2r}-\frac{\ln[\frac{\sqrt{f}}{8\pi^2}]f^3}{60fh^2\pi^2r}$$
$$-\frac{f'f^3}{480f^2h^2\pi^2}-\frac{f'f^3}{12fh^2\pi^2}+\frac{53f'f^3}{1536fh^3m^2\pi^2r^2}-\frac{f'f^3}{256fh^{5/2}m^2\pi^2r^2}$$
$$+\frac{\ln[\frac{\sqrt{f}}{8\pi^2}]f'f^3}{80f^2h^2\pi^2}-\frac{11f'^2f^3}{1536f^2h^3m^2\pi^2r}+\frac{f'^2f^3}{1024f^2h^{5/2}m^2\pi^2r}$$
$$-\frac{f'^3f^3}{2048f^3h^3m^2\pi^2}+\frac{h'f^3}{64h^3\pi^2}-\frac{h'f^3}{160fh^3\pi^2}-\frac{21h'f^3}{512h^4m^2\pi^2r^2}$$
$$+\frac{\ln[\frac{\sqrt{f}}{8\pi^2}]h'f^3}{80fh^3\pi^2}+\frac{29f'h'f^3}{768fh^4m^2\pi^2r}-\frac{53f'^2h'f^3}{6144f^2h^4m^2\pi^2}$$
$$-\frac{55h'^2f^3}{3072h^5m^2\pi^2r}+\frac{55f'h'^2f^3}{6144fh^5m^2\pi^2}-\frac{5f''f^3}{1536fh^3m^2\pi^2r}$$
$$+\frac{5f'f''f^3}{3072f^2h^3m^2\pi^2}+\frac{5h''f^3}{768h^4m^2\pi^2r}-\frac{5f'h''f^3}{1536fh^4m^2\pi^2}$$
$$+\frac{fh^3}{64h^4m^2\pi^2r^3}+\frac{h^3}{240h^3\pi^2r}-\frac{fh^3}{128h^3\pi^2r}-\frac{\ln[\frac{\sqrt{f}}{8\pi^2}]h^3}{240h^3\pi^2r}$$

$$
\begin{aligned}
&+\frac{f'h^3}{384h^3\pi^2}-\frac{f'h^3}{960fh^3\pi^2}-\frac{37f'h^3}{1536h^4m^2\pi^2r^2}+\frac{\ln[\frac{\sqrt{f}}{8\pi^2}]f'h^3}{480fh^3\pi^2}\\
&+\frac{11f'^2h^3}{1024fh^4m^2\pi^2r}-\frac{f'^3h^3}{768f^2h^4m^2\pi^2}+\frac{19fh'h^3}{1536h^5m^2\pi^2r^2}\\
&-\frac{19f'h'h^3}{1536h^5m^2\pi^2r}+\frac{19f'^2h'h^3}{6144fh^5m^2\pi^2}+\frac{5f''h^3}{1536h^4m^2\pi^2r}\\
&-\frac{5f'f''h^3}{3072fh^4m^2\pi^2}-\frac{f^4}{192h^2\pi^2}+\frac{f^4}{480fh^2\pi^2}+\frac{f^4}{96h^3m^2\pi^2r^2}\\
&-\frac{\ln[\frac{\sqrt{f}}{8\pi^2}]f^4}{240fh^2\pi^2}-\frac{f'f^4}{96fh^3m^2\pi^2r}+\frac{f'^2f^4}{384f^2h^3m^2\pi^2}+\frac{5h'f^4}{768h^4m^2\pi^2r}\\
&-\frac{5f'h'f^4}{1536fh^4m^2\pi^2}-\frac{fh^4}{768h^4m^2\pi^2r^2}+\frac{f'h^4}{768h^4m^2\pi^2r}\\
&-\frac{f'^2h^4}{3072fh^4m^2\pi^2}-\frac{f^5}{768h^3m^2\pi^2r}+\frac{f'f^5}{1536fh^3m^2\pi^2}
\end{aligned}
\tag{B1}
$$

$$
\begin{aligned}
< T_r^r >_{ren} \quad = \quad & -\frac{f}{3072h^2\pi^2}+\frac{7\kappa^4}{2880f^2\pi^2}+\frac{fm^2}{16h\pi^2}-\frac{\kappa^2m^2}{48f\pi^2}+\frac{3m^4}{32\pi^2}+\frac{fm^4}{96\pi^2}\\
&-\frac{423f^2}{71680m^2\pi^2r^8}-\frac{7f^2}{15360h^{3/2}m^2\pi^2r^8}-\frac{991f^2}{161280hm^2\pi^2r^8}\\
&-\frac{125f^2}{10752m^2\pi^2r^8}-\frac{1747f^2}{53760\pi^2r^6}-\frac{9f^2}{5120h\pi^2r^6}-\frac{79f^2}{2560\pi^2r^6}\\
&+\frac{937f}{80640m^2\pi^2r^6}-\frac{193f}{192h^3m^2\pi^2r^6}-\frac{2119f}{1920h^{5/2}m^2\pi^2r^6}\\
&-\frac{11f}{96h^2m^2\pi^2r^6}-\frac{f}{192h^{3/2}m^2\pi^2r^6}+\frac{31f}{7680hm^2\pi^2r^6}\\
&+\frac{11f}{3840m^2\pi^2r^6}-\frac{81f}{1280\pi^2r^4}+\frac{5f}{192h^2\pi^2r^4}+\frac{271f}{192h^{3/2}\pi^2r^4}\\
&+\frac{5f}{24h\pi^2r^4}-\frac{59f}{384\pi^2r^4}+\frac{49f^2m^2}{5120\pi^2r^4}-\frac{f^2m^2}{512\pi^2r^4}+\frac{f}{24h^2\pi^2r^3}\\
&+\frac{9f}{64h^{3/2}\pi^2r^3}+\frac{f}{8h\pi^2r^3}-\frac{f}{96\pi^2r^3}-\frac{3f}{128h^2\pi^2r^2}-\frac{3f}{64h^{3/2}\pi^2r^2}\\
&-\frac{f}{64h\pi^2r^2}-\frac{\kappa^2}{288f\pi^2r^2}+\frac{\kappa^2}{288fh\pi^2r^2}+\frac{m^2}{48\pi^2r^2}-\frac{245fm^2}{768\pi^2r^2}
\end{aligned}
$$

$$-\frac{m^2}{48h\pi^2r^2}-\frac{11fm^2}{192h\pi^2r^2}+\frac{9fm^2}{64\pi^2r^2}-\frac{f^2m^4}{1536\pi^2r^2}+\frac{f}{192h^2\pi^2r}$$
$$+\frac{f}{256h^{3/2}\pi^2r}-\frac{9fm^2}{32\pi^2r}+\frac{\ln[\frac{\sqrt{f}}{8\pi^2}]}{240\pi^2r^4}+\frac{\ln[\frac{\sqrt{f}}{8\pi^2}]}{80h^2\pi^2r^4}-\frac{\ln[\frac{\sqrt{f}}{8\pi^2}]}{60h\pi^2r^4}$$
$$+\frac{7ff'}{10240h^{3/2}m^2\pi^2r^7}+\frac{991ff'}{161280hm^2\pi^2r^7}+\frac{125ff'}{21504m^2\pi^2r^7}$$
$$+\frac{143ff'}{15360h\pi^2r^5}+\frac{127ff'}{5120\pi^2r^5}+\frac{4981f'}{1920h^3m^2\pi^2r^5}+\frac{8387f'}{3840h^{5/2}m^2\pi^2r^5}$$
$$+\frac{89f'}{480h^2m^2\pi^2r^5}-\frac{31f'}{7680hm^2\pi^2r^5}-\frac{11f'}{7680m^2\pi^2r^5}-\frac{1327f'}{960h^2\pi^2r^3}$$
$$+\frac{f'}{120fh^2\pi^2r^3}-\frac{307f'}{128h^{3/2}\pi^2r^3}-\frac{7f'}{48h\pi^2r^3}+\frac{119f'}{768\pi^2r^3}$$
$$-\frac{15fm^2f'}{1024\pi^2r^3}-\frac{\kappa^2f'}{288f^2h\pi^2r}-\frac{13m^2f'}{64h\pi^2r}+\frac{m^2f'}{48fh\pi^2r}+\frac{71m^2f'}{128\pi^2r}$$
$$-\frac{\ln[\frac{\sqrt{f}}{8\pi^2}]f'}{60fh^2\pi^2r^3}+\frac{\ln[\frac{\sqrt{f}}{8\pi^2}]f'}{120fh\pi^2r^3}+\frac{\kappa^2f'^2}{1152f^3h\pi^2}+\frac{m^2f'^2}{192f^2h\pi^2}$$
$$-\frac{49m^2f'^2}{256fh\pi^2}-\frac{7f'^2}{20480h^{3/2}m^2\pi^2r^6}-\frac{991f'^2}{645120hm^2\pi^2r^6}$$
$$+\frac{f'^2}{3072h^{3/2}\pi^2r^4}-\frac{23f'^2}{6144h\pi^2r^4}-\frac{17987f'^2}{7680fh^3m^2\pi^2r^4}$$
$$-\frac{2191f'^2}{1536fh^{5/2}m^2\pi^2r^4}-\frac{349f'^2}{3840fh^2m^2\pi^2r^4}+\frac{3f'^2}{512fh^{3/2}m^2\pi^2r^4}$$
$$+\frac{31f'^2}{30720fhm^2\pi^2r^4}-\frac{f'^2}{384f^2h^2\pi^2r^2}+\frac{12647f'^2}{7680fh^2\pi^2r^2}$$
$$+\frac{755f'^2}{768fh^{3/2}\pi^2r^2}+\frac{f'^2}{1152f^2h\pi^2r^2}-\frac{161f'^2}{3072fh\pi^2r^2}-\frac{11m^2f'^2}{6144h\pi^2r^2}$$
$$+\frac{\ln[\frac{\sqrt{f}}{8\pi^2}]f'^2}{320f^2h^2\pi^2r^2}+\frac{7f'^3}{122880fh^{3/2}m^2\pi^2r^5}-\frac{f'^3}{6144fh^{3/2}\pi^2r^3}$$
$$+\frac{1821f'^3}{2560f^2h^3m^2\pi^2r^3}+\frac{343f'^3}{1280f^2h^{5/2}m^2\pi^2r^3}+\frac{7f'^3}{640f^2h^2m^2\pi^2r^3}$$
$$-\frac{f'^3}{768f^2h^{3/2}m^2\pi^2r^3}-\frac{7f'^3}{5760f^3h^2\pi^2r}-\frac{4781f'^3}{7680f^2h^2\pi^2r}$$

$$-\frac{49f'^3}{384f^2h^{3/2}\pi^2r}-\frac{\ln[\frac{\sqrt{f}}{8\pi^2}]f'^3}{960f^3h^2\pi^2r}+\frac{f'^4}{46080f^4h^2\pi^2}+\frac{97f'^4}{1024f^3h^2\pi^2}$$
$$+\frac{277f'^4}{3840f^3h^3m^2\pi^2r^2}+\frac{601f'^4}{15360f^3h^{5/2}m^2\pi^2r^2}+\frac{f'^4}{512f^3h^2m^2\pi^2r^2}$$
$$+\frac{\ln[\frac{\sqrt{f}}{8\pi^2}]f'^4}{1280f^4h^2\pi^2}-\frac{637f'^5}{10240f^4h^3m^2\pi^2r}-\frac{661f'^5}{61440f^4h^{5/2}m^2\pi^2r}$$
$$+\frac{157f'^6}{24576f^5h^3m^2\pi^2}-\frac{fh'}{1024h^3\pi^2}-\frac{5fm^2h'}{128h^2\pi^2}-\frac{191fh'}{480h^4m^2\pi^2r^5}$$
$$-\frac{343fh'}{640h^{7/2}m^2\pi^2r^5}-\frac{7fh'}{160h^3m^2\pi^2r^5}-\frac{fh'}{128h^{5/2}m^2\pi^2r^5}$$
$$+\frac{283fh'}{960h^3\pi^2r^3}+\frac{23fh'}{96h^{5/2}\pi^2r^3}+\frac{fh'}{48h^2\pi^2r^3}-\frac{fh'}{256h^3\pi^2r^2}$$
$$-\frac{fh'}{128h^{5/2}\pi^2r^2}-\frac{fh'}{128h^2\pi^2r^2}+\frac{fh'}{256h^3\pi^2r}+\frac{fh'}{256h^{5/2}\pi^2r}$$
$$-\frac{fm^2h'}{48h^2\pi^2r}-\frac{\ln[\frac{\sqrt{f}}{8\pi^2}]h'}{40h^3\pi^2r^3}+\frac{\ln[\frac{\sqrt{f}}{8\pi^2}]h'}{40h^2\pi^2r^3}+\frac{5m^2f'h'}{128h^2\pi^2}-\frac{ff'h'}{768h^{5/2}\pi^2r^4}$$
$$-\frac{29ff'h'}{15360h^2\pi^2r^4}+\frac{1727f'h'}{1280h^4m^2\pi^2r^4}+\frac{1329f'h'}{1280h^{7/2}m^2\pi^2r^4}$$
$$+\frac{109f'h'}{1920h^3m^2\pi^2r^4}+\frac{5f'h'}{768h^{5/2}m^2\pi^2r^4}-\frac{329f'h'}{480h^3\pi^2r^2}+\frac{f'h'}{480fh^3\pi^2r^2}$$
$$+\frac{5f'h'}{384h^{5/2}\pi^2r^2}-\frac{17f'h'}{768h^2\pi^2r^2}+\frac{fm^2f'h'}{512h^2\pi^2r^2}-\frac{7\ln[\frac{\sqrt{f}}{8\pi^2}]f'h'}{480fh^3\pi^2r^2}$$
$$+\frac{f'^2h'}{1536h^{5/2}\pi^2r^3}-\frac{4003f'^2h'}{2560fh^4m^2\pi^2r^3}-\frac{3593f'^2h'}{5120fh^{7/2}m^2\pi^2r^3}$$
$$-\frac{29f'^2h'}{1280fh^3m^2\pi^2r^3}-\frac{f'^2h'}{3072fh^{5/2}m^2\pi^2r^3}-\frac{f'^2h'}{960f^2h^3\pi^2r}$$
$$+\frac{421f'^2h'}{1280fh^3\pi^2r}-\frac{125f'^2h'}{1536fh^{5/2}\pi^2r}+\frac{\ln[\frac{\sqrt{f}}{8\pi^2}]f'^2h'}{80f^2h^3\pi^2r}+\frac{f'^3h'}{3840f^3h^3\pi^2}$$
$$-\frac{89f'^3h'}{3840f^2h^3\pi^2}+\frac{897f'^3h'}{1280f^2h^4m^2\pi^2r^2}+\frac{43f'^3h'}{240f^2h^{7/2}m^2\pi^2r^2}$$
$$+\frac{17f'^3h'}{3840f^2h^3m^2\pi^2r^2}+\frac{7\ln[\frac{\sqrt{f}}{8\pi^2}]f'^3h'}{1920f^3h^3\pi^2}-\frac{f'^4h'}{2048f^3h^{7/2}m\pi^2}$$

$$-\frac{5f'^4h'}{48f^3h^4m^2\pi^2r}-\frac{701f'^4h'}{61440f^3h^{7/2}m^2\pi^2r}+\frac{37f'^5h'}{15360f^4h^4m^2\pi^2}$$
$$+\frac{863fh'^2}{1920h^5m^2\pi^2r^4}-\frac{11fh'^2}{160h^{9/2}m^2\pi^2r^4}-\frac{29fh'^2}{3840h^4m^2\pi^2r^4}$$
$$-\frac{fh'^2}{384h^{7/2}m^2\pi^2r^4}+\frac{99fh'^2}{2560h^4\pi^2r^2}-\frac{3fh'^2}{64h^{7/2}\pi^2r^2}+\frac{9\ln[\frac{\sqrt{f}}{8\pi^2}]h'^2}{320h^4\pi^2r^2}$$
$$-\frac{61f'h'^2}{480h^5m^2\pi^2r^3}+\frac{29f'h'^2}{256h^{9/2}m^2\pi^2r^3}+\frac{23f'h'^2}{3840h^4m^2\pi^2r^3}$$
$$+\frac{f'h'^2}{768h^{7/2}m^2\pi^2r^3}-\frac{319f'h'^2}{7680h^4\pi^2r}-\frac{7f'h'^2}{960fh^4\pi^2r}+\frac{23f'h'^2}{384h^{7/2}\pi^2r}$$
$$+\frac{7\ln[\frac{\sqrt{f}}{8\pi^2}]f'h'^2}{320fh^4\pi^2r}+\frac{7f'^2h'^2}{7680f^2h^4\pi^2}+\frac{457f'^2h'^2}{10240fh^4\pi^2}$$
$$-\frac{2251f'^2h'^2}{10240fh^5m^2\pi^2r^2}-\frac{409f'^2h'^2}{5120fh^{9/2}m^2\pi^2r^2}+\frac{7f'^2h'^2}{5120fh^4m^2\pi^2r^2}$$
$$+\frac{\ln[\frac{\sqrt{f}}{8\pi^2}]f'^2h'^2}{1280f^2h^4\pi^2}+\frac{291f'^3h'^2}{2048f^2h^5m^2\pi^2r}+\frac{167f'^3h'^2}{10240f^2h^{9/2}m^2\pi^2r}$$
$$-\frac{467f'^4h'^2}{30720f^3h^5m^2\pi^2}+\frac{1337fh'^3}{3840h^6m^2\pi^2r^3}+\frac{19fh'^3}{480h^{11/2}m^2\pi^2r^3}$$
$$-\frac{7fh'^3}{960h^5m^2\pi^2r^3}-\frac{49fh'^3}{1920h^5\pi^2r}+\frac{7f'h'^3}{640h^5\pi^2}-\frac{3379f'h'^3}{7680h^6m^2\pi^2r^2}$$
$$-\frac{77f'h'^3}{1920h^{11/2}m^2\pi^2r^2}+\frac{7f'h'^3}{1920h^5m^2\pi^2r^2}+\frac{1003f'^2h'^3}{10240fh^6m^2\pi^2r}$$
$$+\frac{11f'^2h'^3}{2560fh^{11/2}m^2\pi^2r}+\frac{151f'^3h'^3}{20480f^2h^6m^2\pi^2}+\frac{191fh'^4}{768h^7m^2\pi^2r^2}$$
$$+\frac{7fh'^4}{384h13/2m^2\pi^2r^2}-\frac{357f'h'^4}{1280h^7m^2\pi^2r}-\frac{7f'h'^4}{768h13/2m^2\pi^2r}$$
$$+\frac{311f'^2h'^4}{7680fh^7m^2\pi^2}+\frac{91fh'^5}{768h8m^2\pi^2r}-\frac{91f'h'^5}{1536h^8m^2\pi^2}+\frac{f''}{512h^2\pi^2}$$
$$+\frac{ff''}{384h^{3/2}\pi^2r^4}+\frac{29ff''}{7680h\pi^2r^4}-\frac{73f''}{160h^3m^2\pi^2r^4}-\frac{229f''}{480h^{5/2}m^2\pi^2r^4}$$
$$-\frac{19f''}{480h^2m^2\pi^2r^4}-\frac{f''}{192h^{3/2}m^2\pi^2r^4}+\frac{41f''}{80h^2\pi^2r^2}-\frac{f''}{120fh^2\pi^2r^2}$$
$$-\frac{f''}{192h^{3/2}\pi^2r^2}+\frac{23f''}{384h\pi^2r^2}-\frac{fm^2f''}{256h\pi^2r^2}-\frac{f''}{128h^2\pi^2r}$$

$$-\frac{f''}{128h^{3/2}\pi^2 r}+\frac{\ln[\frac{\sqrt{f}}{8\pi^2}]f''}{120fh^2\pi^2r^2}-\frac{f'f''}{768h^{3/2}\pi^2r^3}+\frac{3773f'f''}{3840fh^3m^2\pi^2r^3}$$
$$+\frac{1623f'f''}{2560fh^{5/2}m^2\pi^2r^3}+\frac{17f'f''}{480fh^2m^2\pi^2r^3}+\frac{f'f''}{1536fh^{3/2}m^2\pi^2r^3}$$
$$+\frac{f'f''}{120f^2h^2\pi^2r}-\frac{887f'f''}{1920fh^2\pi^2r}+\frac{125f'f''}{768fh^{3/2}\pi^2r}-\frac{f'^2f''}{1920f^3h^2\pi^2}$$
$$+\frac{89f'^2f''}{1920f^2h^2\pi^2}-\frac{10057f'^2f''}{15360f^2h^3m^2\pi^2r^2}-\frac{157f'^2f''}{640f^2h^{5/2}m^2\pi^2r^2}$$
$$-\frac{17f'^2f''}{1920f^2h^2m^2\pi^2r^2}-\frac{7\ln[\frac{\sqrt{f}}{8\pi^2}]f'^2f''}{960f^3h^2\pi^2}+\frac{4139f'^3f''}{30720f^3h^3m^2\pi^2r}$$
$$+\frac{701f'^3f''}{30720f^3h^{5/2}m^2\pi^2r}-\frac{37f'^4f''}{7680f^4h^3m^2\pi^2}+\frac{269h'f''}{3840h^4m^2\pi^2r^3}$$
$$-\frac{209h'f''}{2560h^{7/2}m^2\pi^2r^3}-\frac{h'f''}{240h^3m^2\pi^2r^3}-\frac{h'f''}{512h^{5/2}m^2\pi^2r^3}$$
$$+\frac{107h'f''}{1920h^3\pi^2r}+\frac{h'f''}{240fh^3\pi^2r}-\frac{23h'f''}{256h^{5/2}\pi^2r}-\frac{\ln[\frac{\sqrt{f}}{8\pi^2}]h'f''}{30fh^3\pi^2r}$$
$$-\frac{f'h'f''}{960f^2h^3\pi^2}-\frac{731f'h'f''}{7680fh^3\pi^2}+\frac{13f'h'f''}{80fh^4m^2\pi^2r^2}+\frac{271f'h'f''}{2560fh^{7/2}m^2\pi^2r^2}$$
$$-\frac{f'h'f''}{640fh^3m^2\pi^2r^2}-\frac{\ln[\frac{\sqrt{f}}{8\pi^2}]f'h'f''}{120f^2h^3\pi^2}-\frac{5533f'^2h'f''}{30720f^2h^4m^2\pi^2r}$$
$$-\frac{323f'^2h'f''}{10240f^2h^{7/2}m^2\pi^2r}+\frac{1771f'^3h'f''}{61440f^3h^4m^2\pi^2}-\frac{19h'^2f''}{1280h^4\pi^2}$$
$$+\frac{245h'^2f''}{1024h^5m^2\pi^2r^2}+\frac{67h'^2f''}{2560h^{9/2}m^2\pi^2r^2}-\frac{19h'^2f''}{3840h^4m^2\pi^2r^2}$$
$$-\frac{579f'h'^2f''}{5120fh^5m^2\pi^2r}-\frac{37f'h'^2f''}{5120fh^{9/2}m^2\pi^2r}-\frac{563f'^2h'^2f''}{61440f^2h^5m^2\pi^2}$$
$$+\frac{2609h'^3f''}{15360h^6m^2\pi^2r}+\frac{3h'^3f''}{256h^{11/2}m^2\pi^2r}-\frac{1987f'h'^3f''}{30720fh^6m^2\pi^2}$$
$$+\frac{113h'^4f''}{1536h^7m^2\pi^2}-\frac{f''^2}{1920f^2h^2\pi^2}+\frac{347f''^2}{7680fh^2\pi^2}-\frac{7f''^2}{7680fh^3m^2\pi^2r^2}$$
$$-\frac{3f''^2}{160fh^{5/2}m^2\pi^2r^2}-\frac{f''^2}{1280fh^2m^2\pi^2r^2}+\frac{11\ln[\frac{\sqrt{f}}{8\pi^2}]f''^2}{960f^2h^2\pi^2}$$

$$+\frac{541f'f''^2}{15360f^2h^3m^2\pi^2r}+\frac{29f'f''^2}{2560f^2h^{5/2}m^2\pi^2r}-\frac{37f'^2f''^2}{3840f^3h^3m^2\pi^2}$$
$$+\frac{527h'f''^2}{15360fh^4m^2\pi^2r}+\frac{h'f''^2}{512fh^{7/2}m^2\pi^2r}-\frac{13f'h'f''^2}{10240f^2h^4m^2\pi^2}$$
$$+\frac{127h'^2f''^2}{7680fh^5m^2\pi^2}+\frac{f''^3}{7680f^2h^3m^2\pi^2}-\frac{7fh''}{240h^4m^2\pi^2r^4}$$
$$+\frac{113fh''}{3840h^{7/2}m^2\pi^2r^4}+\frac{fh''}{480h^3m^2\pi^2r^4}+\frac{fh''}{768h^{5/2}m^2\pi^2r^4}$$
$$-\frac{13fh''}{960h^3\pi^2r^2}+\frac{3fh''}{128h^{5/2}\pi^2r^2}+\frac{\ln[\frac{\sqrt{f}}{8\pi^2}]h''}{240h^3\pi^2r^2}-\frac{67f'h''}{1920h^4m^2\pi^2r^3}$$
$$-\frac{79f'h''}{1536h^{7/2}m^2\pi^2r^3}-\frac{f'h''}{640h^3m^2\pi^2r^3}-\frac{f'h''}{1536h^{5/2}m^2\pi^2r^3}$$
$$+\frac{13f'h''}{1280h^3\pi^2r}+\frac{f'h''}{240fh^3\pi^2r}-\frac{23f'h''}{768h^{5/2}\pi^2r}-\frac{\ln[\frac{\sqrt{f}}{8\pi^2}]f'h''}{240fh^3\pi^2r}$$
$$-\frac{f'^2h''}{1920f^2h^3\pi^2}-\frac{f'^2h''}{60fh^3\pi^2}+\frac{919f'^2h''}{7680fh^4m^2\pi^2r^2}$$
$$+\frac{173f'^2h''}{5120fh^{7/2}m^2\pi^2r^2}-\frac{f'^2h''}{1280fh^3m^2\pi^2r^2}+\frac{\ln[\frac{\sqrt{f}}{8\pi^2}]f'^2h''}{960f^2h^3\pi^2}$$
$$-\frac{123f'^3h''}{2048f^2h^4m^2\pi^2r}-\frac{69f'^3h''}{10240f^2h^{7/2}m^2\pi^2r}+\frac{131f'^4h''}{20480f^3h^4m^2\pi^2}$$
$$-\frac{467fh'h''}{1920h^5m^2\pi^2r^3}-\frac{31fh'h''}{960h^{9/2}m^2\pi^2r^3}+\frac{13fh'h''}{1920h^4m^2\pi^2r^3}$$
$$+\frac{91fh'h''}{3840h^4\pi^2r}-\frac{13f'h'h''}{1280h^4\pi^2}+\frac{1189f'h'h''}{3840h^5m^2\pi^2r^2}+\frac{f'h'h''}{30h^{9/2}m^2\pi^2r^2}$$
$$-\frac{13f'h'h''}{3840h^4m^2\pi^2r^2}-\frac{2053f'^2h'h''}{30720fh^5m^2\pi^2r}-\frac{19f'^2h'h''}{5120fh^{9/2}m^2\pi^2r}$$
$$-\frac{431f'^3h'h''}{61440f^2h^5m^2\pi^2}-\frac{73fh'^2h''}{240h^6m^2\pi^2r^2}-\frac{47fh'^2h''}{1920h^{11/2}m^2\pi^2r^2}$$
$$+\frac{1333f'h'^2h''}{3840h^6m^2\pi^2r}+\frac{47f'h'^2h''}{3840h^{11/2}m^2\pi^2r}-\frac{531f'^2h'^2h''}{10240fh^6m^2\pi^2}$$
$$-\frac{797fh'^3h''}{3840h^7m^2\pi^2r}+\frac{797f'h'^3h''}{7680h^7m^2\pi^2}+\frac{f''h''}{160h^3\pi^2}-\frac{9f''h''}{128h^4m^2\pi^2r^2}$$
$$-\frac{3f''h''}{320h^{7/2}m^2\pi^2r^2}+\frac{f''h''}{480h^3m^2\pi^2r^2}+\frac{497f'f''h''}{15360fh^4m^2\pi^2r}$$

$$+\frac{7f'f''h''}{2560fh^{7/2}m^2\pi^2r}+\frac{25f'^2f''h''}{6144f^2h^4m^2\pi^2}-\frac{1963h'f''h''}{15360h^5m^2\pi^2r}$$
$$-\frac{5h'f''h''}{512h^{9/2}m^2\pi^2r}+\frac{1559f'h'f''h''}{30720fh^5m^2\pi^2}-\frac{1403h'^2f''h''}{15360h^6m^2\pi^2}$$
$$-\frac{11f''^2h''}{1920fh^4m^2\pi^2}+\frac{287fh''^2}{7680h^5m^2\pi^2r^2}+\frac{13fh''^2}{3840h^{9/2}m^2\pi^2r^2}$$
$$-\frac{167f'h''^2}{3840h^5m^2\pi^2r}-\frac{13f'h''^2}{7680h^{9/2}m^2\pi^2r}+\frac{41f'^2h''^2}{6144fh^5m^2\pi^2}$$
$$+\frac{493fh'h''^2}{7680h^6m^2\pi^2r}-\frac{493f'h'h''^2}{15360h^6m^2\pi^2}+\frac{11f''h''^2}{960h^5m^2\pi^2}+\frac{11f^3}{240h^3m^2\pi^2r^3}$$
$$+\frac{161f^3}{3840h^{5/2}m^2\pi^2r^3}-\frac{f^3}{960h^2m^2\pi^2r^3}+\frac{f^3}{768h^{3/2}m^2\pi^2r^3}$$
$$-\frac{17f^3}{1920h^2\pi^2r}-\frac{f^3}{240fh^2\pi^2r}+\frac{23f^3}{384h^{3/2}\pi^2r}+\frac{\ln[\frac{\sqrt{f}}{8\pi^2}]f^3}{240fh^2\pi^2r}$$
$$+\frac{f'f^3}{960f^2h^2\pi^2}+\frac{f'f^3}{30fh^2\pi^2}-\frac{913f'f^3}{7680fh^3m^2\pi^2r^2}$$
$$-\frac{23f'f^3}{480fh^{5/2}m^2\pi^2r^2}+\frac{f'f^3}{640fh^2m^2\pi^2r^2}-\frac{\ln[\frac{\sqrt{f}}{8\pi^2}]f'f^3}{480f^2h^2\pi^2}$$
$$+\frac{607f'^2f^3}{7680f^2h^3m^2\pi^2r}+\frac{69f'^2f^3}{5120f^2h^{5/2}m^2\pi^2r}-\frac{131f'^3f^3}{10240f^3h^3m^2\pi^2}$$
$$+\frac{3h'f^3}{320h^3\pi^2}-\frac{31h'f^3}{512h^4m^2\pi^2r^2}-\frac{13h'f^3}{1280h^{7/2}m^2\pi^2r^2}+\frac{h'f^3}{320h^3m^2\pi^2r^2}$$
$$+\frac{91f'h'f^3}{3840fh^4m^2\pi^2r}+\frac{29f'h'f^3}{7680fh^{7/2}m^2\pi^2r}+\frac{193f'^2h'f^3}{30720f^2h^4m^2\pi^2}$$
$$-\frac{1027h'^2f^3}{15360h^5m^2\pi^2r}-\frac{11h'^2f^3}{1536h^{9/2}m^2\pi^2r}+\frac{1037f'h'^2f^3}{30720fh^5m^2\pi^2}$$
$$-\frac{45h'^3f^3}{1024h^6m^2\pi^2}-\frac{23f''f^3}{1536fh^3m^2\pi^2r}-\frac{f''f^3}{768fh^{5/2}m^2\pi^2r}$$
$$+\frac{11f'f''f^3}{15360f^2h^3m^2\pi^2}-\frac{h'f''f^3}{80fh^4m^2\pi^2}+\frac{h''f^3}{48h^4m^2\pi^2r}+\frac{h''f^3}{384h^{7/2}m^2\pi^2r}$$
$$-\frac{17f'h''f^3}{1536fh^4m^2\pi^2}+\frac{17h'h''f^3}{512h^5m^2\pi^2}+\frac{f^32}{768fh^3m^2\pi^2}+\frac{fh^3}{40h^4m^2\pi^2r^3}$$
$$+\frac{fh^3}{240h^{7/2}m^2\pi^2r^3}-\frac{fh^3}{960h^3m^2\pi^2r^3}-\frac{7fh^3}{1920h^3\pi^2r}+\frac{f'h^3}{640h^3\pi^2}$$

$$
\begin{aligned}
&-\frac{247f'h^3}{7680h^4m^2\pi^2r^2}-\frac{17f'h^3}{3840h^{7/2}m^2\pi^2r^2}+\frac{f'h^3}{1920h^3m^2\pi^2r^2}\\
&+\frac{33f'^2h^3}{5120fh^4m^2\pi^2r}+\frac{f'^2h^3}{1920fh^{7/2}m^2\pi^2r}+\frac{17f'^3h^3}{15360f^2h^4m^2\pi^2}\\
&+\frac{421fh'h^3}{7680h^5m^2\pi^2r^2}+\frac{19fh'h^3}{3840h^{9/2}m^2\pi^2r^2}-\frac{493f'h'h^3}{7680h^5m^2\pi^2r}\\
&-\frac{19f'h'h^3}{7680h^{9/2}m^2\pi^2r}+\frac{307f'^2h'h^3}{30720fh^5m^2\pi^2}+\frac{359fh'^2h^3}{7680h^6m^2\pi^2r}\\
&-\frac{359f'h'^2h^3}{15360h^6m^2\pi^2}+\frac{23f''h^3}{1536h^4m^2\pi^2r}+\frac{f''h^3}{768h^{7/2}m^2\pi^2r}\\
&-\frac{97f'f''h^3}{15360fh^4m^2\pi^2}+\frac{43h'f''h^3}{2560h^5m^2\pi^2}-\frac{3fh''h^3}{256h^5m^2\pi^2r}+\frac{3f'h''h^3}{512h^5m^2\pi^2}\\
&-\frac{f^3h^3}{256h^4m^2\pi^2}-\frac{f^4}{320h^2\pi^2}+\frac{f^4}{192h^3m^2\pi^2r^2}+\frac{f^4}{480h^{5/2}m^2\pi^2r^2}\\
&-\frac{f^4}{960h^2m^2\pi^2r^2}+\frac{f'f^4}{3840fh^3m^2\pi^2r}-\frac{f'f^4}{960fh^{5/2}m^2\pi^2r}\\
&-\frac{17f'^2f^4}{7680f^2h^3m^2\pi^2}+\frac{11h'f^4}{640h^4m^2\pi^2r}+\frac{h'f^4}{384h^{7/2}m^2\pi^2r}\\
&-\frac{43f'h'f^4}{3840fh^4m^2\pi^2}+\frac{25h'^2f^4}{1536h^5m^2\pi^2}+\frac{11f''f^4}{3840fh^3m^2\pi^2}-\frac{h''f^4}{192h^4m^2\pi^2}\\
&-\frac{19fh^4}{3840h^4m^2\pi^2r^2}-\frac{fh^4}{1920h^{7/2}m^2\pi^2r^2}+\frac{23f'h^4}{3840h^4m^2\pi^2r}\\
&+\frac{f'h^4}{3840h^{7/2}m^2\pi^2r}-\frac{f'^2h^4}{1024fh^4m^2\pi^2}-\frac{13fh'h^4}{1920h^5m^2\pi^2r}\\
&+\frac{13f'h'h^4}{3840h^5m^2\pi^2}-\frac{f''h^4}{640h^4m^2\pi^2}-\frac{3f^5}{1280h^3m^2\pi^2r}-\frac{f^5}{1920h^{5/2}m^2\pi^2r}\\
&+\frac{f'f^5}{512fh^3m^2\pi^2}-\frac{h'f^5}{256h^4m^2\pi^2}+\frac{fh^5}{1920h^4m^2\pi^2r}-\frac{f'h^5}{3840h^4m^2\pi^2}\\
&+\frac{f^6}{1920h^3m^2\pi^2}
\end{aligned}
\tag{B2}
$$

$$
<T^{\theta}_{\theta}>_{ren} \;=\; <T^{\phi}_{\phi}>_{ren}=\frac{7\kappa^4}{2880f^2\pi^2}-\frac{\kappa^2m^2}{48f\pi^2}+\frac{3m^4}{32\pi^2}+\frac{fm^4}{96\pi^2}+\frac{211f}{40320m^2\pi^2r^6}
$$

$$+\frac{95f}{192h^3m^2\pi^2r^6}+\frac{1061f}{1920h^{5/2}m^2\pi^2r^6}+\frac{11f}{192h^2m^2\pi^2r^6}$$
$$-\frac{f}{192h^{3/2}m^2\pi^2r^6}-\frac{f}{960hm^2\pi^2r^6}+\frac{19f}{1920m^2\pi^2r^6}+\frac{13f}{480\pi^2r^4}$$
$$-\frac{61f}{192h^2\pi^2r^4}-\frac{3f}{32h^{3/2}\pi^2r^4}-\frac{f}{96h\pi^2r^4}+\frac{f}{32\pi^2r^4}-\frac{fm^2}{32\pi^2r^2}$$
$$+\frac{fm^2}{16h\pi^2r^2}-\frac{fm^2}{64\pi^2r^2}+\frac{11\ln[\frac{\sqrt{f}}{8\pi^2}]}{240\pi^2r^4}+\frac{3\ln[\frac{\sqrt{f}}{8\pi^2}]}{80h^2\pi^2r^4}-\frac{\ln[\frac{\sqrt{f}}{8\pi^2}]}{12h\pi^2r^4}$$
$$-\frac{5411f'}{3840h^3m^2\pi^2r^5}-\frac{4241f'}{3840h^{5/2}m^2\pi^2r^5}-\frac{89f'}{960h^2m^2\pi^2r^5}$$
$$+\frac{f'}{128h^{3/2}m^2\pi^2r^5}+\frac{f'}{1280hm^2\pi^2r^5}-\frac{19f'}{3840m^2\pi^2r^5}+\frac{1091f'}{960h^2\pi^2r^3}$$
$$-\frac{f'}{240fh^2\pi^2r^3}+\frac{21f'}{64h^{3/2}\pi^2r^3}-\frac{5f'}{96h\pi^2r^3}-\frac{3f'}{64\pi^2r^3}-\frac{\kappa^2f'}{576f^2h\pi^2r}$$
$$+\frac{25m^2f'}{384h\pi^2r}+\frac{m^2f'}{96fh\pi^2r}-\frac{7m^2f'}{128\pi^2r}+\frac{11\ln[\frac{\sqrt{f}}{8\pi^2}]f'}{240fh^2\pi^2r^3}-\frac{\ln[\frac{\sqrt{f}}{8\pi^2}]f'}{24fh\pi^2r^3}$$
$$+\frac{\kappa^2f'^2}{576f^3h\pi^2}+\frac{m^2f'^2}{16fh\pi^2}+\frac{1831f'^2}{1280fh^3m^2\pi^2r^4}+\frac{183f'^2}{256fh^{5/2}m^2\pi^2r^4}$$
$$+\frac{349f'^2}{7680fh^2m^2\pi^2r^4}-\frac{f'^2}{256fh^{3/2}m^2\pi^2r^4}-\frac{633f'^2}{640fh^2\pi^2r^2}$$
$$-\frac{37f'^2}{256fh^{3/2}\pi^2r^2}+\frac{11f'^2}{256fh\pi^2r^2}+\frac{\ln[\frac{\sqrt{f}}{8\pi^2}]f'^2}{48f^2h^2\pi^2r^2}-\frac{533f'^3}{960f^2h^3m^2\pi^2r^3}$$
$$-\frac{333f'^3}{2560f^2h^{5/2}m^2\pi^2r^3}-\frac{7f'^3}{1280f^2h^2m^2\pi^2r^3}+\frac{f'^3}{1536f^2h^{3/2}m^2\pi^2r^3}$$
$$-\frac{f'^3}{1280f^3h^2\pi^2r}+\frac{311f'^3}{960f^2h^2\pi^2r}+\frac{5f'^3}{512f^2h^{3/2}\pi^2r}+\frac{\ln[\frac{\sqrt{f}}{8\pi^2}]f'^3}{960f^3h^2\pi^2r}$$
$$+\frac{29f'^4}{15360f^4h^2\pi^2}-\frac{143f'^4}{3072f^3h^2\pi^2}+\frac{47f'^4}{1920f^3h^3m^2\pi^2r^2}$$
$$-\frac{217f'^4}{10240f^3h^{5/2}m^2\pi^2r^2}-\frac{f'^4}{1024f^3h^2m^2\pi^2r^2}-\frac{19\ln[\frac{\sqrt{f}}{8\pi^2}]f'^4}{3840f^4h^2\pi^2}$$
$$+\frac{527f'^5}{20480f^4h^3m^2\pi^2r}+\frac{113f'^5}{20480f^4h^{5/2}m^2\pi^2r}-\frac{7f'^6}{2048f^5h^3m^2\pi^2}$$

$$+\frac{289fh'}{3840h^4m^2\pi^2r^5}+\frac{133fh'}{480h^{7/2}m^2\pi^2r^5}+\frac{7fh'}{320h^3m^2\pi^2r^5}$$
$$-\frac{fh'}{3840h^2m^2\pi^2r^5}-\frac{209fh'}{960h^3\pi^2r^3}-\frac{7fh'}{192h^{5/2}\pi^2r^3}-\frac{fh'}{96h^2\pi^2r^3}$$
$$-\frac{\kappa^2h'}{576fh^2\pi^2r}+\frac{m^2h'}{96h^2\pi^2r}+\frac{5fm^2h'}{384h^2\pi^2r}-\frac{11\ln[\frac{\sqrt{f}}{8\pi^2}]h'}{240h^3\pi^2r^3}+\frac{\ln[\frac{\sqrt{f}}{8\pi^2}]h'}{24h^2\pi^2r^3}$$
$$+\frac{\kappa^2f'h'}{1152f^2h^2\pi^2}+\frac{m^2f'h'}{256h^2\pi^2}-\frac{m^2f'h'}{192fh^2\pi^2}-\frac{3641f'h'}{7680h^4m^2\pi^2r^4}$$
$$-\frac{257f'h'}{480h^{7/2}m^2\pi^2r^4}-\frac{109f'h'}{3840h^3m^2\pi^2r^4}+\frac{f'h'}{7680h^2m^2\pi^2r^4}$$
$$+\frac{613f'h'}{1920h^3\pi^2r^2}-\frac{f'h'}{160fh^3\pi^2r^2}-\frac{f'h'}{96h^{5/2}\pi^2r^2}+\frac{f'h'}{128h^2\pi^2r^2}$$
$$-\frac{\ln[\frac{\sqrt{f}}{8\pi^2}]f'h'}{160fh^3\pi^2r^2}+\frac{2731f'^2h'}{3840fh^4m^2\pi^2r^3}+\frac{461f'^2h'}{1280fh^{7/2}m^2\pi^2r^3}$$
$$+\frac{29f'^2h'}{2560fh^3m^2\pi^2r^3}-\frac{7f'^2h'}{3840f^2h^3\pi^2r}-\frac{107f'^2h'}{1920fh^3\pi^2r}$$
$$+\frac{11f'^2h'}{384fh^{5/2}\pi^2r}+\frac{\ln[\frac{\sqrt{f}}{8\pi^2}]f'^2h'}{240f^2h^3\pi^2r}+\frac{73f'^3h'}{23040f^3h^3\pi^2}-\frac{83f'^3h'}{3840f^2h^3\pi^2}$$
$$-\frac{2851f'^3h'}{7680f^2h^4m^2\pi^2r^2}-\frac{467f'^3h'}{5120f^2h^{7/2}m^2\pi^2r^2}-\frac{17f'^3h'}{7680f^2h^3m^2\pi^2r^2}$$
$$-\frac{11\ln[\frac{\sqrt{f}}{8\pi^2}]f'^3h'}{1920f^3h^3\pi^2}+\frac{805f'^4h'}{12288f^3h^4m^2\pi^2r}+\frac{29f'^4h'}{5120f^3h^{7/2}m^2\pi^2r}$$
$$-\frac{313f'^5h'}{122880f^4h^4m^2\pi^2}-\frac{291fh'^2}{1280h^5m^2\pi^2r^4}+\frac{11fh'^2}{320h^{9/2}m^2\pi^2r^4}$$
$$+\frac{29fh'^2}{7680h^4m^2\pi^2r^4}-\frac{19fh'^2}{1920h^4\pi^2r^2}+\frac{fh'^2}{96h^{7/2}\pi^2r^2}+\frac{3\ln[\frac{\sqrt{f}}{8\pi^2}]h'^2}{160h^4\pi^2r^2}$$
$$+\frac{681f'h'^2}{2560h^5m^2\pi^2r^3}-\frac{f'h'^2}{16h^{9/2}m^2\pi^2r^3}-\frac{23f'h'^2}{7680h^4m^2\pi^2r^3}$$
$$-\frac{29f'h'^2}{640h^4\pi^2r}-\frac{f'h'^2}{320fh^4\pi^2r}-\frac{f'h'^2}{32h^{7/2}\pi^2r}+\frac{\ln[\frac{\sqrt{f}}{8\pi^2}]f'h'^2}{192fh^4\pi^2r}$$
$$+\frac{31f'^2h'^2}{7680f^2h^4\pi^2}+\frac{11f'^2h'^2}{2560fh^4\pi^2}+\frac{47f'^2h'^2}{15360fh^5m^2\pi^2r^2}$$

$$+\frac{439f'^2h'^2}{10240fh^{9/2}m^2\pi^2r^2}-\frac{7f'^2h'^2}{10240fh^4m^2\pi^2r^2}-\frac{23\ln[\frac{\sqrt{f}}{8\pi^2}]f'^2h'^2}{3840f^2h^4\pi^2}$$
$$-\frac{221f'^3h'^2}{4096f^2h^5m^2\pi^2r}-\frac{177f'^3h'^2}{20480f^2h^{9/2}m^2\pi^2r}+\frac{159f'^4h'^2}{20480f^3h^5m^2\pi^2}$$
$$-\frac{619fh'^3}{2560h^6m^2\pi^2r^3}-\frac{19fh'^3}{960h^{11/2}m^2\pi^2r^3}+\frac{7fh'^3}{1920h^5m^2\pi^2r^3}$$
$$+\frac{7fh'^3}{320h^5\pi^2r}+\frac{7\ln[\frac{\sqrt{f}}{8\pi^2}]h'^3}{480h^5\pi^2r}-\frac{7f'h'^3}{480h^5\pi^2}+\frac{7f'h'^3}{960fh^5\pi^2}$$
$$+\frac{4949f'h'^3}{15360h^6m^2\pi^2r^2}+\frac{77f'h'^3}{3840h^{11/2}m^2\pi^2r^2}-\frac{7f'h'^3}{3840h^5m^2\pi^2r^2}$$
$$-\frac{7\ln[\frac{\sqrt{f}}{8\pi^2}]f'h'^3}{960fh^5\pi^2}-\frac{5719f'^2h'^3}{61440fh^6m^2\pi^2r}-\frac{11f'^2h'^3}{5120fh^{11/2}m^2\pi^2r}$$
$$+\frac{157f'^3h'^3}{122880f^2h^6m^2\pi^2}-\frac{113fh'^4}{768h^7m^2\pi^2r^2}-\frac{7fh'^4}{768h13/2m^2\pi^2r^2}$$
$$+\frac{623f'h'^4}{3840h^7m^2\pi^2r}+\frac{7f'h'^4}{1536h13/2m^2\pi^2r}-\frac{797f'^2h'^4}{30720fh^7m^2\pi^2}$$
$$-\frac{91fh'^5}{1536h8m^2\pi^2r}+\frac{91f'h'^5}{3072h8m^2\pi^2}-\frac{\kappa^2f''}{576f^2h\pi^2}-m^2f''128h\pi^2$$
$$+\frac{m^2f''}{96fh\pi^2}+\frac{721f''}{3840h^3m^2\pi^2r^4}+\frac{39f''}{160h^{5/2}m^2\pi^2r^4}+\frac{19f''}{960h^2m^2\pi^2r^4}$$
$$-\frac{f''}{3840hm^2\pi^2r^4}-\frac{221f''}{960h^2\pi^2r^2}+\frac{f''}{240fh^2\pi^2r^2}+\frac{f''}{96h^{3/2}\pi^2r^2}$$
$$-\frac{f''}{64h\pi^2r^2}-\frac{\ln[\frac{\sqrt{f}}{8\pi^2}]f''}{240fh^2\pi^2r^2}-\frac{1859f'f''}{3840fh^3m^2\pi^2r^3}-\frac{103f'f''}{320fh^{5/2}m^2\pi^2r^3}$$
$$-\frac{17f'f''}{960fh^2m^2\pi^2r^3}+\frac{7f'f''}{2880f^2h^2\pi^2r}+\frac{37f'f''}{640fh^2\pi^2r}-\frac{11f'f''}{192fh^{3/2}\pi^2r}$$
$$-\frac{\ln[\frac{\sqrt{f}}{8\pi^2}]f'f''}{320f^2h^2\pi^2r}-\frac{73f'^2f''}{11520f^3h^2\pi^2}+\frac{83f'^2f''}{1920f^2h^2\pi^2}$$
$$+\frac{931f'^2f''}{2560f^2h^3m^2\pi^2r^2}+\frac{633f'^2f''}{5120f^2h^{5/2}m^2\pi^2r^2}+\frac{17f'^2f''}{3840f^2h^2m^2\pi^2r^2}$$
$$+\frac{11\ln[\frac{\sqrt{f}}{8\pi^2}]f'^2f''}{960f^3h^2\pi^2}-\frac{673f'^3f''}{7680f^3h^3m^2\pi^2r}-\frac{29f'^3f''}{2560f^3h^{5/2}m^2\pi^2r}$$

$$+\frac{313f'^4f''}{61440f^4h^3m^2\pi^2}-\frac{139h'f''}{1280h^4m^2\pi^2r^3}+\frac{7h'f''}{160h^{7/2}m^2\pi^2r^3}$$
$$+\frac{h'f''}{480h^3m^2\pi^2r^3}+\frac{47h'f''}{960h^3\pi^2r}+\frac{11h'f''}{960fh^3\pi^2r}+\frac{3h'f''}{64h^{5/2}\pi^2r}$$
$$-\frac{\ln[\frac{\sqrt{f}}{8\pi^2}]h'f''}{64fh^3\pi^2r}-\frac{f'h'f''}{120f^2h^3\pi^2}-\frac{f'h'f''}{3840fh^3\pi^2}-\frac{79f'h'f''}{7680fh^4m^2\pi^2r^2}$$
$$-\frac{143f'h'f''}{2560fh^{7/2}m^2\pi^2r^2}+\frac{f'h'f''}{1280fh^3m^2\pi^2r^2}+\frac{7\ln[\frac{\sqrt{f}}{8\pi^2}]f'h'f''}{640f^2h^3\pi^2}$$
$$+\frac{187f'^2h'f''}{2560f^2h^4m^2\pi^2r}+\frac{169f'^2h'f''}{10240f^2h^{7/2}m^2\pi^2r}-\frac{37f'^3h'f''}{2560f^3h^4m^2\pi^2}$$
$$+\frac{19h'^2f''}{960h^4\pi^2}-\frac{19h'^2f''}{1920fh^4\pi^2}-\frac{253h'^2f''}{1536h^5m^2\pi^2r^2}-\frac{67h'^2f''}{5120h^{9/2}m^2\pi^2r^2}$$
$$+\frac{19h'^2f''}{7680h^4m^2\pi^2r^2}+\frac{19\ln[\frac{\sqrt{f}}{8\pi^2}]h'^2f''}{1920fh^4\pi^2}+\frac{2897f'h'^2f''}{30720fh^5m^2\pi^2r}$$
$$+\frac{37f'h'^2f''}{10240fh^{9/2}m^2\pi^2r}-\frac{31f'^2h'^2f''}{10240f^2h^5m^2\pi^2}-\frac{3059h'^3f''}{30720h^6m^2\pi^2r}$$
$$-\frac{3h'^3f''}{512h^{11/2}m^2\pi^2r}+\frac{2437f'h'^3f''}{61440fh^6m^2\pi^2}-\frac{113h'^4f''}{3072h^7m^2\pi^2}$$
$$+\frac{7f''^2}{1920f^2h^2\pi^2}-\frac{19f''^2}{1920fh^2\pi^2}-\frac{11f''^2}{1920fh^3m^2\pi^2r^2}$$
$$+\frac{3f''^2}{320fh^{5/2}m^2\pi^2r^2}+\frac{f''^2}{2560fh^2m^2\pi^2r^2}-\frac{\ln[\frac{\sqrt{f}}{8\pi^2}]f''^2}{320f^2h^2\pi^2}$$
$$-\frac{71f'f''^2}{5120f^2h^3m^2\pi^2r}-\frac{29f'f''^2}{5120f^2h^{5/2}m^2\pi^2r}+\frac{23f'^2f''^2}{5120f^3h^3m^2\pi^2}$$
$$-\frac{301h'f''^2}{15360fh^4m^2\pi^2r}-\frac{h'f''^2}{1024fh^{7/2}m^2\pi^2r}+\frac{19f'h'f''^2}{10240f^2h^4m^2\pi^2}$$
$$-\frac{127h'^2f''^2}{15360fh^5m^2\pi^2}-\frac{f''^3}{15360f^2h^3m^2\pi^2}+\frac{9fh''}{160h^4m^2\pi^2r^4}$$
$$-\frac{fh''}{60h^{7/2}m^2\pi^2r^4}-\frac{fh''}{960h^3m^2\pi^2r^4}+\frac{fh''}{240h^3\pi^2r^2}-\frac{fh''}{192h^{5/2}\pi^2r^2}$$
$$-\frac{71f'h''}{1280h^4m^2\pi^2r^3}+\frac{11f'h''}{384h^{7/2}m^2\pi^2r^3}+\frac{f'h''}{1280h^3m^2\pi^2r^3}$$

$$+\frac{11f'h''}{480h^3\pi^2r}+\frac{f'h''}{960fh^3\pi^2r}+\frac{f'h''}{64h^{5/2}\pi^2r}-\frac{\ln[\frac{\sqrt{f}}{8\pi^2}]f'h''}{960fh^3\pi^2r}$$
$$-\frac{f'^2h''}{640f^2h^3\pi^2}-\frac{13f'^2h''}{3840fh^3\pi^2}-\frac{27f'^2h''}{1280fh^4m^2\pi^2r^2}$$
$$-\frac{47f'^2h''}{2560fh^{7/2}m^2\pi^2r^2}+\frac{f'^2h''}{2560fh^3m^2\pi^2r^2}+\frac{\ln[\frac{\sqrt{f}}{8\pi^2}]f'^2h''}{384f^2h^3\pi^2}$$
$$+\frac{49f'^3h''}{2048f^2h^4m^2\pi^2r}+\frac{37f'^3h''}{10240f^2h^{7/2}m^2\pi^2r}-\frac{17f'^4h''}{5120f^3h^4m^2\pi^2}$$
$$+\frac{229fh'h''}{1280h^5m^2\pi^2r^3}+\frac{31fh'h''}{1920h^{9/2}m^2\pi^2r^3}-\frac{13fh'h''}{3840h^4m^2\pi^2r^3}$$
$$-\frac{13fh'h''}{640h^4\pi^2r}-\frac{13\ln[\frac{\sqrt{f}}{8\pi^2}]h'h''}{960h^4\pi^2r}+\frac{13f'h'h''}{960h^4\pi^2}-\frac{13f'h'h''}{1920fh^4\pi^2}$$
$$-\frac{1859f'h'h''}{7680h^5m^2\pi^2r^2}-\frac{f'h'h''}{60h^{9/2}m^2\pi^2r^2}+\frac{13f'h'h''}{7680h^4m^2\pi^2r^2}$$
$$+\frac{13\ln[\frac{\sqrt{f}}{8\pi^2}]f'h'h''}{1920fh^4\pi^2}+\frac{733f'^2h'h''}{10240fh^5m^2\pi^2r}+\frac{19f'^2h'h''}{10240fh^{9/2}m^2\pi^2r}$$
$$-\frac{19f'^3h'h''}{20480f^2h^5m^2\pi^2}+\frac{1403fh'^2h''}{7680h^6m^2\pi^2r^2}+\frac{47fh'^2h''}{3840h^{11/2}m^2\pi^2r^2}$$
$$-\frac{49f'h'^2h''}{240h^6m^2\pi^2r}-\frac{47f'h'^2h''}{7680h^{11/2}m^2\pi^2r}+\frac{2063f'^2h'^2h''}{61440fh^6m^2\pi^2}$$
$$+\frac{797fh'^3h''}{7680h^7m^2\pi^2r}-\frac{797f'h'^3h''}{15360h^7m^2\pi^2}-\frac{f''h''}{120h^3\pi^2}+\frac{f''h''}{240fh^3\pi^2}$$
$$+\frac{5f''h''}{96h^4m^2\pi^2r^2}+\frac{3f''h''}{640h^{7/2}m^2\pi^2r^2}-\frac{f''h''}{960h^3m^2\pi^2r^2}-\frac{\ln[\frac{\sqrt{f}}{8\pi^2}]f''h''}{240fh^3\pi^2}$$
$$-\frac{157f'f''h''}{5120fh^4m^2\pi^2r}-\frac{7f'f''h''}{5120fh^{7/2}m^2\pi^2r}+\frac{f'^2f''h''}{1024f^2h^4m^2\pi^2}$$
$$+\frac{1169h'f''h''}{15360h^5m^2\pi^2r}+\frac{5h'f''h''}{1024h^{9/2}m^2\pi^2r}-\frac{967f'h'f''h''}{30720fh^5m^2\pi^2}$$
$$+\frac{1403h'^2f''h''}{30720h^6m^2\pi^2}+\frac{11f''^2h''}{3840fh^4m^2\pi^2}-\frac{11fh''^2}{480h^5m^2\pi^2r^2}$$
$$-\frac{13fh''^2}{7680h^{9/2}m^2\pi^2r^2}+\frac{133f'h''^2}{5120h^5m^2\pi^2r}+\frac{13f'h''^2}{15360h^{9/2}m^2\pi^2r}$$

$$-\frac{9f'^2h''^2}{2048fh^5m^2\pi^2}-\frac{493fh'h''^2}{15360h^6m^2\pi^2r}+\frac{493f'h'h''^2}{30720h^6m^2\pi^2}$$
$$-\frac{11f''h''^2}{1920h^5m^2\pi^2}-\frac{3f^3}{640h^3m^2\pi^2r^3}-\frac{11f^3}{480h^{5/2}m^2\pi^2r^3}$$
$$+\frac{f^3}{1920h^2m^2\pi^2r^3}-\frac{f^3}{30h^2\pi^2r}-\frac{f^3}{160fh^2\pi^2r}-\frac{f^3}{32h^{3/2}\pi^2r}$$
$$+\frac{\ln[\frac{\sqrt{f}}{8\pi^2}]f^3}{160fh^2\pi^2r}+\frac{f'f^3}{320f^2h^2\pi^2}+\frac{13f'f^3}{1920fh^2\pi^2}+\frac{27f'f^3}{640fh^3m^2\pi^2r^2}$$
$$+\frac{199f'f^3}{7680fh^{5/2}m^2\pi^2r^2}-\frac{f'f^3}{1280fh^2m^2\pi^2r^2}-\frac{\ln[\frac{\sqrt{f}}{8\pi^2}]f'f^3}{192f^2h^2\pi^2}$$
$$-\frac{23f'^2f^3}{640f^2h^3m^2\pi^2r}-\frac{37f'^2f^3}{5120f^2h^{5/2}m^2\pi^2r}+\frac{17f'^3f^3}{2560f^3h^3m^2\pi^2}$$
$$-\frac{h'f^3}{80h^3\pi^2}+\frac{h'f^3}{160fh^3\pi^2}+\frac{13h'f^3}{256h^4m^2\pi^2r^2}+\frac{13h'f^3}{2560h^{7/2}m^2\pi^2r^2}$$
$$-\frac{h'f^3}{640h^3m^2\pi^2r^2}-\frac{\ln[\frac{\sqrt{f}}{8\pi^2}]h'f^3}{160fh^3\pi^2}-\frac{59f'h'f^3}{1920fh^4m^2\pi^2r}$$
$$-\frac{29f'h'f^3}{15360fh^{7/2}m^2\pi^2r}+\frac{3f'^2h'f^3}{2560f^2h^4m^2\pi^2}+\frac{217h'^2f^3}{5120h^5m^2\pi^2r}$$
$$+\frac{11h'^2f^3}{3072h^{9/2}m^2\pi^2r}-\frac{41f'h'^2f^3}{1920fh^5m^2\pi^2}+\frac{45h'^3f^3}{2048h^6m^2\pi^2}$$
$$+\frac{7f''f^3}{768fh^3m^2\pi^2r}+\frac{f''f^3}{1536fh^{5/2}m^2\pi^2r}-\frac{3f'f''f^3}{2560f^2h^3m^2\pi^2}$$
$$+\frac{h'f''f^3}{160fh^4m^2\pi^2}-\frac{7h''f^3}{512h^4m^2\pi^2r}-\frac{h''f^3}{768h^{7/2}m^2\pi^2r}$$
$$+\frac{11f'h''f^3}{1536fh^4m^2\pi^2}-\frac{17h'h''f^3}{1024h^5m^2\pi^2}-\frac{f^{3/2}}{1536fh^3m^2\pi^2}$$
$$-\frac{13fh^3}{640h^4m^2\pi^2r^3}-\frac{fh^3}{480h^{7/2}m^2\pi^2r^3}+\frac{fh^3}{1920h^3m^2\pi^2r^3}$$
$$+\frac{fh^3}{320h^3\pi^2r}+\frac{\ln[\frac{\sqrt{f}}{8\pi^2}]h^3}{480h^3\pi^2r}-\frac{f'h^3}{480h^3\pi^2}+\frac{f'h^3}{960fh^3\pi^2}$$
$$+\frac{9f'h^3}{320h^4m^2\pi^2r^2}+\frac{17f'h^3}{7680h^{7/2}m^2\pi^2r^2}-\frac{f'h^3}{3840h^3m^2\pi^2r^2}$$

$$
\begin{aligned}
&-\frac{\ln[\frac{\sqrt{f}}{8\pi^2}]f'h^3}{960fh^3\pi^2}-\frac{11f'^2h^3}{1280fh^4m^2\pi^2r}-\frac{f'^2h^3}{3840fh^{7/2}m^2\pi^2r}\\
&+\frac{f'^3h^3}{10240f^2h^4m^2\pi^2}-\frac{43fh'h^3}{1280h^5m^2\pi^2r^2}-\frac{19fh'h^3}{7680h^{9/2}m^2\pi^2r^2}\\
&+\frac{49f'h'h^3}{1280h^5m^2\pi^2r}+\frac{19f'h'h^3}{15360h^{9/2}m^2\pi^2r}-\frac{67f'^2h'h^3}{10240fh^5m^2\pi^2}\\
&-\frac{359fh'^2h^3}{15360h^6m^2\pi^2r}+\frac{359f'h'^2h^3}{30720h^6m^2\pi^2}-\frac{7f''h^3}{768h^4m^2\pi^2r}\\
&-\frac{f''h^3}{1536h^{7/2}m^2\pi^2r}+\frac{61f'f''h^3}{15360fh^4m^2\pi^2}-\frac{43h'f''h^3}{5120h^5m^2\pi^2}\\
&+\frac{3fh''h^3}{512h^5m^2\pi^2r}-\frac{3f'h''h^3}{1024h^5m^2\pi^2}+\frac{f^3h^3}{512h^4m^2\pi^2}+\frac{f^4}{240h^2\pi^2}\\
&-\frac{f^4}{480fh^2\pi^2}-\frac{f^4}{128h^3m^2\pi^2r^2}-\frac{f^4}{960h^{5/2}m^2\pi^2r^2}\\
&+\frac{f^4}{1920h^2m^2\pi^2r^2}+\frac{\ln[\frac{\sqrt{f}}{8\pi^2}]f^4}{480fh^2\pi^2}+\frac{13f'f^4}{2560fh^3m^2\pi^2r}\\
&+\frac{f'f^4}{1920fh^{5/2}m^2\pi^2r}-\frac{f'^2f^4}{5120f^2h^3m^2\pi^2}-\frac{91h'f^4}{7680h^4m^2\pi^2r}\\
&-\frac{h'f^4}{768h^{7/2}m^2\pi^2r}+\frac{37f'h'f^4}{5120fh^4m^2\pi^2}-\frac{25h'^2f^4}{3072h^5m^2\pi^2}\\
&-\frac{11f''f^4}{7680fh^3m^2\pi^2}+\frac{h''f^4}{384h^4m^2\pi^2}+\frac{fh^4}{320h^4m^2\pi^2r^2}\\
&+\frac{fh^4}{3840h^{7/2}m^2\pi^2r^2}-\frac{7f'h^4}{1920h^4m^2\pi^2r}-\frac{f'h^4}{7680h^{7/2}m^2\pi^2r}\\
&+\frac{f'^2h^4}{1536fh^4m^2\pi^2}+\frac{13fh'h^4}{3840h^5m^2\pi^2r}-\frac{13f'h'h^4}{7680h^5m^2\pi^2}\\
&+\frac{f''h^4}{1280h^4m^2\pi^2}+\frac{7f^5}{3840h^3m^2\pi^2r}+\frac{f^5}{3840h^{5/2}m^2\pi^2r}\\
&-\frac{f'f^5}{768fh^3m^2\pi^2}+\frac{h'f^5}{512h^4m^2\pi^2}-\frac{fh^5}{3840h^4m^2\pi^2r}+\frac{f'h^5}{7680h^4m^2\pi^2}\\
&-\frac{f^6}{3840h^3m^2\pi^2}
\end{aligned}
\tag{B3}
$$

In these equations, f and h are coefficient functions in Eq. (1.1); m is the mass of the field quantum; and $\kappa = 2\pi T$ with T being the temperature.

Appendix C: Stress-Energy Tensor of the Quantized Neutrino Field and Quantized Proton Field in the Zero-Tidal-Force Wormhole Spacetime

C.1 Zero-temperature vacuum state

C.1.1 Quatized neutrino field

The stress-energy tensor components of a quantized neutrino field in the entire spacetime of the zero-tidal-force wormhole geometry in a zero-temperature vacuum state are computed to be (in units of F_p/l_p^2):

$$\begin{aligned} < T_t^t > \;\; = \;\; & 3.2 \times 10^{54}/r^8 - 2.2 \times 10^{54}/r^6 + 0.2/r^4 + 6.6 \times 10^{-60}/r^2 \\ & -2.0 \times 10^{43}/(r^3 r_0^3) - 1.4 \times 10^{-17}/(r r_0^3) - 4.3 \times 10^{42}/(r^4 r_0^2) \\ & +4.0 \times 10^{-16}/(r^2 r_0^2) - 1.4 \times 10^{42}/(r^5 r_0) + 9.7 \times 10^{-17}/(r^3 r_0) \\ & -1.6 \times 10^{54} r_0/r^9 - 1.5 \times 10^{56} r_0/r^7 - 0.4 r_0/r^5 \end{aligned}$$

$$
\begin{aligned}
&-8.5\times10^{-60}r_0/r^3+2.7\times10^{56}r_0^2/r^8+0.2r_0^2/r^6\\
&-1.2\times10^{56}r_0^3/r^9, \qquad \text{(C1)}
\end{aligned}
$$

$$
\begin{aligned}
<T_r^r> \;=\; & -0.00003-3.16735\times10^{54}/r^8-2.9\times10^{56}/r^6+0.02/r^4\\
&+0.02/r^3-0.004/r^2+0.0005/r-6.6\times10^{43}/(r^3r_0^3)\\
&-1.9\times10^{-16}/(rr_0^3)-1.5\times10^{43}/(r^4r_0^2)-1.0\times10^{-16}/(r^2r_0^2)\\
&-9.0\times10^{42}/(r^5r_0)-7.6\times10^{-17}/(r^3r_0)+1.6\times10^{54}r_0/r^9\\
&+8.7\times10^{56}r_0/r^7-0.06r_0/r^5-0.02r_0/r^4+0.006r_0/r^3\\
&-0.001r_0/r^2+0.00007r_0/r-6.4\times10^{56}r_0^2/r^8+0.03r_0^2/r^6\\
&+0.004r_0^2/r^5-0.002r_0^2/r^4+0.0004r_0^2/r^3-0.00003r_0^2/r^2\\
&+6.3\times10^{55}r_0^3/r^9, \qquad \text{(C2)}
\end{aligned}
$$

$$
\begin{aligned}
<T_\theta^\theta> \;=\; & 1.6\times10^{-117}+1.5\times10^{56}/r^6-0.03/r^4+1.2\times10^{-60}/r^2\\
&-2.4\times10^{43}/(r^3r_0^3)+2.3\times10^{-16}/(rr_0^3)-1.2\times10^{43}/(r^4r_0^2)\\
&+9.4\times10^{-17}/(r^2r_0^2)-4.2\times10^{42}/(r^5r_0)\\
&+5.2\times10^{-17}/(r^3r_0)-(3.6\times10^{56}r_0)/r^7+0.09r_0/r^5\\
&-3.6\times10^{-60}r_0/r^3+1.9\times10^{56}r_0^2/r^8-0.06r_0^2/r^6\\
&+2.8\times10^{55}r_0^3/r^9. \qquad \text{(C3)}
\end{aligned}
$$

C.1.2 Quantized proton field

Similarly, the stress-energy tensor components of a quantized proton field in the entire spacetime of the zero-tidal-force wormhole geometry in a zero-temperature vacuum state are found to be (in units of F_p/l_p^2):

$$\begin{aligned} < T_t^t > \;=\; & 2.1\times 10^{35}/r^8 - 1.4\times 10^{35}/r^6 + 0.2/r^4 + 1.0\times 10^{-40}/r^2 \\ & +3.0\times 10^{23}/(r^3 r_0^3) - 1.4\times 10^{-17}/(r r_0^3) + 2.3\times 10^{23}/(r^4 r_0^2) \\ & +4.0\times 10^{-16}/(r^2 r_0^2) + 7.6\times 10^{22}/(r^5 r_0) \\ & +9.7\times 10^{-17}/(r^3 r_0) - 1.1\times 10^{35} r_0/r^9 - 1.0\times 10^{37} r_0/r^7 \\ & -0.4 r_0/r^5 - 1.3\times 10^{-40} r_0/r^3 + 1.8\times 10^{37} r_0^2/r^8 + 0.2 r_0^2/r^6 \\ & -7.7\times 10^{36} r_0^3/r^9, \end{aligned} \tag{C4}$$

$$\begin{aligned} < T_r^r > \;=\; & -0.00003 - 2.1\times 10^{35}/r^8 - 1.9\times 10^{37}/r^6 + 0.02/r^4 + 0.02/r^3 \\ & -0.004/r^2 + 0.0005/r + 7.4\times 10^{24}/(r^3 r_0^3) - 1.9\times 10^{-16}/(r r_0^3) \\ & +2.3\times 10^{24}/(r^4 r_0^2) - 1.0\times 10^{-16}/(r^2 r_0^2) + 2.1\times 10^{22}/(r^5 r_0) \\ & -7.6\times 10^{-17}/(r^3 r_0) + 1.1\times 10^{35} r_0/r^9 + 5.7\times 10^{37} r_0/r^7 \\ & -0.06 r_0/r^5 - 0.02 r_0/r^4 + 0.006 r_0/r^3 - 0.001 r_0/r^2 \\ & +0.00007 r_0/r - 4.2\times 10^{37} r_0^2/r^8 + 0.03 r_0^2/r^6 + 0.004 r_0^2/r^5 \\ & -0.002 r_0^2/r^4 + 0.0004 r_0^2/r^3 - 0.00003 r_0^2/r^2 \\ & +4.1\times 10^{36} r_0^3/r^9, \end{aligned} \tag{C5}$$

$$
\begin{aligned}
< T_{\theta}^{\theta} > \;\; = \;\; & 3.7 \times 10^{-79} + 9.6 \times 10^{36}/r^6 - 0.03/r^4 + 1.9 \times 10^{-41}/r^2 \\
& -1.7 \times 10^{23}/(r^3 r_0^3) + 2.3 \times 10^{-16}/(r r_0^3) - 5.2 \times 10^{23}/(r^4 r_0^2) \\
& +9.4 \times 10^{-17}/(r^2 r_0^2) + 3.8 \times 10^{22}/(r^5 r_0) \\
& +5.2 \times 10^{-17}/(r^3 r_0) - 2.3 \times 10^{37} r_0/r^7 + 0.09 r_0/r^5 \\
& -5.1 \times 10^{-41} r_0/r^3 + 1.2 \times 10^{37} r_0^2/r^8 - 0.06 r_0^2/r^6 \\
& +1.8 \times 10^{36} r_0^3/r^9 . \qquad \text{(C6)}
\end{aligned}
$$

C.2 Thermal states

C.2.1 Quantized neutrino field

The stress-energy tensor components of a quantized neutrino field in the entire spacetime for the zero-tidal-force wormhole goemetry in thermal states are found to be (in units of F_p/l_p^2):

$$
\begin{aligned}
< T_{t}^{t} > \;\; = \;\; & 3.2 \times 10^{54}/r^8 - 2.2 \times 10^{54}/r^6 + 0.2/r^4 + 6.6 \times 10^{-60}/r^2 \\
& -1.9 \times 10^{43}/(r^3 r_0^3) + 6.0 \times 10^{-15}/(r r_0^3) - 5.4 \times 10^{42}/(r^4 r_0^2) \\
& -3.8 \times 10^{-15}/(r^2 r_0^2) - 2.0 \times 10^{42}/(r^5 r_0) \\
& +1.9 \times 10^{-15}/(r^3 r_0) - 1.6 \times 10^{54} r_0/r^9 - 1.5 \times 10^{56} r_0/r^7 \\
& -0.4 r_0/r^5 - 8.5 \times 10^{-60} r_0/r^3 + 2.7 \times 10^{56} r_0^2/r^8 + 0.2 r_0^2/r^6 \\
& -1.2 \times 10^{56} r_0^3/r^9 + 3.2 \times 10^{-59} T^2 - 1.2 T^4 \\
& -1.8 \times 10^{-16} (\ln T)/(r r_0^3) - 2.8 \times 10^{-17} (\ln T)/(r^2 r_0^2) \\
& -0.0009 r_0^2 (\ln T)/r^6 , \qquad \text{(C7)}
\end{aligned}
$$

$$
\begin{aligned}
< T_r^r > \;=\; & -0.00003 - 3.2\times 10^{54}/r^8 - 2.9\times 10^{56}/r^6 + 0.02/r^4 \\
& +0.02/r^3 - 0.004/r^2 + 0.0005/r + 4.8\times 10^{43}/(r^3 r_0^3) \\
& -5.3\times 10^{-15}/(r r_0^3) + 1.2\times 10^{43}/(r^4 r_0^2) - 3.7\times 10^{-15}/(r^2 r_0^2) \\
& +2.5\times 10^{42}/(r^5 r_0) - 1.6\times 10^{-15}/(r^3 r_0) + 1.6\times 10^{54} r_0/r^9 \\
& +8.7\times 10^{56} r_0/r^7 - 0.06 r_0/r^5 - 0.02 r_0/r^4 + 0.006 r_0/r^3 \\
& -0.001 r_0/r^2 + 0.00007 r_0/r - 6.4\times 10^{56} r_0^2/r^8 - 0.08 r_0^2/r^6 \\
& +0.004 r_0^2/r^5 - 0.002 r_0^2/r^4 + 0.0004 r_0^2/r^3 - 0.00003 r_0^2/r^2 \\
& +6.3\times 10^{55} r_0^3/r^9 - 3.2\times 10^{-59} T^2 - 0.01 r_0 T^2/r^3 + 0.4 T^4 \\
& +3.5\times 10^{-18}(\ln T)/r^4 + 6.9\times 10^{-18}(\ln T)/(r^2 r_0^2) \\
& +6.9\times 10^{-18}(\ln T)/(r^3 r_0) + 1.7\times 10^{-18} r_0 (\ln T)/r^5 \\
& -0.002 r_0^2 (\ln T)/r^6, \qquad \text{(C8)}
\end{aligned}
$$

$$
\begin{aligned}
< T_\theta^\theta > \;=\; & 1.6\times 10^{-117} + 1.5\times 10^{56}/r^6 - 0.03/r^4 + 1.2\times 10^{-60}/r^2 \\
& -7.2\times 10^{43}/(r^3 r_0^3) + 3.9\times 10^{-15}/(r r_0^3) - 2.5\times 10^{43}/(r^4 r_0^2) \\
& +2.8\times 10^{-15}/(r^2 r_0^2) - 5.5\times 10^{42}/(r^5 r_0) \\
& +7.3\times 10^{-16}/(r^3 r_0) - 3.6\times 10^{56} r_0/r^7 + 0.09 r_0/r^5 \\
& -3.4^{-60} r_0/r^3 + 1.9\times 10^{56} r_0^2/r^8 - 0.2 r_0^2/r^6 + 2.8\times 10^{55} r_0^3/r^9 \\
& -3.2\times 10^{-59} T^2 + 0.007 r_0 T^2/r^3 + 0.4 T^4 \\
& +1.0\times 10^{-16}(\ln T)/(r r_0^3) + 3.5\times 10^{-18}(\ln T)/(r^2 r_0^2) \\
& +1.7\times 10^{-18}(\ln T)/(r^3 r_0) - 0.003 r_0^2 (\ln T)/r^6. \qquad \text{(C9)}
\end{aligned}
$$

C.2.2 Quantized proton field

The stress-energy tensor components of a quantized proton field in the entire spacetime for the zero-tidal-force wormhole geometry in thermal states are found to be (in units of F_p/l_p^2):

$$\begin{aligned}
< T_t^t > \;=\; & 2.1\times 10^{35}/r^8 - 1.4\times 10^{35}/r^6 + 0.2/r^4 + 1.0\times 10^{-40}/r^2 \\
& +5.4\times 10^{23}/(r^3 r_0^3) + 9.9\times 10^{-15}/(r r_0^3) + 2.7\times 10^{23}/(r^4 r_0^2) \\
& +5.1\times 10^{-15}/(r^2 r_0^2) + 1.3\times 10^{23}/(r^5 r_0) + 1.9\times 10^{-15}/(r^3 r_0) \\
& -1.1\times 10^{35} r_0/r^9 - 1.0\times 10^{37} r_0/r^7 - 0.4 r_0/r^5 \\
& -1.3\times 10^{-40} r_0/r^3 + 1.8\times 10^{37} r_0^2/r^8 + 0.2 r_0^2/r^6 \\
& -7.7\times 10^{36} r_0^3/r^9 + 4.9\times 10^{-40} T^2 - 1.2 T^4 \\
& -1.8\times 10^{-16}(\ln T)/(r r_0^3) - 2.8\times 10^{-17}(\ln T)/(r^2 r_0^2) \\
& -0.0009 r_0^2 (\ln T)/r^6, \qquad \text{(C10)}
\end{aligned}$$

$$\begin{aligned}
< T_r^r > \;=\; & -0.00003 - 2.0\times 10^{35}/r^8 - 1.9\times 10^{37}/r^6 + 0.02/r^4 + 0.02/r^3 \\
& -0.004/r^2 + 0.0005/r + 3.6\times 10^{24}/(r^3 r_0^3) - 3.0\times 10^{-15}/(r r_0^3) \\
& +1.9\times 10^{24}/(r^4 r_0^2) - 1.5\times 10^{-16}/(r^2 r_0^2) - 1.7\times 10^{22}/(r^5 r_0) \\
& -6.2\times 10^{-17}/(r^3 r_0) + 1.1\times 10^{35} r_0/r^9 + 5.7\times 10^{37} r_0/r^7 \\
& -0.06 r_0/r^5 - 0.02 r_0/r^4 + 0.006 r_0/r^3 - 0.001 r_0/r^2 \\
& +0.00007 r_0/r - 4.2\times 10^{37} r_0^2/r^8 - 0.04 r_0^2/r^6 + 0.004 r_0^2/r^5
\end{aligned}$$

$$
\begin{aligned}
& -0.002 r_0^2/r^4 + 0.0004 r_0^2/r^3 - 0.00003 r_0^2/r^2 + 4.1 \times 10^{36} r_0^3/r^9 \\
& -4.9 \times 10^{-40} T^2 - 0.01 r_0 T^2/r^3 + 0.4 T^4 + 3.5 \times 10^{-18} (\ln T)/r^4 \\
& +6.9 \times 10^{-18} (\ln T)/(r^2 r_0^2) + 6.9 \times 10^{-18} (\ln T)/(r^3 r_0) \\
& +1.7 \times 10^{-18} r_0 (\ln T)/r^5 - 0.002 r_0^2 (\ln T)/r^6. \qquad \text{(C11)}
\end{aligned}
$$

$$
\begin{aligned}
< T_\theta^\theta > \;\; = \;\; & 3.7 \times 10^{-79} + 9.6 \times 10^{36}/r^6 - 0.03/r^4 + 1.9 \times 10^{-41}/r^2 \\
& -6.6 \times 10^{23}/(r^3 r_0^3) - 5.2 \times 10^{-15}/(r r_0^3) - 8.4 \times 10^{22}/(r^4 r_0^2) \\
& -5.8 \times 10^{-16}/(r^2 r_0^2) + 2.9 \times 10^{22}/(r^5 r_0) \\
& -3.0 \times 10^{-16}/(r^3 r_0) - 2.3 \times 10^{37} r_0/r^7 + 0.09 r_0/r^5 \\
& -5.1 \times 10^{-41} r_0/r^3 + 1.2 \times 10^{37} r_0^2/r^8 - 0.2 r_0^2/r^6 \\
& +1.8 \times 10^{36} r_0^3/r^9 - 4.9 \times 10^{-40} T^2 + 0.007 r_0 T^2/r^3 \\
& +0.4 T^4 + 1.0 \times 10^{-16} (\ln T)/(r r_0^3) + 3.5 \times 10^{-18} (\ln T)/(r^2 r_0^2) \\
& +1.7 \times 10^{-18} (\ln T)/(r^3 r_0) - 0.003 r_0^2 (\ln T)/r^6. \qquad \text{(C12)}
\end{aligned}
$$

Appendix D: Stress-Energy Tensor of the Quantized Neutrino Field and Quantized Proton Field in the Simple Wormhole Spacetime

D.1 Zero-temperature vacuum state

D.1.1 Quantized neutrino field

The stress-energy tensor components of a quantized neutrino field in the entire spacetime of the simple wormhole geometry at zero temperature are found to be (in units of F_p/l_p^2):

$$\begin{aligned} < T_t^t > \;\; = \;\; & 3.2 \times 10^{54}/r^8 - 2.2 \times 10^{54}/r^6 + 0.2/r^4 + 6.6 \times 10^{-60}/r^2 \\ & -1.5 \times 10^{43}/(r^4 r_0^2) + 3.5 \times 10^{-16}/(r^2 r_0^2) - 1.6 \times 10^{54} r_0^2/r^{10} \\ & -4.1 \times 10^{56} r_0^2/r^8 - 0.5 r_0^2/r^6 - 8.3 \times 10^{-60} r_0^2/r^4 \\ & +7.4 \times 10^{56} r_0^4/r^{10} + 0.3 r_0^4/r^8 - 3.3 \times 10^{56} r_0^6/r^{12}, \end{aligned} \tag{D1}$$

$$
\begin{aligned}
< T_r^r > \;=\; & -0.00003 - 3.2\times 10^{54}/r^8 - 2.9\times 10^{56}/r^6 + 0.02/r^4 + 0.02/r^3 \\
& -0.004/r^2 + 0.0005/r + 5.0\times 10^{43}/(r^4 r_0^2) - 3.5\times 10^{-16}/(r^2 r_0^2) \\
& +1.6\times 10^{54} r_0^2/r^{10} + 6.4\times 10^{56} r_0^2/r^8 - 0.1 r_0^2/r^6 - 0.02 r_0^2/r^5 \\
& +0.006 r_0^2/r^4 - 0.0009 r_0^2/r^3 + 0.00007 r_0^2/r^2 + 7.6\times 10^{56} r_0^4/r^{10} \\
& +0.03 r_0^4/r^8 + 0.003 r_0^4/r^7 - 0.002 r_0^4/r^6 + 0.0003 r_0^4/r^5 \\
& -0.00003 r_0^4/r^4 - 1.2\times 10^{57} r_0^6/r^{12}, \qquad \text{(D2)}
\end{aligned}
$$

$$
\begin{aligned}
< T_\theta^\theta > \;=\; & 1.6\times 10^{-117} + 1.5\times 10^{56}/r^6 - 0.03/r^4 + 1.2\times 10^{-60}/r^2 \\
& +1.4\times 10^{44}/(r^4 r_0^2) + 4.3\times 10^{-16}/(r^2 r_0^2) - 1.1\times 10^{56} r_0^2/r^8 \\
& +0.1 r_0^2/r^6 - 4.3\times 10^{-60} r_0^2/r^4 - 7.5\times 10^{56} r_0^4/r^{10} \\
& -0.1 r_0^4/r^8 + 7.5\times 10^{56} r_0^6/r^{12}. \qquad \text{(D3)}
\end{aligned}
$$

D.1.2 Quantized proton field

The stress-energy tensor components of a quantized proton field in the entire spacetime of the simple wormhole geometry at zero temperature are found to be (in units of F_p/l_p^2):

$$
\begin{aligned}
< T_t^t > \;=\; & 2.1\times 10^{35}/r^8 - 1.4\times 10^{35}/r^6 + 0.2/r^4 + 1.0\times 10^{-40}/r^2 \\
& +1.2\times 10^{24}/(r^4 r0^2) + 3.5\times 10^{-16}/(r^2 r_0^2) - 1.1\times 10^{35} r_0^2/r^{10} \\
& -2.7\times 10^{37} r_0^2/r^8 - 0.5 r_0^2/r^6 - 1.3\times 10^{-40} r_0^2/r^4 \\
& +4.9\times 10^{37} r_0^4/r^{10} + 0.3 r_0^4/r^8 - 2.2\times 10^{37} r_0^6/r^{12}, \qquad \text{(D4)}
\end{aligned}
$$

$$
\begin{aligned}
< T_r^r > \;=\; & -0.00003 - 2.1\times 10^{35}/r^8 - 1.9\times 10^{37}/r^6 + 0.02/r^4 + 0.02/r^3 \\
& -0.004/r^2 + 0.0005/r + 2.6\times 10^{25}/(r^4 r_0^2) \\
& -3.5\times 10^{-16}/(r^2 r_0^2) + 1.1\times 10^{35} r_0^2/r^{10} + 4.2\times 10^{37} r_0^2/r^8 \\
& -0.1 r_0^2/r^6 - 0.02 r_0^2/r^5 + 0.006 r_0^2/r^4 - 0.0009 r_0^2/r^3 \\
& +0.00007 r_0^2/r^2 + 4.9\times 10^{37} r_0^4/r^{10} + 0.03 r_0^4/r^8 + 0.003 r_0^4/r^7 \\
& -0.002 r_0^4/r^6 + 0.0003 r_0^4/r^5 - 0.00003 r_0^4/r^4 \\
& -7.6\times 10^{37} r_0^6/r^{12}, \qquad \text{(D5)}
\end{aligned}
$$

$$
\begin{aligned}
< T_\theta^\theta > \;=\; & 3.7\times 10^{-79} + 9.6\times 10^{36}/r^6 - 0.03/r^4 + 1.9\times 10^{-41}/r^2 \\
& +1.2\times 10^{25}/(r^4 r_0^2) + 4.3\times 10^{-16}/(r^2 r_0^2) - 7.3\times 10^{36} r_0^2/r^8 \\
& +0.1 r_0^2/r^6 - 6.5\times 10^{-41} r_0^2/r^4 - 4.9\times 10^{37} r_0^4/r^{10} - 0.1 r_0^4/r^8 \\
& +4.9\times 10^{37} r_0^6/r^{12}. \qquad \text{(D6)}
\end{aligned}
$$

D.2 Thermal states

D.2.1 Quantized neutrino field

The stress-energy tensor components of a quantized neutrino field in the entire spacetime for simple wormhole geometry in thermal states are found to be (in units of F_p/l_p^2):

$$
< T_t^t > \;=\; 3.2\times 10^{54}/r^8 - 2.2\times 10^{54}/r^6 + 0.2/r^4 + 6.6\times 10^{-60}/r^2
$$

$$
\begin{aligned}
&-1.6\times 10^{43}/(r^4 r_0^2) - 1.4\times 10^{-14}/(r^2 r_0^2) - 1.6\times 10^{54} r_0^2/r^{10} \\
&-4.1\times 10^{56} r_0^2/r^8 - 0.8 r_0^2/r^6 - 8.3\times 10^{-60} r_0^2/r^4 \\
&+7.4\times 10^{56} r_0^4/r^{10} + 0.6 r_0^4/r^8 - 3.3\times 10^{56} r_0^6/r^{12} \\
&+3.2\times 10^{-59} T^2 - 0.01 r_0^2 T^2/r^4 - 1.2 T^4 - 1.2\times 10^{-16}(\ln T)/r^4 \\
&-3.1\times 10^{-16}(\ln T)/(r^2 r_0^2) - 0.005 r_0^2 (\ln T)/r^6 \\
&+0.005 r_0^4 (\ln T)/r^8, \qquad \text{(D7)}
\end{aligned}
$$

$$
\begin{aligned}
< T_r^r > \;=\; & -0.00003 - 3.2\times 10^{54}/r^8 - 2.9\times 10^{56}/r^6 + 0.02/r^4 + 0.02/r^3 \\
&-0.004/r^2 + 0.0005/r + 4.04724\times 10^{44}/(r^4 r_0^2) \\
&+1.7\times 10^{-15}/(r^2 r_0^2) + 1.6\times 10^{54} r_0^2/r^{10} + 6.4\times 10^{56} r_0^2/r^8 \\
&-0.2 r_0^2/r^6 - 0.02 r_0^2/r^5 + 0.006 r_0^2/r^4 - 0.0009 r_0^2/r^3 \\
&+0.00007 r_0^2/r^2 + 7.6\times 10^{56} r_0^4/r^{10} - 0.5 r_0^4/r^8 + 0.003 r_0^4/r^7 \\
&-0.002 r_0^4/r^6 + 0.0003 r_0^4/r^5 - 0.00003 r_0^4/r^4 - 1.2\times 10^{57} r_0^6/r^{12} \\
&-3.2\times 10^{-59} T^2 - 0.01 r_0^2 T^2/r^4 + 0.4 T^4 - 0.002 r_0^2 (\ln T)/r^6 \\
&-0.008 r_0^4 (\ln T)/r^8, \qquad \text{(D8)}
\end{aligned}
$$

$$
\begin{aligned}
< T_\theta^\theta > \;=\; & 1.6\times 10^{-117} + 1.5\times 10^{56}/r^6 - 0.03/r^4 + 1.2\times 10^{-60}/r^2 \\
&+2.4\times 10^{43}/(r^4 r_0^2) + 8.5\times 10^{-16}/(r^2 r_0^2) - 1.1\times 10^{56} r_0^2/r^8 \\
&+0.3 r_0^2/r^6 - 4.3\times 10^{-60} r_0^2/r^4 - 7.5\times 10^{56} r_0^4/r^{10} - 0.7 r_0^4/r^8 \\
&+7.5\times 10^{56} r_0^6/r^{12} - 3.2\times 10^{-59} T^2 + 0.01 r_0^2 T^2/r^4 + 0.4 T^4
\end{aligned}
$$

$$+0.003r_0^2(\ln T)/r^6 - 0.008r_0^4(\ln T)/r^8. \tag{D9}$$

D.2.2 Quantized proton field

The stress-energy tensor components of a quantized proton field in the entire spacetime for the simple wormhole geometry in thermal states are found to be (in units of F_p/l_p^2):

$$\begin{aligned}
< T_t^t > \;=\; & 2.1\times 10^{35}/r^8 - 1.4\times 10^{35}/r^6 + 0.2/r^4 + 1.0\times 10^{-40}/r^2 \\
& +6.2\times 10^{23}/(r^4 r_0^2) + 2.7\times 10^{-14}/(r^2 r_0^2) - 1.1\times 10^{35} r_0^2/r^{10} \\
& -2.7\times 10^{37} r_0^2/r^8 - 0.7 r_0^2/r^6 - 1.3\times 10^{-40} r_0^2/r^4 \\
& +4.9\times 10^{37} r_0^4/r^{10} + 0.5 r_0^4/r^8 - 2.2\times 10^{37} r_0^6/r^{12} \\
& +4.9\times 10^{-40} T^2 - 0.01 r_0^2 T^2/r^4 - 1.2 T^4 - 1.2\times 10^{-16}(\ln T)/r^4 \\
& -3.1\times 10^{-16}(\ln T)/(r^2 r_0^2) - 0.005 r_0^2(\ln T)/r^6 \\
& +0.005 r_0^4(\ln T)/r^8,
\end{aligned} \tag{D10}$$

$$\begin{aligned}
< T_r^r > \;=\; & -0.00003 - 2.1\times 10^{35}/r^8 - 1.9\times 10^{37}/r^6 + 0.02/r^4 + 0.02/r^3 \\
& -0.004/r^2 + 0.0005/r + 1.9\times 10^{25}/(r^4 r_0^2) - 1.1\times 10^{-16}/(r^2 r_0^2) \\
& +1.1\times 10^{35} r_0^2/r^{10} + 4.2\times 10^{37} r_0^2/r^8 - 0.2 r_0^2/r^6 - 0.02 r_0^2/r^5 \\
& +0.006 r_0^2/r^4 - 0.0009 r_0^2/r^3 + 0.00007 r_0^2/r^2 + 4.9\times 10^{37} r_0^4/r^{10} \\
& -0.3 r_0^4/r^8 + 0.003 r_0^4/r^7 - 0.002 r_0^4/r^6 + 0.0003 r_0^4/r^5 \\
& -0.00003 r_0^4/r^4 - 7.6\times 10^{37} r_0^6/r^{12} - 4.9\times 10^{-40} T^2
\end{aligned}$$

$$-0.01 r_0^2 T^2/r^4 + 0.4 T^4 - 0.002 r_0^2 (\ln T)/r^6$$
$$-0.008 r_0^4 (\ln T)/r^8, \qquad \text{(D11)}$$

$$\begin{aligned} < T_\theta^\theta > \;\; = \;\; & 3.7 \times 10^{-79} + 9.6 \times 10^{36}/r^6 - 0.03/r^4 1.9 \times 10^{-41}/r^2 \\ & + 1.2 \times 10^{25}/(r^4 r_0^2) - 6.9 \times 10^{-15}/(r^2 r_0^2) - 7.3 \times 10^{36} r_0^2/r^8 \\ & + 0.3 r_0^2/r^6 - 6.5 \times 10^{-41} r_0^2/r^4 - 4.9 \times 10^{37} r_0^4/r^{10} - 0.5 r_0^4/r^8 \\ & + 4.9 \times 10^{37} r_0^6/r^{12} - 4.9 \times 10^{-40} T^2 + 0.01 r_0^2 T^2/r^4 + 0.4 T^4 \\ & + 0.003 r_0^2 (\ln T)/r^6 - 0.008 r_0^4 (\ln T)/r^8. \qquad \text{(D12)} \end{aligned}$$

Appendix E: Stress-Energy Tensor of the Quantized Neutrino Field and Quantized Proton Field in the Proximal Schwarzschild Wormhole Spacetime

E.1 Zero-temperature vacuum state

E.1.1 Quantized neutrino field

I have computed the stress-energy tensor components of a quantized neutrino field in the entire spacetime of the proximal Schwarzschild wormhole geometry at zero temperature. Because the expression for each component is lengthy, I list only $< T_t^t >$ and $< T_r^r >$ (in units of F_p/l_p^2) but omit $< T_\theta^\theta >$ since it is irrelevant to the calculations in this paper:

$$\begin{aligned} < T_t^t > \;\; = \;\; & 3.2 \times 10^{54}/r^8 + 3.9 \times 10^{57}/r^6 + 4.0 \times 10^{57}/(\epsilon^4 r^6) \\ & -3.0 \times 10^{58}/(\epsilon^3 r^6) + 6.6 \times 10^{58}/(\epsilon^2 r^6) - 4.5 \times 10^{58}/(\epsilon r^6) \end{aligned}$$

$$+0.5/r^4 - 0.4/(\epsilon^3 r^4) + 2.2/(\epsilon^2 r^4) - 2.7/(\epsilon r^4) - 4.4 \times 10^{-16}\epsilon/r^4$$

$$-6.9 \times 10^{-77}\epsilon^2/r^4 - 1.1 \times 10^{-59}/r^2 - 4.2 \times 10^{-60}/(\epsilon^2 r^2)$$

$$+2.2 \times 10^{-59}/(\epsilon r^2) - 6.9 \times 10^{-77}/r_0^2 - 4.2 \times 10^{-60}/(\epsilon^4 r_0^2)$$

$$+3.1 \times 10^{-59}/(\epsilon^3 r_0^2) - 6.2 \times 10^{-59}/(\epsilon^2 r_0^2) + 2.0 \times 10^{-59}/(\epsilon r_0^2)$$

$$-8.9 \times 10^{43}/(r^4 r_0^2) + 7.0 \times 10^{57}/(\epsilon^6 r^4 r_0^2) - 6.7 \times 10^{58}/(\epsilon^5 r^4 r_0^2)$$

$$+2.2 \times 10^{59}/(\epsilon^4 r^4 r_0^2) - 3.0 \times 10^{59}/(\epsilon^3 r^4 r_0^2)$$

$$+1.3 \times 10^{59}/(\epsilon^2 r^4 r_0^2) - 8.8 \times 10^{57}/(\epsilon r^4 r_0^2) + 4.5 \times 10^{43}\epsilon/(r^4 r_0^2)$$

$$-3.6 \times 10^{-15}/(r^2 r_0^2) - 0.4/(\epsilon^5 r^2 r_0^2) + 2.8/(\epsilon^4 r^2 r_0^2)$$

$$-6.2/(\epsilon^3 r^2 r_0^2) + 3.9/(\epsilon^2 r^2 r_0^2) - 0.2/(\epsilon r^2 r_0^2)$$

$$+2.4 \times 10^{24}/(r^{7/2} r_0^{3/2}) - 1.6 \times 10^{26}/(\epsilon^5 r^{7/2} r_0^{3/2})$$

$$+1.2 \times 10^{27}/(\epsilon^4 r^{7/2} r_0^{3/2}) - 2.6 \times 10^{27}/(\epsilon^3 r^{7/2} r_0^{3/2})$$

$$+1.6 \times 10^{27}/(\epsilon^2 r^{7/2} r_0^{3/2}) - 7.7 \times 10^{25}/(\epsilon r^{7/2} r_0^{3/2})$$

$$-2.8 \times 10^{23}\epsilon/(r^{7/2} r_0^{3/2}) + 3.3 \times 10^{43}/(r^5 r_0)$$

$$+5.4 \times 10^{57}/(\epsilon^5 r^5 r_0) - 4.6 \times 10^{58}/(\epsilon^4 r^5 r_0)$$

$$+1.3 \times 10^{59}/(\epsilon^3 r^5 r_0) - 1.3 \times 10^{59}/(\epsilon^2 r^5 r_0) + 3.2 \times 10^{58}/(\epsilon r^5 r_0)$$

$$-1.1 \times 10^{43}\epsilon/(r^5 r_0) - 1.3 \times 10^{-15}/(r^3 r_0) - 0.4/(\epsilon^4 r^3 r_0)$$

$$+2.5/(\epsilon^3 r^3 r_0) - 4.3/(\epsilon^2 r^3 r_0) + 1.6/(\epsilon r^3 r_0)$$

$$-1.3 \times 10^{-15}\epsilon/(r^3 r_0) + 6.9 \times 10^{-77}\epsilon^2/(r^3 r_0)$$

$$+1.4 \times 10^{-76}/(r r_0) - 4.2 \times 10^{-60}/(\epsilon^3 r r_0) + 2.6 \times 10^{-59}/(\epsilon^2 r r_0)$$

$$-3.7 \times 10^{-59}/(\epsilon r r_0) + 6.6 \times 10^{24}/(r^{9/2}\sqrt{r_0})$$

$$-1.3 \times 10^{26}/(\epsilon^4 r^{9/2}\sqrt{r_0}) + 8.2 \times 10^{26}/(\epsilon^3 r^{9/2}\sqrt{r_0})$$

$$-1.4 \times 10^{27}/(\epsilon^2 r^{9/2}\sqrt{r_0}) + 4.5 \times 10^{26}/(\epsilon r^{9/2}\sqrt{r_0})$$

$$-4.7 \times 10^{23}\epsilon/(r^{9/2}\sqrt{r_0}) + 4.3 \times 10^{25}\sqrt{r_0}/r^{11/2}$$

$$-1.0 \times 10^{26}\sqrt{r_0}/(\epsilon^3 r^{11/2}) + 5.4 \times 10^{26}\sqrt{r_0}/(\epsilon^2 r^{11/2})$$

$$-6.3 \times 10^{26}\sqrt{r_0}/(\epsilon r^{11/2}) - 9.5 \times 10^{23}\epsilon\sqrt{r_0}/r^{11/2}$$

$$-9.6 \times 10^{54} r_0/r^9 - 1.1 \times 10^{58} r_0/r^7 + 2.8 \times 10^{57} r_0/(\epsilon^3 r^7)$$

$$-1.7 \times 10^{58} r_0/(\epsilon^2 r^7) + 2.9 \times 10^{58} r_0/(\epsilon r^7) + 1.1 \times 10^{43}\epsilon r_0/r^7$$

$$-2.2 r_0/r^5 - 0.4 r_0/(\epsilon^2 r^5) + 1.8 r_0/(\epsilon r^5) + 2.2 \times 10^{-16}\epsilon r_0/r^5$$

$$+3.5 \times 10^{-77}\epsilon^2 r_0/r^5 - 1.0 \times 10^{-59} r_0/r^3 - 4.2 \times 10^{-60} r_0/(\epsilon r^3)$$

$$-4.7 \times 10^{-118} r_0/r - 2.0 \times 10^{26} r_0^{3/2}/r^{13/2}$$

$$-8.1 \times 10^{25} r_0^{3/2}/(\epsilon^2 r^{13/2}) + 3.3 \times 10^{26} r_0^{3/2}/(\epsilon r^{13/2})$$

$$-2.5 \times 10^{24}\epsilon r_0^{3/2}/r^{13/2} + 1.0 \times 10^{55} r_0^2/r^{10} + 9.6 \times 10^{54}\epsilon r_0^2/r^{10}$$

$$+1.0 \times 10^{58} r_0^2/r^8 + 1.8 \times 10^{57} r_0^2/(\epsilon^2 r^8) - 8.7 \times 10^{57} r_0^2/(\epsilon r^8)$$

$$+1.3 \times 10^{56}\epsilon r_0^2/r^8 + 2.4 r_0^2/r^6 - 0.4 r_0^2/(\epsilon r^6) - 0.08\epsilon r_0^2/r^6$$

$$-1.7 \times 10^{-77}\epsilon^2 r_0^2/r^6 + 2.0 \times 10^{-59} r_0^2/r^4 + 4.7 \times 10^{-59}\epsilon r_0^2/r^4$$

$$+4.7 \times 10^{-118}\epsilon r_0^2/r^2 + 1.8 \times 10^{26} r_0^{5/2}/r^{15/2}$$

$$-6.0 \times 10^{25} r_0^{5/2}/(\epsilon r^{15/2}) - 1.5 \times 10^{25}\epsilon r_0^{5/2}/r^{15/2}$$

$$-3.6 \times 10^{54} r_0^3/r^{11} - 1.9 \times 10^{55}\epsilon r_0^3/r^{11} - 5.0 \times 10^{57} r_0^3/r^9$$

$$+9.2 \times 10^{56} r_0^3/(\epsilon r^9) - 4.2 \times 10^{57}\epsilon r_0^3/r^9 - 0.7 r_0^3/r^7 + 0.8\epsilon r_0^3/r^7$$

$$-4.8 \times 10^{-59}\epsilon r_0^3/r^5 - 4.0 \times 10^{25} r_0^{7/2}/r^{17/2}$$

$$+6.0 \times 10^{25} \epsilon r_0^{7/2}/r^{17/2} + 9.7 \times 10^{54} \epsilon r_0^4/r^{12} + 8.0 \times 10^{54} \epsilon^2 r_0^4/r^{12}$$

$$+1.3 \times 10^{57} r_0^4/r^{10} + 8.3 \times 10^{57} \epsilon r_0^4/r^{10} + 0.005 \epsilon^2 r_0^4/r^{10}$$

$$-0.7 \epsilon r_0^4/r^8 + 8.2 \times 10^{-61} \epsilon^2 r_0^4/r^8 + 9.8 \times 10^{-120} \epsilon^2 r_0^4/r^6$$

$$-4.0 \times 10^{25} \epsilon r_0^{9/2}/r^{19/2} - 6.5 \times 10^{54} \epsilon^2 r_0^5/r^{13} - 4.3 \times 10^{57} \epsilon r_0^5/r^{11}$$

$$-0.0009 \epsilon^2 r_0^5/r^{11} - 1.3 \times 10^{-60} \epsilon^2 r_0^5/r^9 + 0.007(\ln \epsilon)/r^4$$

$$+0.007(\ln \epsilon)/(\epsilon^2 r^4) - 0.02(\ln \epsilon)/(\epsilon r^4) + 0.004(\ln \epsilon)/(\epsilon^4 r^2 r_0^2)$$

$$-0.02(\ln \epsilon)/(\epsilon^3 r^2 r_0^2) + 0.02(\ln \epsilon)/(\epsilon^2 r^2 r_0^2) - 0.005(\ln \epsilon)/(\epsilon r^2 r_0^2)$$

$$-2.7 \times 10^{-17}(\ln \epsilon)/(r^3 r_0) + 0.006(\ln \epsilon)/(\epsilon^3 r^3 r_0)$$

$$-0.02(\ln \epsilon)/(\epsilon^2 r^3 r_0) + 0.02(\ln \epsilon)/(\epsilon r^3 r_0) - 0.01 r_0(\ln \epsilon)/r^5$$

$$+0.007 r_0(\ln \epsilon)/(\epsilon r^5) + 0.004 r_0^2(\ln \epsilon)/r^6 - 0.01(\ln r)/r^4$$

$$-0.01(\ln r)/(\epsilon^2 r^4) + 0.04(\ln r)/(\epsilon r^4) - 0.008(\ln r)/(\epsilon^4 r^2 r_0^2)$$

$$+0.03(\ln r)/(\epsilon^3 r^2 r_0^2) - 0.04(\ln r)/(\epsilon^2 r^2 r_0^2) + 0.01(\ln r)/(\epsilon r^2 r_0^2)$$

$$+5.6 \times 10^{-17}(\ln r)/(r^3 r_0) - 0.01(\ln r)/(\epsilon^3 r^3 r_0)$$

$$+0.05(\ln r)/(\epsilon^2 r^3 r_0) - 0.04(\ln r)/(\epsilon r^3 r_0) + 0.02 r_0(\ln r)/r^5$$

$$-0.01 r_0(\ln r)/(\epsilon r^5) - 0.008 r_0^2(\ln r)/r^6 + 0.01(\ln r_0)/r^4$$

$$+0.01(\ln r_0)/(\epsilon^2 r^4) - 0.04(\ln r_0)/(\epsilon r^4) + 0.008(\ln r_0)/(\epsilon^4 r^2 r_0^2)$$

$$-0.03(\ln r_0)/(\epsilon^3 r^2 r_0^2) + 0.04(\ln r_0)/(\epsilon^2 r^2 r_0^2)$$

$$-0.01(\ln r_0)/(\epsilon r^2 r_0^2) - 5.6 \times 10^{-17}(\ln r_0)/(r^3 r_0)$$

$$+0.01(\ln r_0)/(\epsilon^3 r^3 r_0) - 0.05(\ln r_0)/(\epsilon^2 r^3 r_0)$$

$$+0.04(\ln r_0)/(\epsilon r^3 r_0) - 0.02 r_0(\ln r_0)/r^5 + 0.01 r_0(\ln r_0)/(\epsilon r^5)$$

$$+0.008 r_0^2 (\ln r_0)/r^6, \tag{E1}$$

$$\begin{aligned}
< T_r^r > \;=\; & -0.00003 - 3.2\times 10^{54}/r^8 + 2.7\times 10^{58}/r^6 + 2.6\times 10^{58}/(\epsilon^4 r^6) \\
& -1.9\times 10^{59}/(\epsilon^3 r^6) + 4.4\times 10^{59}/(\epsilon^2 r^6) - 3.1\times 10^{59}/(\epsilon r^6) \\
& +6.7\times 10^{43}\epsilon/r^6 - 3.3/r^4 + 1.6/(\epsilon^3 r^4) - 10.0/(\epsilon^2 r^4) \\
& +15.5/(\epsilon r^4) + 4.4\times 10^{-16}\epsilon/r^4 + 6.9\times 10^{-77}\epsilon^2/r^4 + 0.02/r^3 \\
& -0.004/r^2 + 7.5\times 10^{-60}/(\epsilon^2 r^2) - 3.7\times 10^{-59}/(\epsilon r^2) \\
& +0.0005/r + 7.5\times 10^{-60}/(\epsilon^4 r_0^2) - 5.3\times 10^{-59}/(\epsilon^3 r_0^2) \\
& +9.8\times 10^{-59}/(\epsilon^2 r_0^2) - 3.0\times 10^{-59}/(\epsilon r_0^2) + 8.9\times 10^{43}/(r^4 r_0^2) \\
& +3.2\times 10^{58}/(\epsilon^6 r^4 r_0^2) - 3.1\times 10^{59}/(\epsilon^5 r^4 r_0^2) \\
& +1.0\times 10^{60}/(\epsilon^4 r^4 r_0^2) - 1.4\times 10^{60}/(\epsilon^3 r^4 r_0^2) \\
& +6.2\times 10^{59}/(\epsilon^2 r^4 r_0^2) - 4.0\times 10^{58}/(\epsilon r^4 r_0^2) \\
& +1.8\times 10^{44}\epsilon/(r^4 r_0^2) + 1.4\times 10^{-15}/(r^2 r_0^2) \\
& +2.0/(\epsilon^5 r^2 r_0^2) - 16.5/(\epsilon^4 r^2 r_0^2) + 42.7/(\epsilon^3 r^2 r_0^2) - 35.3/(\epsilon^2 r^2 r_0^2) \\
& +4.4/(\epsilon r^2 r_0^2) - 2.2\times 10^{-16}\epsilon/(r^2 r_0^2) - 2.4\times 10^{24}/(r^{7/2} r_0^{3/2}) \\
& +1.6\times 10^{26}/(\epsilon^5 r^{7/2} r_0^{3/2}) - 1.2\times 10^{27}/(\epsilon^4 r^{7/2} r_0^{3/2}) \\
& +2.6\times 10^{27}/(\epsilon^3 r^{7/2} r_0^{3/2}) - 1.6\times 10^{27}/(\epsilon^2 r^{7/2} r_0^{3/2}) \\
& +7.7\times 10^{25}/(\epsilon r^{7/2} r_0^{3/2}) + 2.8\times 10^{23}\epsilon/(r^{7/2} r_0^{3/2}) \\
& -4.5\times 10^{43}/(r^5 r_0) + 2.9\times 10^{58}/(\epsilon^5 r^5 r_0) - 2.5\times 10^{59}/(\epsilon^4 r^5 r_0) \\
& +7.0\times 10^{59}/(\epsilon^3 r^5 r_0) - 7.1\times 10^{59}/(\epsilon^2 r^5 r_0) + 1.8\times 10^{59}/(\epsilon r^5 r_0)
\end{aligned}$$

$$+8.9 \times 10^{43}\epsilon/(r^5 r_0) - 8.9 \times 10^{-16}/(r^3 r_0) + 1.8/(\epsilon^4 r^3 r_0)$$

$$-13.0/(\epsilon^3 r^3 r_0) + 27.0/(\epsilon^2 r^3 r_0) - 13.8/(\epsilon r^3 r_0)$$

$$-4.4 \times 10^{-16}\epsilon/(r^3 r_0) - 6.9 \times 10^{-77}\epsilon^2/(r^3 r_0)$$

$$+7.5 \times 10^{-60}/(\epsilon^3 r r_0) - 4.5 \times 10^{-59}/(\epsilon^2 r r_0)$$

$$+6.0 \times 10^{-59}/(\epsilon r r_0) - 6.6 \times 10^{24}/(r^{9/2}\sqrt{r_0})$$

$$+1.3 \times 10^{26}/(\epsilon^4 r^{9/2}\sqrt{r_0}) - 8.2 \times 10^{26}/(\epsilon^3 r^{9/2}\sqrt{r_0})$$

$$+1.4 \times 10^{27}/(\epsilon^2 r^{9/2}\sqrt{r_0}) - 4.5 \times 10^{26}/(\epsilon r^{9/2}\sqrt{r_0})$$

$$+4.7 \times 10^{23}\epsilon/(r^{9/2}\sqrt{r_0}) - 4.3 \times 10^{25}\sqrt{r_0}/r^{11/2}$$

$$+1.0 \times 10^{26}\sqrt{r_0}/(\epsilon^3 r^{11/2}) - 5.4 \times 10^{26}\sqrt{r_0}/(\epsilon^2 r^{11/2})$$

$$+6.3 \times 10^{26}\sqrt{r_0}/(\epsilon r^{11/2}) + 9.5 \times 10^{23}\epsilon\sqrt{r_0}/r^{11/2}$$

$$+9.6 \times 10^{54} r_0/r^9 - 9.7 \times 10^{58} r_0/r^7 + 2.2 \times 10^{58} r_0/(\epsilon^3 r^7)$$

$$-1.4 \times 10^{59} r_0/(\epsilon^2 r^7) + 2.6 \times 10^{59} r_0/(\epsilon r^7) + 1.3 \times 10^{43}\epsilon r_0/r^7$$

$$+7.2 r_0/r^5 + 1.5 r_0/(\epsilon^2 r^5) - 7.5 r_0/(\epsilon r^5) + 2.8 \times 10^{-16}\epsilon r_0/r^5$$

$$-3.5 \times 10^{-77}\epsilon^2 r_0/r^5 - 0.04 r_0/r^4 + 0.009 r_0/r^3$$

$$+7.5 \times 10^{-60} r_0/(\epsilon r^3) - 0.001 r_0/r^2 + 0.0001 r_0/r$$

$$+2.0 \times 10^{26} r_0^{3/2}/r^{13/2} + 8.1 \times 10^{25} r_0^{3/2}/(\epsilon^2 r^{13/2})$$

$$-3.3 \times 10^{26} r_0^{3/2}/(\epsilon r^{13/2}) + 2.5 \times 10^{24}\epsilon r_0^{3/2}/r^{13/2}$$

$$-1.0 \times 10^{55} r_0^2/r^{10} - 9.6 \times 10^{54}\epsilon r_0^2/r^{10} + 1.2 \times 10^{59} r_0^2/r^8$$

$$+1.9 \times 10^{58} r_0^2/(\epsilon^2 r^8) - 1.0 \times 10^{59} r_0^2/(\epsilon r^8) - 1.7 \times 10^{58}\epsilon r_0^2/r^8$$

$$-4.3 r_0^2/r^6 + 1.3 r_0^2)/(\epsilon r^6) + 3.0\epsilon r_0^2/r^6 + 1.7 \times 10^{-77}\epsilon^2 r_0^2/r^6$$

$$+0.02r_0^2/r^5 + 0.01\epsilon r_0^2/r^5 - 0.007r_0^2/r^4 - 0.003\epsilon r_0^2/r^4$$

$$+0.001r_0^2/r^3 + 0.0005\epsilon r_0^2/r^3 - 0.0001r_0^2/r^2 - 0.00003\epsilon r_0^2/r^2$$

$$-1.8 \times 10^{26} r_0^{5/2}/r^{15/2} + 6.0 \times 10^{25} r_0^{5/2}/(\epsilon r^{15/2})$$

$$+1.5 \times 10^{25} \epsilon r_0^{5/2}/r^{15/2} + 3.6 \times 10^{54} r_0^3/r^{11} + 1.9 \times 10^{55} \epsilon r_0^3/r^{11}$$

$$-6.1 \times 10^{58} r_0^3/r^9 + 1.6 \times 10^{58} r_0^3/(\epsilon r^9) + 5.3 \times 10^{58} \epsilon r_0^3/r^9$$

$$+0.3r_0^3/r^7 - 6.3\epsilon r_0^3/r^7 - 0.002r_0^3/r^6 - 0.01\epsilon r_0^3/r^6 + 0.002r_0^3/r^5$$

$$+0.004\epsilon r_0^3/r^5 - 0.0004r_0^3/r^4 - 0.001\epsilon r_0^3/r^4 + 0.00003r_0^3/r^3$$

$$+0.00007\epsilon r_0^3/r^3 + 4.0 \times 10^{25} r_0^{7/2}/r^{17/2} - 6.0 \times 10^{25} \epsilon r_0^{7/2}/r^{17/2}$$

$$-9.7 \times 10^{54} \epsilon r_0^4/r^{12} - 8.0 \times 10^{54} \epsilon^2 r_0^4/r^{12} + 9.9 \times 10^{57} r_0^4/r^{10}$$

$$-5.2 \times 10^{58} \epsilon r_0^4/r^{10} - 0.005\epsilon^2 r_0^4/r^{10} + 3.4\epsilon r_0^4/r^8$$

$$-8.2 \times 10^{-61} \epsilon^2 r_0^4/r^8 - 0.0009\epsilon r_0^4/r^7 - 0.0008\epsilon r_0^4/r^6$$

$$-9.8 \times 10^{-120} \epsilon^2 r_0^4/r^6 + 0.0004\epsilon r_0^4/r^5 - 0.00003\epsilon r_0^4/r^4$$

$$+4.0 \times 10^{25} \epsilon r_0^{9/2}/r^{19/2} + 6.5 \times 10^{54} \epsilon^2 r_0^5/r^{13} + 1.6 \times 10^{58} \epsilon r_0^5/r^{11}$$

$$+0.0009\epsilon^2 r_0^5/r^{11} + 1.3 \times 10^{-60} \epsilon^2 r_0^5/r^9 + 0.007(\ln \epsilon)/r^4$$

$$+0.009(\ln \epsilon)/(\epsilon^2 r^4) - 0.02(\ln \epsilon)/(\epsilon r^4) - 2.8 \times 10^{-17}(\ln \epsilon)/(r^2 r_0^2)$$

$$+0.009(\ln \epsilon)/(\epsilon^4 r^2 r_0^2) - 0.04(\ln \epsilon)/(\epsilon^3 r^2 r_0^2)$$

$$+0.05(\ln \epsilon)/(\epsilon^2 r^2 r_0^2) - 0.008(\ln \epsilon)/(\epsilon r^2 r_0^2)$$

$$+1.4 \times 10^{-17}(\ln \epsilon)/(r^3 r_0) + 0.01(\ln \epsilon)/(\epsilon^3 r^3 r_0)$$

$$-0.04(\ln \epsilon)/(\epsilon^2 r^3 r_0) + 0.03(\ln \epsilon)/(\epsilon r^3 r_0) - 0.01 r_0 (\ln \epsilon)/r^5$$

$$+0.007 r_0 (\ln \epsilon)/(\epsilon r^5) + 0.004 r_0^2 (\ln \epsilon)/r^6 - 0.01(\ln r)/r^4$$

$$
\begin{aligned}
&-0.02(\ln r)/(\epsilon^2 r^4) + 0.05(\ln r)/(\epsilon r^4) + 5.6\times 10^{-17}(\ln r)/(r^2 r_0^2) \\
&-0.02(\ln r)/(\epsilon^4 r^2 r_0^2) + 0.08(\ln r)/(\epsilon^3 r^2 r_0^2) - 0.1(\ln r)/(\epsilon^2 r^2 r_0^2) \\
&+0.02(\ln r)/(\epsilon r^2 r_0^2) - 2.8\times 10^{-17}(\ln r)/(r^3 r_0) \\
&-0.02(\ln r)/(\epsilon^3 r^3 r_0) + 0.07(\ln r)/(\epsilon^2 r^3 r_0) - 0.05(\ln r)/(\epsilon r^3 r_0) \\
&+0.02 r_0(\ln r)/r^5 - 0.01 r_0(\ln r)/(\epsilon r^5) - 0.008 r_0^2(\ln r)/r^6 \\
&+0.01(\ln r_0)/r^4 + 0.02(\ln r_0)/(\epsilon^2 r^4) - 0.05(\ln r_0)/(\epsilon r^4) \\
&-5.6\times 10^{-17}(\ln r_0)/(r^2 r_0^2) + 0.02(\ln r_0)/(\epsilon^4 r^2 r_0^2) \\
&-0.08(\ln r_0)/(\epsilon^3 r^2 r_0^2) + 0.1(\ln r_0)/(\epsilon^2 r^2 r_0^2) - 0.02(\ln r_0)/(\epsilon r^2 r_0^2) \\
&+2.8\times 10^{-17}(\ln r_0)/(r^3 r_0) + 0.02(\ln r_0)/(\epsilon^3 r^3 r_0) \\
&-0.07(\ln r_0)/(\epsilon^2 r^3 r_0) + 0.05(\ln r_0)/(\epsilon r^3 r_0) - 0.02 r_0(\ln r_0)/r^5 \\
&+0.01 r_0(\ln r_0)/(\epsilon r^5) + 0.008 r_0^2(\ln r_0)/r^6, \qquad \text{(E2)}
\end{aligned}
$$

By setting $r = r_0$, we get the stress-energy tensor components of a quantized neutrino field at the throat of the proximal Schwarzschild wormhole (in units of F_p/l_p^2):

$$
\begin{aligned}
< T_t^t >_0 \;=\; & -4.7\times 10^{-118} + 4.7\times 10^{-118}\epsilon + 2.7\times 10^{39}/r_0^8 \\
& +4.1\times 10^{39}\epsilon/r_0^8 + 1.6\times 10^{54}\epsilon^2/r_0^8 + 6.8\times 10^{52}/r_0^6 \\
& +7.0\times 10^{57}/(\epsilon^6 r_0^6) - 6.2\times 10^{58}/(\epsilon^5 r_0^6) + 1.8\times 10^{59}/(\epsilon^4 r_0^6) \\
& -2.0\times 10^{59}/(\epsilon^3 r_0^6) + 5.6\times 10^{58}/(\epsilon^2 r_0^6) + 5.6\times 10^{42}/(\epsilon r_0^6) \\
& -6.1\times 10^{54}\epsilon/r_0^6 + 0.004\epsilon^2/r_0^6 - 3.6\times 10^{24}/r_0^5
\end{aligned}
$$

$$
\begin{aligned}
& -1.6\times 10^{26}/(\epsilon^5 r_0^5) + 1.0\times 10^{27}/(\epsilon^4 r_0^5) - 1.9\times 10^{27}/(\epsilon^3 r_0^5) \\
& +7.2\times 10^{26}/(\epsilon^2 r_0^5) + 1.7\times 10^{25}/(\epsilon r_0^5) + 8.3\times 10^{23}\epsilon/r_0^5 \\
& +0.02/r_0^4 - 0.4/(\epsilon^5 r_0^4) + 2.4/(\epsilon^4 r_0^4) - 4.0/(\epsilon^3 r_0^4) + 1.3/(\epsilon^2 r_0^4) \\
& +0.001/(\epsilon r_0^4) - 0.03\epsilon/r_0^4 - 5.3\times 10^{-61}\epsilon^2/r_0^4 - 1.1\times 10^{-60}/r_0^2 \\
& -4.2\times 10^{-60}/(\epsilon^4 r_0^2) + 2.7\times 10^{-59}/(\epsilon^3 r_0^2) - 3.9\times 10^{-59}/(\epsilon^2 r_0^2) \\
& +4.1\times 10^{-61}/(\epsilon r_0^2) - 1.4\times 10^{-60}\epsilon/r_0^2 + 9.8\times 10^{-120}\epsilon^2/r_0^2 \\
& -0.0002(\ln\epsilon)/r_0^4 + 0.004(\ln\epsilon)/(\epsilon^4 r_0^4) - 0.01(\ln\epsilon)/(\epsilon^3 r_0^4) \\
& +0.007(\ln\epsilon)/(\epsilon^2 r_0^4) - 0.0003(\ln\epsilon)/(\epsilon r_0^4) \qquad \text{(E3)}
\end{aligned}
$$

$$
\begin{aligned}
< T_r^r >_0 \;=\; & -1.4\times 10^{39}/r_0^8 - 4.1\times 10^{39}\epsilon/r_0^8 - 1.6\times 10^{54}\epsilon^2/r_0^8 \\
& +1.9\times 10^{55}/r_0^6 + 5.0\times 10^{58}/(\epsilon^{12} r_0^6) - 7.4\times 10^{59}/(\epsilon^{11} r_0^6) \\
& +4.4\times 10^{60}/(\epsilon^{10} r_0^6) - 1.3\times 10^{61}/(\epsilon^9 r_0^6) + 2.1\times 10^{61}/(\epsilon^8 r_0^6) \\
& -1.7\times 10^{61}/(\epsilon^7 r_0^6) + 6.0\times 10^{60}/(\epsilon^6 r_0^6) - 5.9\times 10^{59}/(\epsilon^5 r_0^6) \\
& +1.6\times 10^{44}/(\epsilon^4 r_0^6) - 1.0\times 10^{45}/(\epsilon^3 r_0^6) + 4.3\times 10^{51}/(\epsilon^2 r_0^6) \\
& -1.6\times 10^{54}/(\epsilon r_0^6) - 4.2\times 10^{55}\epsilon/r_0^6 - 0.004\epsilon^2/r_0^6 \\
& +8.0\times 10^{23}/r_0^5 + 3.8\times 10^{26}/(\epsilon^{11} r_0^5) - 4.9\times 10^{27}/(\epsilon^{10} r_0^5) \\
& +2.4\times 10^{28}/(\epsilon^9 r_0^5) - 5.6\times 10^{28}/(\epsilon^8 r_0^5) + 6.2\times 10^{28}/(\epsilon^7 r_0^5) \\
& -2.8\times 10^{28}/(\epsilon^6 r_0^5) + 2.9\times 10^{27}/(\epsilon^5 r_0^5) + 2.1\times 10^{25}/(\epsilon^4 r_0^5) \\
& -2.4\times 10^{24}/(\epsilon^3 r_0^5) + 1.2\times 10^{24}/(\epsilon^2 r_0^5) - 1.1\times 10^{24}/(\epsilon r_0^5) \\
& -2.8\times 10^{23}\epsilon/r_0^5 - 0.004/r_0^4 + 3.3/(\epsilon^{11} r_0^4) - 44.7/(\epsilon^{10} r_0^4)
\end{aligned}
$$

$$
\begin{aligned}
&+231.8/(\epsilon^9 r_0^4) - 579.3/(\epsilon^8 r_0^4) + 708.0/(\epsilon^7 r_0^4) - 373.4/(\epsilon^6 r_0^4) \\
&+56.7/(\epsilon^5 r_0^4) + 7.1 \times 10^{-15}/(\epsilon^4 r_0^4) + 3.4 \times 10^{-14}/(\epsilon^3 r_0^4) \\
&-0.001/(\epsilon^2 r_0^4) + 0.0004/(\epsilon r_0^4) - 0.005\epsilon/r_0^4 + 5.3 \times 10^{-61}\epsilon^2/r_0^4 \\
&+3.7 \times 10^{-16}(\ln\epsilon)/r_0^4 - 0.02(\ln\epsilon)/(\epsilon^{10} r_0^4) + 0.2(\ln\epsilon)/(\epsilon^9 r_0^4) \\
&-0.9(\ln\epsilon)/(\epsilon^8 r_0^4) + 1.5(\ln\epsilon)/(\epsilon^7 r_0^4) - 1.0(\ln\epsilon)/(\epsilon^6 r_0^4) \\
&+0.2(\ln\epsilon)/(\epsilon^5 r_0^4) - 5.9 \times 10^{-17}(\ln\epsilon)/(\epsilon^4 r_0^4) \\
&-1.5 \times 10^{-16}(\ln\epsilon)/(\epsilon^3 r_0^4) + 0.0001(\ln\epsilon)/(\epsilon^2 r_0^4) \\
&+0.0001(\ln\epsilon)/(\epsilon r_0^4) - 6.9 \times 10^{-18}/r_0^3 + 0.0008\epsilon/r_0^3 \\
&+7.5 \times 10^{-60}/(\epsilon^{10} r_0^2) - 9.1 \times 10^{-59}/(\epsilon^9 r_0^2) \\
&+4.1 \times 10^{-58}/(\epsilon^8 r_0^2) - 8.2 \times 10^{-58}/(\epsilon^7 r_0^2) + 6.8 \times 10^{-58}/(\epsilon^6 r_0^2) \\
&-1.6 \times 10^{-58}/(\epsilon^5 r_0^2) + 5.3 \times 10^{-74}/(\epsilon^4 r_0^2) - 8.8 \times 10^{-74}/(\epsilon^3 r_0^2) \\
&-4.4 \times 10^{-75}/(\epsilon^2 r_0^2) - 8.8 \times 10^{-75}/(\epsilon r_0^2) \\
&-9.8 \times 10^{-120}\epsilon^2/r_0^2, \qquad \text{(E4)}
\end{aligned}
$$

E.1.2 Quantized proton field

The stress-energy tensor components of a quantized proton field for the entire spacetime of the proximal Schwarzschild wormhole geometry at zero temperature are found to be (in units of F_p/l_p^2):

$$
\begin{aligned}
< T_t^t > \;=\; & 2.1 \times 10^{35}/r^8 + 2.5 \times 10^{38}/r^6 + 2.6 \times 10^{38}/(\epsilon^4 r^6) \\
& -1.9 \times 10^{39}/(\epsilon^3 r^6) + 4.3 \times 10^{39}/(\epsilon^2 r^6) - 2.9 \times 10^{39}/(\epsilon r^6)
\end{aligned}
$$

$$+3.8 \times 10^{24}\epsilon/r^6 + 0.5/r^4 - 0.4/(\epsilon^3 r^4) + 2.2/(\epsilon^2 r^4) - 2.7/(\epsilon r^4)$$

$$-5.6 \times 10^{-16}\epsilon/r^4 + 1.3 \times 10^{-57}\epsilon^2/r^4 - 1.7 \times 10^{-40}/r^2$$

$$-6.4 \times 10^{-41}/(\epsilon^2 r^2) + 3.3 \times 10^{-40}/(\epsilon r^2) - 1.8 \times 10^{-15}/r_0^4$$

$$-0.3/(\epsilon^7 r_0^4) + 3.2/(\epsilon^6 r_0^4) - 10.0/(\epsilon^5 r_0^4) + 11.9/(\epsilon^4 r_0^4)$$

$$-4.1/(\epsilon^3 r_0^4) + 0.09/(\epsilon^2 r_0^4) + 3.1 \times 10^{-15}/(\epsilon r_0^4)$$

$$-4.7 \times 10^{-15}\epsilon/r_0^4 + 7.0 \times 10^{38}/(\epsilon^8 r^2 r_0^4) - 8.2 \times 10^{39}/(\epsilon^7 r^2 r_0^4)$$

$$+3.6 \times 10^{40}/(\epsilon^6 r^2 r_0^4) - 7.2 \times 10^{40}/(\epsilon^5 r^2 r_0^4)$$

$$+6.5 \times 10^{40}/(\epsilon^4 r^2 r_0^4) - 2.1 \times 10^{40}/(\epsilon^3 r^2 r_0^4)$$

$$+1.0 \times 10^{39}/(\epsilon^2 r^2 r_0^4) + 4.8 \times 10^{24}/(\epsilon r^2 r_0^4) - 4.8 \times 10^{24}\epsilon/(r^2 r_0^4)$$

$$-1.3 \times 10^{-56} r^2/r_0^4 - 6.4 \times 10^{-41} r^2/(\epsilon^6 r_0^4)$$

$$+6.2 \times 10^{-40} r^2/(\epsilon^5 r_0^4) - 1.9 \times 10^{-39} r^2/(\epsilon^4 r_0^4)$$

$$+2.0 \times 10^{-39} r^2/(\epsilon^3 r_0^4) - 3.4 \times 10^{-40} r^2/(\epsilon^2 r_0^4)$$

$$-1.3 \times 10^{-57} r^2/(\epsilon r_0^4) + 1.7 \times 10^{14}/(r^{3/2} r_0^{7/2})$$

$$-5.6 \times 10^{16}/(\epsilon^7 r^{3/2} r_0^{7/2}) + 5.4 \times 10^{17}/(\epsilon^6 r^{3/2} r_0^{7/2})$$

$$-1.8 \times 10^{18}/(\epsilon^5 r^{3/2} r_0^{7/2}) + 2.3 \times 10^{18}/(\epsilon^4 r^{3/2} r_0^{7/2})$$

$$-9.1 \times 10^{17}/(\epsilon^3 r^{3/2} r_0^{7/2}) + 2.9 \times 10^{16}/(\epsilon^2 r^{3/2} r_0^{7/2})$$

$$-8.3 \times 10^{14}/(\epsilon r^{3/2} r_0^{7/2}) - 3.1 \times 10^{13}\epsilon)/(r^{3/2} r_0^{7/2})$$

$$-7.3 \times 10^{24}/(r^3 r_0^3) + 5.7 \times 10^{38}/(\epsilon^7 r^3 r_0^3) - 6.1 \times 10^{39}/(\epsilon^6 r^3 r_0^3)$$

$$+2.4 \times 10^{40}/(\epsilon^5 r^3 r_0^3) - 3.9 \times 10^{40}/(\epsilon^4 r^3 r_0^3)$$

$$+2.6 \times 10^{40}/(\epsilon^3 r^3 r_0^3) - 4.7 \times 10^{39}/(\epsilon^2 r^3 r_0^3) + 1.2 \times 10^{24}/(\epsilon r^3 r_0^3)$$

$$+1.5 \times 10^{25}\epsilon/(r^3 r_0^3) + 3.0/(\epsilon^5 r r_0^3) - 8.1/(\epsilon^4 r r_0^3) + 7.4/(\epsilon^3 r r_0^3)$$

$$-1.4/(\epsilon^2 r r_0^3) + 1.3 \times 10^{-15}/(\epsilon r r_0^3) - 3.6 \times 10^{-15}\epsilon/(r r_0^3)$$

$$-1.8 \times 10^{-56} r/r_0^3 - 6.4 \times 10^{-41} r/(\epsilon^5 r_0^3) + 5.5 \times 10^{-40} r/(\epsilon^4 r_0^3)$$

$$-1.4 \times 10^{-39} r/(\epsilon^3 r_0^3) + 9.5 \times 10^{-40} r/(\epsilon^2 r_0^3)$$

$$+1.3 \times 10^{-57} r/(\epsilon r_0^3) + 2.9 \times 10^{14}/(r^{5/2} r_0^{5/2})$$

$$-4.8 \times 10^{16}/(\epsilon^6 r^{5/2} r_0^{5/2}) + 4.1 \times 10^{17}/(\epsilon^5 r^{5/2} r_0^{5/2})$$

$$-1.1 \times 10^{18}/(\epsilon^4 r^{5/2} r_0^{5/2}) + 1.1 \times 10^{18}/(\epsilon^3 r^{5/2} r_0^{5/2})$$

$$-2.2 \times 10^{17}/(\epsilon^2 r^{5/2} r_0^{5/2}) - 2.6 \times 10^{15}/(\epsilon r^{5/2} r_0^{5/2})$$

$$-4.5 \times 10^{13}\epsilon/(r^{5/2} r_0^{5/2}) - 2.5 \times 10^{-57}/r_0^2 - 6.4 \times 10^{-41}/(\epsilon^4 r_0^2)$$

$$+4.8 \times 10^{-40}/(\epsilon^3 r_0^2) - 9.4 \times 10^{-40}/(\epsilon^2 r_0^2) + 3.1 \times 10^{-40}/(\epsilon r_0^2)$$

$$-2.4 \times 10^{24}/(r^4 r_0^2) + 4.5 \times 10^{38}/(\epsilon^6 r^4 r_0^2) - 4.4 \times 10^{39}/(\epsilon^5 r^4 r_0^2)$$

$$+1.5 \times 10^{40}/(\epsilon^4 r^4 r_0^2) - 1.9 \times 10^{40}/(\epsilon^3 r^4 r_0^2)$$

$$+8.7 \times 10^{39}/(\epsilon^2 r^4 r_0^2) - 5.7 \times 10^{38}/(\epsilon r^4 r_0^2) + 8.5 \times 10^{24}\epsilon/(r^4 r_0^2)$$

$$-1.8 \times 10^{-15}/(r^2 r_0^2) - 0.4/(\epsilon^5 r^2 r_0^2) + 2.8/(\epsilon^4 r^2 r_0^2)$$

$$-6.2/(\epsilon^3 r^2 r_0^2) + 3.9/(\epsilon^2 r^2 r_0^2) - 0.2/(\epsilon r^2 r_0^2)$$

$$-8.9 \times 10^{-16}\epsilon/(r^2 r_0^2) + 6.0 \times 10^{14}/(r^{7/2} r_0^{3/2})$$

$$-4.0 \times 10^{16}/(\epsilon^5 r^{7/2} r_0^{3/2}) + 3.0 \times 10^{17}/(\epsilon^4 r^{7/2} r_0^{3/2})$$

$$-6.7 \times 10^{17}/(\epsilon^3 r^{7/2} r_0^{3/2}) + 4.2 \times 10^{17}/(\epsilon^2 r^{7/2} r_0^{3/2})$$

$$-2.0 \times 10^{16}/(\epsilon r^{7/2} r_0^{3/2}) - 7.1 \times 10^{13}\epsilon/(r^{7/2} r_0^{3/2})$$

$$+3.5 \times 10^{38}/(\epsilon^5 r^5 r_0) - 3.0 \times 10^{39}/(\epsilon^4 r^5 r_0)$$

$$+8.4 \times 10^{39}/(\epsilon^3 r^5 r_0) - 8.4 \times 10^{39}/(\epsilon^2 r^5 r_0) + 2.1 \times 10^{39}/(\epsilon r^5 r_0)$$

$$+6.0 \times 10^{23}\epsilon/(r^5 r_0) + 4.4 \times 10^{-16}/(r^3 r_0) - 0.4/(\epsilon^4 r^3 r_0)$$

$$+2.5/(\epsilon^3 r^3 r_0) - 4.3/(\epsilon^2 r^3 r_0) + 1.6/(\epsilon r^3 r_0)$$

$$-1.3 \times 10^{-15}\epsilon/(r^3 r_0) - 1.3 \times 10^{-57}\epsilon^2/(r^3 r_0)$$

$$-7.6 \times 10^{-57}/(r r_0) - 6.4 \times 10^{-41}/(\epsilon^3 r r_0) + 4.0 \times 10^{-40}/(\epsilon^2 r r_0)$$

$$-5.7 \times 10^{-40}/(\epsilon r r_0) + 1.7 \times 10^{15}/(r^{9/2}\sqrt{r_0})$$

$$-3.3 \times 10^{16}/(\epsilon^4 r^{9/2}\sqrt{r_0}) + 2.1 \times 10^{17}/(\epsilon^3 r^{9/2}\sqrt{r_0})$$

$$-3.6 \times 10^{17}/(\epsilon^2 r^{9/2}\sqrt{r_0}) + 1.2 \times 10^{17}/(\epsilon r^{9/2}\sqrt{r_0})$$

$$-1.2 \times 10^{14}\epsilon/(r^{9/2}\sqrt{r_0}) + 1.1 \times 10^{16}\sqrt{r_0}/r^{11/2}$$

$$-2.6 \times 10^{16}\sqrt{r_0}/(e^3 r^{11/2}) + 1.4 \times 10^{17}\sqrt{r_0}/(\epsilon^2 r^{11/2})$$

$$-1.6 \times 10^{17}\sqrt{r_0}/(\epsilon r^{11/2}) - 2.4 \times 10^{14}\epsilon\sqrt{r_0}/r^{11/2}$$

$$-6.3 \times 10^{35} r_0/r^9 - 6.9 \times 10^{38} r_0/r^7 + 1.8 \times 10^{38} r_0/(\epsilon^3 r^7)$$

$$-1.1 \times 10^{39} r_0/(\epsilon^2 r^7) + 1.9 \times 10^{39} r_0/(\epsilon r^7) + 6.0 \times 10^{23}\epsilon r_0/r^7$$

$$-2.2 r_0/r^5 - 0.4 r_0/(\epsilon^2 r^5) + 1.8 r_0/(\epsilon r^5) + 2.2 \times 10^{-16}\epsilon r_0/r^5$$

$$-6.4 \times 10^{-58}\epsilon^2 r_0/r^5 - 1.6 \times 10^{-40} r_0/r^3 - 6.4 \times 10^{-41} r_0/(\epsilon r^3)$$

$$-1.1 \times 10^{-79} r_0/r - 5.0 \times 10^{16} r_0^{3/2}/r^{13/2}$$

$$-2.1 \times 10^{16} r_0^{3/2}/(\epsilon^2 r^{13/2}) + 8.5 \times 10^{16} r_0^{3/2}/(\epsilon r^{13/2})$$

$$-6.4 \times 10^{14}\epsilon r_0^{3/2}/r^{13/2} + 6.6 \times 10^{35} r_0^2/r^{10} + 6.3 \times 10^{35}\epsilon r_0^2/r^{10}$$

$$+6.8 \times 10^{38} r_0^2/r^8 + 1.2 \times 10^{38} r_0^2/(\epsilon^2 r^8) - 5.7 \times 10^{38} r_0^2/(\epsilon r^8)$$

$$+8.4 \times 10^{36}\epsilon r_0^2/r^8 + 2.4 r_0^2/r^6 - 0.4 r_0^2/(\epsilon r^6) - 0.08\epsilon r_0^2/r^6$$

$$+3.2 \times 10^{-58}\epsilon^2 r_0^2/r^6 + 3.1 \times 10^{-40} r_0^2/r^4 + 7.1 \times 10^{-40}\epsilon r_0^2/r^4$$

$$+1.1 \times 10^{-79}\epsilon r_0^2/r^2 + 4.6 \times 10^{16} r_0^{5/2}/r^{15/2}$$

$$-1.5 \times 10^{16} r_0^{5/2}/(\epsilon r^{15/2}) - 3.9 \times 10^{15}\epsilon r_0^{5/2}/r^{15/2}$$

$$-2.4 \times 10^{35} r_0^3/r^{11} - 1.3 \times 10^{36}\epsilon r_0^3/r^{11} - 3.3 \times 10^{38} r_0^3/r^9$$

$$+6.0 \times 10^{37} r_0^3/(\epsilon r^9) - 2.7 \times 10^{38}\epsilon r_0^3/r^9 - 0.7 r_0^3/r^7 + 0.8\epsilon r_0^3/r^7$$

$$-7.3 \times 10^{-40}\epsilon r_0^3/r^5 - 1.0 \times 10^{16} r_0^{7/2}/r^{17/2}$$

$$+1.5 \times 10^{16}\epsilon r_0^{7/2}/r^{17/2} + 6.3 \times 10^{35}\epsilon r_0^4/r^{12} + 5.2 \times 10^{35}\epsilon^2 r_0^4/r^{12}$$

$$+8.3 \times 10^{37} r_0^4/r^{10} + 5.5 \times 10^{38}\epsilon r_0^4/r^{10} + 0.005\epsilon^2 r_0^4/r^{10}$$

$$-0.7\epsilon r_0^4/r^8 + 1.3 \times 10^{-41}\epsilon^2 r_0^4/r^8 + 2.3 \times 10^{-81}\epsilon^2 r_0^4/r^6$$

$$-1.0 \times 10^{16}\epsilon r_0^{9/2}/r^{19/2} - 4.2 \times 10^{35}\epsilon^2 r_0^5/r^{13} - 2.8 \times 10^{38}\epsilon r_0^5/r^{11}$$

$$-0.0009\epsilon^2 r_0^5/r^{11} - 2.1 \times 10^{-41}\epsilon^2 r_0^5/r^9 + 0.007(\ln\epsilon)/r^4$$

$$+0.007(\ln\epsilon)/(\epsilon^2 r^4) - 0.02(\ln\epsilon)/(\epsilon r^4) + 2.2 \times 10^{-16}(\ln\epsilon)/r_0^4$$

$$-0.0005(\ln\epsilon)/(\epsilon^6 r_0^4) + 0.004(\ln\epsilon)/(\epsilon^5 r_0^4) - 0.005(\ln\epsilon)/(\epsilon^4 r_0^4)$$

$$-0.004(\ln\epsilon)/(\epsilon^3 r_0^4) + 0.002(\ln\epsilon)/(\epsilon^2 r_0^4)$$

$$+3.3 \times 10^{-16}(\ln\epsilon)/(r r_0^3) + 0.001(\ln\epsilon)/(\epsilon^5 r r_0^3)$$

$$-0.006(\ln\epsilon)/(\epsilon^4 r r_0^3) + 0.01(\ln\epsilon)/(\epsilon^3 r r_0^3) - 0.008(\ln\epsilon)/(\epsilon^2 r r_0^3)$$

$$+1.7 \times 10^{-16}(\ln\epsilon)/(\epsilon r r_0^3) + 2.2 \times 10^{-16}(\ln\epsilon)/(r^2 r_0^2)$$

$$+0.004(\ln\epsilon)/(\epsilon^4 r^2 r_0^2) - 0.02(\ln\epsilon)/(\epsilon^3 r^2 r_0^2) + 0.02(\ln\epsilon)/(\epsilon^2 r^2 r_0^2)$$

$$-0.005(\ln\epsilon)/(\epsilon r^2 r_0^2) + 5.6 \times 10^{-17}(\ln\epsilon)/(r^3 r_0)$$

$$+0.006(\ln\epsilon)/(\epsilon^3 r^3 r_0) - 0.02(\ln\epsilon)/(\epsilon^2 r^3 r_0) + 0.02(\ln\epsilon)/(\epsilon r^3 r_0)$$

$$-0.01r_0(\ln\epsilon)/r^5 + 0.007r_0(\ln\epsilon)/(\epsilon r^5) + 0.004r_0^2(\ln\epsilon)/r^6$$

$$-0.01(\ln r)/r^4 - 0.01(\ln r)/(\epsilon^2 r^4) + 0.04(\ln r)/(\epsilon r^4)$$

$$-4.4\times10^{-16}(\ln r)/r_0^4 + 0.001(\ln r)/(\epsilon^6 r_0^4) - 0.008(\ln r)/(\epsilon^5 r_0^4)$$

$$+0.01(\ln r)/(\epsilon^4 r_0^4) + 0.008(\ln r)/(\epsilon^3 r_0^4) - 0.003(\ln r)/(\epsilon^2 r_0^4)$$

$$-6.7\times10^{-16}(\ln r)/(r r_0^3) - 0.003(\ln r)/(\epsilon^5 r r_0^3)$$

$$+0.01(\ln r)/(\epsilon^4 r r_0^3) - 0.02(\ln r)/(\epsilon^3 r r_0^3) + 0.02(\ln r)/(\epsilon^2 r r_0^3)$$

$$-3.3\times10^{-16}(\ln r)/(\epsilon r r_0^3) - 4.4\times10^{-16}(\ln r)/(r^2 r_0^2)$$

$$-0.008(\ln r)/(\epsilon^4 r^2 r_0^2) + 0.03(\ln r)/(\epsilon^3 r^2 r_0^2)$$

$$-0.04(\ln r)/(\epsilon^2 r^2 r_0^2) + 0.01(\ln r)/(\epsilon r^2 r_0^2)$$

$$-1.1\times10^{-16}(\ln r)/(r^3 r_0) - 0.01(\ln r)/(\epsilon^3 r^3 r_0)$$

$$+0.05(\ln r)/(\epsilon^2 r^3 r_0) - 0.04(\ln r)/(\epsilon r^3 r_0) + 0.02r_0(\ln r)/r^5$$

$$-0.01r_0(\ln r)/(\epsilon r^5) - 0.008r_0^2(\ln r)/r^6 + 0.01(\ln r)/r^4$$

$$+0.01(\ln r_0)/(\epsilon^2 r^4) - 0.041795(\ln r_0)/(\epsilon r^4)$$

$$+4.4\times10^{-16}(\ln r_0)/r_0^4 - 0.001(\ln r_0)/(\epsilon^6 r_0^4)$$

$$+0.008(\ln r_0)/(\epsilon^5 r_0^4) - 0.01(\ln r_0)/(\epsilon^4 r_0^4)$$

$$-0.008(\ln r_0)/(\epsilon^3 r_0^4) + 0.003(\ln r_0)/(\epsilon^2 r_0^4)$$

$$+6.7\times10^{-16}(\ln r_0)/(r r_0^3) + 0.003(\ln r_0)/(\epsilon^5 r r_0^3)$$

$$-0.01(\ln r_0)/(\epsilon^4 r r_0^3) + 0.02(\ln r_0)/(\epsilon^3 r r_0^3)$$

$$-0.02(\ln r_0)/(\epsilon^2 r r_0^3) + 3.3\times10^{-16}(\ln r_0)/(\epsilon r r_0^3)$$

$$+4.4\times10^{-16}(\ln r_0)/(r^2 r_0^2) + 0.008(\ln r_0)/(\epsilon^4 r^2 r_0^2)$$

$$
\begin{aligned}
& -0.03(\ln r_0)/(\epsilon^3 r^2 r_0^2) + 0.04(\ln r_0)/(\epsilon^2 r^2 r_0^2) \\
& -0.01(\ln r_0)/(\epsilon r^2 r_0^2) + 1.1 \times 10^{-16}(\ln r_0)/(r^3 r_0) \\
& +0.01(\ln r_0)/(\epsilon^3 r^3 r_0) - 0.05(\ln r_0)/(\epsilon^2 r^3 r_0) \\
& +0.04(\ln r_0)/(\epsilon r^3 r_0) - 0.02 r_0 (\ln r_0)/r^5 + 0.01 r_0 (\ln r_0)/(\epsilon r^5) \\
& +0.008 r_0^2 (\ln r_0)/r^6, \qquad \text{(E5)}
\end{aligned}
$$

$$
\begin{aligned}
< T_r^r > \;=\; & -0.00003 - 2.1 \times 10^{35}/r^8 + 1.8 \times 10^{39}/r^6 + 1.7 \times 10^{39}/(\epsilon^4 r^6) \\
& -1.3 \times 10^{40}/(\epsilon^3 r^6) + 2.9 \times 10^{40}/(\epsilon^2 r^6) - 2.0 \times 10^{40}/(\epsilon r^6) \\
& +7.7 \times 10^{24}\epsilon/r^6 - 3.3/r^4 + 1.6/(\epsilon^3 r^4) - 10.0/(\epsilon^2 r^4) \\
& +15.5/(\epsilon r^4) + 5.0 \times 10^{-16}\epsilon/r^4 - 1.3 \times 10^{-57}\epsilon^2/r^4 + 0.01/r^3 \\
& -0.004/r^2 + 1.1 \times 10^{-40}/(\epsilon^2 r^2) - 5.7 \times 10^{-40}/(\epsilon r^2) + 0.0005/r \\
& +8.9 \times 10^{-16}/r_0^4 + 2.4/(\epsilon^7 r_0^4) - 24.8/(\epsilon^6 r_0^4) + 89.6/(\epsilon^5 r_0^4) \\
& -132.7/(\epsilon^4 r_0^4) + 68.7/(\epsilon^3 r_0^4) - 5.6/(\epsilon^2 r_0^4) - 2.2 \times 10^{-16}/(\epsilon r_0^4) \\
& -2.7 \times 10^{-15}\epsilon/r_0^4 + 7.7 \times 10^{25}/(r^2 r_0^4) + 2.6 \times 10^{39}/(\epsilon^8 r^2 r_0^4) \\
& -3.0 \times 10^{40}/(\epsilon^7 r^2 r_0^4) + 1.3 \times 10^{41}/(\epsilon^6 r^2 r_0^4) \\
& -2.6 \times 10^{41}/(\epsilon^5 r^2 r_0^4) + 2.3 \times 10^{41}/(\epsilon^4 r^2 r_0^4) \\
& -7.2 \times 10^{40}/(\epsilon^3 r^2 r_0^4) + 3.4 \times 10^{39}/(\epsilon^2 r^2 r_0^4) + 9.7 \times 10^{24}/(\epsilon r^2 r_0^4) \\
& +3.3 \times 10^{26}\epsilon/(r^2 r_0^4) + 1.1 \times 10^{-40} r^2/(\epsilon^6 r_0^4) \\
& -1.0 \times 10^{-39} r^2/(\epsilon^5 r_0^4) + 3.0 \times 10^{-39} r^2/(\epsilon^4 r_0^4) \\
& -3.0 \times 10^{-39} r^2/(\epsilon^3 r_0^4) + 4.7 \times 10^{-40} r^2/(\epsilon^2 r_0^4)
\end{aligned}
$$

$$-1.7 \times 10^{14}/(r^{3/2}r_0^{7/2}) + 5.6 \times 10^{16}/(\epsilon^7 r^{3/2}r_0^{7/2})$$

$$-5.4 \times 10^{17}/(\epsilon^6 r^{3/2}r_0^{7/2}) + 1.8 \times 10^{18}/(\epsilon^5 r^{3/2}r_0^{7/2})$$

$$-2.3 \times 10^{18}/(\epsilon^4 r^{3/2}r_0^{7/2}) + 9.1 \times 10^{17}/(\epsilon^3 r^{3/2}r_0^{7/2})$$

$$-2.9 \times 10^{16}/(\epsilon^2 r^{3/2}r_0^{7/2}) + 8.3 \times 10^{14}/(\epsilon r^{3/2}r_0^{7/2})$$

$$+3.1 \times 10^{13}\epsilon/(r^{3/2}r_0^{7/2}) + 2.9 \times 10^{25}/(r^3 r_0^3)$$

$$+2.3 \times 10^{39}/(\epsilon^7 r^3 r_0^3) - 2.5 \times 10^{40}/(\epsilon^6 r^3 r_0^3)$$

$$+9.6 \times 10^{40}/(\epsilon^5 r^3 r_0^3) - 1.6 \times 10^{41}/(\epsilon^4 r^3 r_0^3)$$

$$+1.0 \times 10^{41}/(\epsilon^3 r^3 r_0^3) - 1.8 \times 10^{40}/(\epsilon^2 r^3 r_0^3)$$

$$-2.4 \times 10^{24}/(\epsilon r^3 r_0^3) + 1.1 \times 10^{26}\epsilon/(r^3 r_0^3) + 8.9 \times 10^{-16}/(r r_0^3)$$

$$+2.2/(\epsilon^6 r r_0^3) - 20.4/(\epsilon^5 r r_0^3) + 63.3/(\epsilon^4 r r_0^3) - 72.9/(\epsilon^3 r r_0^3)$$

$$+22.5/(\epsilon^2 r r_0^3) + 4.4 \times 10^{-16}/(\epsilon r r_0^3) - 3.3 \times 10^{-16}\epsilon/(r r_0^3)$$

$$+1.1 \times 10^{-40} r/(\epsilon^5 r_0^3) - 9.2 \times 10^{-40} r/(\epsilon^4 r_0^3)$$

$$+2.2 \times 10^{-39} r/(\epsilon^3 r_0^3) - 1.4 \times 10^{-39} r/(\epsilon^2 r_0^3)$$

$$-2.9 \times 10^{14}/(r^{5/2}r_0^{5/2}) + 4.8 \times 10^{16}/(\epsilon^6 r^{5/2}r_0^{5/2})$$

$$-4.1 \times 10^{17}/(\epsilon^5 r^{5/2}r_0^{5/2}) + 1.1 \times 10^{18}/(\epsilon^4 r^{5/2}r_0^{5/2})$$

$$-1.1 \times 10^{18}/(\epsilon^3 r^{5/2}r_0^{5/2}) + 2.2 \times 10^{17}/(\epsilon^2 r^{5/2}r_0^{5/2})$$

$$+2.6 \times 10^{15}/(\epsilon r^{5/2}r_0^{5/2}) + 4.5 \times 10^{13}\epsilon/(r^{5/2}r_0^{5/2})$$

$$+1.1 \times 10^{-40}/(\epsilon^4 r_0^2) - 8.1 \times 10^{-40}/(\epsilon^3 r_0^2) + 1.5 \times 10^{-39}/(\epsilon^2 r_0^2)$$

$$-4.6 \times 10^{-40}/(\epsilon r_0^2) + 9.7 \times 10^{24}/(r^4 r_0^2) + 2.1 \times 10^{39}/(\epsilon^6 r^4 r_0^2)$$

$$-2.0 \times 10^{40}/(\epsilon^5 r^4 r_0^2) + 6.8 \times 10^{40}/(\epsilon^4 r^4 r_0^2)$$

$$-9.1 \times 10^{40}/(\epsilon^3 r^4 r_0^2) + 4.1 \times 10^{40}/(\epsilon^2 r^4 r_0^2)$$

$$-2.6 \times 10^{39}/(\epsilon r^4 r_0^2) + 4.8 \times 10^{24}\epsilon/(r^4 r_0^2) + 8.9 \times 10^{-16}/(r^2 r_0^2)$$

$$+2.0/(\epsilon^5 r^2 r_0^2) - 16.5/(\epsilon^4 r^2 r_0^2) + 42.7/(\epsilon^3 r^2 r_0^2) - 35.3/(\epsilon^2 r^2 r_0^2)$$

$$+4.4/(\epsilon r^2 r_0^2) - 4.4 \times 10^{-16}\epsilon/(r^2 r_0^2) - 6.0 \times 10^{14}/(r^{7/2} r_0^{3/2})$$

$$+4.0 \times 10^{16}/(\epsilon^5 r^{7/2} r_0^{3/2}) - 3.0 \times 10^{17}/(\epsilon^4 r^{7/2} r_0^{3/2})$$

$$+6.7 \times 10^{17}/(\epsilon^3 r^{7/2} r_0^{3/2}) - 4.2 \times 10^{17}/(\epsilon^2 r^{7/2} r_0^{3/2})$$

$$+2.0 \times 10^{16}/(\epsilon r^{7/2} r_0^{3/2}) + 7.1 \times 10^{13}\epsilon/(r^{7/2} r_0^{3/2})$$

$$-2.4 \times 10^{24}/(r^5 r_0) + 1.9 \times 10^{39}/(\epsilon^5 r^5 r_0) - 1.6 \times 10^{40}/(\epsilon^4 r^5 r_0)$$

$$+4.6 \times 10^{40}/(\epsilon^3 r^5 r_0) - 4.6 \times 10^{40}/(\epsilon^2 r^5 r_0) + 1.2 \times 10^{40}/(\epsilon r^5 r_0)$$

$$+1.6 \times 10^{25}\epsilon/(r^5 r_0) + 4.4 \times 10^{-16}/(r^3 r_0) + 1.8/(\epsilon^4 r^3 r_0)$$

$$-13.0/(\epsilon^3 r^3 r_0) + 27.0/(\epsilon^2 r^3 r_0) - 13.8/(\epsilon r^3 r_0)$$

$$+1.3 \times 10^{-57}\epsilon^2/(r^3 r_0) + 1.1 \times 10^{-40}/(\epsilon^3 r r_0)$$

$$-6.9 \times 10^{-40}/(\epsilon^2 r r_0) + 9.1 \times 10^{-40}/(\epsilon r r_0)$$

$$-1.7 \times 10^{15}/(r^{9/2}\sqrt{r_0}) + 3.3 \times 10^{16}/(\epsilon^4 r^{9/2}\sqrt{r_0})$$

$$-2.1 \times 10^{1}7/(\epsilon^3 r^{9/2}\sqrt{r_0}) + 3.6 \times 10^{17}/(\epsilon^2 r^{9/2}\sqrt{r_0})$$

$$-1.2 \times 10^{17}/(\epsilon r^{9/2}\sqrt{r_0}) + 1.2 \times 10^{14}\epsilon/(r^{9/2}\sqrt{r_0})$$

$$-1.1 \times 10^{16}\sqrt{r_0}/r^{11/2} + 2.6 \times 10^{16}\sqrt{r_0}/(\epsilon^3 r^{11/2})$$

$$-1.4 \times 10^{17}\sqrt{r_0}/(\epsilon^2 r^{11/2}) + 1.6 \times 10^{17}\sqrt{r_0}/(\epsilon r^{11/2})$$

$$+2.4 \times 10^{14}\epsilon\sqrt{r_0}/r^{11/2} + 6.3 \times 10^{35} r_0/r^9 - 6.3 \times 10^{39} r_0/r^7$$

$$+1.5 \times 10^{39} r_0/(\epsilon^3 r^7) - 9.4 \times 10^{39} r_0/(\epsilon^2 r^7)$$

$$+1.7 \times 10^{40} r_0/(\epsilon r^7) + 4.5 \times 10^{23} \epsilon r_0/r^7 + 7.2 r_0/r^5$$

$$+1.4 r_0/(\epsilon^2 r^5) - 7.4 r_0/(\epsilon r^5) + 2.2 \times 10^{-16} \epsilon r_0/r^5$$

$$+6.4 \times 10^{-58} \epsilon^2 r_0/r^5 - 0.04 r_0/r^4 + 0.009 r_0/r^3$$

$$+1.1 \times 10^{-40} r_0/(\epsilon r^3) - 0.001 r_0/r^2 + 0.0001 r_0/r$$

$$+5.0 \times 10^{16} r_0^{3/2}/r^{13/2} + 2.1 \times 10^{16} r_0^{3/2}/(\epsilon^2 r^{13/2})$$

$$-8.5 \times 10^{16} r_0^{3/2}/(\epsilon r^{13/2}) + 6.4 \times 10^{14} \epsilon r_0^{3/2}/r^{13/2}$$

$$-6.6 \times 10^{35} r_0^2/r^{10} - 6.3 \times 10^{35} \epsilon r_0^2/r^{10} + 7.9 \times 10^{39} r_0^2/r^8$$

$$+1.2 \times 10^{39} r_0^2/(\epsilon^2 r^8) - 6.7 \times 10^{39} r_0^2/(\epsilon r^8) - 1.1 \times 10^{39} \epsilon r_0^2/r^8$$

$$-4.3 r_0^2/r^6 + 1.3 r_0^2/(\epsilon r^6) + 3.0 \epsilon r_0^2/r^6 - 3.2 \times 10^{-58} \epsilon^2 r_0^2/r^6$$

$$+0.02 r_0^2/r^5 + 0.01 \epsilon r_0^2/r^5 - 0.007 r_0^2/r^4 - 0.003 \epsilon r_0^2/r^4$$

$$+0.001 r_0^2/r^3 + 0.0005 \epsilon r_0^2/r^3 - 0.0001 r_0^2/r^2 - 0.00003 \epsilon r_0^2/r^2$$

$$-4.6 \times 10^{16} r_0^{5/2}/r^{15/2} + 1.5 \times 10^{16} r_0^{5/2}/(\epsilon r^{15/2})$$

$$+3.9 \times 10^{15} \epsilon r_0^{5/2}/r^{15/2} + 2.4 \times 10^{35} r_0^3/r^{11} + 1.3 \times 10^{36} \epsilon r_0^3/r^{11}$$

$$-4.0 \times 10^{39} r_0^3/r^9 + 1.0 \times 10^{39} r_0^3/(\epsilon r^9) + 3.5 \times 10^{39} \epsilon r_0^3/r^9$$

$$+0.3 r_0^3/r^7 - 6.3 \epsilon r_0^3/r^7 - 0.002 r_0^3/r^6 - 0.01 \epsilon r_0^3/r^6$$

$$+0.002 r_0^3/r^5 + 0.004 \epsilon r_0^3/r^5 - 0.0004 r_0^3/r^4 - 0.001 \epsilon r_0^3/r^4$$

$$+0.00003 r_0^3/r^3 + 0.00007 \epsilon r_0^3/r^3 + 1.0 \times 10^{16} r_0^{7/2}/r^{17/2}$$

$$-1.5 \times 10^{16} \epsilon r_0^{7/2}/r^{17/2} - 6.3 \times 10^{35} \epsilon r_0^4/r^{12}$$

$$-5.2 \times 10^{35} \epsilon^2 r_0^4/r^{12} + 6.5 \times 10^{38} r_0^4/r^{10} - 3.4 \times 10^{39} \epsilon r_0^4/r^{10}$$

$$-0.005 \epsilon^2 r_0^4/r^{10} + 3.4 \epsilon r_0^4/r^8 - 1.3 \times 10^{-41} \epsilon^2 r_0^4/r^8$$

$$-0.0009\epsilon r_0^4/r^7 - 0.0008\epsilon r_0^4/r^6 - 2.3\times10^{-81}\epsilon^2 r_0^4/r^6$$

$$+0.0004\epsilon r_0^4/r^5 - 0.00003\epsilon r_0^4/r^4 + 1.0\times10^{16}\epsilon r_0^{9/2}/r^{19/2}$$

$$+4.2\times10^{35}\epsilon^2 r_0^5/r^{13} + 1.1\times10^{39}\epsilon r_0^5/r^{11} + 0.0009\epsilon^2 r_0^5/r^{11}$$

$$+2.1\times10^{-41}\epsilon^2 r_0^5/r^9 + 0.007(\ln\epsilon)/r^4 + 0.009(\ln\epsilon)/(\epsilon^2 r^4)$$

$$-0.02(\ln\epsilon)/(\epsilon r^4) + 1.7\times10^{-16}(\ln\epsilon)/r_0^4 + 0.004(\ln\epsilon)/(\epsilon^6 r_0^4)$$

$$-0.02(\ln\epsilon)/(\epsilon^5 r_0^4) + 0.04(\ln\epsilon)/(\epsilon^4 r_0^4) - 0.02(\ln\epsilon)/(\epsilon^3 r_0^4)$$

$$+0.003(\ln\epsilon)/(\epsilon^2 r_0^4) - 2.8\times10^{-17}(\ln\epsilon)/(\epsilon r_0^4)$$

$$+9.7\times10^{-17}(\ln\epsilon)/(r r_0^3) + 0.007(\ln\epsilon)/(\epsilon^5 r r_0^3)$$

$$-0.04(\ln\epsilon)/(\epsilon^4 r r_0^3) + 0.06(\ln\epsilon)/(\epsilon^3 r r_0^3) - 0.02(\ln\epsilon)/(\epsilon^2 r r_0^3)$$

$$+2.8\times10^{-17}(\ln\epsilon)/(r^2 r_0^2) + 0.009(\ln\epsilon)/(\epsilon^4 r^2 r_0^2)$$

$$-0.04(\ln\epsilon)/(\epsilon^3 r^2 r_0^2) + 0.05(\ln\epsilon)/(\epsilon^2 r^2 r_0^2) - 0.008(\ln\epsilon)/(\epsilon r^2 r_0^2)$$

$$+6.9\times10^{-18}(\ln\epsilon)/(r^3 r_0) + 0.01(\ln\epsilon)/(\epsilon^3 r^3 r_0)$$

$$-0.04(\ln\epsilon)/(\epsilon^2 r^3 r_0) + 0.03(\ln\epsilon)/(\epsilon r^3 r_0) - 0.01 r_0(\ln\epsilon)/r^5$$

$$+0.007 r_0(\ln\epsilon)/(\epsilon r^5) + 0.004 r_0^2(\ln\epsilon)/r^6 - 0.01(\ln r)/r^4$$

$$-0.02(\ln r)/(\epsilon^2 r^4) + 0.05(\ln r)/(\epsilon r^4) - 3.3\times10^{-16}(\ln r)/r_0^4$$

$$-0.009(\ln r)/(\epsilon^6 r_0^4) + 0.05(\ln r)/(\epsilon^5 r_0^4) - 0.08(\ln r)/(\epsilon^4 r_0^4)$$

$$+0.05(\ln r)/(\epsilon^3 r_0^4) - 0.007(\ln r)/(\epsilon^2 r_0^4)$$

$$+5.6\times10^{-17}(\ln r)/(\epsilon r_0^4) - 1.9\times10^{-16}(\ln r)/(r r_0^3)$$

$$-0.01(\ln r)/(\epsilon^5 r r_0^3) + 0.08(\ln r)/(\epsilon^4 r r_0^3) - 0.1(\ln r)/(\epsilon^3 r r_0^3)$$

$$+0.05(\ln r)/(\epsilon^2 r r_0^3) - 5.6\times10^{-17}(\ln r)/(r^2 r_0^2)$$

$$
\begin{aligned}
&-0.02(\ln r)/(\epsilon^4 r^2 r_0^2) + 0.08(\ln r)/(\epsilon^3 r^2 r_0^2) - 0.1(\ln r)/(\epsilon^2 r^2 r_0^2) \\
&+0.02(\ln r)/(\epsilon r^2 r_0^2) - 1.4 \times 10^{-17}(\ln r)/(r^3 r_0) \\
&-0.02(\ln r)/(\epsilon^3 r^3 r_0) + 0.07(\ln r)/(\epsilon^2 r^3 r_0) - 0.05(\ln r)/(\epsilon r^3 r_0) \\
&+0.02 r_0(\ln r)/r^5 - 0.01 r_0(\ln r)/(\epsilon r^5) - 0.008 r_0^2(\ln r)/r^6 \\
&+0.01(\ln r_0)/r^4 + 0.02(\ln r_0)/(\epsilon^2 r^4) - 0.05(\ln r_0)/(\epsilon r^4) \\
&+3.3 \times 10^{-16}(\ln r_0)/r_0^4 + 0.009(\ln r_0)/(\epsilon^6 r_0^4) \\
&-0.05(\ln r_0)/(\epsilon^5 r_0^4) + 0.08(\ln r_0)/(\epsilon^4 r_0^4) - 0.05(\ln r_0)/(\epsilon^3 r_0^4) \\
&+0.007(\ln r_0)/(\epsilon^2 r_0^4) - 5.6 \times 10^{-17}(\ln r_0)/(\epsilon r_0^4) \\
&+1.9 \times 10^{-16}(\ln r_0)/(r r_0^3) + 0.01(\ln r_0)/(\epsilon^5 r r_0^3) \\
&-0.08(\ln r_0)/(\epsilon^4 r r_0^3) + 0.1(\ln r_0)/(\epsilon^3 r r_0^3) - 0.05(\ln r_0)/(\epsilon^2 r r_0^3) \\
&+5.6 \times 10^{-17}(\ln r)/(r^2 r_0^2) + 0.02(\ln r_0)/(\epsilon^4 r^2 r_0^2) \\
&-0.08(\ln r_0)/(\epsilon^3 r^2 r_0^2) + 0.1(\ln r_0)/(\epsilon^2 r^2 r_0^2) \\
&-0.02(\ln r_0)/(\epsilon r^2 r_0^2) + 1.4 \times 10^{-17}(\ln r_0)/(r^3 r_0) \\
&+0.02(\ln r_0)/(\epsilon^3 r^3 r_0) - 0.07(\ln r_0)/(\epsilon^2 r^3 r_0) \\
&+0.05(\ln r_0)/(\epsilon r^3 r_0) - 0.02 r_0(\ln r_0)/r^5 + 0.01 r_0(\ln r_0)/(\epsilon r^5) \\
&+0.008 r_0^2(\ln r_0)/r^6. \qquad \text{(E6)}
\end{aligned}
$$

By setting $r = r_0$ in Eqs. (E5) and (E6), we get the stress-energy tensor components of a quantized proton field at the throat of the proximal Schwarzschild wormhole (in units of F_p/l_p^2):

$$
\begin{aligned}
< T_t^t >_0 \;=\; & -1.1\times 10^{-79} + 1.1\times 10^{-79}\epsilon + 7.4\times 10^{19}/r_0^8 + 1.5\times 10^{20}\epsilon/r_0^8 \\
& +1.0\times 10^{35}\epsilon^2/r_0^8 + 4.5\times 10^{33}/r_0^6 + 1.4\times 10^{39}/(\epsilon^{12}r_0^6) \\
& -2.0\times 10^{40}/(\epsilon^{11}r_0^6) + 1.2\times 10^{41}/(\epsilon^{10}r_0^6) - 3.8\times 10^{41}/(\epsilon^9 r_0^6) \\
& +6.2\times 10^{41}/(\epsilon^8 r_0^6) - 5.2\times 10^{41}/(\epsilon^7 r_0^6) + 1.9\times 10^{41}/(\epsilon^6 r_0^6) \\
& -2.1\times 10^{40}/(\epsilon^5 r_0^6) + 1.5\times 10^{25}/(\epsilon^4 r_0^6) - 9.1\times 10^{24}/(\epsilon^3 r_0^6) \\
& +1.8\times 10^{25}/(\epsilon^2 r_0^6) - 3.1\times 10^{25}/(\epsilon r_0^6) - 4.0\times 10^{35}\epsilon/r_0^6 \\
& +0.004\epsilon^2/r_0^6 - 2.0\times 10^{14}/r_0^5 - 9.6\times 10^{16}/(\epsilon^{11}r_0^5) \\
& +1.2\times 10^{18}/(\epsilon^{10}r_0^5) - 6.1\times 10^{18}/(\epsilon^9 r_0^5) + 1.4\times 10^{19}/(\epsilon^8 r_0^5) \\
& -1.6\times 10^{19}/(\epsilon^7 r_0^5) + 7.2\times 10^{18}/(\epsilon^6 r_0^5) - 7.4\times 10^{17}/(\epsilon^5 r_0^5) \\
& -5.3\times 10^{15}/(\epsilon^4 r_0^5) + 6.2\times 10^{14}/(\epsilon^3 r_0^5) - 3.2\times 10^{14}/(\epsilon^2 r_0^5) \\
& +2.8\times 10^{14}/(\epsilon r_0^5) + 7.2\times 10^{13}\epsilon/r_0^5 + 0.02/r_0^4 - 0.2/(\epsilon^{11}r_0^4) \\
& +2.4/(\epsilon^{10}r_0^4) - 8.4/(\epsilon^9 r_0^4) + 8.7/(\epsilon^8 r_0^4) + 8.3/(\epsilon^7 r_0^4) \\
& -17.4/(\epsilon^6 r_0^4) + 5.4/(\epsilon^5 r_0^4) + 3.2\times 10^{-14}/(\epsilon^4 r_0^4) \\
& +5.7\times 10^{-15}/(\epsilon^3 r_0^4) - 0.002/(\epsilon^2 r_0^4) + 0.001/(\epsilon r_0^4) - 0.03\epsilon/r_0^4 \\
& -8.0\times 10^{-42}\epsilon^2/r_0^4 - 0.0002(\ln\epsilon)/r_0^4 + 0.01(\ln\epsilon)/(\epsilon^{10}r_0^4) \\
& -0.2(\ln\epsilon)/(\epsilon^9 r_0^4) + 0.8(\ln\epsilon)/(\epsilon^8 r_0^4) - 1.7(\ln\epsilon)/(\epsilon^7 r_0^4) \\
& +1.4(\ln\epsilon)/(\epsilon^6 r_0^4) - 0.3(\ln\epsilon)/(\epsilon^5 r_0^4) - 1.4\times 10^{-16}(\ln\epsilon)/(\epsilon^4 r_0^4) \\
& -4.0\times 10^{-16}(\ln\epsilon)/(\epsilon^3 r_0^4) + 0.0003(\ln\epsilon)/(\epsilon^2 r_0^4) \\
& -0.0003(\ln\epsilon)/(\epsilon r_0^4) - 1.7\times 10^{-41}/r_0^2 - 6.4\times 10^{-41}/(\epsilon^{10}r_0^2)
\end{aligned}
$$

$$
\begin{aligned}
&+8.5\times10^{-40}/(\epsilon^9 r_0^2)-4.2\times10^{-39}/(\epsilon^8 r_0^2)+9.0\times10^{-39}/(\epsilon^7 r_0^2)\\
&-8.1\times10^{-39}/(\epsilon^6 r_0^2)+2.1\times10^{-39}/(\epsilon^5 r_0^2)+8.2\times10^{-55}/(\epsilon^4 r_0^2)\\
&+1.6\times10^{-55}/(\epsilon^2 r_0^2)+6.2\times10^{-42}/(\epsilon r_0^2)-2.1\times10^{-41}\epsilon/r_0^2\\
&+2.3\times10^{-81}\epsilon^2/r_0^2, \qquad \text{(E7)}
\end{aligned}
$$

$$
\begin{aligned}
< T_r^r >_0 \;=\;& -7.4\times10^{19}/r_0^8-1.5\times10^{20}\epsilon/r_0^8-1.0\times10^{35}\epsilon^2/r_0^8\\
&+1.2\times10^{36}/r_0^6+3.3\times10^{39}/(\epsilon^{12}r_0^6)-4.9\times10^{40}/(\epsilon^{11}r_0^6)\\
&+2.9\times10^{41}/(\epsilon^{10}r_0^6)-8.6\times10^{41}/(\epsilon^9 r_0^6)+1.4\times10^{42}/(\epsilon^8 r_0^6)\\
&-1.1\times10^{42}/(\epsilon^7 r_0^6)+3.9\times10^{41}/(\epsilon^6 r_0^6)-3.9\times10^{40}/(\epsilon^5 r_0^6)\\
&-1.6\times10^{25}/(\epsilon^4 r_0^6)-2.2\times10^{25}/(\epsilon^3 r_0^6)+2.8\times10^{32}/(\epsilon^2 r_0^6)\\
&-1.1\times10^{35}/(\epsilon r_0^6)-2.7\times10^{36}\epsilon/r_0^6-0.004\epsilon^2/r_0^6\\
&+2.0\times10^{14}/r_0^5+9.6\times10^{16}/(\epsilon^{11}r_0^5)-1.2\times10^{18}/(\epsilon^{10}r_0^5)\\
&+6.1\times10^{18}/(\epsilon^9 r_0^5)-1.4\times10^{19}/(\epsilon^8 r_0^5)+1.6\times10^{19}/(\epsilon^7 r_0^5)\\
&-7.2\times10^{18}/(\epsilon^6 r_0^5)+7.4\times10^{17}/(\epsilon^5 r_0^5)+5.3\times10^{15}/(\epsilon^4 r_0^5)\\
&-6.2\times10^{14}/(\epsilon^3 r_0^5)+3.2\times10^{14}/(\epsilon^2 r_0^5)-2.8\times10^{14}/(\epsilon r_0^5)\\
&-7.2\times10^{13}\epsilon/r_0^5-0.004/r_0^4+3.3/(\epsilon^{11}r_0^4)-44.7/(\epsilon^{10}r_0^4)\\
&+231.8/(\epsilon^9 r_0^4)-579.3/(\epsilon^8 r_0^4)+708.0/(\epsilon^7 r_0^4)-373.4/(\epsilon^6 r_0^4)\\
&+56.7/(\epsilon^5 r_0^4)+7.1\times10^{-15}/(\epsilon^4 r_0^4)+3.4\times10^{-14}/(\epsilon^3 r_0^4)\\
&-0.001/(\epsilon^2 r_0^4)+0.0004/(\epsilon r_0^4)-0.005\epsilon/r_0^4+8.0\times10^{-42}\epsilon^2/r_0^4\\
&+3.7\times10^{-16}(\ln\epsilon)/r_0^4-0.02(\ln\epsilon)/(\epsilon^{10}r_0^4)+0.2(\ln\epsilon)/(\epsilon^9 r_0^4)
\end{aligned}
$$

$$
\begin{aligned}
&-0.9(\ln\epsilon)/(\epsilon^8 r_0^4) + 1.5(\ln\epsilon)/(\epsilon^7 r_0^4) - 1.0(\ln\epsilon)/(\epsilon^6 r_0^4) \\
&+0.2(\ln\epsilon)/(\epsilon^5 r_0^4) - 5.9\times 10^{-17}(\ln\epsilon)/(\epsilon^4 r_0^4) \\
&-1.5\times 10^{-16}(\ln\epsilon)/(\epsilon^3 r_0^4) + 0.0001(\ln\epsilon)/(\epsilon^2 r_0^4) \\
&+0.0001(\ln\epsilon)/(\epsilon r_0^4) - 6.9\times 10^{-18}/r_0^3 + 0.0008\epsilon/r_0^3 \\
&+1.1\times 10^{-40}/(\epsilon^{10} r_0^2) - 1.4\times 10^{-39}/(\epsilon^9 r_0^2) + 6.3\times 10^{-39}/(\epsilon^8 r_0^2) \\
&-1.3\times 10^{-38}/(\epsilon^7 r_0^2) + 1.0\times 10^{-38}/(\epsilon^6 r_0^2) - 2.5\times 10^{-39}/(\epsilon^5 r_0^2) \\
&+3.3\times 10^{-55}/(\epsilon^4 r_0^2) - 3.3\times 10^{-55}/(\epsilon^3 r_0^2) + 1.6\times 10^{-55}/(\epsilon r_0^2) \\
&-2.3\times 10^{-81}\epsilon^2/r_0^2, \qquad \text{(E8)}
\end{aligned}
$$

E.2 Thermal states

E.2.1 Quantized neutrino field

The stress-energy tensor components of a quantized neutrino field in the entire spacetime for the proximal Schwarzschild wormhole geometry are lengthy and complicated. So I list only $< T_t^t >$ and $< T_r^r >$ (in units of F_p/l_p^2) but omit $< T_\theta^\theta >$ because it is irrelevant to the calculations in this thesis.

$$
\begin{aligned}
< T_t^t > \;=\; & 3.2\times 10^{54}/r^8 + 3.9\times 10^{57}/r^6 + 4.0\times 10^{57}/(\epsilon^4 r^6) \\
& -3.0\times 10^{58}/(\epsilon^3 r^6) + 6.6\times 10^{58}/(\epsilon^2 r^6) - 4.5\times 10^{58}/(\epsilon r^6) \\
& -1.1\times 10^{43}\epsilon/r^6 - 0.4/r^4 - 0.4/(\epsilon^3 r^4) + 1.2/(\epsilon^2 r^4) + 0.06/(\epsilon r^4) \\
& -1.3\times 10^{-15}\epsilon/r^4 - 6.9\times 10^{-77}\epsilon^2/r^4 + 0.007(\ln\epsilon)/r^4
\end{aligned}
$$

$$+0.007(\ln\epsilon)/(\epsilon^2 r^4) - 0.02(\ln\epsilon)/(\epsilon r^4) - 0.01(\ln r)/r^4$$

$$-0.01(\ln r)/(\epsilon^2 r^4) + 0.04(\ln r)/(\epsilon r^4) + 0.01(\ln r_0)/r^4$$

$$+0.01(\ln r_0)/(\epsilon^2 r^4) - 0.04(\ln r_0)/(\epsilon r^4) - 0.01(\ln T)/r^4$$

$$-0.01(\ln T)/(\epsilon^2 r^4) + 0.04(\ln T)/(\epsilon r^4) - 1.1 \times 10^{-59}/r^2$$

$$-4.2 \times 10^{-60}/(\epsilon^2 r^2) + 2.2 \times 10^{-59}/(\epsilon r^2) - 6.9 \times 10^{-77}/r_0^2$$

$$-4.2 \times 10^{-60}/(\epsilon^4 r_0^2) + 3.1 \times 10^{-59}/(\epsilon^3 r_0^2) - 6.2 \times 10^{-59}/(\epsilon^2 r_0^2)$$

$$+2.0 \times 10^{-59}/(\epsilon r_0^2) + 7.0 \times 10^{57}/(\epsilon^6 r^4 r_0^2) - 6.7 \times 10^{58}/(\epsilon^5 r^4 r_0^2)$$

$$+2.2 \times 10^{59}/(\epsilon^4 r^4 r_0^2) - 3.0 \times 10^{59}/(\epsilon^3 r^4 r_0^2)$$

$$+1.3 \times 10^{59}/(\epsilon^2 r^4 r_0^2) - 8.8 \times 10^{57}/(\epsilon r^4 r_0^2) - 8.9 \times 10^{43}\epsilon/(r^4 r_0^2)$$

$$+2.3 \times 10^{-14}/(r^2 r_0^2) - 0.4/(\epsilon^5 r^2 r_0^2) + 2.3/(\epsilon^4 r^2 r_0^2)$$

$$-3.9/(\epsilon^3 r^2 r_0^2) + 0.9/(\epsilon^2 r^2 r_0^2) + 0.4/(\epsilon r^2 r_0^2)$$

$$+8.9 \times 10^{-16}\epsilon/(r^2 r_0^2) + 5.6 \times 10^{-17}(\ln\epsilon)/(r^2 r_0^2)$$

$$+0.004(\ln\epsilon)/(\epsilon^4 r^2 r_0^2) - 0.02(\ln\epsilon)/(\epsilon^3 r^2 r_0^2) + 0.02(\ln\epsilon)/(\epsilon^2 r^2 r_0^2)$$

$$-0.005(\ln\epsilon)/(\epsilon r^2 r_0^2) - 1.1 \times 10^{-16}(\ln r)/(r^2 r_0^2)$$

$$-0.008(\ln r)/(\epsilon^4 r^2 r_0^2) + 0.03(\ln r)/(\epsilon^3 r^2 r_0^2) - 0.04(\ln r)/(\epsilon^2 r^2 r_0^2)$$

$$+0.01(\ln r)/(\epsilon r^2 r_0^2) + 1.1 \times 10^{-16}(\ln r_0)/(r^2 r_0^2)$$

$$+0.008(\ln r_0)/(\epsilon^4 r^2 r_0^2) - 0.03(\ln r_0)/(\epsilon^3 r^2 r_0^2)$$

$$+0.04(\ln r_0)/(\epsilon^2 r^2 r_0^2) - 0.01(\ln r_0)/(\epsilon r^2 r_0^2)$$

$$-2.8 \times 10^{-17}(\ln T)/(r^2 r_0^2) - 0.008(\ln T)/(\epsilon^4 r^2 r_0^2)$$

$$+0.03(\ln T)/(\epsilon^3 r^2 r_0^2) - 0.04(\ln T)/(\epsilon^2 r^2 r_0^2)$$

$$+0.01(\ln T)/(\epsilon r^2 r_0^2) + 2.4 \times 10^{24}/(r^{7/2} r_0^{3/2})$$

$$-1.6 \times 10^{26}/(\epsilon^5 r^{7/2} r_0^{3/2}) + 1.2 \times 10^{27}/(\epsilon^4 r^{7/2} r_0^{3/2})$$

$$-2.6 \times 10^{27}/(\epsilon^3 r^{7/2} r_0^{3/2}) + 1.6 \times 10^{27}/(\epsilon^2 r^{7/2} r_0^{3/2})$$

$$-7.7 \times 10^{25}/(\epsilon r^{7/2} r_0^{3/2}) - 2.8 \times 10^{23}\epsilon/(r^{7/2} r_0^{3/2})$$

$$+5.4 \times 10^{57}/(\epsilon^5 r^5 r_0) - 4.6 \times 10^{58}/(\epsilon^4 r^5 r_0)$$

$$+1.3 \times 10^{59}/(\epsilon^3 r^5 r_0) - 1.3 \times 10^{59}/(\epsilon^2 r^5 r_0) + 3.2 \times 10^{58}/(\epsilon r^5 r_0)$$

$$-4.5 \times 10^{43}\epsilon/(r^5 r_0) - 1.8 \times 10^{-15}/(r^3 r_0) - 0.4/(\epsilon^4 r^3 r_0)$$

$$+1.7/(\epsilon^3 r^3 r_0) - 1.3/(\epsilon^2 r^3 r_0) - 0.9/(\epsilon r^3 r_0)$$

$$-1.3 \times 10^{-15}\epsilon/(r^3 r_0) + 6.9 \times 10^{-77}\epsilon^2/(r^3 r_0)$$

$$+0.006(\ln \epsilon)/(\epsilon^3 r^3 r_0) - 0.02(\ln \epsilon)/(\epsilon^2 r^3 r_0) + 0.02(\ln \epsilon)/(\epsilon r^3 r_0)$$

$$-0.01(\ln r)/(\epsilon^3 r^3 r_0) + 0.05(\ln r)/(\epsilon^2 r^3 r_0) - 0.04(\ln r)/(\epsilon r^3 r_0)$$

$$+0.01(\ln r_0)/(\epsilon^3 r^3 r_0) - 0.05(\ln r_0)/(\epsilon^2 r^3 r_0)$$

$$+0.04(\ln r_0)/(\epsilon r^3 r_0) - 5.6 \times 10^{-17}(\ln T)/(r^3 r_0)$$

$$-0.01(\ln T)/(\epsilon^3 r^3 r_0) + 0.05(\ln T)/(\epsilon^2 r^3 r_0) - 0.04(\ln T)/(\epsilon r^3 r_0)$$

$$+1.4 \times 10^{-76}/(r r_0) - 4.2 \times 10^{-60}/(\epsilon^3 r r_0) + 2.6 \times 10^{-59}/(\epsilon^2 r r_0)$$

$$-3.7 \times 10^{-59}/(\epsilon r r_0) + 6.6 \times 10^{24}/(r^{9/2}\sqrt{r_0})$$

$$-1.3 \times 10^{26}/(\epsilon^4 r^{9/2}\sqrt{r_0}) + 8.2 \times 10^{26}/(\epsilon^3 r^{9/2}\sqrt{r_0})$$

$$-1.4 \times 10^{27}/(\epsilon^2 r^{9/2}\sqrt{r_0}) + 4.5 \times 10^{26}/(\epsilon r^{9/2}\sqrt{r_0})$$

$$-4.7 \times 10^{23}\epsilon/(r^{9/2}\sqrt{r_0}) + 4.3 \times 10^{25}\sqrt{r_0}/r^{11/2}$$

$$-1.0 \times 10^{26}\sqrt{r_0}/(\epsilon^3 r^{11/2}) + 5.4 \times 10^{26}\sqrt{r_0}/(\epsilon^2 r^{11/2})$$

$$-6.3 \times 10^{26}\sqrt{r_0}/(\epsilon r^{11/2}) - 9.5 \times 10^{23}\epsilon\sqrt{r_0}/r^{11/2}$$

$$-9.6 \times 10^{54} r_0/r^9 - 1.1 \times 10^{58} r_0/r^7 + 2.8 \times 10^{57} r_0/(\epsilon^3 r^7)$$

$$-1.7 \times 10^{58} r_0/(\epsilon^2 r^7) + 2.9 \times 10^{58} r_0/(\epsilon r^7) + 2.2 \times 10^{43} \epsilon r_0/r^7$$

$$-0.7 r_0/r^5 - 0.4 r_0/(\epsilon^2 r^5) + 0.9 r_0/(\epsilon r^5) + 2.2 \times 10^{-16} \epsilon r_0/r^5$$

$$+3.5 \times 10^{-77} \epsilon^2 r_0/r^5 - 0.01(\ln \epsilon) r_0/r^5 + 0.007(\ln \epsilon) r_0/(\epsilon r^5)$$

$$+0.02(\ln r) r_0/r^5 - 0.01(\ln r) r_0/(\epsilon r^5) - 0.02(\ln r_0) r_0/r^5$$

$$+0.01(\ln r_0) r_0/(\epsilon r^5) + 0.02(\ln T) r_0/r^5 - 0.01(\ln T) r_0/(\epsilon r^5)$$

$$-1.0 \times 10^{-59} r_0/r^3 - 4.2 \times 10^{-60} r_0/(\epsilon r^3) - 4.7 \times 10^{-118} r_0/r$$

$$-2.0 \times 10^{26} r_0^{3/2}/r^{13/2} - 8.1 \times 10^{25} r_0^{3/2}/(\epsilon^2 r^{13/2})$$

$$+3.3 \times 10^{26} r_0^{3/2}/(\epsilon r^{13/2}) - 2.5 \times 10^{24} \epsilon r_0^{3/2}/r^{13/2}$$

$$+1.0 \times 10^{55} r_0^2/r^{10} + 9.6 \times 10^{54} \epsilon r_0^2/r^{10} + 1.0 \times 10^{58} r_0^2/r^8$$

$$+1.8 \times 10^{57} r_0^2/(\epsilon^2 r^8) - 8.7 \times 10^{57} r_0^2/(\epsilon r^8) + 1.3 \times 10^{56} \epsilon r_0^2/r^8$$

$$+1.8 r_0^2/r^6 - 0.4 r_0^2/(\epsilon r^6) - 0.08 \epsilon r_0^2/r^6 - 1.7 \times 10^{-77} \epsilon^2 r_0^2/r^6$$

$$+0.004(\ln \epsilon) r_0^2/r^6 - 0.008(\ln r) r_0^2/r^6 + 0.008(\ln r_0) r_0^2/r^6$$

$$-0.008(\ln T) r_0^2/r^6 + 2.0 \times 10^{-59} r_0^2/r^4 + 4.7 \times 10^{-59} \epsilon r_0^2/r^4$$

$$+4.7 \times 10^{-118} \epsilon r_0^2/r^2 + 1.8 \times 10^{26} r_0^{5/2}/r^{15/2}$$

$$-6.0 \times 10^{25} r_0^{5/2}/(\epsilon r^{15/2}) - 1.5 \times 10^{25} \epsilon r_0^{5/2}/r^{15/2}$$

$$-3.6 \times 10^{54} r_0^3/r^{11} - 1.9 \times 10^{55} \epsilon r_0^3/r^{11} - 5.0 \times 10^{57} r_0^3/r^9$$

$$+9.2 \times 10^{56} r_0^3/(\epsilon r^9) - 4.2 \times 10^{57} \epsilon r_0^3/r^9 - 0.7 r_0^3/r^7 + 0.8 \epsilon r_0^3/r^7$$

$$-4.8 \times 10^{-59} \epsilon r_0^3/r^5 - 4.0 \times 10^{25} r_0^{7/2}/r^{17/2}$$

$$
\begin{aligned}
&+6.0\times10^{25}\epsilon r_0^{7/2}/r^{17/2}+9.7\times10^{54}\epsilon r_0^4/r^{12}+8.0\times10^{54}\epsilon^2 r_0^4/r^{12}\\
&+1.3\times10^{57}r_0^4/r^{10}+8.3\times10^{57}\epsilon r_0^4/r^{10}+0.005\epsilon^2 r_0^4/r^{10}\\
&-0.7\epsilon r_0^4/r^8+8.2\times10^{-61}\epsilon^2 r_0^4/r^8+9.8\times10^{-120}\epsilon^2 r_0^4/r^6\\
&-4.0\times10^{25}\epsilon r_0^{9/2}/r^{19/2}-6.5\times10^{54}\epsilon^2 r_0^5/r^{13}-4.3\times10^{57}\epsilon r_0^5/r^{11}\\
&-0.0009\epsilon^2 r_0^5/r^{11}-1.3\times10^{-60}\epsilon^2 r_0^5/r^9+0.06T^2/(\epsilon^2 r_0^2)\\
&-0.04T^2/(\epsilon r_0^2)+3.2\times10^{-59}r^2T^2/(\epsilon r_0^2)+0.03T^2/(\epsilon r r_0), \qquad \text{(E9)}
\end{aligned}
$$

$$
\begin{aligned}
< T_r^r > \;=\; & -0.00003-3.2\times10^{54}/r^8+2.7\times10^{58}/r^6+2.6\times10^{58}/(\epsilon^4 r^6)\\
&-1.9\times10^{59}/(\epsilon^3 r^6)+4.4\times10^{59}/(\epsilon^2 r^6)-3.1\times10^{59}/(\epsilon r^6)\\
&+4.5\times10^{43}\epsilon/r^6-4.2/r^4+1.6/(\epsilon^3 r^4)-11.3/(\epsilon^2 r^4)\\
&+18.8/(\epsilon r^4)+6.7\times10^{-16}\epsilon/r^4+6.9\times10^{-77}\epsilon^2/r^4\\
&+0.007(\ln\epsilon)/r^4+0.009(\ln\epsilon)/(\epsilon^2 r^4)-0.02(\ln\epsilon)/(\epsilon r^4)\\
&-0.01(\ln r)/r^4-0.02(\ln r)/(\epsilon^2 r^4)+0.05(\ln r)/(\epsilon r^4)\\
&+0.01(\ln r_0)/r^4+0.02(\ln r_0)/(\epsilon^2 r^4)-0.05(\ln r_0)/(\epsilon r^4)\\
&-0.01(\ln T)/r^4-0.02(\ln T)/(\epsilon^2 r^4)+0.05(\ln T)/(\epsilon r^4)\\
&+0.02/r^3-0.004/r^2+7.5\times10^{-60}/(\epsilon^2 r^2)-3.7\times10^{-59}/(\epsilon r^2)\\
&+0.0005/r+7.5\times10^{-60}/(\epsilon^4 r_0^2)-5.3\times10^{-59}/(\epsilon^3 r_0^2)\\
&+9.8\times10^{-59}/(\epsilon^2 r_0^2)-3.0\times10^{-59}/(\epsilon r_0^2)+3.6\times10^{44}/(r^4 r_0^2)\\
&+3.2\times10^{58}/(\epsilon^6 r^4 r_0^2)-3.1\times10^{59}/(\epsilon^5 r^4 r_0^2)\\
&+1.0\times10^{60}/(\epsilon^4 r^4 r_0^2)-1.4\times10^{60}/(\epsilon^3 r^4 r_0^2)
\end{aligned}
$$

$$+6.2 \times 10^{59}/(\epsilon^2 r^4 r_0^2) - 4.0 \times 10^{58}/(\epsilon r^4 r_0^2) - 8.9 \times 10^{43}\epsilon/(r^4 r_0^2)$$

$$+2.1 \times 10^{-15}/(r^2 r_0^2) + 2.0/(\epsilon^5 r^2 r_0^2) - 17.7/(\epsilon^4 r^2 r_0^2)$$

$$+48.3/(\epsilon^3 r^2 r_0^2) - 41.7/(\epsilon^2 r^2 r_0^2) + 5.5/(\epsilon r^2 r_0^2)$$

$$-4.4 \times 10^{-16}\epsilon/(r^2 r_0^2) - 5.6 \times 10^{-17}(\ln \epsilon)/(r^2 r_0^2)$$

$$+0.009(\ln \epsilon)/(\epsilon^4 r^2 r_0^2) - 0.04(\ln \epsilon)/(\epsilon^3 r^2 r_0^2)$$

$$+0.05(\ln \epsilon)/(\epsilon^2 r^2 r_0^2) - 0.008(\ln \epsilon)/(\epsilon r^2 r_0^2)$$

$$+1.1 \times 10^{-16}(\ln r)/(r^2 r_0^2) - 0.02(\ln r)/(\epsilon^4 r^2 r_0^2)$$

$$+0.08(\ln r)/(\epsilon^3 r^2 r_0^2) - 0.1(\ln r)/(\epsilon^2 r^2 r_0^2) + 0.02(\ln r)/(\epsilon r^2 r_0^2)$$

$$-1.1 \times 10^{-16}(\ln r_0)/(r^2 r_0^2) + 0.02(\ln r_0)/(\epsilon^4 r^2 r_0^2)$$

$$-0.08(\ln r_0)/(\epsilon^3 r^2 r_0^2) + 0.1(\ln r_0)/(\epsilon^2 r^2 r_0^2) - 0.02(\ln r_0)/(\epsilon r^2 r_0^2)$$

$$+2.8 \times 10^{-17}(\ln T)/(r^2 r_0^2) - 0.02(\ln T)/(\epsilon^4 r^2 r_0^2)$$

$$+0.08(\ln T)/(\epsilon^3 r^2 r_0^2) - 0.1(\ln T)/(\epsilon^2 r^2 r_0^2) + 0.02(\ln T)/(\epsilon r^2 r_0^2)$$

$$-2.4 \times 10^{24}/(r^{7/2} r_0^{3/2}) + 1.6 \times 10^{26}/(\epsilon^5 r^{7/2} r_0^{3/2})$$

$$-1.2 \times 10^{27}/(\epsilon^4 r^{7/2} r_0^{3/2}) + 2.6 \times 10^{27}/(\epsilon^3 r^{7/2} r_0^{3/2})$$

$$-1.6 \times 10^{27}/(\epsilon^2 r^{7/2} r_0^{3/2}) + 7.7 \times 10^{25}/(\epsilon r^{7/2} r_0^{3/2})$$

$$+2.8 \times 10^{23}\epsilon/(r^{7/2} r_0^{3/2}) + 2.9 \times 10^{58}/(\epsilon^5 r^5 r_0)$$

$$-2.5 \times 10^{59}/(\epsilon^4 r^5 r_0) + 7.0 \times 10^{59}/(\epsilon^3 r^5 r_0)$$

$$-7.1 \times 10^{59}/(\epsilon^2 r^5 r_0) + 1.8 \times 10^{59}/(\epsilon r^5 r_0) - 4.5 \times 10^{43}\epsilon/(r^5 r_0)$$

$$+2.4 \times 10^{-15}/(r^3 r_0) + 1.8/(\epsilon^4 r^3 r_0) - 14.4/(\epsilon^3 r^3 r_0)$$

$$+31.8/(\epsilon^2 r^3 r_0) - 17.2/(\epsilon r^3 r_0) + 4.4 \times 10^{-16}\epsilon/(r^3 r_0)$$

$$-6.9 \times 10^{-77}\epsilon^2/(r^3 r_0) + 6.9 \times 10^{-18}(\ln\epsilon)/(r^3 r_0)$$

$$+0.01(\ln\epsilon)/(\epsilon^3 r^3 r_0) - 0.04(\ln\epsilon)/(\epsilon^2 r^3 r_0) + 0.03(\ln\epsilon)/(\epsilon r^3 r_0)$$

$$-1.4 \times 10^{-17}(\ln r)/(r^3 r_0) - 0.02(\ln r)/(\epsilon^3 r^3 r_0)$$

$$+0.07(\ln r)/(\epsilon^2 r^3 r_0) - 0.05(\ln r)/(\epsilon r^3 r_0)$$

$$+1.4 \times 10^{-17}(\ln r_0)/(r^3 r_0) + 0.02(\ln r_0)/(\epsilon^3 r^3 r_0)$$

$$-0.07(\ln r_0)/(\epsilon^2 r^3 r_0) + 0.05(\ln r_0)/(\epsilon r^3 r_0)$$

$$-0.02(\ln T)/(\epsilon^3 r^3 r_0) + 0.07(\ln T)/(\epsilon^2 r^3 r_0)$$

$$-0.05(\ln T)/(\epsilon r^3 r_0) + 7.5 \times 10^{-60}/(\epsilon^3 r r_0)$$

$$-4.5 \times 10^{-59}/(\epsilon^2 r r_0) + 6.0 \times 10^{-59}/(\epsilon r r_0)$$

$$-6.6 \times 10^{24}/(r^{9/2}\sqrt{r_0}) + 1.3 \times 10^{26}/(\epsilon^4 r^{9/2}\sqrt{r_0})$$

$$-8.2 \times 10^{26}/(\epsilon^3 r^{9/2}\sqrt{r_0}) + 1.4 \times 10^{27}/(\epsilon^2 r^{9/2}\sqrt{r_0})$$

$$-4.5 \times 10^{26}/(\epsilon r^{9/2}\sqrt{r_0}) + 4.7 \times 10^{23}\epsilon/(r^{9/2}\sqrt{r_0})$$

$$-4.3 \times 10^{25}\sqrt{r_0}/r^{11/2} + 1.0 \times 10^{26}\sqrt{r_0}/(\epsilon^3 r^{11/2})$$

$$-5.4 \times 10^{26}\sqrt{r_0}/(\epsilon^2 r^{11/2}) + 6.3 \times 10^{26}\sqrt{r_0}/(\epsilon r^{11/2})$$

$$+9.5 \times 10^{23}\epsilon\sqrt{r_0}/r^{11/2} + 9.6 \times 10^{54} r_0/r^9 - 9.7 \times 10^{58} r_0/r^7$$

$$+2.2 \times 10^{58} r_0/(\epsilon^3 r^7) - 1.4 \times 10^{59} r_0/(\epsilon^2 r^7) + 2.6 \times 10^{59} r_0/(\epsilon r^7)$$

$$+5.6 \times 10^{42}\epsilon r_0/r^7 + 8.7 r_0/r^5 + 1.5 r_0/(\epsilon^2 r^5) - 8.4 r_0/(\epsilon r^5)$$

$$+5.6 \times 10^{-17}\epsilon r_0/r^5 - 3.5 \times 10^{-77}\epsilon^2 r_0/r^5 - 0.01(\ln\epsilon) r_0/r^5$$

$$+0.007(\ln\epsilon) r_0/(\epsilon r^5) + 0.02(\ln r) r_0/r^5 - 0.01(\ln r) r_0/(\epsilon r^5)$$

$$-0.02(\ln r_0) r_0/r^5 + 0.01(\ln r_0) r_0/(\epsilon r^5) + 0.02(\ln T) r_0/r^5$$

$$-0.01(\ln T)r_0/(\epsilon r^5) - 0.04r_0/r^4 + 0.009r_0/r^3$$

$$+7.5 \times 10^{-60} r_0/(\epsilon r^3) - 0.001r_0/r^2 + 0.0001r_0/r$$

$$+2.0 \times 10^{26} r_0^{3/2}/r^{13/2} + 8.1 \times 10^{25} r_0^{3/2}/(\epsilon^2 r^{13/2})$$

$$-3.3 \times 10^{26} r_0^{3/2}/(\epsilon r^{13/2}) + 2.5 \times 10^{24} \epsilon r_0^{3/2}/r^{13/2}$$

$$-1.0 \times 10^{55} r_0^2/r^{10} - 9.6 \times 10^{54} \epsilon r_0^2/r^{10} + 1.2 \times 10^{59} r_0^2/r^8$$

$$+1.9 \times 10^{58} r_0^2/(\epsilon^2 r^8) - 1.0 \times 10^{59} r_0^2/(\epsilon r^8) - 1.7 \times 10^{58} \epsilon r_0^2/r^8$$

$$-4.8 r_0^2/r^6 + 1.3 r_0^2/(\epsilon r^6) + 3.0 \epsilon r_0^2/r^6 + 1.7 \times 10^{-77} \epsilon^2 r_0^2/r^6$$

$$+0.004(\ln \epsilon) r_0^2/r^6 - 0.008(\ln r) r_0^2/r^6 + 0.008(\ln r_0) r_0^2/r^6$$

$$-0.008(\ln T) r_0^2/r^6 + 0.02 r_0^2/r^5 + 0.01 \epsilon r_0^2/r^5$$

$$-0.007 r_0^2/r^4 - 0.003 \epsilon r_0^2/r^4 + 0.001 r_0^2/r^3 + 0.0005 \epsilon r_0^2/r^3$$

$$-0.0001 r_0^2/r^2 - 0.00003 \epsilon r_0^2/r^2 - 1.8 \times 10^{26} r_0^{5/2}/r^{15/2}$$

$$+6.0 \times 10^{25} r_0^{5/2}/(\epsilon r^{15/2}) + 1.5 \times 10^{25} \epsilon r_0^{5/2}/r^{15/2}$$

$$+3.6 \times 10^{54} r_0^3/r^{11} + 1.9 \times 10^{55} \epsilon r_0^3/r^{11} - 6.1 \times 10^{58} r_0^3/r^9$$

$$+1.6 \times 10^{58} r_0^3/(\epsilon r^9) + 5.3 \times 10^{58} \epsilon r_0^3/r^9 + 0.3 r_0^3/r^7 - 6.3 \epsilon r_0^3/r^7$$

$$-0.002 r_0^3/r^6 - 0.01 \epsilon r_0^3/r^6 + 0.002 r_0^3/r^5 + 0.004 \epsilon r_0^3/r^5$$

$$-0.0004 r_0^3/r^4 - 0.001 \epsilon r_0^3/r^4 + 0.00003 r_0^3/r^3 + 0.00007 \epsilon r_0^3/r^3$$

$$+4.0 \times 10^{25} r_0^{7/2}/r^{17/2} - 6.0 \times 10^{25} \epsilon r_0^{7/2}/r^{17/2}$$

$$-9.7 \times 10^{54} \epsilon r_0^4/r^{12} - 8.0 \times 10^{54} \epsilon^2 r_0^4/r^{12} + 9.9 \times 10^{57} r_0^4/r^{10}$$

$$-5.2 \times 10^{58} \epsilon r_0^4/r^{10} - 0.005 \epsilon^2 r_0^4/r^{10} + 3.4 \epsilon r_0^4/r^8$$

$$-8.2 \times 10^{-61} \epsilon^2 r_0^4/r^8 - 0.0009 \epsilon r_0^4/r^7 - 0.0008 \epsilon r_0^4/r^6$$

$$
\begin{aligned}
&-9.8\times 10^{-120}\epsilon^2 r_0^4/r^6+0.0004\epsilon r_0^4/r^5-0.00003\epsilon r_0^4/r^4\\
&+4.0\times 10^{25}\epsilon r_0^{9/2}/r^{19/2}+6.5\times 10^{54}\epsilon^2 r_0^5/r^{13}\\
&+1.6\times 10^{58}\epsilon r_0^5/r^{11}+0.0009\epsilon^2 r_0^5/r^{11}+1.3\times 10^{-60}\epsilon^2 r_0^5/r^9\\
&-0.08T^2/(\epsilon^2 r_0^2)+0.04T^2/(\epsilon r_0^2)-3.2\times 10^{-59}r^2T^2/(\epsilon r_0^2)\\
&-0.06T^2/(\epsilon r r_0). \qquad \text{(E10)}
\end{aligned}
$$

Setting $r = r_0$ in Eqs. (E9) and (E10), we get the expressions of the stress-energy components of a quantized neutrino field at the throat of the wormhole (in units of F_p/l_p^2):

$$
\begin{aligned}
< T_t^t >_0 \;=\;& -4.7\times 10^{-118}+4.7\times 10^{-118}\epsilon+2.7\times 10^{39}/r_0^8\\
&+4.1\times 10^{39}\epsilon/r_0^8+1.6\times 10^{54}\epsilon^2/r_0^8+6.8\times 10^{52}/r_0^6\\
&+7.0\times 10^{57}/(\epsilon^6 r_0^6)-6.2\times 10^{58}/(\epsilon^5 r_0^6)+1.8\times 10^{59}/(\epsilon^4 r_0^6)\\
&-2.0\times 10^{59}/(\epsilon^3 r_0^6)+5.6\times 10^{58}/(\epsilon^2 r_0^6)+5.6\times 10^{42}/(\epsilon r_0^6)\\
&-6.1\times 10^{54}\epsilon/r_0^6+0.004\epsilon^2/r_0^6-3.6\times 10^{24}/r_0^5\\
&-1.6\times 10^{26}/(\epsilon^5 r_0^5)+1.0\times 10^{27}/(\epsilon^4 r_0^5)-1.9\times 10^{27}/(\epsilon^3 r_0^5)\\
&+7.2\times 10^{26}/(\epsilon^2 r_0^5)+1.7\times 10^{25}/(\epsilon r_0^5)+8.3\times 10^{23}\epsilon/r_0^5\\
&+0.04/r_0^4-0.4/(\epsilon^5 r_0^4)+1.9/(\epsilon^4 r_0^4)-2.6/(\epsilon^3 r_0^4)+0.4/(\epsilon^2 r_0^4)\\
&+0.04/(\epsilon r_0^4)-0.03\epsilon/r_0^4-5.3\times 10^{-61}\epsilon^2/r_0^4-0.0002(\ln\epsilon)/r_0^4\\
&+0.004(\ln\epsilon)/(\epsilon^4 r_0^4)-0.01(\ln\epsilon)/(\epsilon^3 r_0^4)+0.007(\ln\epsilon)/(\epsilon^2 r_0^4)\\
&-0.0003(\ln\epsilon)/(\epsilon r_0^4)+0.0004(\ln r)/r_0^4-0.008(\ln r)/(\epsilon^4 r_0^4)
\end{aligned}
$$

$$
\begin{aligned}
&+0.02(\ln r)/(\epsilon^3 r_0^4) - 0.01(\ln r)/(\epsilon^2 r_0^4) + 0.0006(\ln r)/(\epsilon r_0^4) \\
&-0.0004(\ln r_0)/r_0^4 + 0.008(\ln r_0)/(\epsilon^4 r_0^4) - 0.02(\ln r_0)/(\epsilon^3 r_0^4) \\
&+0.01(\ln r_0)/(\epsilon^2 r_0^4) - 0.0006(\ln r_0)/(\epsilon r_0^4) + 0.0004(\ln T)/r_0^4 \\
&-0.008(\ln T)/(\epsilon^4 r_0^4) + 0.02(\ln T)/(\epsilon^3 r_0^4) - 0.01(\ln T)/(\epsilon^2 r_0^4) \\
&+0.0006(\ln T)/(\epsilon r_0^4) - 1.1 \times 10^{-60}/r_0^2 - 4.2 \times 10^{-60}/(\epsilon^4 r_0^2) \\
&+2.7 \times 10^{-59}/(\epsilon^3 r_0^2) - 3.9 \times 10^{-59}/(\epsilon^2 r_0^2) + 4.1 \times 10^{-61}/(\epsilon r_0^2) \\
&-1.4 \times 10^{-60}\epsilon/r_0^2 + 9.8 \times 10^{-120}\epsilon^2/r_0^2 + 3.2 \times 10^{-59}T^2/\epsilon \\
&+0.06T^2/(\epsilon^2 r_0^2) - 0.01T^2/(\epsilon r_0^2) \qquad \text{(E11)}
\end{aligned}
$$

$$
\begin{aligned}
< T_r^r >_0 \;=\; & -1.4 \times 10^{39}/r_0^8 - 2.7 \times 10^{39}\epsilon/r_0^8 - 1.6 \times 10^{54}\epsilon^2/r_0^8 \\
&+1.9 \times 10^{55}/r_0^6 + 3.2 \times 10^{58}/(\epsilon^6 r_0^6) - 2.8 \times 10^{59}/(\epsilon^5 r_0^6) \\
&+8.2 \times 10^{59}/(\epsilon^4 r_0^6) - 8.6 \times 10^{59}/(\epsilon^3 r_0^6) + 2.3 \times 10^{59}/(\epsilon^2 r_0^6) \\
&-1.6 \times 10^{54}/(\epsilon r_0^6) - 4.2 \times 10^{55}\epsilon/r_0^6 - 0.004\epsilon^2/r_0^6 \\
&+3.6 \times 10^{24}/r_0^5 + 1.6 \times 10^{26}/(\epsilon^5 r_0^5) - 1.0 \times 10^{27}/(\epsilon^4 r_0^5) \\
&+1.9 \times 10^{27}/(\epsilon^3 r_0^5) - 7.2 \times 10^{26}/(\epsilon^2 r_0^5) - 1.7 \times 10^{25}/(\epsilon r_0^5) \\
&-8.3 \times 10^{23}\epsilon/r_0^5 - 0.004/r_0^4 + 2.0/(\epsilon^5 r_0^4) - 15.9/(\epsilon^4 r_0^4) \\
&+35.6/(\epsilon^3 r_0^4) - 19.7/(\epsilon^2 r_0^4) - 0.01/(\epsilon r_0^4) - 0.005\epsilon/r_0^4 \\
&+5.3 \times 10^{-61}\epsilon^2/r_0^4 - 4.2 \times 10^{-17}(\ln \epsilon)/r_0^4 + 0.009(\ln \epsilon)/(\epsilon^4 r_0^4) \\
&-0.03(\ln \epsilon)/(\epsilon^3 r_0^4) + 0.02(\ln \epsilon)/(\epsilon^2 r_0^4) + 0.0001(\ln \epsilon)/(\epsilon r_0^4) \\
&+8.3 \times 10^{-17}(\ln r)/r_0^4 - 0.02(\ln r)/(\epsilon^4 r_0^4) + 0.06(\ln r)/(\epsilon^3 r_0^4)
\end{aligned}
$$

$$
\begin{aligned}
&-0.04(\ln r)/(\epsilon^2 r_0^4) - 0.0002(\ln r)/(\epsilon r_0^4) \\
&-8.3\times 10^{-17}(\ln r)_0)/r_0^4 + 0.02(\ln r)_0)/(\epsilon^4 r_0^4) \\
&-0.06(\ln r_0)/(\epsilon^3 r_0^4) + 0.04(\ln r_0)/(\epsilon^2 r_0^4) + 0.0002(\ln r_0)/(\epsilon r_0^4) \\
&+4.2\times 10^{-17}(\ln T)/r_0^4 - 0.02(\ln T)/(\epsilon^4 r_0^4) + 0.06(\ln T)/(\epsilon^3 r_0^4) \\
&-0.04(\ln T)/(\epsilon^2 r_0^4) - 0.0002(\ln T)/(\epsilon r_0^4) - 1.0\times 10^{-17}/r_0^3 \\
&+0.0008\epsilon/r_0^3 + 7.5\times 10^{-60}/(\epsilon^4 r_0^2) - 4.5\times 10^{-59}/(\epsilon^3 r_0^2) \\
&+6.1\times 10^{-59}/(\epsilon^2 r_0^2) - 9.8\times 10^{-120}\epsilon^2/r_0^2 - 3.2\times 10^{-59}T^2/\epsilon \\
&-0.08T^2/(\epsilon^2 r_0^2) - 0.01T^2/(\epsilon r_0^2) \qquad \text{(E12)}
\end{aligned}
$$

E.2.2 Quantized proton field

The stress-energy tensor components of a quantized proton field in the entire spacetime for the proximal Schwarzschild wormhole in thermal states are computed to be (in units of F_p/l_p^2):

$$
\begin{aligned}
< T_t^t > \;=\; & 2.1\times 10^{35}/r^8 + 2.5\times 10^{38}/r^6 + 2.6\times 10^{38}/(\epsilon^4 r^6) \\
& -1.9\times 10^{39}/(\epsilon^3 r^6) + 4.3\times 10^{39}/(\epsilon^2 r^6) - 2.9\times 10^{39}/(\epsilon r^6) \\
& +1.2\times 10^{24}\epsilon/r^6 - 0.1/r^4 - 0.4/(\epsilon^3 r^4) + 1.5/(\epsilon^2 r^4) - 0.9/(\epsilon r^4) \\
& -1.3\times 10^{-15}\epsilon/r^4 + 1.3\times 10^{-57}\epsilon^2/r^4 + 0.007(\ln\epsilon)/r^4 \\
& +0.007(\ln\epsilon)/(\epsilon^2 r^4) - 0.02(\ln\epsilon)/(\epsilon r^4) - 0.01(\ln r)/r^4 \\
& -0.01(\ln r)/(\epsilon^2 r^4) + 0.04(\ln r)/(\epsilon r^4) + 0.01(\ln r)_0)/r^4 \\
& +0.01(\ln r_0)/(\epsilon^2 r^4) - 0.04(\ln r_0)/(\epsilon r^4) - 0.01(\ln T)/r^4
\end{aligned}
$$

$$-0.01(\ln T)/(\epsilon^2 r^4) + 0.04(\ln T)/(\epsilon r^4) - 1.7 \times 10^{-40}/r^2$$

$$-6.4 \times 10^{-41}/(\epsilon^2 r^2) + 3.3 \times 10^{-40}/(\epsilon r^2) + 1.3 \times 10^{-57}/r_0^2$$

$$-6.4 \times 10^{-41}/(\epsilon^4 r_0^2) + 4.8 \times 10^{-40}/(\epsilon^3 r_0^2) - 9.4 \times 10^{-40}/(\epsilon^2 r_0^2)$$

$$+3.1 \times 10^{-40}/(\epsilon r_0^2) + 4.6 \times 10^{38}/(\epsilon^6 r^4 r_0^2)$$

$$-4.4 \times 10^{39}/(\epsilon^5 r^4 r_0^2) + 1.5 \times 10^{40}/(\epsilon^4 r^4 r_0^2)$$

$$-1.9 \times 10^{40}/(\epsilon^3 r^4 r_0^2) + 8.7 \times 10^{39}/(\epsilon^2 r^4 r_0^2)$$

$$-5.7 \times 10^{38}/(\epsilon r^4 r_0^2) + 4.8 \times 10^{24}\epsilon/(r^4 r_0^2)$$

$$-5.3 \times 10^{-15}/(r^2 r_0^2) - 0.4/(\epsilon^5 r^2 r_0^2) + 2.5/(\epsilon^4 r^2 r_0^2)$$

$$-4.6/(\epsilon^3 r^2 r_0^2) + 1.9/(\epsilon^2 r^2 r_0^2) + 0.2/(\epsilon r^2 r_0^2)$$

$$+5.6 \times 10^{-17}(\ln \epsilon)/(r^2 r_0^2) + 0.004(\ln \epsilon)/(\epsilon^4 r^2 r_0^2)$$

$$-0.02(\ln \epsilon)/(\epsilon^3 r^2 r_0^2) + 0.02(\ln \epsilon)/(\epsilon^2 r^2 r_0^2) - 0.005(\ln \epsilon)/(\epsilon r^2 r_0^2)$$

$$-1.1 \times 10^{-16}(\ln r)/(r^2 r_0^2) - 0.008(\ln r)/(\epsilon^4 r^2 r_0^2)$$

$$+0.03(\ln r)/(\epsilon^3 r^2 r_0^2) - 0.04(\ln r)/(\epsilon^2 r^2 r_0^2) + 0.01(\ln r)/(\epsilon r^2 r_0^2)$$

$$+1.1 \times 10^{-16}(\ln r_0)/(r^2 r_0^2) + 0.008(\ln r_0)/(\epsilon^4 r^2 r_0^2)$$

$$-0.03(\ln r_0)/(\epsilon^3 r^2 r_0^2) + 0.04(\ln r_0)/(\epsilon^2 r^2 r_0^2)$$

$$-0.01(\ln r_0)/(\epsilon r^2 r_0^2) - 2.8 \times 10^{-17}(\ln T)/(r^2 r_0^2)$$

$$-0.008(\ln T)/(\epsilon^4 r^2 r_0^2) + 0.03(\ln T)/(\epsilon^3 r^2 r_0^2)$$

$$-0.04(\ln T)/(\epsilon^2 r^2 r_0^2) + 0.01(\ln T)/(\epsilon r^2 r_0^2)$$

$$+6.0 \times 10^{14}/(r^{7/2} r_0^{3/2}) - 4.0 \times 10^{16}/(\epsilon^5 r^{7/2} r_0^{3/2})$$

$$+3.0 \times 10^{17}/(\epsilon^4 r^{7/2} r_0^{3/2}) - 6.7 \times 10^{17}/(\epsilon^3 r^{7/2} r_0^{3/2})$$

$$+4.2 \times 10^{17}/(\epsilon^2 r^{7/2} r_0^{3/2}) - 2.0 \times 10^{16}/(\epsilon r^{7/2} r_0^{3/2})$$

$$-7.1 \times 10^{13}\epsilon/(r^{7/2} r_0^{3/2}) + 3.5 \times 10^{38}/(\epsilon^5 r^5 r_0)$$

$$-3.0 \times 10^{39}/(\epsilon^4 r^5 r_0) + 8.4 \times 10^{39}/(\epsilon^3 r^5 r_0)$$

$$-8.4 \times 10^{39}/(\epsilon^2 r^5 r_0) + 2.1 \times 10^{39}/(\epsilon r^5 r_0) + 3.6 \times 10^{24}\epsilon/(r^5 r_0)$$

$$-8.9 \times 10^{-16}/(r^3 r_0) - 0.4/(\epsilon^4 r^3 r_0) + 2.0/(\epsilon^3 r^3 r_0)$$

$$-2.3/(\epsilon^2 r^3 r_0) - 0.1/(\epsilon r^3 r_0) - 1.3 \times 10^{-15}\epsilon/(r^3 r_0)$$

$$-1.3 \times 10^{-57}\epsilon^2/(r^3 r_0) + 0.006(\ln \epsilon)/(\epsilon^3 r^3 r_0)$$

$$-0.02(\ln \epsilon)/(\epsilon^2 r^3 r_0) + 0.02(\ln \epsilon)/(\epsilon r^3 r_0) - 0.01(\ln r)/(\epsilon^3 r^3 r_0)$$

$$+0.05(\ln r)/(\epsilon^2 r^3 r_0) - 0.04(\ln r)/(\epsilon r^3 r_0) + 0.01(\ln r_0)/(\epsilon^3 r^3 r_0)$$

$$-0.05(\ln r_0)/(\epsilon^2 r^3 r_0) + 0.04(\ln r_0)/(\epsilon r^3 r_0)$$

$$-5.6 \times 10^{-17}(\ln T)/(r^3 r_0) - 0.01(\ln T)/(\epsilon^3 r^3 r_0)$$

$$+0.05(\ln T)/(\epsilon^2 r^3 r_0) - 0.04(\ln T)/(\epsilon r^3 r_0) - 7.6 \times 10^{-57}/(r r_0)$$

$$-6.4 \times 10^{-41}/(\epsilon^3 r r_0) + 4.0 \times 10^{-40}/(\epsilon^2 r r_0)$$

$$-5.7 \times 10^{-40}/(\epsilon r r_0) + 1.7 \times 10^{15}/(r^{9/2}\sqrt{r_0})$$

$$-3.3 \times 10^{16}/(\epsilon^4 r^{9/2}\sqrt{r_0}) + 2.1 \times 10^{17}/(\epsilon^3 r^{9/2}\sqrt{r_0})$$

$$-3.6 \times 10^{17}/(\epsilon^2 r^{9/2}\sqrt{r_0}) + 1.2 \times 10^{17}/(\epsilon r^{9/2}\sqrt{r_0})$$

$$-1.2 \times 10^{14}\epsilon/(r^{9/2}\sqrt{r_0}) + 1.1 \times 10^{16}\sqrt{r_0}/r^{11/2}$$

$$-2.6 \times 10^{16}\sqrt{r_0}/(\epsilon^3 r^{11/2}) + 1.4 \times 10^{17}\sqrt{r_0}/(\epsilon^2 r^{11/2})$$

$$-1.6 \times 10^{17}\sqrt{r_0}/(\epsilon r^{11/2}) - 2.4 \times 10^{14}\epsilon\sqrt{r_0}/r^{11/2}$$

$$-6.3 \times 10^{35} r_0/r^9 - 6.9 \times 10^{38} r_0/r^7 + 1.8 \times 10^{38} r_0/(\epsilon^3 r^7)$$

$$-1.1 \times 10^{39} r_0/(\epsilon^2 r^7) + 1.9 \times 10^{39} r_0/(\epsilon r^7) + 1.2 \times 10^{24} \epsilon r_0/r^7$$

$$-1.2 r_0/r^5 - 0.4 r_0/(\epsilon^2 r^5) + 1.2 r_0/(\epsilon r^5) + 2.2 \times 10^{-16} \epsilon r_0/r^5$$

$$-6.4 \times 10^{-58} \epsilon^2 r_0/r^5 - 0.01(\ln \epsilon) r_0/r^5 + 0.007(\ln \epsilon) r_0/(\epsilon r^5)$$

$$+0.02(\ln r) r_0)/r^5 - 0.01(\ln r) r_0/(\epsilon r^5) - 0.02(\ln r_0) r_0/r^5$$

$$+0.01(\ln r_0) r_0/(\epsilon r^5) + 0.02(\ln T) r_0/r^5 - 0.01(\ln T) r_0/(\epsilon r^5)$$

$$-1.6 \times 10^{-40} r_0/r^3 - 6.4 \times 10^{-41} r_0/(\epsilon r^3) - 1.1 \times 10^{-79} r_0/r$$

$$-5.0 \times 10^{16} r_0^{3/2}/r^{13/2} - 2.1 \times 10^{16} r_0^{3/2}/(\epsilon^2 r^{13/2})$$

$$+8.5 \times 10^{16} r_0^{3/2}/(\epsilon r^{13/2}) - 6.4 \times 10^{14} \epsilon r_0^{3/2}/r^{13/2}$$

$$+6.6 \times 10^{35} r_0^2/r^{10} + 6.3 \times 10^{35} \epsilon r_0^2/r^{10} + 6.8 \times 10^{38} r_0^2/r^8$$

$$+1.2 \times 10^{38} r_0^2/(\epsilon^2 r^8) - 5.7 \times 10^{38} r_0^2/(\epsilon r^8) + 8.4 \times 10^{36} \epsilon r_0^2/r^8$$

$$+2.0 r_0^2/r^6 - 0.4 r_0^2/(\epsilon r^6) - 0.08 \epsilon r_0^2/r^6 + 3.2 \times 10^{-58} \epsilon^2 r_0^2/r^6$$

$$+0.004(\ln \epsilon) r_0^2/r^6 - 0.008(\ln r) r_0^2/r^6 + 0.008(\ln r_0) r_0^2/r^6$$

$$-0.008(\ln T) r_0^2)/r^6 + 3.1 \times 10^{-40} r_0^2/r^4 + 7.1 \times 10^{-40} \epsilon r_0^2/r^4$$

$$+1.1 \times 10^{-79} \epsilon r_0^2/r^2 + 4.6 \times 10^{16} r_0^{5/2}/r^{15/2}$$

$$-1.5 \times 10^{16} r_0^{5/2}/(\epsilon r^{15/2}) - 3.9 \times 10^{15} \epsilon r_0^{5/2}/r^{15/2}$$

$$-2.4 \times 10^{35} r_0^3/r^{11} - 1.3 \times 10^{36} \epsilon r_0^3/r^{11} - 3.3 \times 10^{38} r_0^3/r^9$$

$$+6.0 \times 10^{37} r_0^3/(\epsilon r^9) - 2.7 \times 10^{38} \epsilon r_0^3/r^9 - 0.7 r_0^3/r^7 + 0.8 \epsilon r_0^3/r^7$$

$$-7.3 \times 10^{-40} \epsilon r_0^3/r^5 - 1.0 \times 10^{16} r_0^{7/2}/r^{17/2}$$

$$+1.5 \times 10^{16} \epsilon r_0^{7/2}/r^{17/2} + 6.3 \times 10^{35} \epsilon r_0^4/r^{12} + 5.2 \times 10^{35} \epsilon^2 r_0^4/r^{12}$$

$$+8.3 \times 10^{37} r_0^4/r^{10} + 5.5 \times 10^{38} \epsilon r_0^4/r^{10} + 0.005 \epsilon^2 r_0^4/r^{10}$$

$$-0.7\epsilon r_0^4/r^8 + 1.3\times 10^{-41}\epsilon^2 r_0^4/r^8 + 2.8\times 10^{-81}\epsilon^2 r_0^4/r^6$$
$$-1.0\times 10^{16}\epsilon r_0^{9/2}/r^{19/2} - 4.2\times 10^{35}\epsilon^2 r_0^5/r^{13}$$
$$-2.8\times 10^{38}\epsilon r_0^5/r^{11} - 0.0009\epsilon^2 r_0^5/r^{11} - 2.1\times 10^{-41}\epsilon^2 r_0^5/r^9$$
$$+0.06T^2/(\epsilon^2 r_0^2) - 0.04T^2/(\epsilon r_0^2) + 4.9\times 10^{-40} r^2 T^2/(\epsilon r_0^2)$$
$$+0.03T^2/(\epsilon r r_0) \tag{E13}$$

$$\begin{aligned} < T_r^r > = & -0.00003 - 2.1\times 10^{35}/r^8 + 1.8\times 10^{39}/r^6 + 1.7\times 10^{39}/(\epsilon^4 r^6) \\ & -1.3\times 10^{40}/(\epsilon^3 r^6) + 2.9\times 10^{40}/(\epsilon^2 r^6) - 2.0\times 10^{40}/(\epsilon r^6) \\ & +4.8\times 10^{24}\epsilon/r^6 - 3.9/r^4 + 1.6/(\epsilon^3 r^4) - 10.9/(\epsilon^2 r^4) \\ & +17.7/(\epsilon r^4) + 6.7\times 10^{-16}\epsilon/r^4 - 1.3\times 10^{-57}\epsilon^2/r^4 \\ & +0.007(\ln\epsilon)/r^4 + 0.009(\ln\epsilon)/(\epsilon^2 r^4) - 0.02(\ln\epsilon)/(\epsilon r^4) \\ & -0.01(\ln r)/r^4 - 0.02(\ln r)/(\epsilon^2 r^4) + 0.05(\ln r)/(\epsilon r^4) \\ & +0.01(\ln r_0)/r^4 + 0.02(\ln r_0)/(\epsilon^2 r^4) - 0.05(\ln r_0)/(\epsilon r^4) \\ & -0.01(\ln T)/r^4 - 0.02(\ln T)/(\epsilon^2 r^4) + 0.05(\ln T)/(\epsilon r^4) \\ & +0.02/r^3 - 0.004/r^2 + 1.1\times 10^{-40}/(\epsilon^2 r^2) - 5.7\times 10^{-40}/(\epsilon r^2) \\ & +0.0005/r + 1.1\times 10^{-40}/(\epsilon^4 r_0^2) - 8.1\times 10^{-40}/(\epsilon^3 r_0^2) \\ & +1.5\times 10^{-39}/(\epsilon^2 r_0^2) - 4.6\times 10^{-40}/(\epsilon r_0^2) - 4.8\times 10^{24}/(r^4 r_0^2) \\ & +2.1\times 10^{39}/(\epsilon^6 r^4 r_0^2) - 2.0\times 10^{40}/(\epsilon^5 r^4 r_0^2) \\ & +6.8\times 10^{40}/(\epsilon^4 r^4 r_0^2) - 9.1\times 10^{40}/(\epsilon^3 r^4 r_0^2) \\ & +4.1\times 10^{40}/(\epsilon^2 r^4 r_0^2) - 2.6\times 10^{39}/(\epsilon r^4 r_0^2) - 2.4\times 10^{25}\epsilon/(r^4 r_0^2) \end{aligned}$$

$$-2.3 \times 10^{-15}/(r^2 r_0^2) + 2.0/(\epsilon^5 r^2 r_0^2) - 17.3/(\epsilon^4 r^2 r_0^2)$$

$$+46.4/(\epsilon^3 r^2 r_0^2) - 39.6/(\epsilon^2 r^2 r_0^2) + 5.2/(\epsilon r^2 r_0^2)$$

$$-4.4 \times 10^{-16}\epsilon/(r^2 r_0^2) - 5.6 \times 10^{-17}(\ln \epsilon)/(r^2 r_0^2)$$

$$+0.009(\ln \epsilon)/(\epsilon^4 r^2 r_0^2) - 0.04(\ln \epsilon)/(\epsilon^3 r^2 r_0^2)$$

$$+0.05(\ln \epsilon)/(\epsilon^2 r^2 r_0^2) - 0.008(\ln \epsilon)/(\epsilon r^2 r_0^2)$$

$$+1.1 \times 10^{-16}(\ln r)/(r^2 r_0^2) - 0.02(\ln r)/(\epsilon^4 r^2 r_0^2)$$

$$+0.08(\ln r)/(\epsilon^3 r^2 r_0^2) - 0.1(\ln r)/(\epsilon^2 r^2 r_0^2) + 0.02(\ln r)/(\epsilon r^2 r_0^2)$$

$$-1.1 \times 10^{-16}(\ln r_0)/(r^2 r_0^2) + 0.02(\ln r_0)/(\epsilon^4 r^2 r_0^2)$$

$$-0.08(\ln r_0)/(\epsilon^3 r^2 r_0^2) + 0.1(\ln r_0)/(\epsilon^2 r^2 r_0^2) - 0.02(\ln r_0)/(\epsilon r^2 r_0^2)$$

$$+2.8 \times 10^{-17}(\ln T)/(r^2 r_0^2) - 0.02(\ln T)/(\epsilon^4 r^2 r_0^2)$$

$$+0.08(\ln T)/(\epsilon^3 r^2 r_0^2) - 0.1(\ln T)/(\epsilon^2 r^2 r_0^2)$$

$$+0.02(\ln T)/(\epsilon r^2 r_0^2) - 6.0 \times 10^{14}/(r^{7/2} r_0^{3/2})$$

$$+4.0 \times 10^{16}/(\epsilon^5 r^{7/2} r_0^{3/2}) - 3.0 \times 10^{17}/(\epsilon^4 r^{7/2} r_0^{3/2})$$

$$+6.7 \times 10^{17}/(\epsilon^3 r^{7/2} r_0^{3/2}) - 4.2 \times 10^{17}/(\epsilon^2 r^{7/2} r_0^{3/2})$$

$$+2.0 \times 10^{16}/(\epsilon r^{7/2} r_0^{3/2}) + 7.0 \times 10^{13}\epsilon/(r^{7/2} r_0^{3/2})$$

$$-2.4 \times 10^{24}/(r^5 r_0) + 1.9 \times 10^{39}/(\epsilon^5 r^5 r_0) - 1.6 \times 10^{40}/(\epsilon^4 r^5 r_0)$$

$$+4.6 \times 10^{40}/(\epsilon^3 r^5 r_0) - 4.6 \times 10^{40}/(\epsilon^2 r^5 r_0) + 1.2 \times 10^{40}/(\epsilon r^5 r_0)$$

$$+1.2 \times 10^{25}\epsilon/(r^5 r_0) + 2.2 \times 10^{-16}/(r^3 r_0) + 1.8/(\epsilon^4 r^3 r_0)$$

$$-13.9/(\epsilon^3 r^3 r_0) + 30.2/(\epsilon^2 r^3 r_0) - 16.1/(\epsilon r^3 r_0)$$

$$+4.4 \times 10^{-16}\epsilon/(r^3 r_0) + 1.3 \times 10^{-57}\epsilon^2/(r^3 r_0)$$

$$+6.9 \times 10^{-18}(\ln \epsilon)/(r^3 r_0) + 0.01(\ln \epsilon)/(\epsilon^3 r^3 r_0)$$

$$-0.04(\ln \epsilon)/(\epsilon^2 r^3 r_0) + 0.03(\ln \epsilon)/(\epsilon r^3 r_0)$$

$$-1.4 \times 10^{-17}(\ln r)/(r^3 r_0) - 0.02(\ln r)/(\epsilon^3 r^3 r_0)$$

$$+0.07(\ln r)/(\epsilon^2 r^3 r_0) - 0.05(\ln r)/(\epsilon r^3 r_0)$$

$$+1.4 \times 10^{-17}(\ln r_0)/(r^3 r_0) + 0.02(\ln r_0)/(\epsilon^3 r^3 r_0)$$

$$-0.07(\ln r_0)/(\epsilon^2 r^3 r_0) + 0.05(\ln r_0)/(\epsilon r^3 r_0)$$

$$-0.02(\ln T)/(\epsilon^3 r^3 r_0) + 0.07(\ln T)/(\epsilon^2 r^3 r_0) - 0.05(\ln T)/(\epsilon r^3 r_0)$$

$$+1.1 \times 10^{-40}/(\epsilon^3 r r_0) - 6.9 \times 10^{-40}/(\epsilon^2 r r_0)$$

$$+9.1 \times 10^{-40}/(\epsilon r r_0) - 1.7 \times 10^{15}/(r^{9/2}\sqrt{r_0})$$

$$+3.3 \times 10^{16}/(\epsilon^4 r^{9/2}\sqrt{r_0}) - 2.1 \times 10^{17}/(\epsilon^3 r^{9/2}\sqrt{r_0})$$

$$+3.6 \times 10^{17}/(\epsilon^2 r^{9/2}\sqrt{r_0}) - 1.2 \times 10^{17}/(\epsilon r^{9/2}\sqrt{r_0})$$

$$+1.2 \times 10^{14}\epsilon/(r^{9/2}\sqrt{r_0}) - 1.1 \times 10^{16}\sqrt{r_0}/r^{11/2}$$

$$+2.6 \times 10^{16}\sqrt{r_0}/(\epsilon^3 r^{11/2}) - 1.4 \times 10^{17}\sqrt{r_0}/(\epsilon^2 r^{11/2})$$

$$+1.6 \times 10^{17}\sqrt{r_0}/(\epsilon r^{11/2}) + 2.4 \times 10^{14}\epsilon\sqrt{r_0}/r^{11/2}$$

$$+6.3 \times 10^{35} r_0/r^9 - 6.3 \times 10^{39} r_0/r^7 + 1.5 \times 10^{39} r_0/(\epsilon^3 r^7)$$

$$-9.4 \times 10^{39} r_0/(\epsilon^2 r^7) + 1.7 \times 10^{40} r_0/(\epsilon r^7) + 7.6 \times 10^{23}\epsilon r_0/r^7$$

$$+8.2 r_0/r^5 + 1.5 r_0/(\epsilon^2 r^5) - 8.1 r_0/(\epsilon r^5) + 5.6 \times 10^{-17}\epsilon r_0/r^5$$

$$+6.4 \times 10^{-58}\epsilon^2 r_0/r^5 - 0.01(\ln \epsilon) r_0/r^5 + 0.007(\ln \epsilon) r_0/(\epsilon r^5)$$

$$+0.02(\ln r) r_0/r^5 - 0.01(\ln r) r_0/(\epsilon r^5) - 0.02(\ln r_0) r_0/r^5$$

$$+0.01(\ln r_0) r_0/(\epsilon r^5) + 0.02(\ln T) r_0/r^5 - 0.01(\ln T) r_0/(\epsilon r^5)$$

$$-0.04r_0/r^4 + 0.009r_0/r^3 + 1.1 \times 10^{-40} r_0/(\epsilon r^3) - 0.001r_0/r^2$$

$$+0.0001r_0/r + 5.0 \times 10^{16} r_0^{3/2}/r^{13/2} + 2.1 \times 10^{16} r_0^{3/2}/(\epsilon^2 r^{13/2})$$

$$-8.5 \times 10^{16} r_0^{3/2}/(\epsilon r^{13/2}) + 6.4 \times 10^{14} \epsilon r_0^{3/2}/r^{13/2}$$

$$-6.6 \times 10^{35} r_0^2/r^{10} - 6.3 \times 10^{35} \epsilon r_0^2/r^{10} + 7.9 \times 10^{39} r_0^2/r^8$$

$$+1.2 \times 10^{39} r_0^2/(\epsilon^2 r^8) - 6.7 \times 10^{39} r_0^2/(\epsilon r^8) - 1.1 \times 10^{39} \epsilon r_0^2/r^8$$

$$-4.6 r_0^2/r^6 + 1.3 r_0^2/(\epsilon r^6) + 3.0 \epsilon r_0^2/r^6 - 3.2 \times 10^{-58} \epsilon^2 r_0^2/r^6$$

$$+0.004(\ln \epsilon) r_0^2/r^6 - 0.008(\ln r) r_0^2/r^6 + 0.008(\ln r_0) r_0^2/r^6$$

$$-0.008(\ln T) r_0^2/r^6 + 0.02 r_0^2/r^5 + 0.01 \epsilon r_0^2/r^5 - 0.007 r_0^2/r^4$$

$$-0.003 \epsilon r_0^2/r^4 + 0.001 r_0^2/r^3 + 0.0005 \epsilon r_0^2/r^3 - 0.0001 r_0^2/r^2$$

$$-0.00003 \epsilon r_0^2/r^2 - 4.6 \times 10^{16} r_0^{5/2}/r^{15/2} + 1.5 \times 10^{16} r_0^{5/2}/(\epsilon r^{15/2})$$

$$+3.9 \times 10^{15} \epsilon r_0^{5/2}/r^{15/2} + 2.4 \times 10^{35} r_0^3/r^{11} + 1.3 \times 10^{36} \epsilon r_0^3/r^{11}$$

$$-4.0 \times 10^{39} r_0^3/r^9 + 1.0 \times 10^{39} r_0^3/(\epsilon r^9) + 3.5 \times 10^{39} \epsilon r_0^3/r^9$$

$$+0.3 r_0^3/r^7 - 6.3 \epsilon r_0^3/r^7 - 0.002 r_0^3/r^6 - 0.01 \epsilon r_0^3/r^6 + 0.002 r_0^3/r^5$$

$$+0.004 \epsilon r_0^3/r^5 - 0.0004 r_0^3/r^4 - 0.001 \epsilon r_0^3/r^4 + 0.00003 r_0^3/r^3$$

$$+0.00007 \epsilon r_0^3/r^3 + 1.0 \times 10^{16} r_0^{7/2}/r^{17/2} - 1.5 \times 10^{16} \epsilon r_0^{7/2}/r^{17/2}$$

$$-6.3 \times 10^{35} \epsilon r_0^4/r^{12} - 5.2 \times 10^{35} \epsilon^2 r_0^4/r^{12} + 6.5 \times 10^{38} r_0^4/r^{10}$$

$$-3.4 \times 10^{39} \epsilon r_0^4/r^{10} - 0.005 \epsilon^2 r_0^4/r^{10} + 3.4 \epsilon r_0^4/r^8$$

$$-1.3 \times 10^{-41} \epsilon^2 r_0^4/r^8 - 0.0009 \epsilon r_0^4/r^7 - 0.0008 \epsilon r_0^4/r^6$$

$$-2.3 \times 10^{-81} \epsilon^2 r_0^4/r^6 + 0.0004 \epsilon r_0^4/r^5 - 0.00003 \epsilon r_0^4/r^4$$

$$+1.0 \times 10^{16} \epsilon r_0^{9/2}/r^{19/2} + 4.2 \times 10^{35} \epsilon^2 r_0^5/r^{13} + 1.1 \times 10^{39} \epsilon r_0^5/r^{11}$$

$$+0.0009\epsilon^2 r_0^5/r^{11} + 2.1\times10^{-41}\epsilon^2 r_0^5/r^9 - 0.08T^2/(\epsilon^2 r_0^2)$$
$$+0.04T^2/(\epsilon r_0^2) - 4.9\times10^{-40} r^2T^2/(\epsilon r_0^2) - 0.05T^2/(\epsilon r r_0). \quad \text{(E14)}$$

Setting $r = r_0$ in Eqs. (E13) and (E14), we obtain the stress-energy tensor components of a quantized proton field at the throat of the wormhole (in units of F_p/l_p^2):

$$\begin{aligned}
< T_t^t >_0 \;=\; & -1.1\times10^{-79} + 1.1\times10^{-79}\epsilon + 7.4\times10^{19}/r_0^8 + 1.5\times10^{20}\epsilon/r_0^8 \\
& +1.0\times10^{35}\epsilon^2/r_0^8 + 4.5\times10^{33}/r_0^6 + 4.6\times10^{38}/(\epsilon^6 r_0^6) \\
& -4.0\times10^{39}/(\epsilon^5 r_0^6) + 1.2\times10^{40}/(\epsilon^4 r_0^6) - 1.3\times10^{40}/(\epsilon^3 r_0^6) \\
& +3.7\times10^{39}/(\epsilon^2 r_0^6) + 4.2\times10^{24}/(\epsilon r_0^6) - 4.0\times10^{35}\epsilon/r_0^6 \\
& +0.004\epsilon^2/r_0^6 - 9.3\times10^{14}/r_0^5 - 4.0\times10^{16}/(\epsilon^5 r_0^5) \\
& +2.7\times10^{17}/(\epsilon^4 r_0^5) - 4.8\times10^{17}/(\epsilon^3 r_0^5) + 1.8\times10^{17}/(\epsilon^2 r_0^5) \\
& +4.5\times10^{15}/(\epsilon r_0^5) + 2.1\times10^{14}\epsilon/r_0^5 + 0.03/r_0^4 - 0.4/(\epsilon^5 r_0^4) \\
& +2.1/(\epsilon^4 r_0^4) - 3.1/(\epsilon^3 r_0^4) + 0.7/(\epsilon^2 r_0^4) + 0.03/(\epsilon r_0^4) - 0.03\epsilon/r_0^4 \\
& -8.0\times10^{-42}\epsilon^2/r_0^4 - 0.0002(\ln\epsilon)/r_0^4 + 0.004(\ln\epsilon)/(\epsilon^4 r_0^4) \\
& -0.01(\ln\epsilon)/(\epsilon^3 r_0^4) + 0.007(\ln\epsilon)/(\epsilon^2 r_0^4) - 0.0003(\ln\epsilon)/(\epsilon r_0^4) \\
& +0.0004(\ln r)/r_0^4 - 0.008(\ln r)/(\epsilon^4 r_0^4) + 0.02(\ln r)/(\epsilon^3 r_0^4) \\
& -0.01(\ln r)/(\epsilon^2 r_0^4) + 0.0006(\ln r)/(\epsilon r_0^4) - 0.0004(\ln r_0)/r_0^4 \\
& +0.008(\ln r_0)/(\epsilon^4 r_0^4) - 0.02(\ln r_0)/(\epsilon^3 r_0^4) + 0.01(\ln r_0)/(\epsilon^2 r_0^4) \\
& -0.0006(\ln r_0)/(\epsilon r_0^4) + 0.0004(\ln T)/r_0^4 - 0.008(\ln T)/(\epsilon^4 r_0^4)
\end{aligned}$$

$$
\begin{aligned}
&+0.02(\ln T)/(\epsilon^3 r_0^4) - 0.01(\ln T)/(\epsilon^2 r_0^4) + 0.0006(\ln T)/(\epsilon r_0^4) \\
&-1.7 \times 10^{-41}/r_0^2 - 6.4 \times 10^{-41}/(\epsilon^4 r_0^2) + 4.1 \times 10^{-40}/(\epsilon^3 r_0^2) \\
&-6.0 \times 10^{-40}/(\epsilon^2 r_0^2) + 6.2 \times 10^{-42}/(\epsilon r_0^2) - 2.1 \times 10^{-41}\epsilon/r_0^2 \\
&+2.3 \times 10^{-81}\epsilon^2/r_0^2 + 4.9 \times 10^{-40}T^2/\epsilon + 0.06T^2/(\epsilon^2 r_0^2) \\
&-0.01T^2/(\epsilon r_0^2) \qquad \text{(E15)}
\end{aligned}
$$

$$
\begin{aligned}
< T_r^r >_0 \;=\; & -1.5 \times 10^{20}\epsilon/r_0^8 - 1.0 \times 10^{35}\epsilon^2/r_0^8 + 1.2 \times 10^{36}/r_0^6 \\
&+2.1 \times 10^{39}/(\epsilon^6 r_0^6) - 1.9 \times 10^{40}/(\epsilon^5 r_0^6) + 5.4 \times 10^{40}/(\epsilon^4 r_0^6) \\
&-5.6 \times 10^{40}/(\epsilon^3 r_0^6) + 1.5 \times 10^{40}/(\epsilon^2 r_0^6) - 1.1 \times 10^{35}/(\epsilon r_0^6) \\
&-2.7 \times 10^{36}\epsilon/r_0^6 - 0.004\epsilon^2/r_0^6 + 9.3 \times 10^{14}/r_0^5 \\
&+4.0 \times 10^{16}/(\epsilon^5 r_0^5) - 2.7 \times 10^{17}/(\epsilon^4 r_0^5) + 4.8 \times 10^{17}/(\epsilon^3 r_0^5) \\
&-1.8 \times 10^{17}/(\epsilon^2 r_0^5) - 4.5 \times 10^{15}/(\epsilon r_0^5) - 2.1 \times 10^{14}\epsilon/r_0^5 \\
&-0.004/r_0^4 + 2.0/(\epsilon^5 r_0^4) - 15.5/(\epsilon^4 r_0^4) + 34.1/(\epsilon^3 r_0^4) \\
&-18.8/(\epsilon^2 r_0^4) - 0.009/(\epsilon r_0^4) - 0.005\epsilon/r_0^4 + 8.0 \times 10^{-42}\epsilon^2/r_0^4 \\
&-4.2 \times 10^{-17}(\ln \epsilon)/r_0^4 + 0.009(\ln \epsilon)/(\epsilon^4 r_0^4) - 0.03(\ln \epsilon)/(\epsilon^3 r_0^4) \\
&+0.02(\ln \epsilon)/(\epsilon^2 r_0^4) + 0.0001(\ln \epsilon)/(\epsilon r_0^4) + 8.3 \times 10^{-17}(\ln r)/r_0^4 \\
&-0.02(\ln r)/(\epsilon^4 r_0^4) + 0.06(\ln r)/(\epsilon^3 r_0^4) - 0.04(\ln r)/(\epsilon^2 r_0^4) \\
&-0.0002(\ln r)/(\epsilon r_0^4) - 8.3 \times 10^{-17}(\ln r_0)/r_0^4 \\
&+0.02(\ln r_0)/(\epsilon^4 r_0^4) - 0.06(\ln r_0)/(\epsilon^3 r_0^4) + 0.04(\ln r_0)/(\epsilon^2 r_0^4) \\
&+0.0002(\ln r_0)/(\epsilon r_0^4) + 4.2 \times 10^{-17}(\ln T)/r_0^4
\end{aligned}
$$

$$
\begin{aligned}
&-0.02(\ln T)/(\epsilon^4 r_0^4) + 0.06(\ln T)/(\epsilon^3 r_0^4) - 0.04(\ln T)/(\epsilon^2 r_0^4) \\
&-0.0002(\ln T)/(\epsilon r_0^4) - 1.04 \times 10^{-17}/r_0^3 + 0.0008\epsilon/r_0^3 \\
&+1.1 \times 10^{-40}/(\epsilon^4 r_0^2) - 6.9 \times 10^{-40}/(\epsilon^3 r_0^2) + 9.3 \times 10^{-40}/(\epsilon^2 r_0^2) \\
&-1.6 \times 10^{-55}/(\epsilon r_0^2) - 2.3 \times 10^{-81}\epsilon^2/r_0^2 - 4.9 \times 10^{-40}T^2/\epsilon \\
&-0.08T^2/(\epsilon^2 r_0^2) - 0.01T^2/(\epsilon r_0^2). \qquad \text{(E16)}
\end{aligned}
$$

Appendix F: Stress-Energy Tensor of the Quantized Neutrino Field and Quantized Proton Field in the Spacetime of Wormhole with Finite Radial Energy Cutoff

F.1 Zero-temperature vacuum state

F.1.1 Quantized neutrino field

I have computed the stress-energy tensor components of a quantized neutrino field for the wormhole with finite radial cutoff of the stress-energy in the entire spacetime. Because the expression for each component is lengthy, I list only $< T_t^t >$ and $< T_r^r >$ (in units of F_p/l_p^2) but omit $< T_\phi^\phi >$ since it is irrelevant to the calculations in this thesis:

$$\begin{aligned} < T_t^t > \;\; = \;\; & 1.6 \times 10^{54}/r^8 + 1.6 \times 10^{54}\eta(\ln r)/r^8 - 8.1 \times 10^{53}\eta^2(\ln r)^2/r^8 \\ & -1.6 \times 10^{54}\eta(\ln r_0)/r^8 + 1.6 \times 10^{54}\eta^2(\ln r)(\ln r_0)/r^8 \end{aligned}$$

$$-8.1 \times 10^{53}\eta^2(\ln r_0)^2/r^8 - 5.8 \times 10^{54}/r^6 - 1.4 \times 10^{53}\eta/r^6$$

$$-1.1 \times 10^{41}\eta^2/r^6 - 5.1 \times 10^{53}\eta(\ln r)/r^6 + 1.4 \times 10^{53}\eta^2(\ln r)/r^6$$

$$+2.6 \times 10^{53}\eta^2(\ln r^2)/r^6 + 5.7 \times 10^{41}/[(\ln r_0)^2 r^6]$$

$$-8.7 \times 10^{40}/[\eta(\ln r_0)^2 r^6] - 3.7 \times 10^{42}\eta/[(\ln r_0)^2 r^6]$$

$$+1.7 \times 10^{43}\eta^2/[(\ln r_0)^2 r^6] - 2.2 \times 10^{41}(\ln r)/[(\ln r_0)^2 r^6]$$

$$-1.1 \times 10^{42}\eta(\ln r)/[(\ln r_0)^2 r^6] + 8.6 \times 10^{43}\eta^2(\ln r)/[(\ln r_0)^2 r^6]$$

$$+7.8 \times 10^{41}\eta(\ln r)^2/[(\ln r_0)^2 r^6]$$

$$+7.7 \times 10^{42}\eta^2(\ln r)^2/[(\ln r_0)^2 r^6]$$

$$+4.2 \times 10^{42}\eta^2(\ln r)^3/[(\ln r_0)^2 r^6] - 1.3 \times 10^{41}/[(\ln r_0) r^6]$$

$$-6.5 \times 10^{40}\eta/[(\ln r_0) r^6] + 1.1 \times 10^{43}\eta^2/[(\ln r_0) r^6]$$

$$+2.2 \times 10^{40}\eta(\ln r)/[(\ln r_0) r^6] + 1.7 \times 10^{42}\eta^2(\ln r)/[(\ln r_0) r^6]$$

$$-1.9 \times 10^{42}\eta^2(\ln r)^2/[(\ln r_0) r^6] + 5.1 \times 10^{53}\eta(\ln r_0)/r^6$$

$$-1.4 \times 10^{53}\eta^2(\ln r_0)/r^6 - 5.1 \times 10^{53}\eta^2(\ln r)(\ln r_0)/r^6$$

$$+2.6 \times 10^{53}\eta^2(\ln r_0)^2/r^6 - 0.007/r^4 - 0.004\eta/r^4 - 0.002\eta^2/r^4$$

$$+0.007\eta(\ln r)/r^4 - 0.03\eta^2(\ln r)/r^4 + 0.2\eta^2(\ln r)^2/r^4$$

$$-2.3 \times 10^{-17}/[(\ln r_0)^2 r^4] - 4.1 \times 10^{-16}\eta/[(\ln r_0)^2 r^4]$$

$$-1.4 \times 10^{-17}(\ln r)/[(\ln r_0)^2 r^4] - 6.1 \times 10^{-18}\eta(\ln r)/[(\ln r_0)^2 r^4]$$

$$+4.3 \times 10^{-15}\eta^2(\ln r)/[(\ln r_0)^2 r^4]$$

$$+1.4 \times 10^{-17}\eta(\ln r)^2/(\ln r_0)^2 r^4]$$

$$-5.7 \times 10^{-17}\eta^2(\ln r)^2/[(\ln r_0)^2 r^4]$$

$$
\begin{aligned}
& +2.0\times10^{-16}\eta^2(\ln r)^3/[(\ln r_0)^2 r^4] - 6.9\times10^{-18}/[(\ln r_0) r^4] \\
& -8.7\times10^{-18}\eta/[(\ln r_0) r^4] + 4.7\times10^{-16}\eta^2/[(\ln r_0) r^4] \\
& +6.9\times10^{-18}\eta(\ln r)/[(\ln r_0) r^4] - 1.5\times10^{-17}\eta^2(\ln r)/[(\ln r_0) r^4] \\
& -4.4\times10^{-17}\eta^2(\ln r)^2/[(\ln r_0) r^4] - 0.007\eta(\ln r_0)/r^4 \\
& +0.03\eta^2(\ln r_0)/r^4 - 0.4\eta^2(\ln r)(\ln r_0)/r^4 + 0.2\eta^2(\ln r_0)^2/r^4 \\
& -2.2\times10^{-60}/r^2 + 2.0\times10^{-61}\eta/r^2 + 8.7\times10^{-60}\eta(\ln r)/r^2 \\
& -2.0\times10^{-61}\eta^2(\ln r)/r^2 - 4.4\times10^{-60}\eta^2(\ln r)^2/r^2 \\
& -6.9\times10^{-77}\eta(\ln r)^2/[(\ln r_0)^2 r^2] \\
& +8.2\times10^{-76}\eta^2(\ln r)^3/[(\ln r_0)^2 r^2] \\
& -3.5\times10^{-77}\eta(\ln r)/[(\ln r_0) r^2] + 2.6\times10^{-76}\eta^2(\ln r)^2/[(\ln r_0) r^2] \\
& -8.7\times10^{-60}\eta(\ln r_0)/r^2 + 2.0\times10^{-61}\eta^2(\ln r_0)/r^2 \\
& +8.7\times10^{-60}\eta^2(\ln r)(\ln r_0)/r^2 - 4.4\times10^{-60}\eta^2(lnr_0)^2/r^2, \quad \text{(F1)}
\end{aligned}
$$

$$
\begin{aligned}
< T_r^r > \;=\; & -0.00003\eta^2(\ln r)^2 + 0.00007\eta^2(\ln r)(\ln r_0) - 0.00003\eta^2(\ln r_0)^2 \\
& -1.6\times10^{54}/r^8 - 1.6\times10^{54}\eta(\ln r)/r^8 + 8.1\times10^{53}\eta^2(\ln r)^2/r^8 \\
& +1.6\times10^{54}\eta(\ln r_0)/r^8 - 1.6\times10^{54}\eta^2(\ln r)(\ln r_0)/r^8 \\
& +8.1\times10^{53}\eta^2(\ln r_0)^2/r^8 + 1.5\times10^{56}/[(\ln r_0) r^6] \\
& +3.1\times10^{54}/r^6 + 6.5\times10^{40}\eta/r^6 - 1.0\times10^{54}\eta^2/r^6 \\
& +1.1\times10^{54}\eta(\ln r)/r^6 + 1.3\times10^{55}\eta^2(\ln r)/r^6 \\
& -3.1\times10^{55}\eta^2(\ln r^2)/r^6 - 7.0\times10^{41}/[(\ln r_0)^2 r^6]
\end{aligned}
$$

$$-3.3 \times 10^{43}\eta/[(\ln r_0)^2 r^6] + 1.9 \times 10^{44}\eta^2/[(\ln r_0)^2 r^6]$$

$$-4.4 \times 10^{40}(\ln r)/[(\ln r_0)^2 r^6] - 3.1 \times 10^{42}\eta(\ln r)/[(\ln r_0)^2 r^6]$$

$$+3.8 \times 10^{44}\eta^2(\ln r)/[(\ln r_0)^2 r^6] - 4.4 \times 10^{40}\eta(\ln r)^2/[(\ln r_0)^2 r^6]$$

$$+6.3 \times 10^{43}\eta^2(\ln r)^2/[(\ln r_0)^2 r^6]$$

$$-4.0 \times 10^{42}\eta^2(\ln r)^3/[(\ln r_0)^2 r^6] - 1.5 \times 10^{56}/[(\ln r_0) r^6]$$

$$-2.4 \times 10^{42}\eta/[(\ln r_0) r^6] + 3.9 \times 10^{43}\eta^2/[(\ln r_0) r^6]$$

$$+1.4 \times 10^{43}\eta^2(\ln r)/[(\ln r_0) r^6] + 1.4 \times 10^{42}\eta^2(\ln r)^2/[(\ln r_0) r^6]$$

$$-1.1 \times 10^{54}\eta(\ln r_0)/r^6 - 1.3 \times 10^{55}\eta^2(\ln r_0)/r^6$$

$$+6.1 \times 10^{55}\eta^2(\ln r)(\ln r_0)/r^6 - 3.1 \times 10^{55}\eta^2(\ln r_0)^2/r^6$$

$$-0.009/[(\ln r_0) r^4] - 0.008/r^4 + 0.009\eta/r^4 - 0.02\eta^2/r^4$$

$$+0.03\eta(\ln r)/r^4 - 0.05\eta^2(\ln r)/r^4 - 0.02\eta^2(\ln r)^2/r^4$$

$$-3.5 \times 10^{-17}/[(\ln r_0)^2 r^4] + 9.7 \times 10^{-17}\eta/[(\ln r_0)^2 r^4]$$

$$-1.4 \times 10^{-17}(\ln r)/[(\ln r_0)^2 r^4] + 1.7 \times 10^{-17}\eta(\ln r)/[(\ln r_0)^2 r^4]$$

$$-1.1 \times 10^{-15}\eta^2(\ln r)/[(\ln r_0)^2 r^4]$$

$$-9.7 \times 10^{-17}\eta(\ln r)^2/[(\ln r_0)^2 r^4]$$

$$-6.2 \times 10^{-16}\eta^2(\ln r)^2/[(\ln r_0)^2 r^4]$$

$$+1.5 \times 10^{-15}\eta^2(\ln r)^3/[(\ln r_0)^2 r^4] + 0.009/[(\ln r_0) r^4]$$

$$-1.7 \times 10^{-17}\eta/[(\ln r_0) r^4] - 1.2 \times 10^{-16}\eta^2/[(\ln r_0) r^4]$$

$$+6.9 \times 10^{-18}\eta(\ln r)/[(\ln r_0) r^4] - 1.8 \times 10^{-16}\eta^2(\ln r)/[(\ln r_0) r^4]$$

$$+2.3 \times 10^{-16}\eta^2(\ln r)^2/[(\ln r_0) r^4] - 0.03\eta(\ln r_0)/r^4$$

$$
\begin{aligned}
&+0.05\eta^2(\ln r_0)/r^4 + 0.03\eta^2(\ln r)(\ln r_0)/r^4 - 0.02\eta^2(\ln r_0)^2/r^4 \\
&-0.0008/[(\ln r_0)r^3] + 0.0008\eta/r^3 + 0.01\eta(\ln r)/r^3 \\
&-0.0004\eta^2(\ln r)/r^3 - 0.002\eta^2(\ln r)^2/r^3 \\
&-4.3\times 10^{-19}\eta(\ln r)^2/[(\ln r_0)^2 r^3] \\
&-7.5\times 10^{-18}\eta^2(\ln r)^3/[(\ln r_0)^2 r^3] + 0.0008/[(\ln r_0)r^3] \\
&-2.2\times 10^{-19}\eta(\ln r)/[(\ln r_0)r^3] \\
&-1.2\times 10^{-18}\eta^2(\ln r)^2/[(\ln r_0)r^3] - 0.01\eta(\ln r_0)/r^3 \\
&+0.0004\eta^2(\ln r_0)/r^3 + 0.004\eta^2(\ln r)(\ln r_0)/r^3 \\
&-0.002\eta^2(\ln r_0)^2/r^3 - 0.002\eta(\ln r)/r^2 - 0.0004\eta^2(\ln r)/r^2 \\
&-0.002\eta^2(\ln r)^2/r^2 + 2.2\times 10^{-19}\eta(\ln r)^2/[(\ln r_0)^2 r^2] \\
&+1.0\times 10^{-17}\eta^2(\ln r)^3/[(\ln r_0)^2 r^2] + 1.1\times 10^{-19}\eta(\ln r)/[(\ln r_0)r^2] \\
&+1.6\times 10^{-18}\eta^2(\ln r)^2/[(\ln r_0)r^2] + 0.002\eta(\ln r_0)/r^2 \\
&+0.0004\eta^2(\ln r_0)/r^2 + 0.003\eta^2(\ln r)(\ln r_0)/r^2 \\
&-0.002\eta^2(\ln r_0)^2/r^2 - 6.8\times 10^{-21}\eta/r + 0.0001\eta^2(\ln r)/r \\
&+0.0005\eta^2(\ln r)^2/r - 5.4\times 10^{-20}\eta(\ln r)^2/[(\ln r_0)^2 r] \\
&-2.5\times 10^{-18}\eta^2(\ln r^3)/[(\ln r_0)^2 r] - 2.7\times 10^{-20}\eta(\ln r)/[(\ln r_0)r] \\
&-4.1\times 10^{-19}\eta^2(\ln r)^2/[(\ln r_0)r] - 0.0001\eta^2(\ln r_0)/r \\
&-0.001\eta^2(\ln r)(\ln r_0)/r + 0.0005\eta^2(\ln r_0)^2/r. \qquad \text{(F2)}
\end{aligned}
$$

By setting $r = r_0$ in Eqs. (F1) and (F2), we get the stress-energy tensor components of a quantized neutrino field at the throat of the wormhole (in

units of F_p/l_p^2):

$$
\begin{aligned}
< T_t^t >_0 \;=\; & 1.6\times 10^{54}/r_0^8 - 5.8\times 10^{54}/r_0^6 - 1.4\times 10^{53}\eta/r_0^6 \\
& +9.3\times 10^{42}\eta^2/r_0^6 + 5.7\times 10^{41}/[(\ln r_0)^2 r_0^6] \\
& -8.7\times 10^{40}/[(\eta(\ln r_0)^2 r_0^6] - 3.7\times 10^{42}\eta/[(\ln r_0)^2 r_0^6] \\
& +1.7\times 10^{43}\eta^2/[(\ln r_0)^2 r_0^6] - 3.5\times 10^{41}/[(\ln r_0) r_0^6] \\
& -1.2\times 10^{42}\eta/[(\ln r_0) r_0^6] + 9.7\times 10^{43}\eta^2/[(\ln r_0) r_0^6] \\
& +1.2\times 10^{42}\eta^2(\ln r_0)/r_0^6 - 0.007/r_0^4 - 0.004\eta/r_0^4 - 0.002\eta^2/r_0^4 \\
& -2.3\times 10^{-17}/[(\ln r_0)^2 r_0^4] - 4.1\times 10^{-16}\eta/[(\ln r_0)^2 r_0^4] \\
& -2.1\times 10^{-17}/[(\ln r_0) r_0^4] - 1.5\times 10^{-17}\eta/[(\ln r_0) r_0^4] \\
& +4.7\times 10^{-15}\eta^2/[(\ln r_0) r_0^4] + 2.0\times 10^{-16}\eta^2(\ln r_0)/r_0^4 \\
& -2.2\times 10^{-60}/r_0^2 + 2.0\times 10^{-61}\eta/r_0^2 \\
& +1.0\times 10^{-75}\eta^2(\ln r_0)/r_0^2, \qquad \text{(F3)}
\end{aligned}
$$

$$
\begin{aligned}
< T_r^r >_0 \;=\; & -1.6\times 10^{54}/r_0^8 + 1.5\times 10^{56}/[(\ln r_0) r_0^6] + 3.1\times 10^{54}/r_0^6 \\
& +2.2\times 10^{40}\eta/r_0^6 - 1.0\times 10^{54}\eta^2/r_0^6 - 7.0\times 10^{41}/[(\ln r_0)^2 r_0^6] \\
& -3.3\times 10^{43}\eta/[(\ln r0^2 r_0^6] + 1.9\times 10^{44}\eta^2/[(\ln r_0)^2 r_0^6] \\
& -1.5\times 10^{56}/[(\ln r_0) r_0^6] - 5.6\times 10^{42}\eta/[(\ln r_0) r_0^6] \\
& +4.1\times 10^{44}\eta^2/[(\ln r_0) r_0^6] - 1.8\times 10^{42}\eta^2(\ln r_0)/r_0^6 \\
& -0.009/[(\ln r_0) r_0^4] - 0.008/r_0^4 + 0.009\eta/r_0^4 - 0.02\eta^2/r_0^4
\end{aligned}
$$

$$
\begin{aligned}
&-3.5\times10^{-17}/[(\ln r_0)^2 r_0^4]+9.7\times10^{-17}\eta/[(\ln r_0)^2 r_0^4]\\
&+0.009/[(\ln r_0) r_0^4]-1.2\times10^{-15}\eta^2/[(\ln r_0 r_0^4]\\
&+1.7\times10^{-15}\eta^2(\ln r_0)/r_0^4-0.0008/[(\ln r_0) r_0^3]+0.0008\eta/r_0^3\\
&+0.0008/[(\ln r_0) r_0^3]-8.8\times10^{-18}\eta^2(\ln r_0)/r_0^3\\
&+3.3\times10^{-19}\eta/r_0^2+1.2\times10^{-17}\eta^2(\ln r_0)/r_0^2-8.8\times10^{-20}\eta/r_0\\
&-2.9\times10^{-18}\eta^2(\ln r_0)/r_0. \qquad \text{(F4)}
\end{aligned}
$$

F.1.2 Quantized proton field

The stress-energy tensor components of a quantized proton field for wormholes with finite radial cutoff of stress-energy tensor in the entire spacetime are found to be (in units of F_p/l_p^2):

$$
\begin{aligned}
< T_t^t > \;=\;& 1.0\times10^{35}/r^8+1.1\times10^{35}\eta(\ln r)/r^8-5.3\times10^{34}\eta^2(\ln r^2)/r^8\\
&-1.1\times10^{35}\eta(\ln r_0)/r^8+1.1\times10^{35}\eta^2(\ln r)(\ln r_0)/r^8\\
&-5.3\times10^{34}\eta^2(\ln r_0)^2/r^8-3.8\times10^{35}/r^6-9.0\times10^{33}\eta/r^6\\
&-1.8\times10^{21}\eta^2/r^6-3.4\times10^{34}\eta(\ln r)/r^6\\
&+9.0\times10^{33}\eta^2(\ln r)/r^6+1.7\times10^{34}\eta^2(\ln r)^2/r^6\\
&-4.2\times10^{23}\eta/[(\ln r_0)^2 r^6]+1.2\times10^{24}\eta^2/[(\ln r_0)^2 r^6]\\
&+1.4\times10^{22}(\ln r)/[(\ln r_0)^2 r^6]-2.1\times10^{22}\eta(\ln r)/[(\ln r_0)^2 r^6]\\
&+5.8\times10^{24}\eta^2(\ln r)/[(\ln r_0)^2 r^6]+2.4\times10^{21}\eta(\ln r)^2/[(\ln r_0)^2 r^6]\\
&+5.6\times10^{23}\eta^2(\ln r)^2/[(\ln r_0)^2 r^6]
\end{aligned}
$$

$$-1.9 \times 10^{23}\eta^2(\ln r)^3/[(\ln r_0)^2 r^6]$$

$$+9.4 \times 10^{21}/[(\ln r_0)r^6] + 1.7 \times 10^{22}\eta/[(\ln r_0)r^6]$$

$$+5.7 \times 10^{23}\eta^2/[(\ln r_0)r^6] + 1.2 \times 10^{21}\eta(\ln r)/[(lnr_0)r^6]$$

$$+1.2 \times 10^{23}\eta^2(\ln r)/[(\ln r_0)r^6] - 7.0 \times 10^{22}\eta^2(\ln r)^2/[(\ln r_0)r^6]$$

$$+3.4 \times 10^{34}\eta(\ln r_0)/r^6 - 9.0 \times 10^{33}\eta^2(\ln r_0)/r^6$$

$$-3.4 \times 10^{34}\eta^2(\ln r)(\ln r_0)/r^6 + 1.7 \times 10^{34}\eta^2(\ln r_0)^2/r^6$$

$$-0.007/r^4 - 0.004\eta/r^4 - 0.002\eta^2/r^4 + 0.007\eta(\ln r)/r^4$$

$$-0.03\eta^2(\ln r)/r^4 + 0.2\eta^2(\ln r)^2/r^4 - 2.3 \times 10^{-17}/[(\ln r_0)^2 r^4]$$

$$-4.1 \times 10^{-16}\eta/[(\ln r_0)^2 r^4] - 1.4 \times 10^{-17}(\ln r)/[(\ln r_0)^2 r^4]$$

$$-6.1 \times 10^{-18}\eta(\ln r)/[(\ln r_0)^2 r^4]$$

$$+4.3 \times 10^{-15}\eta^2(\ln r)/[(\ln r_0)^2 r^4]$$

$$+1.4 \times 10^{-17}\eta(\ln r)^2/[(\ln r_0)^2 r^4]$$

$$-5.7 \times 10^{-17}\eta^2(\ln r)^2/[(\ln r_0)^2 r^4]$$

$$+2.0 \times 10^{-16}\eta^2(\ln r)^3/[(\ln r_0)^2 r^4] - 8.7 \times 10^{-18}\eta/[(\ln r_0)r^4]$$

$$+4.7 \times 10^{-16}\eta^2/[(\ln r_0)r^4] + 6.9 \times 10^{-18}\eta(\ln r)/[(\ln r_0)r^4]$$

$$-1.5 \times 10^{-17}\eta^2(\ln r)/[(\ln r_0)r^4]$$

$$-4.4 \times 10^{-17}\eta^2(\ln r)^2/[(\ln r_0)r^4] - 0.007\eta(\ln r_0)/r^4$$

$$+0.03\eta^2(\ln r_0)/r^4 - 0.4\eta^2(\ln r)(\ln r_0)/r^4 + 0.2\eta^2(\ln r_0)^2/r^4$$

$$-3.3 \times 10^{-41}/r^2 + 3.1 \times 10^{-42}\eta/r^2 + 1.3 \times 10^{-40}\eta(\ln r)/r^2$$

$$-3.1 \times 10^{-42}\eta^2(\ln r)/r^2 - 6.7 \times 10^{-41}\eta^2(\ln r^2)/r^2$$

$$
\begin{aligned}
&-6.4\times10^{-58}\eta(\ln r)^2/[(\ln r_0)^2r^2]\\
&+3.2\times10^{-57}\eta^2(\ln r)^3/[(\ln r_0)^2r^2]\\
&-3.2\times10^{-58}\eta(\ln r)/[(\ln r_0)r^2]+1.9\times10^{-57}\eta^2(\ln r)^2/[(\ln r_0)r^2]\\
&-1.3\times10^{-40}\eta(\ln r_0)/r^2+3.1\times10^{-42}\eta^2(\ln r_0)/r^2\\
&+1.3\times10^{-40}\eta^2(\ln r)(\ln r_0)/r^2-6.7\times10^{-41}\eta^2(\ln r_0)^2/r^2, \quad \text{(F5)}
\end{aligned}
$$

$$
\begin{aligned}
< T_r^r > \;=\; & -0.00003\eta^2(\ln r)^2+0.00007\eta^2(\ln r)(\ln r_0)-0.00003\eta^2(\ln r_0)^2\\
&-1.0\times10^{35}/r^8-1.1\times10^{35}\eta(\ln r)/r^8+5.3\times10^{34}\eta^2(\ln r)^2)/r^8\\
&+1.1\times10^{35}\eta(\ln r_0)/r^8-1.1\times10^{35}\eta^2(\ln r)(\ln r_0)/r^8\\
&+5.3\times10^{34}\eta^2(\ln r_0)^2/r^8+2.0\times10^{35}/r^6+1.4\times10^{22}\eta/r^6\\
&-6.7\times10^{34}\eta^2/r^6+6.9\times10^{34}\eta(\ln r)/r^6+8.2\times10^{35}\eta^2(\ln r)/r^6\\
&-2.0\times10^{36}\eta^2(\ln r)^2/r^6+7.6\times10^{22}/[(\ln r_0)^2r^6]\\
&+4.7\times10^{21}/[\eta(\ln r_0)^2r^6]-2.2\times10^{24}\eta/[(\ln r_0)^2r^6]\\
&+1.1\times10^{25}\eta^2/[(\ln r_0)^2r^6]+9.4\times10^{21}(\ln r)/[(\ln r_0)^2r^6]\\
&-9.4\times10^{22}\eta(\ln r)/[(\ln r_0)^2r^6]+2.2\times10^{25}\eta^2(\ln r)/[(\ln r_0)^2r^6]\\
&-7.8\times10^{22}\eta(\ln r)^2/[(\ln r_0)^2r^6]+5.0\times10^{24}\eta^2(\ln r)^2/[(\ln r_0)^2r^6]\\
&+3.5\times10^{23}\eta^2(\ln r)^3/[(lnr_0)^2r^6]+9.4\times10^{21}/[(\ln r_0)r^6]\\
&+2.8\times10^{22}\eta/[(\ln r_0)r^6]+2.1\times10^{24}\eta^2/[(\ln r_0)r^6]\\
&-1.2\times10^{21}\eta(\ln r)/[(\ln r_0)r^6]+1.2\times10^{24}\eta^2(\ln r)/[(\ln r_0)r^6]\\
&+1.4\times10^{23}\eta^2(\ln r)^2/[(\ln r_0)r^6]-6.9\times10^{34}\eta(\ln r_0)/r^6
\end{aligned}
$$

$$-8.2 \times 10^{35}\eta^2(\ln r_0)/r^6 + 4.0 \times 10^{36}\eta^2(\ln r)(\ln r_0)/r^6$$

$$-2.0 \times 10^{36}\eta^2(\ln r_0)^2/r^6 - 0.008/r^4 + 0.009\eta/r^4 - 0.02\eta^2/r^4$$

$$+0.03\eta(\ln r)/r^4 - 0.05\eta^2(\ln r)/r^4 - 0.02\eta^2(\ln r)^2/r^4$$

$$-2.8 \times 10^{-17}/[(\ln r_0)^2 r^4] + 9.7 \times 10^{-17}\eta/[(\ln r_0)^2 r^4]$$

$$-1.4 \times 10^{-17}(\ln r)/[(\ln r_0)^2 r^4] + 1.7 \times 10^{-17}\eta(\ln r)/[(\ln r_0)^2 r^4]$$

$$-1.1 \times 10^{-15}\eta^2(\ln r)/[(\ln r_0)^2 r^4]$$

$$-9.7 \times 10^{-17}\eta(\ln r)^2/[(\ln r_0)^2 r^4]$$

$$-6.2 \times 10^{-16}\eta^2(\ln r)^2/[(\ln r_0)^2 r^4]$$

$$+1.5 \times 10^{-15}\eta^2(\ln r)^3/[(\ln r_0)^2 r^4] - 1.7 \times 10^{-17}\eta/[(\ln r_0) r^4]$$

$$-1.2 \times 10^{-16}\eta^2/[(\ln r_0) r^4] + 6.9 \times 10^{-18}\eta(\ln r)/[(\ln r_0) r^4]$$

$$-1.8 \times 10^{-16}\eta^2(\ln r)/(\ln r_0) r^4]$$

$$+2.3 \times 10^{-16}\eta^2(\ln r)^2/[(\ln r_0) r^4] - 0.03\eta(\ln r_0)/r^4$$

$$+0.05\eta^2(\ln r_0)/r^4 + 0.03\eta^2(\ln r)(\ln r_0)/r^4 - 0.02\eta^2(\ln r_0)^2/r^4$$

$$+0.0008\eta/r^3 + 0.01\eta(\ln r)/r^3 - 0.0004\eta^2(\ln r)/r^3$$

$$-0.002\eta^2(\ln r)^2/r^3 - 4.3 \times 10^{-19}\eta(\ln r)^2/[(\ln r_0)^2 r^3]$$

$$-7.5 \times 10^{-18}\eta^2(\ln r)^3/[(\ln r_0)^2 r^3]$$

$$-2.2 \times 10^{-19}\eta(\ln r)/[(\ln r_0) r^3] - 1.2 \times 10^{-18}\eta^2(\ln r)^2/[(\ln r_0) r^3]$$

$$-0.01\eta(\ln r_0)/r^3 + 0.0004\eta^2(\ln r_0)/r^3 + 0.004\eta^2(\ln r)(\ln r_0)/r^3$$

$$-0.002\eta^2(\ln r_0)^2/r^3 - 0.002\eta(\ln r)/r^2 - 0.0004\eta^2(\ln r)/r^2$$

$$-0.002\eta^2(\ln r)^2/r^2 + 2.2 \times 10^{-19}\eta(\ln r)^2/[(\ln r_0)^2 r^2]$$

$$
\begin{aligned}
&+1.0\times10^{-17}\eta^2(\ln r)^3/[(\ln r_0)^2r^2]\\
&+1.1\times10^{-19}\eta(\ln r)/[(\ln r_0)r^2]+1.6\times10^{-18}\eta^2(\ln r)^2/[(\ln r_0)r^2]\\
&+0.002\eta(\ln r_0)/r^2+0.0004\eta^2(\ln r_0)/r^2+0.003\eta^2(\ln r)(\ln r_0)/r^2\\
&-0.002\eta^2(\ln r_0)^2/r^2-6.8\times10^{-21}\eta/r+0.0001\eta^2(\ln r)/r\\
&+0.0005\eta^2(\ln r)^2/r-5.4\times10^{-20}\eta(\ln r)^2/[(\ln r_0)^2r]\\
&-2.5\times10^{-18}\eta^2(\ln r)^3/[(\ln r_0)^2r]-2.7\times10^{-20}\eta(\ln r)/[(\ln r_0)r]\\
&-4.1\times10^{-19}\eta^2(\ln r)^2/[(\ln r_0)r]-0.0001\eta^2(\ln r_0)/r\\
&-0.001\eta^2(\ln r)(\ln r_0)/r+0.0005\eta^2(\ln r_0)^2/r. \qquad \text{(F6)}
\end{aligned}
$$

By setting $r=r_0$ in Eqs. (F5) and (F6), we get the stress-energy components of a quantized proton field at the throat of the wormhole (in units of F_p/l_p^2):

$$
\begin{aligned}
<T_t^t>_0 \;=\;& 1.0\times10^{35}/r_0^8-3.8\times10^{35}/r_0^6-9.0\times10^{33}\eta/r_0^6\\
&+6.8\times10^{23}\eta^2/r_0^6-4.2\times10^{23}\eta/[(\ln r_0)^2r_0^6]\\
&+1.2\times10^{24}\eta^2/[(\ln r_0)^2r_0^6]+2.4\times10^{22}/[(\ln r_0)r_0^6]\\
&-4.7\times10^{21}\eta/[(\ln r_0)r_0^6]+6.4\times10^{24}\eta^2/[(\ln r_0)r_0^6]\\
&-3.0\times10^{23}\eta^2(\ln r_0)/r_0^6-0.007/r_0^4-0.004\eta/r_0^4-0.002\eta^2/r_0^4\\
&-2.3\times10^{-17}/[(\ln r_0)^2r_0^4]-4.1\times10^{-16}\eta/[(\ln r_0)^2r_0^4]\\
&-1.4\times10^{-17}/[(\ln r_0)r_0^4]-1.5\times10^{-17}\eta/[(\ln r_0)r_0^4]\\
&+4.8\times10^{-15}\eta^2/[(\ln r_0)r_0^4]+2.0\times10^{-16}\eta^2(\ln r_0)/r_0^4
\end{aligned}
$$

$$
\begin{aligned}
&-3.3\times 10^{-41}/r_0^2+3.1\times 10^{-42}\eta/r_0^2\\
&+5.7\times 10^{-57}\eta^2(\ln r_0)/r_0^2, \qquad \text{(F7)}
\end{aligned}
$$

$$
\begin{aligned}
< T_r^r >_0 \;=\; & -1.0\times 10^{35}/r_0^8+2.0\times 10^{35}/r_0^6-6.5\times 10^{22}\eta/r_0^6\\
&-6.7\times 10^{34}\eta^2/r_0^6+7.6\times 10^{22}/[(\ln r_0)^2 r_0^6]\\
&+4.7\times 10^{21}/[\eta(\ln r_0)^2 r_0^6]-2.2\times 10^{24}\eta/[(\ln r_0)^2 r_0^6]\\
&+1.1\times 10^{25}\eta^2/[(\ln r0^2 r_0^6]+1.9\times 10^{22}/[(\ln r_0) r_0^6]\\
&-6.6\times 10^{22}\eta/[(\ln r_0) r_0^6]+2.4\times 10^{25}\eta^2/[(\ln r_0) r_0^6]\\
&+5.1\times 10^{23}\eta^2(\ln r_0)/r_0^6-0.008/r_0^4+0.009\eta/r_0^4-0.02\eta^2/r_0^4\\
&-2.8\times 10^{-17}/[(\ln r_0)^2 r_0^4]+9.7\times 10^{-17}\eta/[(\ln r_0)^2 r_0^4]\\
&-1.4\times 10^{-17}/[(\ln r_0) r_0^4]-1.2\times 10^{-15}\eta^2/[(\ln r_0) r_0^4]\\
&+1.7\times 10^{-15}\eta^2(\ln r_0)/r_0^4+0.0008\eta/r_0^3\\
&-8.78204\times 10^{-18}\eta^2(\ln r_0)/r_0^3+3.3\times 10^{-19}\eta/r_0^2\\
&+1.2\times 10^{-17}\eta^2(\ln r_0)/r_0^2-8.8\times 10^{-20}\eta/r_0\\
&-2.9\times 10^{-18}\eta^2(\ln r_0)/r_0. \qquad \text{(F8)}
\end{aligned}
$$

F.2 Thermal states

F.2.1 Quantized neutrino field

I have computed the stress-energy tensor components in the entire spacetime for the wormhole with finite radial cutoff of stress-energy tensor in

thermal states. Each component is lengthy and complicated. So I list only $< T_t^t >$ and $< T_r^r >$ (in units of F_p/l_p^2), but omit $< T_\theta^\theta >$ because it is irrelevant to the calculations in this thesis.

$$
\begin{aligned}
< T_t^t > \;=\; & 3.2\times 10^{54}/r^8 - 1.6\times 10^{54}/r^8 + 1.6\times 10^{54}\eta(\ln r)/r^8 \\
& -8.1\times 10^{53}\eta^2(\ln r)^2/r^8 - 1.6\times 10^{54}\eta(\ln r_0)/r^8 \\
& +1.6\times 10^{54}\eta^2(\ln r)(\ln r_0)/r^8 - 8.1\times 10^{53}\eta^2(\ln r_0)^2/r^8 \\
& -2.2\times 10^{54}/r^6 - 3.6\times 10^{54}/r^6 - 1.4\times 10^{53}\eta/r^6 \\
& -1.1\times 10^{42}\eta^2/r^6 - 5.1\times 10^{53}\eta(\ln r)/r^6 + 1.4\times 10^{53}\eta^2(\ln r)/r^6 \\
& +2.6\times 10^{53}\eta^2(\ln r)^2/r^6 - 3.0\times 10^{41}/[(\ln r_0)^2 r^6] \\
& -8.7\times 10^{40}/[\eta(\ln r_0)^2 r^6] - 6.5\times 10^{42}\eta/[(\ln r_0)^2 r^6] \\
& +1.7\times 10^{43}\eta^2/[(\ln r_0)^2 r^6] - 2.2\times 10^{41}(\ln r)/[(\ln r_0)^2 r^6] \\
& -1.1\times 10^{42}\eta(\ln r)/[(\ln r_0)^2 r^6] + 9.1\times 10^{43}\eta^2(\ln r)/[(\ln r_0)^2 r^6] \\
& +7.8\times 10^{41}\eta(\ln r)^2/[(\ln r_0)^2 r^6] + 8.9\times 10^{42}\eta^2(\ln r)^2/[(\ln r_0)^2 r^6] \\
& +4.2\times 10^{42}\eta^2(\ln r)^3/[(\ln r_0)^2 r^6] - 1.3\times 10^{41}/[(\ln r_0) r^6] \\
& -5.9\times 10^{41}\eta/[(\ln r_0) r^6] + 1.0\times 10^{43}\eta^2/[(\ln r_0) r^6] \\
& +2.2\times 10^{40}\eta(\ln r)/[(\ln r_0) r^6] + 1.4\times 10^{42}\eta^2(\ln r)/[(\ln r_0) r^6] \\
& -1.9\times 10^{42}\eta^2(\ln r)^2/[(\ln r_0) r^6] + 5.1\times 10^{53}\eta(\ln r_0)/r^6 \\
& -1.4\times 10^{53}\eta^2(\ln r_0)/r^6 - 5.1\times 10^{53}\eta^2(\ln r)(\ln r_0)/r^6 \\
& +2.6\times 10^{53}\eta^2(\ln r_0)^2/r^6 + 0.2/r^4 - 0.2/r^4 - 0.06\eta/r^4 \\
& +0.005\eta^2/r^4 + 0.1\eta(\ln r)/r^4 + 0.1\eta^2(\ln r)/r^4 + 0.04\eta^2(\ln r)^2/r^4
\end{aligned}
$$

$$-3.1 \times 10^{-16}/[(\ln r_0)^2 r^4] - 5.6 \times 10^{-17}/[(\eta(\ln r_0)^2 r^4]$$

$$-5.0 \times 10^{-15}\eta/[(\ln r_0)^2 r^4] - 3.5 \times 10^{-17}(\ln r)/[(\ln r_0)^2 r^4]$$

$$-1.4 \times 10^{-15}\eta(\ln r)/[(\ln r_0)^2 r^4]$$

$$+8.1 \times 10^{-14}\eta^2(\ln r)/[(\ln r_0)^2 r^4]$$

$$-5.9 \times 10^{-17}\eta(\ln r)^2/[(\ln r_0)^2 r^4]$$

$$+1.1 \times 10^{-14}\eta^2(\ln r)^2/[(\ln r_0)^2 r^4]$$

$$-8.0 \times 10^{-16}\eta^2(\ln r)^3/[(\ln r_0)^2 r^4] - 4.9 \times 10^{-17}/[(\ln r_0) r^4]$$

$$-5.0 \times 10^{-16}\eta/[(\ln r_0) r^4] + 1.1 \times 10^{-14}\eta^2/[(\ln r_0) r^4]$$

$$-1.7 \times 10^{-18}\eta(\ln r)/[(\ln r_0) r^4] + 2.5 \times 10^{-15}\eta^2(\ln r)/[(\ln r_0) r^4]$$

$$-3.3 \times 10^{-17}\eta^2(\ln r)^2/[(\ln r_0) r^4] - 0.1\eta(\ln r_0)/r^4$$

$$-0.1\eta^2(\ln r_0)/r^4 - 0.07\eta^2(\ln r)(\ln r_0)/r^4 + 0.04\eta^2(\ln r_0)^2/r^4$$

$$-0.0004(\ln T)/r^4 - 0.0008\eta(\ln T)/r^4 + 0.0001\eta^2(\ln T)/r^4$$

$$+0.002\eta(\ln r)(\ln T)/r^4 + 0.002\eta^2(\ln r)(\ln T)/r^4$$

$$-0.002\eta^2(\ln r)^2(\ln T)/r^4 - 1.1 \times 10^{-16}\eta(\ln T)/[(\ln r_0)^2 r^4]$$

$$-5.6 \times 10^{-18}\eta(\ln r)(\ln T)/[(\ln r_0)^2 r^4]$$

$$+1.3 \times 10^{-15}\eta^2(\ln r)(\ln T)/[(\ln r_0)^2 r^4]$$

$$-2.3 \times 10^{-19}\eta(\ln r)^2(\ln T)/[(\ln r_0)^2 r^4]$$

$$+1.5 \times 10^{-16}\eta^2(\ln r)^2(\ln T)/[(\ln r_0)^2 r^4]$$

$$-2.0 \times 10^{-17}\eta^2(\ln r)^3(\ln T)/[(\ln r_0)^2 r^4]$$

$$-1.5 \times 10^{-18}\eta(\ln T)/[(\ln r_0) r^4] + 1.4 \times 10^{-16}\eta^2(\ln T)/[(\ln r_0) r^4]$$

$$
\begin{aligned}
&-1.2\times10^{-19}\eta(\ln r)(\ln T)/[(\ln r_0)r^4]\\
&+2.5\times10^{-17}\eta^2(\ln r)(\ln T)/[(\ln r_0)r^4]\\
&-2.0\times10^{-18}\eta^2(\ln r)^2(\ln T)/[(\ln r_0)r^4]-0.002\eta(\ln r_0)(\ln T)/r^4\\
&-0.002\eta^2(\ln r_0)(\ln T)/r^4+0.004\eta^2(\ln r)(\ln r_0)(\ln T)/r^4\\
&-0.002\eta^2(\ln r_0)^2(\ln T)/r^4+6.6\times10^{-60}/r^2-8.7\times10^{-60}/r^2\\
&+2.0\times10^{-61}\eta/r^2+8.7\times10^{-60}\eta(\ln r)/r^2\\
&-2.0\times10^{-61}\eta^2(\ln r)/r^2-4.4\times10^{-60}\eta^2(\ln r)^2/r^2\\
&-6.9\times10^{-77}\eta(\ln r)^2/[(\ln r_0)^2r^2]\\
&+8.2\times10^{-76}\eta^2(\ln r)^3/[(\ln r_0)^2r^2]\\
&-3.5\times10^{-77}\eta(\ln r)/[(\ln r_0)r^2]\\
&+2.6\times10^{-76}\eta^2(\ln r)^2/[(\ln r_0)r^2]-8.7\times10^{-60}\eta(\ln r_0)/r^2\\
&+2.0\times10^{-61}\eta^2(\ln r_0)/r^2+8.7\times10^{-60}\eta^2(\ln r)(\ln r_0)/r^2\\
&-4.4\times10^{-60}\eta^2(\ln r_0)^2/r^2+3.2\times10^{-59}T^2+0.01T^2/r^2\\
&-0.01\eta T^2/r^2-0.01\eta(\ln r)T^2/r^2+0.01\eta^2(\ln r)T^2/r^2\\
&+0.007\eta^2(\ln r)^2T^2/r^2+3.1\times10^{-18}\eta(\ln r)^2T^2/[(\ln r_0)^2r^2]\\
&+1.1\times10^{-17}\eta^2(\ln r)^3T^2/[(\ln r_0)^2r^2]\\
&+1.5\times10^{-18}\eta(\ln r)T^2/[(\ln r_0)r^2]\\
&+6.6\times10^{-18}\eta^2(\ln r)^2T^2/[(\ln r_0)r^2]+0.01\eta(\ln r_0)T^2/r^2\\
&-0.01\eta^2(\ln r_0)T^2/r^2-0.01\eta^2(\ln r)(\ln r_0)T^2/r^2\\
&+0.007\eta^2(\ln r_0)^2T^2/r^2-1.2T^4,
\end{aligned}
\tag{F9}
$$

$$
\begin{aligned}
< T_r^r > \;=\; & -0.00003\eta^2(\ln r)^2 + 0.00007\eta^2(\ln r)(\ln r_0) - 0.00003\eta^2(\ln r_0)^2 \\
& -3.2\times 10^{54}/r^8 + 1.6\times 10^{54}/r^8 - 1.6\times 10^{54}\eta(\ln r)/r^8 \\
& +8.1\times 10^{53}\eta^2(\ln r)^2/r^8 + 1.6\times 10^{54}\eta(\ln r_0)/r^8 \\
& -1.6\times 10^{54}\eta^2(\ln r)(\ln r_0)/r^8 + 8.1\times 10^{53}\eta^2(\ln r_0)^2/r^8 \\
& -2.9\times 10^{56}/r^6 + 2.9\times 10^{56}/r^6 + 6.5\times 10^{40}\eta/r^6 \\
& -1.0\times 10^{54}\eta^2/r^6 + 1.1\times 10^{54}\eta(\ln r)/r^6 + 1.3\times 10^{55}\eta^2(\ln r)/r^6 \\
& -3.1\times 10^{55}\eta^2(\ln r)^2/r^6 - 7.0\times 10^{41}/[(\ln r_0)^2 r^6) \\
& -2.2\times 10^{43}\eta/[(\ln r_0)^2 r^6] + 1.7\times 10^{44}\eta^2/[(\ln r_0)^2 r^6] \\
& -4.4\times 10^{40}(\ln r)/[(\ln r_0)^2 r^6] - 3.1\times 10^{42}\eta(\ln r)/[(\ln r_0)^2 r^6] \\
& +3.6\times 10^{44}\eta^2(\ln r)/[(\ln r_0)^2 r^6] \\
& -4.4\times 10^{40}\eta(\ln r)^2/[(\ln r_0)^2 r^6] \\
& +7.4\times 10^{43}\eta^2(\ln r)^2/[(\ln r_0)^2 r^6] \\
& -4.0\times 10^{42}\eta^2(\ln r)^3/[(\ln r_0)^2 r^6] - 4.4\times 10^{40}/[(\ln r_0) r^6] \\
& -1.0\times 10^{4}2\eta/[(\ln r_0) r^6] + 4.3\times 10^{43}\eta^2/[(\ln r_0) r^6] \\
& +1.4\times 10^{43}\eta^2(\ln r)/[(\ln r_0) r^6] + 1.4\times 10^{42}\eta^2(\ln r)^2/[(\ln r_0) r^6] \\
& -1.1\times 10^{54}\eta(\ln r_0)/r^6 - 1.3\times 10^{55}\eta^2(\ln r_0)/r^6 \\
& +6.1\times 10^{55}\eta^2(\ln r)(\ln r_0)/r^6 - 3.1\times 10^{55}\eta^2(\ln r_0)^2/r^6 \\
& +0.02/r^4 - 0.05/r^4 + 0.2\eta/r^4 - 0.3\eta^2/r^4 + 0.1\eta(\ln r)/r^4 \\
& -0.4\eta^2(\ln r)/r^4 - 0.2\eta^2(\ln r)^2/r^4 - 8.9\times 10^{-16}/[(\ln r_0)^2 r^4] \\
& +9.7\times 10^{-17}\eta/[(\ln r_0)^2 r^4] - 3.6\times 10^{-16}(\ln r)/[(\ln r_0)^2 r^4]
\end{aligned}
$$

$$+7.2\times10^{-16}\eta(\ln r)/[(\ln r_0)^2r^4]$$

$$-1.1\times10^{-15}\eta^2(\ln r)/[(\ln r_0)^2r^4]$$

$$+5.6\times10^{-17}\eta(\ln r)^2/[(\ln r_0)^2r^4]$$

$$-9.0\times10^{-15}\eta^2(\ln r)^2/[(\ln r_0)^2r^4]$$

$$+1.5\times10^{-15}\eta^2(\ln r)^3/[(\ln r_0)^2r^4]-3.9\times10^{-16}/[(\ln r_0)r^4]$$

$$+2.2\times10^{-16}\eta/[(\ln r_0)r^4]-1.2\times10^{-16}\eta^2/[(\ln r_0)r^4]$$

$$+2.8\times10^{-17}\eta(\ln r)/[(\ln r_0)r^4]-2.5\times10^{-15}\eta^2(\ln r)/[(\ln r_0)r^4]$$

$$-1.0\times10^{-15}\eta^2(\ln r)^2/[(\ln r_0)r^4]-0.1\eta(\ln r_0)/r^4$$

$$+0.4\eta^2(\ln r_0)/r^4+0.3\eta^2(\ln r)(\ln r_0)/r^4-0.2\eta^2(\ln r_0)^2/r^4$$

$$-0.0004(\ln T)/r^4+0.003\eta(\ln T)/r^4-0.004\eta^2(\ln T)/r^4$$

$$+0.002\eta(\ln r)(\ln T)/r^4-0.005\eta^2(\ln r)(\ln T)/r^4$$

$$-0.002\eta^2(\ln r)^2(\ln T)/r^4+8.7\times10^{-18}\eta(\ln r)(\ln T)/[(\ln r_0)^2r^4]$$

$$+4.2\times10^{-19}\eta(\ln r)^2(\ln T)/[(\ln r_0)^2r^4]$$

$$-2.3\times10^{-16}\eta^2(\ln r)^2(\ln T)/[(\ln r_0)^2r^4$$

$$+4.5\times10^{-17}\eta^2(\ln r)^3(\ln T)/[(\ln r_0)^2r^4]$$

$$+2.6\times10^{-18}\eta(\ln T)/[(\ln r_0)r^4]$$

$$+2.1\times10^{-19}\eta(\ln r)(\ln T)/[(\ln r_0)r^4]$$

$$-4.3\times10^{-17}\eta^2(\ln r)(\ln T)/[(\ln r_0)r^4]$$

$$+4.5\times10^{-18}\eta^2(\ln r)^2(\ln T)/[(\ln r_0)r^4]-0.002\eta(\ln r_0)(\ln T)/r^4$$

$$+0.005\eta^2(\ln r_0)(\ln T)/r^4+0.004\eta^2(\ln r)(\ln r_0)(\ln T)/r^4$$

$$
\begin{aligned}
&-0.002\eta^2(\ln r_0)^2(\ln T)/r^4 + 0.02/r^3 - 0.02/r^3 + 0.0008\eta/r^3 \\
&+0.01\eta(\ln r)/r^3 - 0.0004\eta^2(\ln r)/r^3 - 0.002\eta^2(\ln r)^2/r^3 \\
&-4.3\times 10^{-19}\eta(\ln r)^2/[(\ln r_0)^2 r^3] \\
&-7.5\times 10^{-18}\eta^2(\ln r)^3/[(\ln r_0)^2 r^3] \\
&-2.2\times 10^{-19}\eta(\ln r)/[(\ln r_0) r^3] - 1.2\times 10^{-18}\eta^2(\ln r)^2/[(\ln r_0) r^3] \\
&-0.01\eta(\ln r_0)/r^3 + 0.0004\eta^2(\ln r_0)/r^3 + 0.004\eta^2(\ln r)(\ln r_0)/r^3 \\
&-0.002\eta^2(\ln r_0)^2/r^3 - 0.004/r^2 + 0.004/r^2 - 0.002\eta(\ln r)/r^2 \\
&-0.0004\eta^2(\ln r)/r^2 - 0.002\eta^2(\ln r)^2/r^2 \\
&+2.2\times 10^{-19}\eta(\ln r)^2/[(\ln r_0)^2 r^2] \\
&+1.0\times 10^{-17}\eta^2(\ln r)^3/[(\ln r_0)^2 r^2] \\
&+1.1\times 10^{-19}\eta(\ln r)/[(\ln r_0) r^2] + 1.6\times 10^{-18}\eta^2(\ln r)^2/[(\ln r_0) r^2] \\
&+0.002\eta(\ln r_0)/r^2 + 0.0004\eta^2(\ln r_0)/r^2 + 0.003\eta^2(\ln r)(\ln r_0)/r^2 \\
&-0.002\eta^2(\ln r_0)^2/r^2 - 6.8\times 10^{-21}\eta/r + 0.0001\eta^2(\ln r)/r \\
&+0.0005\eta^2(\ln r)^2/r - 5.4\times 10^{-20}\eta(\ln r)^2/[(\ln r_0)^2 r] \\
&-2.5\times 10^{-18}\eta^2(\ln r)^3/[(\ln r_0)^2 r] - 2.7\times 10^{-20}\eta(\ln r)/[(\ln r_0) r] \\
&-4.1\times 10^{-19}\eta^2(\ln r)^2/[(\ln r_0) r] - 0.0001\eta^2(\ln r_0)/r \\
&-0.001\eta^2(\ln r)(\ln r_0)/r + 0.0005\eta^2(\ln r_0)^2/r - 3.2\times 10^{-59}T^2 \\
&-0.01T^2/r^2 + 0.01\eta(\ln r)T^2/r^2 - 0.007\eta^2(\ln r)^2T^2/r^2 \\
&-0.01\eta(\ln r_0)T^2/r^2 + 0.01\eta^2(\ln r)(\ln r_0)T^2/r^2 \\
&-0.007\eta^2(\ln r_0)^2T^2/r^2 + 0.4T^4. \qquad \text{(F10)}
\end{aligned}
$$

Setting $r = r_0$ in Eqs. (F9) and (F10), we obtain the expressions of the stress-energy tensor components of a quantized neutrino field at the throat of the wormhole (in units of F_p/l_p^2):

$$
\begin{aligned}
< T_t^t >_0 \;=\; & 3.2\times 10^{54}/r_0^8 - 1.6\times 10^{54}/r_0^8 - 2.2\times 10^{54}/r_0^6 - 3.6\times 10^{54}/r_0^6 \\
& -1.4\times 10^{53}\eta/r_0^6 + 9.2\times 10^{42}\eta^2/r_0^6 - 3.0\times 10^{41}/[(\ln r_0)^2 r_0^6] \\
& -8.7\times 10^{40}/[\eta(\ln r_0)^2 r_0^6] - 6.5\times 10^{42}\eta/[(\ln r_0)^2 r_0^6] \\
& +1.7\times 10^{43}\eta^2/[(\ln r_0)^2 r_0^6] - 3.5\times 10^{41}/[(\ln r_0) r_0^6] \\
& -1.7\times 10^{42}\eta/[(\ln r_0) r_0^6] + 1.0\times 10^{44}\eta^2/[(\ln r_0) r_0^6] \\
& +1.2\times 10^{42}\eta^2(\ln r_0)/r_0^6 - 0.06\eta/r_0^4 + 0.005\eta^2/r_0^4 \\
& -3.1\times 10^{-16}/[(\ln r_0)^2 r_0^4] - 5.6\times 10^{-17}/[\eta(\ln r_0)^2 r_0^4] \\
& -5.0\times 10^{-15}\eta/[(\ln r_0)^2 r_0^4] - 8.3\times 10^{-17}/[(\ln r_0) r_0^4] \\
& -1.9\times 10^{-15}\eta/[(\ln r_0) r_0^4] + 9.2\times 10^{-14}\eta^2/[(\ln r_0) r_0^4] \\
& -7.5\times 10^{-16}\eta^2(\ln r_0)/r_0^4 - 0.0004(\ln T)/r_0^4 - 0.0008\eta(\ln T)/r_0^4 \\
& +0.0001\eta^2(\ln T)/r_0^4 - 1.1\times 10^{-16}\eta(\ln T)/[(\ln r_0)^2 r_0^4] \\
& -7.2\times 10^{-18}\eta(\ln T)/[(\ln r_0) r_0^4] + 1.4\times 10^{-15}\eta^2(\ln T)/[(\ln r_0) r_0^4] \\
& -1.9\times 10^{-17}\eta^2(\ln r_0)(\ln T)/r_0^4 + 6.6\times 10^{-60}/r_0^2 \\
& -8.7\times 10^{-60}/r_0^2 + 2.0\times 10^{-61}\eta/r_0^2 + 1.0\times 10^{-75}\eta^2(\ln r_0)/r_0^2 \\
& +3.2\times 10^{-59}T^2 + 0.01T^2/r_0^2 - 0.01\eta T^2/r_0^2 \\
& +1.2\times 10^{-17}\eta^2(\ln r_0)T^2/r_0^2 - 1.2T^4, \qquad \text{(F11)}
\end{aligned}
$$

$$
\begin{aligned}
< T_r^r >_0 \;=\; & -3.2\times 10^{54}/r_0^8 + 1.6\times 10^{54}/r_0^8 + 2.2\times 10^{40}\eta/r_0^6 \\
& -1.0\times 10^{54}\eta^2/r_0^6 - 7.0\times 10^{41}/[(\ln r_0)^2 r_0^6] \\
& -2.2\times 10^{43}\eta/[(\ln r_0)^2 r_0^6] + 1.7\times 10^{44}\eta^2/[(\ln r_0)^2 r_0^6] \\
& -8.7\times 10^{40}/[(\ln r_0) r_0^6] - 4.2\times 10^{42}\eta/[(\ln r_0) r_0^6] \\
& +4.1\times 10^{44}\eta^2/[(\ln r_0) r_0^6] - 1.8\times 10^{42}\eta^2(\ln r_0)/r_0^6 + 0.02/r_0^4 \\
& -0.05/r_0^4 + 0.2\eta/r_0^4 - 0.3\eta^2/r_0^4 - 8.9\times 10^{-16}/[(\ln r_0)^2 r_0^4] \\
& +9.7\times 10^{-17}\eta/[(\ln r_0)^2 r_0^4] - 7.5\times 10^{-16}/[(\ln r_0) r_0^4] \\
& +9.4\times 10^{-16}\eta/[(\ln r_0) r_0^4] - 1.2\times 10^{-15}\eta^2/[(\ln r_0) r_0^4] \\
& +2.2\times 10^{-16}\eta^2(\ln r_0)/r_0^4 - 0.0004(\ln T)/r_0^4 + 0.003\eta(\ln T)/r_0^4 \\
& -0.004\eta^2(\ln T)/r_0^4 + 1.1\times 10^{-17}\eta(\ln T)/[(\ln r_0) r_0^4] \\
& +4.4\times 10^{-17}\eta^2(\ln r_0)(\ln T)/r_0^4 + 0.0008\eta/r_0^3 \\
& -8.8\times 10^{-18}\eta^2(\ln r_0)/r_0^3 + 3.3\times 10^{-19}\eta/r_0^2 \\
& +1.2\times 10^{-17}\eta^2(\ln r_0)/r_0^2 - 8.8\times 10^{-20}\eta/r_0 \\
& -2.9\times 10^{-18}\eta^2(\ln r_0)/r_0 - 3.2\times 10^{-59}T^2 - 0.01T^2/r_0^2 \\
& +0.4T^4 \qquad \text{(F12)}
\end{aligned}
$$

F.2.2 Quantized proton field

The stress-energy tensor components of a quantized proton field in the entire spacetime for the wormhole with finite radial cutoff of stress-energy tensor in thermal states are computed to be (in units of F_p/l_p^2):

$$
\begin{aligned}
< T_t^t > \;=\; & 2.1 \times 10^{35}/r^8 - 1.1 \times 10^{35}/r^8 + 1.1 \times 10^{35}\eta(\ln r)/r^8 \\
& -5.3 \times 10^{34}\eta^2(\ln r)^2/r^8 - 1.1 \times 10^{35}\eta(\ln r_0)/r^8 \\
& +1.1 \times 10^{35}\eta^2(\ln r)(\ln r_0)/r^8 - 5.3 \times 10^{34}\eta^2(\ln r_0)^2/r^8 \\
& -1.4 \times 10^{35}/r^6 - 2.4 \times 10^{35}/r^6 - 9.0 \times 10^{33}\eta/r^6 \\
& -2.1 \times 10^{22}\eta^2/r^6 - 3.4 \times 10^{34}\eta(\ln r)/r^6 + 9.0 \times 10^{33}\eta^2(\ln r)/r^6 \\
& +1.7 \times 10^{34}\eta^2(\ln r)^2/r^6 - 2.4 \times 10^{22}/[(\ln r_0)^2 r^6] \\
& -4.2 \times 10^{23}\eta/[(\ln r_0)^2 r^6] + 1.2 \times 10^{24}\eta^2/[(\ln r_0)^2 r^6] \\
& +1.4 \times 10^{22}(\ln r)/[(\ln r_0)^2 r^6] - 2.1 \times 10^{22}\eta(\ln r)/[(\ln r_0)^2 r^6] \\
& +5.8 \times 10^{24}\eta^2(\ln r)/[(\ln r_0)^2 r^6] + 2.4 \times 10^{21}\eta(\ln r)^2/[(\ln r_0)^2 r^6] \\
& +3.4 \times 10^{23}\eta^2(\ln r)^2/[(\ln r_0)^2 r^6] \\
& -1.9 \times 10^{23}\eta^2(\ln r)^3)/[(\ln r_0)^2 r^6] + 9.4 \times 10^{21}/[(\ln r_0) r^6] \\
& -2.1 \times 10^{22}\eta/[(\ln r_0) r^6] + 6.0 \times 10^{23}\eta^2/[(\ln r_0) r^6] \\
& +1.2 \times 10^{21}\eta(\ln r)/[(\ln r_0) r^6] + 1.4 \times 10^{23}\eta^2(\ln r)/[(\ln r_0) r^6] \\
& -7.0 \times 10^{22}\eta^2(\ln r)^2/[(\ln r_0) r^6] + 3.4 \times 10^{34}\eta(\ln r_0)/r^6 \\
& -9.0 \times 10^{33}\eta^2(\ln r_0)/r^6 - 3.4 \times 10^{34}\eta^2(\ln r)(\ln r_0)/r^6 \\
& +1.7 \times 10^{34}\eta^2(\ln r_0)^2/r^6 - 0.04\eta/r^4 + 0.003\eta^2/r^4 \\
& +0.08\eta(\ln r)/r^4 + 0.06\eta^2(\ln r)/r^4 + 0.08\eta^2(\ln r)^2/r^4 \\
& +1.2 \times 10^{-16}/[(\ln r_0)^2 r^4] - 5.3 \times 10^{-15}\eta/[(\ln r_0)^2 r^4] \\
& -2.1 \times 10^{-17}(\ln r)/[(\ln r_0)^2 r^4] - 1.7 \times 10^{-16}\eta(\ln r)/[(\ln r_0)^2 r^4]
\end{aligned}
$$

$$+6.1 \times 10^{-14}\eta^2(\ln r)/[(\ln r_0)^2 r^4]$$

$$+1.7 \times 10^{-18}\eta(\ln r)^2/[(\ln r_0)^2 r^4]$$

$$+6.6 \times 10^{-15}\eta^2(\ln r)^2/[(\ln r_0)^2 r^4]$$

$$+4.8 \times 10^{-17}\eta^2(\ln r)^3/[(\ln r_0)^2 r^4] - 1.4 \times 10^{-17}/[(\ln r_0) r^4]$$

$$-2.4 \times 10^{-16}\eta/[(\ln r_0) r^4] + 7.5 \times 10^{-15}\eta^2/[(\ln r_0) r^4]$$

$$+8.7 \times 10^{-19}\eta(\ln r)/[(\ln r_0) r^4] + 1.3 \times 10^{-15}\eta^2(\ln r)/[(\ln r_0) r^4]$$

$$-3.4 \times 10^{-17}\eta^2(\ln r)^2/[(\ln r_0) r^4] - 0.08\eta(\ln r_0)/r^4$$

$$-0.06\eta^2(\ln r_0)/r^4 - 0.2\eta^2(\ln r)(\ln r_0)/r^4 + 0.08\eta^2(\ln r_0)^2/r^4$$

$$-0.0004(\ln T)/r^4 - 0.0008\eta(\ln T)/r^4 + 0.0001\eta^2(\ln T)/r^4$$

$$+0.002\eta(\ln r)(\ln T)/r^4 + 0.002\eta^2(\ln r)(\ln T)/r^4$$

$$-0.002\eta^2(\ln r)^2(\ln T)/r^4 - 1.1 \times 10^{-16}\eta(\ln T)/[(\ln r_0)^2 r^4]$$

$$-5.6 \times 10^{-18}\eta(\ln r)(\ln T)/[(\ln r_0)^2 r^4]$$

$$+1.3 \times 10^{-15}\eta^2(\ln r)(\ln T)/[(\ln r_0)^2 r^4)$$

$$-2.3 \times 10^{-19}\eta(\ln r)^2(\ln T)/[(\ln r_0)^2 r^4]$$

$$+1.5 \times 10^{-16}\eta^2(\ln r)^2(\ln T)/[(\ln r_0)^2 r^4]$$

$$-2.0 \times 10^{-17}\eta^2(\ln r)^3(\ln T)/[(\ln r_0)^2 r^4]$$

$$-1.5 \times 10^{-18}\eta(\ln T)/[(\ln r_0) r^4] + 1.4 \times 10^{-16}\eta^2(\ln T)/[(\ln r_0) r^4]$$

$$-1.2 \times 10^{-19}\eta(\ln r)(\ln T)/[(\ln r_0) r^4]$$

$$+2.5 \times 10^{-17}\eta^2(\ln r)(\ln T)/[(\ln r_0) r^4]$$

$$-2.0 \times 10^{-18}\eta^2(\ln r)^2(\ln T)/[(\ln r_0) r^4] - 0.002\eta(\ln r_0)(\ln T)/r^4$$

$$
\begin{aligned}
& -0.002\eta^2(\ln r_0)(\ln T)/r^4 + 0.004\eta^2(\ln r)(\ln r_0)(\ln T)/r^4 \\
& -0.002\eta^2(\ln r_0)^2(\ln T)/r^4 + 1.0\times 10^{-40}/r^2 - 1.3\times 10^{-40}/r^2 \\
& +3.1\times 10^{-42}\eta/r^2 + 1.3\times 10^{-40}\eta(\ln r)/r^2 \\
& -3.1\times 10^{-42}\eta^2(\ln r)/r^2 - 6.7\times 10^{-41}\eta^2(\ln r)^2/r^2 \\
& -6.4\times 10^{-58}\eta(\ln r)^2/[(\ln r_0)^2 r^2] \\
& +3.2\times 10^{-57}\eta^2(\ln r)^3/[(\ln r_0)^2 r^2] \\
& -3.2\times 10^{-58}\eta(\ln r)/[(\ln r_0) r^2] + 1.9\times 10^{-57}\eta^2(\ln r)^2/[(\ln r_0) r^2] \\
& -1.3\times 10^{-40}\eta(\ln r_0)/r^2 + 3.1\times 10^{-42}\eta^2(\ln r_0)/r^2 \\
& +1.3\times 10^{-40}\eta^2(\ln r)(\ln r_0)/r^2 - 6.7\times 10^{-41}\eta^2(\ln r_0)^2/r^2 \\
& +4.9\times 10^{-40}T^2 + 0.01T^2/r^2 - 0.01\eta T^2/r^2 - 0.01\eta(\ln r)T^2/r^2 \\
& +0.01\eta^2(\ln r)T^2/r^2 + 0.007\eta^2(\ln r)^2T^2/r^2 \\
& +3.1\times 10^{-18}\eta(\ln r)^2T^2/[(\ln r_0)^2 r^2] \\
& +1.1\times 10^{-17}\eta^2(\ln r)^3T^2/[(\ln r_0)^2 r^2] \\
& +1.5\times 10^{-18}\eta(\ln r)T^2/[(\ln r_0) r^2] \\
& +6.6\times 10^{-18}\eta^2(\ln r)^2T^2/[(\ln r_0) r^2] + 0.01\eta(\ln r_0)T^2/r^2 \\
& -0.01\eta^2(\ln r_0)T^2/r^2 - 0.01\eta^2(\ln r)(\ln r_0)T^2/r^2 \\
& +0.007\eta^2(\ln r_0)^2T^2/r^2 - 1.2T^4, \qquad \text{(F13)}
\end{aligned}
$$

$$
\begin{aligned}
< T^r_r > \;=\; & -0.00003\eta^2(\ln r)^2 + 0.00007\eta^2(\ln r)(\ln r_0) - 0.00003\eta^2(\ln r_0)^2 \\
& -2.1\times 10^{35}/r^8 + 1.1\times 10^{35}/r^8 - 1.1\times 10^{35}\eta(\ln r)/r^8
\end{aligned}
$$

$$+5.3 \times 10^{34}\eta^2(\ln r)^2/r^8 + 1.1 \times 10^{35}\eta(\ln r_0)/r^8$$

$$-1.1 \times 10^{35}\eta^2(\ln r)(\ln r_0)/r^8 + 5.3 \times 10^{34}\eta^2(\ln r_0)^2/r^8$$

$$-1.9 \times 10^{37}/r^6 + 1.9 \times 10^{37}/r^6 - 6.7 \times 10^{34}\eta^2/r^6$$

$$+6.9 \times 10^{34}\eta(\ln r)/r^6 + 8.2 \times 10^{35}\eta^2(\ln r)/r^6$$

$$-2.0 \times 10^{36}\eta^2(\ln r)^2/r^6 + 7.6 \times 10^{22}/[(\ln r_0)^2 r^6]$$

$$-1.8 \times 10^{24}\eta/[(\ln r_0)^2 r^6] + 1.1 \times 10^{25}\eta^2/[(\ln r_0)^2 r^6]$$

$$-9.4 \times 10^{22}\eta(\ln r)/[(\ln r_0)^2 r^6] + 2.3 \times 10^{25}\eta^2(\ln r)/[(\ln r_0)^2 r^6]$$

$$-2.4 \times 10^{21}\eta(\ln r)^2/[(\ln r_0)^2 r^6]$$

$$+5.2 \times 10^{24}\eta^2(\ln r)^2/[(\ln r_0)^2 r^6]$$

$$+5.0 \times 10^{23}\eta^2(\ln r)^3/[(\ln r_0)^2 r^6] + 3.8 \times 10^{22}\eta/[(\ln r_0) r^6]$$

$$+2.6 \times 10^{24}\eta^2/[(\ln r_0) r^6] - 1.2 \times 10^{21}\eta(\ln r)/[(\ln r_0) r^6]$$

$$+1.2 \times 10^{24}\eta^2(\ln r)/[(\ln r_0) r^6] + 2.1 \times 10^{23}\eta^2(\ln r)^2/[(\ln r_0) r^6]$$

$$-6.9 \times 10^{34}\eta(\ln r_0)/r^6 - 8.2 \times 10^{35}\eta^2(\ln r_0)/r^6$$

$$+4.0 \times 10^{36}\eta^2(\ln r)(\ln r_0)/r^6 - 2.0 \times 10^{36}\eta^2(\ln r_0)^2/r^6$$

$$+0.02/r^4 - 0.003(\ln T)/[(\ln r_0) r^4] - 0.04/r^4 + 0.1\eta/r^4$$

$$-0.2\eta^2/r^4 + 0.1\eta(\ln r)/r^4 - 0.3\eta^2(\ln r)/r^4 - 0.1\eta^2(\ln r)^2/r^4$$

$$-2.2 \times 10^{-16}/[(\ln r_0)^2 r^4] + 9.7 \times 10^{-17}\eta/[(\ln r_0)^2 r^4]$$

$$+1.1 \times 10^{-16}(\ln r)/[(\ln r_0)^2 r^4] - 1.1 \times 10^{-16}\eta(\ln r)/[(\ln r_0)^2 r^4]$$

$$-1.1 \times 10^{-15}\eta^2(\ln r)/[(\ln r_0)^2 r^4]$$

$$+3.1 \times 10^{-16}\eta(\ln r)^2/[(\ln r_0)^2 r^4]$$

$$-6.0 \times 10^{-15}\eta^2(\ln r)^2/[(\ln r_0)^2 r^4]$$

$$+6.3 \times 10^{-15}\eta^2(\ln r)^3/[(\ln r_0)^2 r^4] - 3.3 \times 10^{-16}\eta/[(\ln r_0) r^4]$$

$$-1.2 \times 10^{-16}\eta^2/[(\ln r_0) r^4] + 2.8 \times 10^{-17}\eta(\ln r)/[(\ln r_0) r^4]$$

$$-2.1 \times 10^{-15}\eta^2(\ln r)/[(\ln r_0) r^4]$$

$$+7.0 \times 10^{-16}\eta^2(\ln r)^2/[(\ln r_0) r^4] - 0.1\eta(\ln r_0)/r^4$$

$$+0.3\eta^2(\ln r_0)/r^4 + 0.2\eta^2(\ln r)(\ln r_0)/r^4 - 0.1\eta^2(\ln r_0)^2/r^4$$

$$-0.0004(\ln T)/r^4 + 0.003\eta(\ln T)/r^4 - 0.004\eta^2(\ln T)/r^4$$

$$+0.002\eta(\ln r)(\ln T)/r^4 - 0.005\eta^2(\ln r)(\ln T)/r^4$$

$$-0.002\eta^2(\ln r)^2(\ln T)/r^4 + 8.7 \times 10^{-18}\eta(\ln r)(\ln T)/[(\ln r_0)^2 r^4]$$

$$+4.2 \times 10^{-19}\eta(\ln r)^2(\ln T)/[(\ln r_0)^2 r^4]$$

$$-2.3 \times 10^{-16}\eta^2(\ln r)^2(\ln T)/[(\ln r_0)^2 r^4]$$

$$+4.5 \times 10^{-17}\eta^2(\ln r)^3(\ln T)/[(\ln r_0)^2 r^4] + 0.003(\ln T)/[(\ln r_0) r^4]$$

$$+2.6 \times 10^{-18}\eta(\ln T)/[(\ln r_0) r^4]$$

$$+2.1 \times 10^{-19}\eta(\ln r)(\ln T)/[(\ln r_0) r^4]$$

$$-4.3 \times 10^{-17}\eta^2(\ln r)(\ln T)/[(\ln r_0) r^4]$$

$$+4.5 \times 10^{-18}\eta^2(\ln r)^2(\ln T)/[(\ln r_0) r^4] - 0.002\eta(\ln r_0)(\ln T)/r^4$$

$$+0.005\eta^2(\ln r_0)(\ln T)/r^4 + 0.004\eta^2(\ln r)(\ln r_0)(\ln T)/r^4$$

$$-0.002\eta^2(\ln r_0)^2(\ln T)/r^4 + 0.0008\eta/r^3 + 0.01\eta(\ln r)/r^3$$

$$-0.0004\eta^2(\ln r)/r^3 - 0.002\eta^2(\ln r)^2/r^3$$

$$-4.3 \times 10^{-19}\eta(\ln r)^2/[(\ln r_0)^2 r^3]$$

$$
\begin{aligned}
&-7.5\times10^{-18}\eta^2(\ln r)^3/[(\ln r_0)^2r^3]\\
&-2.2\times10^{-19}\eta(\ln r)/[(\ln r_0)r^3]-1.2\times10^{-18}\eta^2(\ln r)^2/[(\ln r_0)r^3]\\
&-0.01\eta(\ln r_0)/r^3+0.0004\eta^2(\ln r_0)/r^3+0.004\eta^2(\ln r)(\ln r_0)/r^3\\
&-0.002\eta^2(\ln r_0)^2/r^3-0.002\eta(\ln r)/r^2\\
&-0.0004\eta^2(\ln r)/r^2-0.002\eta^2(\ln r)^2/r^2\\
&+2.2\times10^{-19}\eta(\ln r)^2/[(\ln r_0)^2r^2]\\
&+1.0\times10^{-17}\eta^2(\ln r)^3)/[(\ln r_0)^2r^2]\\
&+1.1\times10^{-19}\eta(\ln r)/[(\ln r_0)r^2]+1.6\times10^{-18}\eta^2(\ln r)^2/[(\ln r_0)r^2]\\
&+0.002\eta(\ln r_0)/r^2+0.0004\eta^2(\ln r_0)/r^2+0.003\eta^2(\ln r)(\ln r_0)/r^2\\
&-0.002\eta^2(\ln r_0)^2/r^2-6.8\times10^{-21}\eta/r+0.0001\eta^2(\ln r)/r\\
&+0.0005\eta^2(\ln r)^2/r-5.4\times10^{-20}\eta(\ln r)^2/[(\ln r_0)^2r]\\
&-2.5\times10^{-18}\eta^2(\ln r)^3/[(\ln r_0)^2r]-2.7\times10^{-20}\eta(\ln r)/[(\ln r_0)r]\\
&-4.1\times10^{-19}\eta^2(\ln r)^2/[(\ln r_0)r]-0.0001\eta^2(\ln r_0)/r\\
&-0.001\eta^2(\ln r)(\ln r_0)/r+0.0005\eta^2(\ln r_0)^2/r-4.9\times10^{-40}T^2\\
&-0.01T^2/r^2+0.01\eta(\ln r)T^2/r^2-0.007\eta^2(\ln r)^2T^2/r^2\\
&-0.01\eta(\ln r_0)T^2/r^2+0.01\eta^2(\ln r)(\ln r_0)T^2/r^2\\
&-0.007\eta^2(\ln r_0)^2T^2/r^2+0.4T^4. \qquad \text{(F14)}
\end{aligned}
$$

Setting $r = r_0$ in Eqs. (F13) and (F14), we obtain the stress-energy tensor components of a quantized proton field at the throat of the wormhole (in units of F_p/l_p^2):

$$
\begin{aligned}
< T_t^t >_0 \;=\;& 1.0\times 10^{35}/r_0^8 - 3.8\times 10^{35}/r_0^6 - 9.0\times 10^{33}\eta/r_0^6 \\
& +4.6\times 10^{23}\eta^2/r_0^6 - 2.4\times 10^{22}/[(\ln r_0)^2 r_0^6] \\
& -4.2\times 10^{23}\eta/[(\ln r_0)^2 r_0^6] + 1.2\times 10^{24}\eta^2/[(\ln r_0)^2 r_0^6] \\
& +2.4\times 10^{22}/[(\ln r_0) r_0^6] - 4.3\times 10^{22}\eta/[(\ln r_0) r_0^6] \\
& +6.4\times 10^{24}\eta^2/[(\ln r_0) r_0^6] - 3.0\times 10^{23}\eta^2(\ln r_0)/r_0^6 - 0.04\eta/r_0^4 \\
& +0.003\eta^2/r_0^4 + 1.2\times 10^{-16}/[(\ln r_0)^2 r_0^4] \\
& -5.3\times 10^{-15}\eta/[(\ln r_0)^2 r_0^4] - 3.5\times 10^{-17}/[(\ln r_0) r_0^4] \\
& -4.0\times 10^{-16}\eta/[(\ln r_0) r_0^4] + 6.9\times 10^{-14}\eta^2/[(\ln r_0) r_0^4] \\
& +4.2\times 10^{-17}\eta^2(\ln r_0)/r_0^4 - 0.0004(\ln T)/r_0^4 - 0.0008\eta(\ln T)/r_0^4 \\
& +0.0001\eta^2(\ln T)/r_0^4 - 1.1\times 10^{-16}\eta(\ln T)/[(\ln r_0)^2 r_0^4] \\
& -7.2\times 10^{-18}\eta(\ln T)/[(\ln r_0) r_0^4] \\
& +1.4\times 10^{-15}\eta^2(\ln T)/[(\ln r_0) r_0^4] - 1.9\times 10^{-17}\eta^2(\ln r_0)(\ln T)/r_0^4 \\
& +1.0\times 10^{-40}/r_0^2 - 1.3\times 10^{-40}/r_0^2 + 3.1\times 10^{-42}\eta/r_0^2 \\
& +5.7\times 10^{-57}\eta^2(\ln r_0)/r_0^2 + 4.9\times 10^{-40}T^2 + 0.01T^2/r_0^2 \\
& -0.01\eta T^2/r_0^2 + 1.2\times 10^{-17}\eta^2(\ln r_0)T^2/r_0^2 - 1.2T^4, \qquad \text{(F15)}
\end{aligned}
$$

$$
\begin{aligned}
< T_r^r >_0 \;=\;& -1.0\times 10^{35}/r_0^8 - 3.5\times 10^{21}\eta/r_0^6 - 6.7\times 10^{34}\eta^2/r_0^6 \\
& +7.6\times 10^{22}/[(\ln r_0)^2 r_0^6] - 1.8\times 10^{24}\eta/[(\ln r_0)^2 r_0^6]
\end{aligned}
$$

$$
\begin{aligned}
&+1.1\times10^{25}\eta^2/[(\ln r_0)^2 r_0^6] - 5.7\times10^{22}\eta/[(\ln r_0) r_0^6] \\
&+2.5\times10^{25}\eta^2/[(\ln r_0) r_0^6] + 7.6\times10^{23}\eta^2(\ln r_0)/r_0^6 + 0.02/r_0^4 \\
&-0.003(\ln T)/[(\ln r_0) r_0^4] - 0.04/r_0^4 + 0.1\eta/r_0^4 - 0.2\eta^2/r_0^4 \\
&-2.2\times10^{-16}/[(\ln r_0)^2 r_0^4] + 9.7\times10^{-17}\eta/[(\ln r_0)^2 r_0^4] \\
&+1.1\times10^{-16}/[(\ln r_0) r_0^4] - 4.4\times10^{-16}\eta/[(\ln r_0) r_0^4] \\
&-1.2\times10^{-15}\eta^2/[(\ln r_0) r_0^4] + 7.0\times10^{-15}\eta^2(\ln r_0)/r_0^4 \\
&-0.0004(\ln T)/r_0^4 + 0.003\eta(\ln T)/r_0^4 - 0.004\eta^2(\ln T)/r_0^4 \\
&+0.003(\ln T)/[(\ln r_0) r_0^4] + 1.1\times10^{-17}\eta(\ln T)/[(\ln r_0) r_0^4 \\
&+4.4\times10^{-17}\eta^2(\ln r_0)(\ln T)/r_0^4 + 0.0008\eta/r_0^3 \\
&-8.8\times10^{-18}\eta^2(\ln r_0)/r_0^3 - 0.008/r_0^2 + 3.3\times10^{-19}\eta/r_0^2 \\
&+1.2\times10^{-17}\eta^2(\ln r_0)/r_0^2 - 8.8\times10^{-20}\eta/r_0 \\
&-2.9\times10^{-18}\eta^2(\ln r_0)/r_0 - 4.9\times10^{-40}T^2 - 0.01T^2/r_0^2 \\
&+0.4T^4. \qquad \text{(F16)}
\end{aligned}
$$

BIBLIOGRAPHY

[1] A. Einstein and N. Rosen. The particle problem in the general theory of relativity. *Phys. Rev.*, 48:73, 1935.

[2] R.W. Fuller and J.A. Wheeler. *Phys. Rev.*, 128:919, 1962.

[3] J.A. Wheeler. *Geometrodynamics*. Academic Press, 1962.

[4] R.P. Geroch. Topology in General Relativity. *J. Math. Phys*. 8:782, 1967.

[5] M.S. Morris and K.S. Thorne. Wormholes in spacetime and their use for interstellar travel: a tool for teaching general relativity. *Am. J. Phys.*, 56:395, 1988.

[6] S.W. Hawking and G.F.R. Ellis. *The Large Scale Structure of Space-time*. Cambridge University Press, 1973.

[7] G.L. Klimchitskaya, U. Mohideen, V.M. Mostepanenko. The Casimir force between real materials: experiment and theory. *Rev. Mod. Phys.* v.81, N4:1827, 2009 [arXiv:0902.4022].

[8] B. E. Taylor, W. A. Hiscock, and P. R. Anderson. *Phys. Rev. D* 55:6116, 1997.

[9] W. H. Hirsch, Ph.D. thesis, Wake Forest University, 2009.

[10] C. Barcelo, and M. Visser, *Phys. Lett. B* 466:127, 1999.

[11] D. Hochberg, A. Popov, and S. N. Sushkov, *Phys. Rev. Lett.*, 78:2050, 1997.

[12] R. Garattini. Self Sustained Traversable Wormholes? *Class. Quant. Grav*. 221105-1118, 2005 [arXiv:gr-qc/0501105].

[13] L.H. Ford and T.A. Roman. Averaged energy conditions and quantum inequalities.

Phys. Rev. D 51:4277, 1995 [arXiv:gr-qc/9410043].

[14] M.J. Pfenning, L.H. Ford. Quantum inequalities on the energy density in static Robertson-Walker spacetimes. *Phys. Rev. D* 55:4813, 1997.

[15] L.H. Ford and T.A. Roman. Averaged energy conditions and quantum inequalities. *Phys. Rev. D* 51:4277, 1995 [arXiv:gr-qc/9410043].

[16] S. V. Krasnikov, arXiv:gr-qc/0003092 **v1**, 2000.

[17] S. V. Krasnikov, *Phys. Rev. D* 62:084028, 2000.

[18] O.B. Zaslavskii. Exactly solvable model of wormhole supported by phantom energy. *Phys. Rev. D* 72:061303, 2005 [arXiv:gr-qc/0508057].

[19] S. Sushkov. Wormholes supported by a phantom energy. *Phys. Rev. D* 71: 043520, 2005 [arXiv:gr-qc/0502084].

[20] F.S.N. Lobo. Phantom energy traversable wormholes. *Phys. Rev. D* 71:084011, 2005 [arXiv:gr-qc/0502099].

[21] P.F. Gonzalez-Diaz. Wormholes and ringholes in the dark-energy universe. *Phys. Rev. D* 68:084016, 2003 [arXiv:astro-ph/0308382].

[22] R.M. Wald. *Quantum Field Theory in Curved Spacetime and Black Hole Thermodynamics*. The University of Chicago Press, 1994.

[23] N.D. Birrell and P.C.W. Davies. *Quantum Fields in Curved Space*. Cambridge University Press, 1982.

[24] L.E. Parker and D.J. Toms. *Quantum Field Theory in Curved Spacetime*. Cambridge University Press, 2009.

[25] P. B. Groves, P. R. Anderson, and E. D. Carlson, *Phys. Rev. D* 66:124017, 2002.

[26] S.M. Christensen and S.A. Fulling, *Phys. Rev. D* 15:2088, 1977.

[27] F.D. Mazzitelli and C.O. Lousto, *Phys. Rev. D* 43:468, 1991.

[28] D.N. Page, Phys. Rev. D 25:1499, 1982.

[29] K.W. Howard and P. Candelas, *Phys. Rev. Lett*. 53:403, 1984.

[30] B.S. DeWitt, in *Relativity, Groups and Topology*, edited by B.S. DeWitt and C. DeWitt. Gordon and Breach, New York, 1965; B.S. DeWitt, *Phys. Rep.* 9:295, 1975.

[31] V.P. Frolov and A.I. Zel'nikov, *Phys. Lett.* 115B:372, 1982.

[32] P.R. Anderson, W.A. Hiscock, and D.A. Samuel, *Phys. Rev. Lett.* 70:1739, 1993; *Phys. Rev. D* 51:4337, 1995.

[33] J. Matyjasek, *Phys. Rev. D* 63:084004, 2001.

[34] P. Candelas, *Phys. Rev. D* 21:2185, 1980.

[35] M.S. Fawcett, *Commun. Math. Phys.* 89:103, 1983.

[36] J.S. Dowker and R. Critchley, *Phys. Rev. D* 13:3224, 1976.

[37] B. Allen and A. Folacci, *Phys. Rev. D* 35:3771, 1987.

[38] E.R. Bezerra de Mello, V.B. Bezerra, and N.R. Khusnutdinov, *Phys. Rev. D* 60:063506, 1999.

[39] S. M. Christensen, Ph.D. thesis, University of Texas at Austin, 1975.

[40] Peter Bernard Groves, Ph.D. thesis, Wake Forest University, 2003.

[41] L.H.Ryder. *Quantum Field Theory*. Cambridge University Press, Cambridge, England, 1996.

[42] P.A.M. Dirac. *Proc. Roy. Soc.*, 118:352, 1928.

[43] P.A.M. Dirac. *Quantum Mechanics*. Oxford University Press, London, 1958.

[44] J.D. Bjorken and S.D. Drell. *Relativistic Quantum Fields*. McGraw-Hill, New York, 1965.

[45] S.M. Christensen, *Phys. Rev. D* 17:946, 1978.

[46] B.S. DeWitt. In B.S. DeWitt and C. DeWitt, editors, *Relativity, Groups, and Topology*, New York, 1965. Gordon and Breach.

[47] S.M. Christensen, *Phys. Rev. D* 14:2490, 1976.

[48] P.R. Anderson, W.A. Hiscock, and D.A. Samuel. Stress-energy tensor of quantized scalar fields in static spherically symmetric spacetimes. *Phys. Rev. D* 51:4337, 1995.

[49] Available from *http://arstechnica.com/science/news/2010/07/neutrino-mass-less-of-a-mystery-thanks-to-deep-space-imaging.ars*.

[50] Available from *http://www.physorg.com/news196447658.html*.

[51] Available from *http://cupp.oulu.fi/neutrino/nd-mass.html*.

[52] C. W. Misner, K. S. Thorne, and J. A. Wheeler. *Gravitation*, Freeman, San

Francisco, 1973.

[53] M. Visser, *Lorentzian Wormholes – From Einstein to Hawking*, AIP, New York, 1995.

[54] S. Weinberg. *Gravitation and Cosmology: Principles and Applications of the General Theory of Relativity*, John Wiley & Sons, Inc. New York, London, Sydney, Toronto, 1972.

VITA

I was born in Beijing, China. I loved physics and was determined to study physics when I was in the middle school. However, when I entered Fudan University in Shanghai, I was enrolled into the Chemistry Department. I tried to transfer to the Physics Department but could not because China adopted a "planned system" in education that forbade students to change their Departments. Later, I shifted to the Department of Journalism because of a special opportunity. After graduation from Fudan University, I had worked as a journalist for 9 years in China's Xinhua News Agency, The People's Daily, and China Materials News. In 1996, I came to the U.S. to pursue graduate studies. At first, I got a Master's degree in Anthropology at Northern Illinois University (NIU). By that time, I realized that my mission is in physics. So I began to study physics at NIU and got a Master's degree. In 2005, I transferred to the University of Oklahoma and began to pursue my Ph.D. degree in physics. I finished my Ph.D. degree at the University of Missouri in 2012.

I plan to do academic research in theoretical physics in the future. At present, I try to find an academic position of either teaching or doing research.